

UNIVERSITY OF OKLAHOMA

GRADUATE COLLEGE

DEVELOPMENT OF POLYMER GEL SYSTEMS FOR LOST CIRCULATION
TREATMENT AND WELLBORE STRENGTHENING

A DISSERTATION

SUBMITTED TO THE GRADUATE FACULTY

in partial fulfillment of the requirements for the

Degree of

DOCTOR OF PHILOSOPHY

By

MUSAAB IBRAHIM MAGZOUN ELHAG

Norman, Oklahoma

2021

DEVELOPMENT OF POLYMER GEL SYSTEMS FOR LOST CIRCULATION
TREATMENT AND WELLBORE STRENGTHENING

A DISSERTATION APPROVED FOR THE
MEWBOURNE SCHOOL OF PETROLEUM AND GEOLOGICAL ENGINEERING

BY THE COMMITTEE CONSISTING OF

Dr. Saeed Salehi, Chair

Dr. Hamidreza Karami

Dr. Catalin Teodoriu

Dr. Benjamin (Bor-Jier) Shiau

Dr. Ibnelwaleed A. Hussein

Dr. Harold L. Stalford

Dedication

I dedicate this Ph.D. dissertation to my lovely wife Wafa and my gorgeous daughters, Rahaf and Raneem. And to my wonderful family, my father Ibrahim Magzoub, my mother Samia, my brothers Suhaib and Babiker, and my sister Aya. Love you all.

Acknowledgment

Foremost, I would like to express my sincere gratitude to my Ph.D. advisor, Dr. Saeed Salehi, for always being there to provide technical guidance and support throughout my Ph.D. journey. From day one, he has constantly motivated me to challenge my aptitude and competence to deliver quality research. Dr. Salehi has continuously encouraged and supported me to participate in technical conferences, workshops, and competitions that refined my skills. Not only was it academic supervision, but Dr. Salehi has been an advisor, mentor, and older brother who was endlessly keen to help and be in my social and professional life. I will be forever indebted to you and your boundless support.

I am very grateful to all of my committee members for the time and effort devoted to my dissertation. I was honored to have Dr. Harold Stalford as my outside committee member. His valuable comments on the dissertation objectives made my work more focused. Special thanks to Dr. Ibnelwaleed Hussein for his valuable inputs and suggestions on using organic and inorganic crosslinkers that produced promising findings. I am also thankful to Dr. Catalin Teodoriu for his sustained support and practical insights on fractured disc preparation that significantly improved the experimental part of my work. My sincere gratitude to Dr. Benjamin Shiau for the great insights and consultations on the wellbore cleaning and filter cake removal part. I would also like to extend my appreciation to Dr. Hamidreza Karami. His fruitful feedback, suggestions, and time he devoted were constructive in improving my dissertation quality. Thank you all for your significant inputs on my work.

I am immensely grateful to the University of Oklahoma, especially Mewbourne School of Petroleum and Geological Engineering and the Well Construction Technology Center, for providing resources and financial support. I am also grateful to the Qatar National Research Fund

(QNRf) for partial financial support for this dissertation work. I want to thank with gratitude SNF Floerger Company for providing the polyacrylamide samples. The acknowledgment is also extended to the Gas Processing Center at Qatar University for helping with the gelation study.

I would like to express my deepest gratitude to my colleagues at the Well Construction Technology Center, especially my research group, for their continuous support, cooperation, discussions, and consultations that helped me achieve and improve my research work. Dr. Shawgi Ahmed and Mr. Cesar Vivas helped me with cores and fracture preparations. Dr. Raj Kiran's contribution to the machine learning part has improved my dissertation and opened more opportunities for this work to be efficiently applied in the field. Special thanks go to Mr. Jeff McCaskill for the endless technical support on the experimental setup, his consultations were very significant in resolving the technical issues. For that, I am very grateful to you all.

Last but not least, I am deeply thankful to my dear family, my parents, my wife, my two lovely daughters, and my siblings for their love and blessing. I am deeply indebted to my parents' prayers, encouragement, and support. Thanks for always believing in me. I can't thank my wife enough for the sacrifices she made and for always standing by my side; without her, I wouldn't have made it so far.

Table of Contents

| | |
|--|------|
| Dedication..... | iv |
| Acknowledgment..... | v |
| Table of Contents | vii |
| List of Tables | xi |
| List of Figures..... | xiii |
| Abstract..... | xxii |
| Chapter 1: Introduction..... | 1 |
| 1.1 Overview of Lost Circulation Problem and Wellbore Strengthening | 1 |
| 1.2 Problem Statement and Motivation | 4 |
| 1.3 Research Objectives | 5 |
| 1.4 Research Hypotheses | 6 |
| 1.5 Research Scope and Methodology | 7 |
| Chapter 2: Literature Review | 9 |
| 2.1 Mechanisms of Mud Loss and Affecting Factors..... | 9 |
| 2.2 Review of Applied Solutions in the Field and Current Gaps | 14 |
| 2.2.1 <i>Corrective and Preventive Treatments</i> | 14 |
| 2.2.2 <i>Solutions from Drilling Technologies and Techniques</i> | 19 |
| 2.2.3 <i>Review of LCM Types, Formulations, and Applications</i> | 23 |
| 2.3 Implications of Mud Loss and Operational Challenges | 33 |
| 2.3.1 <i>Chemical and Geochemical Challenges</i> | 33 |
| 2.3.2 <i>Thermal and In-situ Stresses Complications Impacting Mud Loss</i> | 39 |

| | | |
|--|--|----|
| 2.3.3 | <i>Wellbore Strengthening</i> | 40 |
| 2.3.4 | <i>Thermal Complications Affecting Mud Loss</i> | 41 |
| 2.4 | Effect of Operational Factors on Mud Loss | 43 |
| 2.4.1 | <i>Effect of Mud Rheology on Mud Loss</i> | 44 |
| 2.4.2 | <i>Effect of Pressure on Mud loss</i> | 46 |
| 2.4.3 | <i>Effect of Drill Pipe Rotational Speed, Flow Rate, and Wellbore Geometry on Mud Loss</i> | 49 |
| 2.4.4 | <i>Effect of Temperature on Mud Loss</i> | 50 |
| 2.5 | Outcomes from Literature Review and Current Research Gap..... | 52 |
| Chapter 3: Polymer Gels as Lost Circulation Solution | | 54 |
| 3.1 | Theory and Chemistry of Crosslinking | 54 |
| 3.2 | The Onset Temperature of Crosslinking | 55 |
| 3.3 | Organic and Inorganic Crosslinkers | 59 |
| 3.4 | Gels as Lost Circulation Materials | 60 |
| Chapter 4: Laboratory Experimental Methods and Machine Learning..... | | 65 |
| 4.1 | Design of Experiments (DoE) | 65 |
| 4.2 | Experimental Methods and Laboratory Procedures | 67 |
| 4.2.1 | <i>Material Selection and Preparation of Polymeric Gel Systems</i> | 67 |
| 4.2.2 | <i>Gel Description According to Sydansk's Codes</i> | 69 |
| 4.2.3 | <i>Cores, Filter Disks, and Fractured Disks Preparation</i> | 70 |
| 4.2.4 | <i>Experiments, Apparatus, and Procedures</i> | 72 |
| 4.3 | Machine Learning Approach | 79 |
| Chapter 5: Experimental Results and Discussions | | 85 |

| | | |
|--|--|-----|
| 5.1 | <i>Optimization of Polymeric Gel Formulation.....</i> | 85 |
| 5.1.1 | <i>Rheological Screening of Non-Cross-Linked Polyacrylamide.....</i> | 86 |
| 5.1.2 | <i>Optimization of crosslinkers in the polymeric gel formulation.....</i> | 91 |
| 5.2 | <i>Development of Crosslinked PAM/PEI-Based Pill</i> | 93 |
| 5.3 | <i>Development of Crosslinked PAM/PEI-Based Mud.....</i> | 99 |
| 5.4 | <i>Development of Crosslinked PAM/AlAc-Based Pill.....</i> | 106 |
| 5.5 | <i>Development of Crosslinked PAM/FNS-Based Pill</i> | 113 |
| 5.6 | <i>Study of Gelation Kinetics of Polymeric Gel Formulations.....</i> | 116 |
| 5.6.1 | <i>Study of Gelation Kinetics of PAM/PEI Based-Mud and Pill.....</i> | 116 |
| 5.6.2 | <i>Study of Gelation Kinetics of PAM/AlAc Based-Pill.....</i> | 125 |
| 5.6.3 | <i>Study of Gelation Kinetics of PAM/FNS Based-Pill.....</i> | 128 |
| 5.7 | <i>Drilling Fluid Filtration and Wellbore Strengthening Experiments.....</i> | 130 |
| 5.7.1 | <i>Pore-Scale Static Drilling Fluids Filtration.....</i> | 131 |
| 5.7.2 | <i>Fracture-Scale Static Drilling Fluids Filtration</i> | 136 |
| 5.7.3 | <i>Fracture-Scale Dynamic Drilling Fluids Filtration.....</i> | 144 |
| 5.8 | <i>Investigation of Filter Cake Evolution</i> | 146 |
| 5.8.1 | <i>Evolution of the Internal Filter Cake</i> | 147 |
| 5.8.2 | <i>Formation Damage and Secondary Filtration.....</i> | 151 |
| Chapter 6: Machine Learning Analysis Results and Discussion..... | | 153 |
| 6.1 | <i>Modeling and Tuning of Models Parameters</i> | 153 |
| 6.2 | <i>Performance and Accuracy of Predictions.....</i> | 156 |
| Chapter 7: Environmental Impacts, Economic Feasibility, and Case Studies | | 158 |
| 7.1 | <i>Environmental Impact Assessment</i> | 158 |

| | | |
|-------|---|-----|
| 7.2 | Gel Cleaning and Filter Cake Removal..... | 161 |
| 7.3 | Economic Feasibility Analysis: Case Studies | 165 |
| 7.3.1 | <i>Cost Analysis</i> | 165 |
| 7.3.2 | <i>Case Studies</i> | 168 |
| | Chapter 8: Summary, Conclusions, and Recommendations | 173 |
| 8.1 | Summary..... | 173 |
| 8.2 | Conclusions | 173 |
| 8.3 | Recommendations | 175 |
| | Nomenclature | 177 |
| | References | 181 |
| | APPENDIX A: Cost Analysis for The Gelling Mud, Pills, and Commercially Available Formulations..... | 205 |

List of Tables

| | |
|--|----|
| Table 2. 1: Loss rate and mud pit level at different loss mechanisms, modified after (Chilingarian and Vorabutr 1981)..... | 12 |
| Table 2. 2: Loss classifications based on mechanisms and formation characteristics | 13 |
| Table 2. 3: Broad types of LCM and their applications | 26 |
| Table 2. 4: Boundaries for sensitivity analysis of the three factors affecting mud loss (Ezeakacha and Salehi 2019b)..... | 29 |
| Table 2. 5: Recommended particle size specification with respect to the pore throat size (Vickers and Elkin 2006) | 31 |
| Table 2. 6: Importance of particle size in different models of wellbore strengthening (Dupriest 2005)..... | 33 |
| | |
| Table 3. 1: Differences between organic and inorganic crosslinkers | 60 |
| Table 3. 2: Example of polymers and crosslinkers used as LCMs..... | 64 |
| | |
| Table 4. 1: Composition of Ref.Mud#1 [20 lb/bbl Bentonite] | 68 |
| Table 4. 2: Composition of Ref.Mud#2 [9.6 ppg] | 68 |
| Table 4. 3: Composition of Ref.Mud#3 [9.6 ppg] | 68 |
| Table 4. 4: Details of the investigated component and parameters | 69 |
| Table 4. 5: Sydnak gel strength codes (Sydansk 1990)..... | 69 |
| Table 4. 6: Types and properties of used ceramic filter disks | 71 |
| Table 4. 7: Types and properties of used fractured aluminum filter mediums..... | 71 |
| Table 4. 8: Mud component and their range of concentrations | 84 |

| | |
|--|-----|
| Table 5. 1: Composition of the polymer-based mud (PBM-2.5, 9.6 ppg)..... | 104 |
| Table 5. 2: Effect of Nanosilica on viscosity and phase separation of PAM/AlAc system | 113 |
| Table 5. 3: Sydansk code of the formed gels using TAS only to crosslink PAM and silica settling | 130 |
| Table 6. 1: Performance of algorithms in predicting plastic and apparent viscosity (R^2)..... | 157 |
| Table 7. 1: Pricing list and range of concentrations of the developed gelling mud and pill | 166 |

List of Figures

| | |
|--|----|
| Figure 1. 1: Types of conditions and formations that cause lost circulations. | 2 |
| Figure 1. 2: Strengthening mechanisms based on (a) stress cage model, (b) fracture-closure stress model, and (c) fracture-propagation resistance model (Mehrabian et al. 2015). | 4 |
| Figure 1. 3: Complications of mud loss problem in narrow operational window and limitations of LCM selection at different formations. | 5 |
| Figure 1. 4: Research methodology framework | 7 |
| | |
| Figure 2. 1: Lost circulation mechanisms..... | 10 |
| Figure 2. 2: Selection chart of preventive and corrective treatment and methods. | 18 |
| Figure 2. 3: Annular space in regular drilling and casing while drilling contributing to plastering effect (Karimi et al. 2011). | 22 |
| Figure 2. 4: Cross-sectional view of filter cake during a) conventional drilling and b) casing while drilling (Meza et al. 2017). | 23 |
| Figure 2. 5: A schematic representation of mud losses while drilling in the case of (a) typical LCM and (b) NPs (Modified from Borisov et al. 2015)..... | 25 |
| Figure 2. 6: Effect of high temperature on carrying capacity of drilling fluid (Echt and Plank 2019)..... | 28 |
| Figure 2. 7: Effect of temperature with LCM concentration on dynamic filtration (Ezeakacha and Salehi 2019b)..... | 29 |
| Figure 2. 8: Illustration of the significance of fine and coarse particles on LCM performance (Kageson-Loe et al. 2009).. | 32 |

| | |
|---|----|
| Figure 2. 9: Typical composition of a) OBM and b) WBM, excluding weighting agents (Wenger et al. 2004)..... | 34 |
| Figure 2. 10: Effect of deflocculant on clay dispersion (Ghazali et al. 2018)..... | 35 |
| Figure 2. 11: Effect of rock type on dynamic filtration (Ezeakacha et al. 2018). | 37 |
| Figure 2. 12: Dynamic filtration using cylindrical cores from a) Austin chalk and b) limestone (Ezeakacha,Salehi, and Bi 2017)..... | 38 |
| Figure 2. 13:: SEM of Michigan core after the filtration test (Salehi et al. 2015)..... | 38 |
| Figure 2. 14: Effect of temperature variations on failure pressure (Peter-Borie et al. 2018). | 42 |
| Figure 2. 15: Correlation between mud loss and drop in mud temperature in a deepwater well in the GoM (Gonzalez et al. 2004). | 43 |
| Figure 2. 16: Effect of yield stress on the ultimate volume of losses, b) effect of shear-thinning on mud loses (Majidi et al. 2010)..... | 46 |
| Figure 2. 17: Status of the wellbore with respect to wellbore pressure..... | 48 |
| Figure 2. 18: variation in loss rate with the variation of differential pressure of overbalance drilling in BP wells (Dyke et al. 1995)..... | 48 |
| Figure 2. 19: Thermal impact on hoop stress along the wellbore wall (Wang 2018). | 51 |
| Figure 3. 1: DSC curve of the gel system composed of 0.6 wt.% PAM and 0.6 wt.% crosslinkers (Liu et al. 2016). | 56 |
| Figure 3. 2: Effect of salts (43.2 g/L) on fractional gelation of emulsified PAM/PEI, 9:1 ratio (Mohamed et al. 2015). | 57 |
| Figure 3. 3: Effect of pH on the gelation process of PAM/PEI gels (Liu et al. 2016). | 58 |
| Figure 3. 4: Chemical structures of different types of acrylamide polymers used as LCMs (Kurenkov et al. 2001; Al-Muntasheri et al. 2008; Omer 2012)..... | 62 |

| | |
|--|----|
| Figure 3. 5: Chemical structure of chitosan and highly branched PEI (Zhang et al. 2015; Reddy et al. 2003)..... | 62 |
| Figure 4. 1: Workflow of the polymeric LCM developing study..... | 65 |
| Figure 4. 2: Flow process of the optimization study for the crosslinked polymer. | 66 |
| Figure 4. 3: Process of carbonate coring and filter disks preparation, (a) rock after coring, (b) core 2.5 x 3 inches, and (3) disks 2.5 x 0.25 inches. | 70 |
| Figure 4. 4: Schematic of the permeability plugging tester (PPA) and the fractured aluminum disk. | 76 |
| Figure 4. 5: M2200 dynamic drilling simulator, modified after (Ezeakacha and Salehi 2019a). | 77 |
| Figure 4. 6: Fractured cylindrical wellbore-shaped aluminum. | 77 |
| Figure 4. 7: Preparation of filter disks for SEM and EDX post-experimental analysis. | 78 |
| Figure 4. 8: Workflow of the ML study. | 83 |
| Figure 5. 1: Viscosity versus temperature for PAM samples (10 wt.%) having different molecular weights, compared to the Ref.Mud#2..... | 87 |
| Figure 5. 2: Plastic viscosities of PAM samples (10 wt.%) of different molecular weights, compared to the Ref.Mud#2. | 88 |
| Figure 5. 3: Viscosity versus temperature of the low molecular weight PAM at different concentrations, compared to the Ref.Mud#2..... | 89 |
| Figure 5. 4: Viscosity of PAM (<math> < 2 \times 10^5 < /math> Da) with different concentrations at 75°F and 200°F. 90 | 90 |
| Figure 5. 5: The (a) AV, (b) PV, and (c) YP of the low molecular weight PAM at different concentrations compared with Ref.Mud#1 at 200°F. | 91 |

| | |
|---|-----|
| Figure 5. 6: Impact of PAM molecular weight on gelation kinetics on Salt-free water..... | 93 |
| Figure 5. 7: Effect of crosslinking with PEI on gel strength of 10 wt.% PAM compared with Ref.Mud#2 at 200°F. | 95 |
| Figure 5. 8: Effect of crosslinking with PEI on AV, PV, and YP of 10 wt.% PAM compared with Ref.Mud#1 at 200°F (93°C)..... | 96 |
| Figure 5. 9: Effect of PEI concentration on AV, PV, and Gel strength. | 97 |
| Figure 5. 10: Effect of PEI concentration on the viscosity of 7.5 wt.% PAM (a) before, and (b) after gelation starts. | 98 |
| Figure 5. 11: Dynamic shear experiment for a) optimized PAM/PEI system..... | 99 |
| Figure 5. 12: Effect of bentonite on PAM/PEI [7.5:1] viscosity compared with the Ref.Mud#2 (indicated by the slotted lines)..... | 100 |
| Figure 5. 13: Effect of bentonite on gel strength of 7.5 wt.% PAM/PEI compared with Ref.Mud#1 and Ref.Mud#2. | 101 |
| Figure 5. 14: Effect of mixing order on the viscosity of the PAM/PEI mud when Bentonite is added first. | 103 |
| Figure 5. 15: Effect of mixing order on the viscosity of the PAM/PEI mud when PAM/PEI is added first. | 103 |
| Figure 5. 16: AV, PV, and YP of the optimized polymer-based mud at 120°F compared with Ref. Mud#2 (illustrated by the slotted line). | 105 |
| Figure 5. 17: AV, PV, and YP of the optimized polymer-based mud at 200°F compared with Ref.Mud#2 (illustrated by the slotted line)..... | 105 |
| Figure 5. 18: Effect of aluminum acetate (AlAc) on storage modulus of 7.5 wt.% PAM. | 106 |

| | |
|---|-----|
| Figure 5. 19: (a) gelation of PAM/AlAc with time at different concentrations, and (b) Effect of AlAc concentration on the final gel strength (storage modulus)..... | 107 |
| Figure 5. 20: Effect of AlAc concentration on the apparent viscosity. | 108 |
| Figure 5. 21: Figure Gel formation on the rotating viscometer pop during the gradual heating. | 109 |
| Figure 5. 22: Viscosity measurements at room temperature. | 110 |
| Figure 5. 23: Effect of AlAc concentration on (a) apparent viscosity and (b) plastic viscosity of 7.5 wt.% PAM. | 110 |
| Figure 5. 24: Phase separation without nanosilica observed in PAM/AlAc [7.5:3]..... | 111 |
| Figure 5. 25: Effect of nanosilica concentration on the AV, PV, and YP of PAM/AlAc [7.5:3]. | 112 |
| Figure 5. 26: Final gel strength of PAM/FNS with different NS concentrations and sizes. | 114 |
| Figure 5. 27: Schematic illustration of the dispersion with respect to the size of nanosilica and molecular weight of the PAM. | 115 |
| Figure 5. 28: Viscosity measurements at room temperature. | 115 |
| Figure 5. 29: Effect of temperature on gelation of PAM/PEI [7.5:1], (a) at 200°F, and (b) at 266°F. | 117 |
| Figure 5. 30: (a) viscosity versus time with gelation by different PEI concentration, and (b) effect on gelation time. | 118 |
| Figure 5. 31: Viscosity evolution of pure PAM/PEI [7.5:1] gel and PAM/PEI gels containing NH ₄ Cl up to 5 wt.%. | 119 |
| Figure 5. 32: Viscosity evolution of pure PAM/PEI [7.5:0.5] gel and PAM/PEI gels containing NH ₄ Cl up to 5 wt.%. | 120 |

| | |
|--|-----|
| Figure 5. 33: Gelation time of PAM/PEI containing NH ₄ Cl from viscosity evaluation. | 121 |
| Figure 5. 34: Effect of bentonite concentration on (a) gelation process and (b) gelation time and storage modulus of PAM/PEI [7.5:1] at 130°C..... | 122 |
| Figure 5. 35: Mud weight effect on (a) the gelation process with time, and (b) gelation time and final storage modulus of PAM/PEI [7.5:1]..... | 123 |
| Figure 5. 36: Summary of the gelation behavior of the different PAM/PEI based systems. ... | 124 |
| Figure 5. 37: Effect of temperature and time on PAM/AlAc (7:1) (a) storage modulus and (b) loss modulus. | 125 |
| Figure 5. 38: Gelation profile of PAM/AlAc system. | 126 |
| Figure 5. 39: Effect of pH and nanosilica on (a) storage modulus of PAM/AlAc, and (b) frequency Sweep of PAM/Alac [9:3]. | 127 |
| Figure 5. 40: Effect of pH on gelation formation and stability indicated by the zeta potential. | 127 |
| Figure 5. 41: (a) Gelation time estimation for PAM/AlAc without NH ₄ Cl retardation, and (b) with retardation effect..... | 128 |
| Figure 5. 42: Effect of NH ₄ Cl concentration on the gelation process with time..... | 128 |
| Figure 5. 43: Effect of adding 50 nm of nanosilica at different concentrations on the gel strength of 9 wt. % PAM crosslinked by 2 wt. % FNS..... | 129 |
| Figure 5. 44: Effect of nanosilica particle size on zeta potential of PAM/FNS solution. | 129 |
| Figure 5. 45: Comparison of filtration control performance of the PBM-2.5 and Ref.Mud#2. | 132 |
| Figure 5. 46: Filter cake on the ceramic disc, calcium carbonate (left), and PBM-25 (right). | 132 |
| Figure 5. 47: Results of static filtration with ceramic filter disks using PAM/PEI pill and Ref.Mud#2..... | 133 |

| | |
|--|-----|
| Figure 5. 48: Filtrates volume by PAM/PEI and WBM Ref.Mud#2 from the static filtration experiments in carbonate cores. | 135 |
| Figure 5. 49: Effect of bentonite on filtration volume of PAM/PEI compared with WBM (Ref.Mud#2) in carbonate cores. | 136 |
| Figure 5. 50: Summary of cumulative filtration volumes and sealing pressure from pore-scale static filtration experiments. | 136 |
| Figure 5. 51: Fracture-scale filtration by the PAM/PEI-based mud..... | 137 |
| Figure 5. 52: Summary of cumulative loss volume and sealing pressure from the fractured scale static filtration experiments. | 138 |
| Figure 5. 53: Images of 1000 microns fractures after static filtration experiment with different formulations..... | 138 |
| Figure 5. 54: Sealing of a complex fracture with PAM/FNS pill..... | 139 |
| Figure 5. 55: Sealing of fractures of different sizes with PAM/PEI pill. | 140 |
| Figure 5. 56: Effect of temperature on the cumulative loss of (a) PAM/NFS and (b) PAM/PEI pill by static filtration experiments in 1000 microns fracture. | 141 |
| Figure 5. 57: Effect of temperature on the cumulative loss of PAM/AlAc pill by static filtration experiments in 1000 microns fracture. | 142 |
| Figure 5. 58: Mud loss versus time at different gelation times using PPA with 1000-micron fractured disc. | 144 |
| Figure 5. 59: Cumulative mud and maximum sealing pressure using PPA with 1000-micron fractured disc. | 144 |
| Figure 5. 60: Dynamic fluid loss profiles for PAM/PEI [7.5:1] in 1000 μ m vertical fracture. | 145 |
| Figure 5. 61: 1000 μ m sealed with PAM/PEI gel in dynamic filtration experiment. | 146 |

| | |
|--|-----|
| Figure 5. 62: External filter cake formation on different filter disks. | 147 |
| Figure 5. 63: SEM images for the (a) carbonate blank core and the internal filter cake after the PPA test with (b) WBM and (c) PAM/PEI. | 148 |
| Figure 5. 64: EDX analysis of the internal filter cake forming in carbonate by WBM and PAM/PEI. | 149 |
| Figure 5. 65: SEM images for the internal filter on ceramic filter disks #170-53 and #170-55 before and after PPA test with PAM/PEI. | 150 |
| Figure 5. 66: SEM images for the invasion of WBM filtrates inside carbonate disk..... | 151 |
| Figure 5. 67: SEM images for the invasion of PAM/PEI filtrates inside carbonate disk..... | 152 |
| Figure 6. 1: Accuracy of the kNN algorithm regarding the number of nearest neighbors for (a) plastic viscosity and (b) apparent viscosity. | 154 |
| Figure 6. 2: Random Forest classification accuracy vs. the number of trees for (a) plastic viscosity and (b) apparent viscosity..... | 155 |
| Figure 6. 3: The test dataset accuracy corresponding to the number of boosting stages for Gradient Boosting algorithm for (a) plastic viscosity and (b) apparent viscosity. | 155 |
| Figure 6. 4: Accuracy in the prediction of plastic viscosity and apparent viscosity using AdaBoosting algorithm. | 156 |
| Figure 6. 5: Predicted Vs. Actual values of (a) PV and (b) AV of the testing dataset for different algorithms at high shear rate..... | 157 |
| Figure 6. 6: Predicted Vs. Actual values of AV at (a) 6 rpm (10 s ⁻¹) and (b) at 3 rpm (5 s ⁻¹) of the testing dataset for different algorithms. | 157 |
| Figure 7. 1: Polymerization of acrylamide with acrylic acid. | 159 |

| | |
|--|-----|
| Figure 7. 2: Effect of polyacrylamide/H ₂ S/CO ₂ on the corrosion mechanism of N80 steel (Dong et al. 2020). | 160 |
| Figure 7. 3: Observation on gel dissolving using ammonium chloride (NH ₄ Cl). | 165 |
| Figure 7. 4: Cost of PAM/PEI-based mud in comparison with a typical WBM. | 167 |
| Figure 7. 5: Cost of gelling PAM/PEI based LCM in comparison with commercial pills. | 167 |
| Figure 7. 6: Well-A performance plot, after (Mannon 2013). | 169 |
| Figure 7. 7: Well-B performance plot, after (Mannon 2013). | 169 |
| Figure 7. 8: Events contributed to NPT in Well-A and Well-B, data from (Mannon2013). | 170 |
| Figure 7. 9: Design chart for lost circulation at different depths and temperatures. | 172 |

Abstract

Lost circulation is a frequent problem and a significant contributor to the non-productive time (NPT) in the drilling operation. Field reports and experimental studies have revealed that conventional solutions are doomed to fail in many complex loss situations. Factors such as fracture sizes, depth, temperature, pressure, and type of formation, complicate the problem and limit the lost circulation materials (LCM) options.

The primary objective of this research was to develop a flowing crosslinked polymer-based drilling fluid by introducing a gelling polymer and a crosslinker to the LCM and drilling mud formulations. The goal is to enhance wellbore strength by increasing the fracture resistance of weak formations to avoid potential mud losses. Other objectives of this research covered developing different fast-curing LCM pills to treat lost circulation in challenging situations. Different types and combinations of polymers, crosslinkers, and reinforcing nanoparticles were utilized. Further, in this research, machine learning (ML) algorithms were used to assess the relationship between the crosslinked polymer recipes and drilling fluids additives. The ML approach aims to expand the developing study and to open more opportunities for this work to be efficiently applied in the field.

The novelty of this study is in the use of the organic and inorganic crosslinker in controllable gelling polymeric LCMs that can seal near wellbore fractures and stable unconsolidated formations. Besides, this research introduces a new concept of gelation kinetics of polymeric gels in drilling fluids. This concept and the post-experimental analysis conducted in this study are essential for the petroleum industry to develop new lost circulation preventive and corrective methods.

Chapter 1: Introduction

1.1 Overview of Lost Circulation Problem and Wellbore Strengthening

Lost circulation is often ranked as the top issue in drilling. Many drilling problems are directly related to lost circulation, such as differential sticking and hole instabilities. Severe well control implications can arise in the event of loss of hydrostatic pressure inside the wellbore due to the loss of a large volume of drilling fluid. Besides, the time spent solving the lost circulation and the associated problems can lead to substantial non-productive time (NPT). The NPT refers to any time that drilling stops, or any time spent on unplanned operations. Rehm et al. (2013) reported a statistical study on lost circulation in the Gulf of Mexico (GoM) for ten years. The study revealed that more than 12% of the NPT was due to lost circulation events. Moreover, about 18% of NPT was due to kicks and wellbore instabilities.

As a common field practice, loss circulation materials (LCM) are added to fill any pores and pre-existing or induced fractures. Other methods include drilling techniques and technologies such as under-balanced drilling (UBD), managed pressure drilling (MPD), and casing while drilling (CwD). However, the application of some of these unconventional drilling methods can be costly or associated with equipment, personnel, or technical challenges. The problem often becomes very complicated when large fractures exist in the formation or drilling in challenging downhole conditions. Highly fractured formations, weak rocks, depleted reservoirs, and abnormally pressurized intervals have driven the need for wellbore strengthening technologies. Technically, the concept of wellbore strengthening is based on anticipating the wellbore issues and design drilling fluids that can seal and plug near wellbore fractures efficiently to strengthen unstable formations.

The wellbore strengthening or touching is a currently widely used term in drilling. The objectives of wellbore strengthening are to expand the drilling window and allow drilling operation to continue with less risk of lost circulation events, and to minimize the number of casing strings, especially in deep and ultra-deepwater applications. The methods applied in wellbore strengthening aim to increase formations resistance to break by plugging and sealing near wellbore fractures. Successful application of wellbore strengthening helped in accessing difficult reserves with varying fracture gradients (Kiran et al. 2017). Figure 1.1 shows the types of conditions and formations that cause lost circulations. In such formations, the margin of safe drilling window between pore pressure and formation fracture pressure is very narrow, which increases the tendency to breakdown and mud loss. This safe margin dictates well design, mud program, and well control (Salehi and Nygaard 2011).

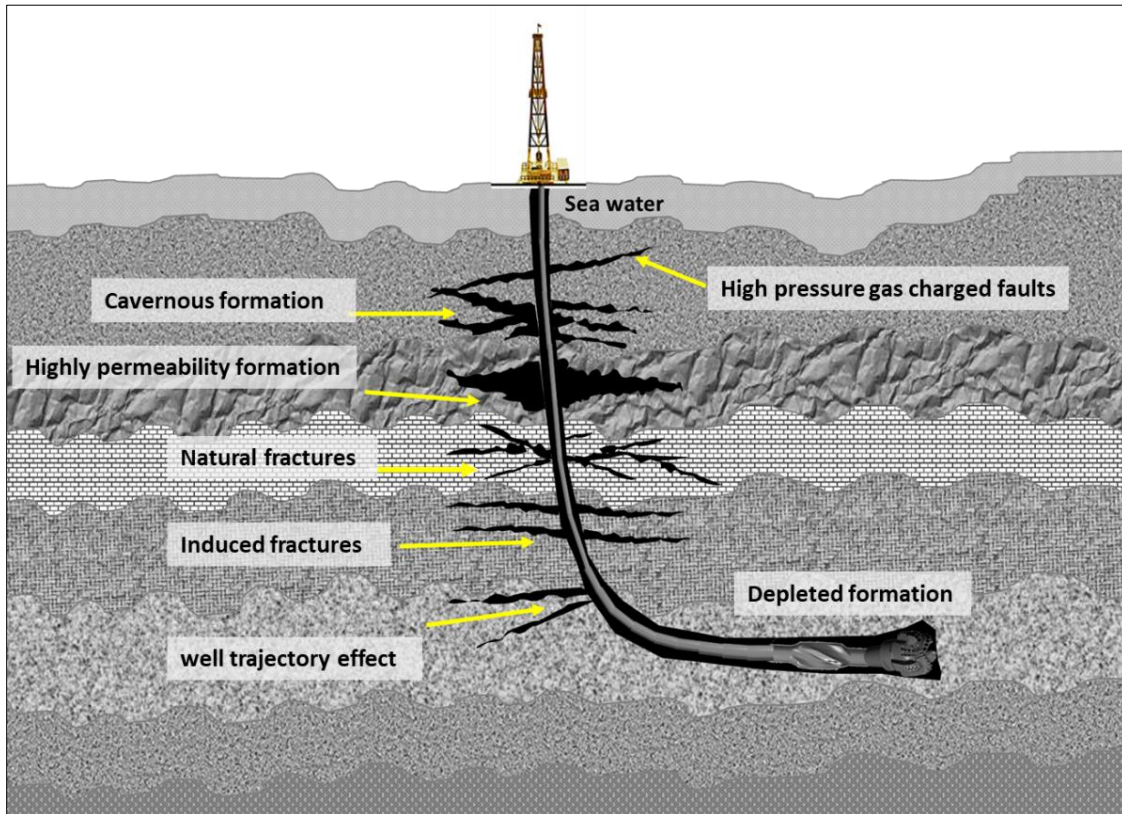


Figure 1. 1: Types of conditions and formations that cause lost circulations.

The wellbore should be protected from fracture initiation or propagation to stop or prevent lost circulation. For that reason, wellbore strengthening techniques enhance the wellbore hoop stress or increase the formation's resistance to fracture propagation. Generally, there are two common hypotheses of how a wellbore can be strengthened: increasing wellbore hoop stress when fractures are sealed. The other is by enhancing fracture propagation pressure by fracture tip isolation with proper LCM (Salehi 2012). The commonly used physical models for wellbore strengthening are the stress cage, fracture closure stress (FCS), and fracture propagation resistance (FPR).

The stress cage model assumes fracture bridging occurs close to the wellbore, and fluid filtrates from the fracture walls into the formation. The increase in hoop stress in the stress cage model is assumed due to the compressive forces transferred to the bridging particles at the fracture mouth (Alberty and McLean 2004a). In the FCS model, the fracture must be initiated first, then bridging particles forced into the fracture. The low permeable plug formed by particles bridging will isolate the fracture tip from wellbore pressure. The fracture tip isolation and increased fracture closure stress will prevent the fracture from reopening (Dupriest 2005). The FPR model, instead of increasing hoop stress, aims to increase the resistance to fracture propagation. This is attained by evaluation of mud cake inside the fracture. A good mud cake built inside the fracture will isolate the tip and prevent further propagation (Morita et al. 1996).

There are several available numerical models for wellbore strengthening to simulate lost circulation due to fracture propagation. However, most of them assume linear rock elasticity and fail to consider porous features of the formation; therefore, the effect of fluid flow and pore pressure are not considered (Alberty and McLean 2004b). Salehi (2012) introduced a new numerical three-dimensional model to solve three-dimensional poroelastic models and identifies

potential loss zones. Figure 1.2 illustrates the common hypothesis of improving wellbore strength (Mehrabian et al. 2015).

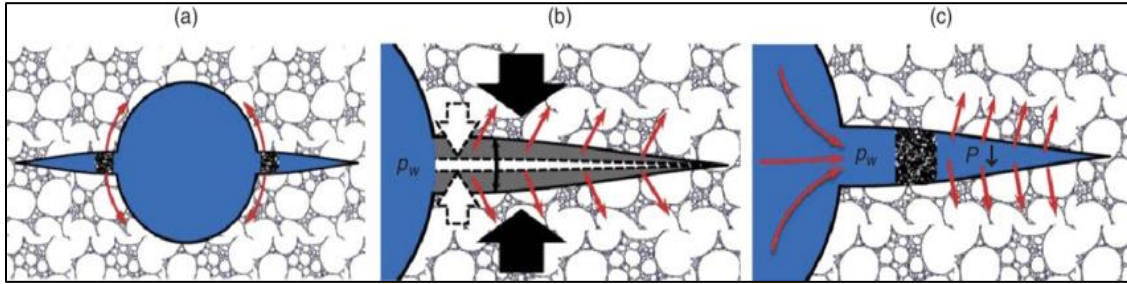


Figure 1. 2: Strengthening mechanisms based on (a) stress cage model, (b) fracture-closure stress model, and (c) fracture-propagation resistance model (Mehrabian et al. 2015).

1.2 Problem Statement and Motivation

Lost circulation problem often complicates in narrow operational windows. It becomes more challenging, as selecting proper LCM is most often limited by temperature, depth, and fracture sizes. Figure 1.3a shows three examples of the common formations that cause lost circulation, which are highly permeable rocks, fractured formations, and depleted reservoirs. Due to this situation, the operational drilling window becomes very narrow, as shown in Figure 1.3c.

Over the past years, LCMs have evolved considerably. Innovative and engineered materials have been introduced to treat various types of loss zones. However, due to many uncertainties, their success rates are still meager. The selection of types, concentrations, and particle size of the bridging materials needs a comprehensive study of the mud loss mechanisms. Besides, when large particle size is required to seal large fractures, as shown in Figure 1.3b, the risk of plugging and difficulties in pumping increases.

The motivation of this study is promoted by the success of several deployments of crosslinked polymers in high permeable formation to shut-off water zones in oil production wells. Therefore, the crosslinked polymers have great potential for application as lost circulation materials. Developing and optimizing a controlled gelling polymer can produce efficient and cost-

effective crosslinked polymers capable of sealing and strengthen the near-wellbore area to solve the root cause of the loss circulation problem.

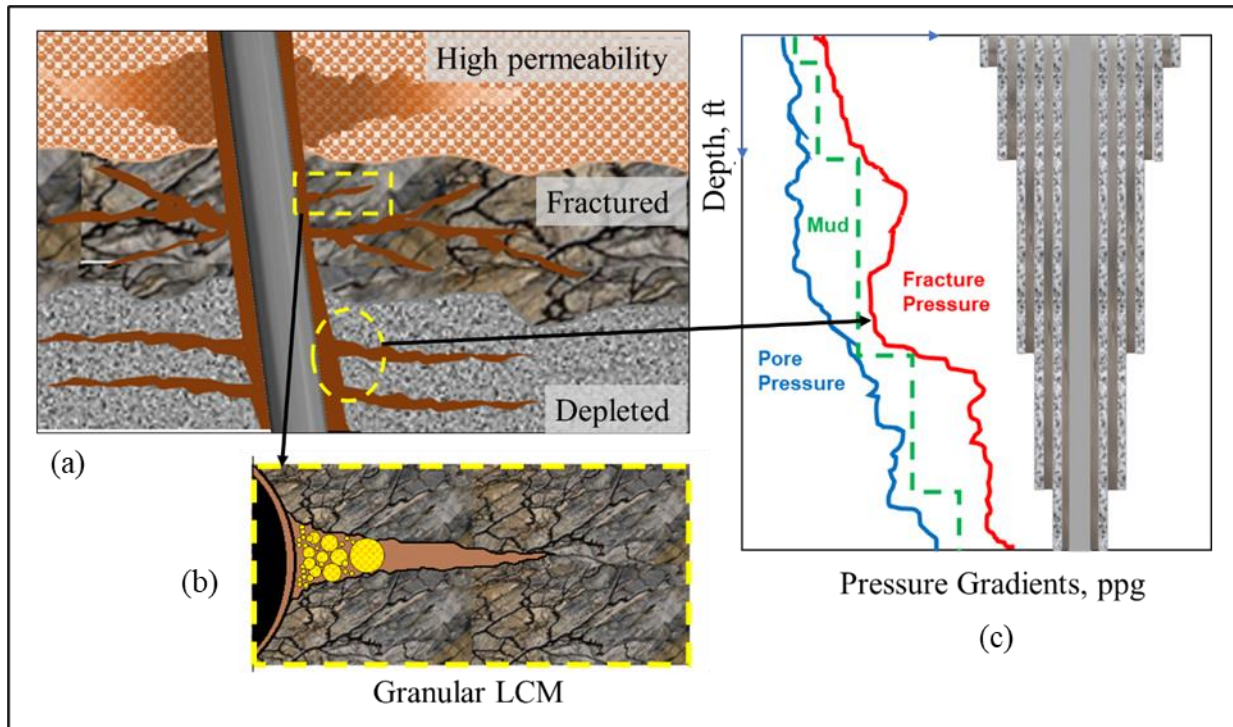


Figure 1. 3: Complications of mud loss problem in narrow operational window and limitations of LCM selection at different formations.

1.3 Research Objectives

This study investigates the application of polyacrylamide cross-linkable polymer gel in the drilling mud formulation to enhance wellbore strengthening. Organic and inorganic crosslinkers were considered. Further, this study seeks to develop procedures and novel polymer gel systems to be applied in naturally fractured formations. The main objective of this study is to provide a responsive, adaptive, and efficient solution to the loss circulation problem in challenging situations such as high fractured formations. The treatment will be independent of fracture size and can solve the lost circulation problem in one trial, saving a lot of non-productive time (NPT). The proposed solution will be based on a controlled gelling polymer which will be developed in this study. The

objectives of developing a crosslinked polymer for lost circulation treatment and wellbore strengthening can be summarized in the following sub-objectives:

1. Develop formulas of a flowing cross-linkable polyacrylamide-based drilling fluid with a controlled gelation rate.
2. Develop cross-linkable polyacrylamide-based pills for lost circulation treatment.
3. Study the gelation kinetics of the gelling LCMs in drilling fluid formulations.
4. Investigate the efficiency of the polymeric gel systems in sealing and plugging multiple near wellbore fractures as a corrective treatment.
5. Investigate the feasibility of using the developed formulations for drilling fluid loss prevention as a proactive treatment.

1.4 Research Hypotheses

The research hypotheses were based on the studied literature where the challenging situations of lost circulation and the affecting factors of polymers crosslinking were investigated. The following hypotheses are considered for this research:

- A crosslinked polymer can form a strong gel capable of sealing near wellbore fractures if the formula is well designed.
- The gelation process may occur in the pipes and drill string if the gelation process is not adequately controlled.
- Crosslinked polymers are compatible with water-based drilling fluid. However, flocculation and instabilities may occur in some conditions.
- The crosslinked polymers cause minor formation damage.

1.5 Research Scope and Methodology

The research methodology of this study was classified into four levels of investigation to cover the scope and meet the objectives. The research levels include theoretical literature review, experimental investigation, post-experimental analysis, and machine learning modeling. The workflow of four these levels is structured in the framework shown in Figure 1.1.

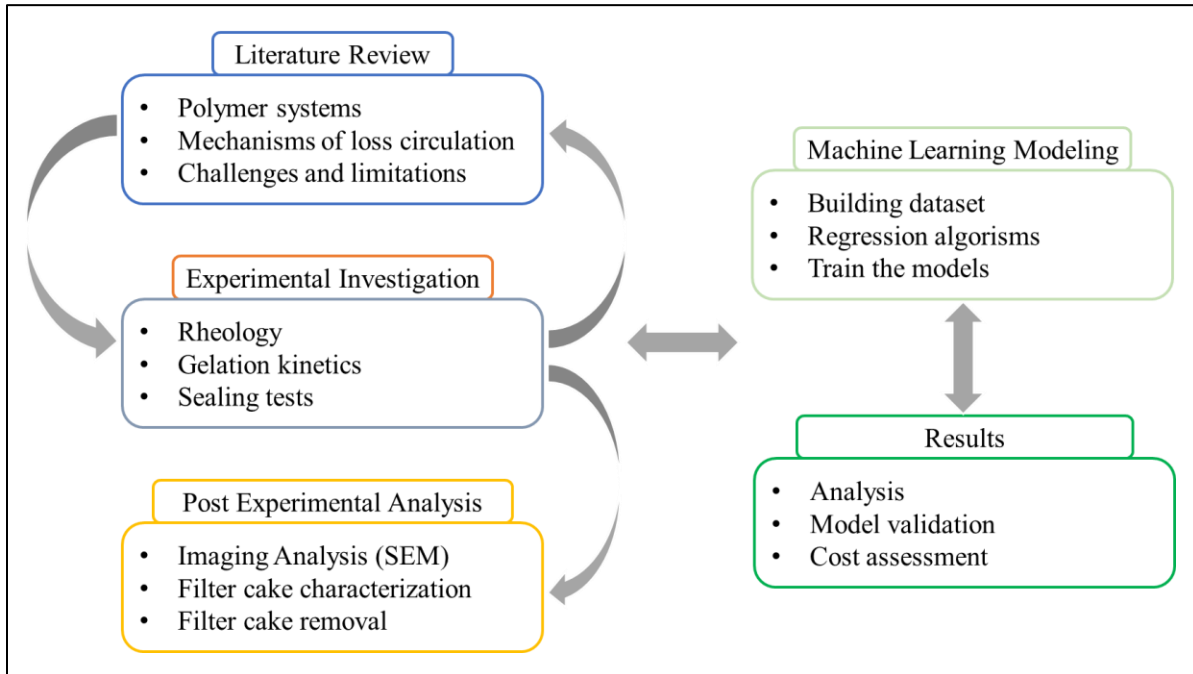


Figure 1. 4: Research methodology framework

The scope of each investigation level is discussed in the following methodologies:

- i. *Theoretical Review*: The objective of the theoretical review conducted in this study is to provide a comprehensive review of literature on the lost circulation problem, drilling fluid filtration mechanism, and lost circulation materials. The gap in the literature, operational challenges, and limitations were defined. Understanding of literature and lost circulation problem provide the base for selecting potential polymers and crosslinkers to meet the specific conditions and applications. This review aims to provide an in-depth evaluation of the commercially available polymers and crosslinkers to characterize their working conditions,

gelation factors, stability, and cost. Findings and outcomes from this review study also helped design the research framework by identifying the required experimental analysis and required investigations.

- ii. *Experimental work:* In this study, three stages of experimental studies were conducted to develop the polymeric gels and evaluate their performance as LCM. In the first stage, the potentials polymers and crosslinkers were screened based on their rheology. The screening was conducted for all components in drilling fluid formulations. The goal was to select the proper materials and concentrations to establish the crosslinked polymer-based fluid formulation to be used as LCM. In the second stage, static and dynamic sealing experiments were conducted to test the performance of the optimized formulations in sealing both permeable rocks and fractures in different conditions. In the third stage, post-experimental analyses were carried out to evaluate sealing efficiency and formation damage potential risks. It is worth mentioning that this is the first time the filter cake and formation damage of crosslinked polymer is investigated. The details of all the experiments are described in Sec 4.3.
- iii. *Machine Learning Modeling:* A machine learning (ML) approach was used in this study to expand the rheological assessment of the crosslinked polymers formulations. The approach depended on the nonlinear regressions using several machine learning algorithms. The data generated in the experimental work was utilized to build datasets used as inputs for the ML models. The ML algorithms, model training, parameters tuning, and model validation are explained in Sec 4.

Chapter 2: Literature Review

This chapter summarizes the findings of the literature study and emphasizes the complications of mud loss, LCM selection criteria, particle size, and concentration considerations. A comprehensive background study was conducted on drilling fluid loss, filtration mechanisms in different fluid and rock systems, and applied solutions. The challenges, limitations, and current gaps were highlighted.

2.1 Mechanisms of Mud Loss and Affecting Factors

A mud loss or lost circulation can be defined as the uncontrolled mud flow from the wellbore to the formation driven by differential pressure. The mud escapes the wellbore by different mechanisms depending on the formation type. Loss formation can be highly permeable or unconsolidated formations, natural fractures, or fractures induced by wellbore pressure and drilling operation. In overbalanced drilling, the hydrostatic mud pressure is maintained slightly above the formation pressure to hold formation fluids from entering the well. This pressure should be less than the formation fracturing pressure to avoid wellbore breakdown and fluid loss.

Moreover, the equivalent circulating density (ECD), which represents the dynamic circulation density exerted in the wellbore, should not exceed the formation fracturing gradient. The ECD is expressed as the sum of hydrostatic mud pressure and annulus pressure loss due to friction. Hence, high circulating pressure loss makes ECD exceeds the near-wellbore hoop stress and tensile strength of the rock, causing loss of circulation (Salehi and Nygaard 2012b; Ghalambor et al. 2014). In microfractures, the excessive pressure imposed by the fluid circulation can propagate these fractures and increase the loss rate. Therefore, the drilling operation window between the pore pressure and fracture pressure should be carefully considered in mud design and during drilling operation.

The commonly used classification for lost circulation was based on the amount of loss. The industry has classified loss into three categories; seepage, when mud loss is below 25 bbl/hr, partial, when the loss rate is between 25-100 bbl/hr, and total, when the loss rate is higher than 100 bbl/hr or there is no return. Sometimes, this classification is different for static and dynamic wellbore or other types of mud; for instance, for the oil-based mud (OBM), when the loss is greater than 30 bbl/hr, it is considered a severe loss (Rabia 2002). This classification was used for many years to assess the lost circulation problems and how to address them. However, it does not provide enough essential information for designing a preventive or corrective strategy, such as the formation type, the loss mechanism, or abnormally pressurized zones. A better classification is based on the formation type in which the loss occurs as it gives more information on the loss mechanisms. Figure 2.1 illustrates the difference between these three types of loss zones.

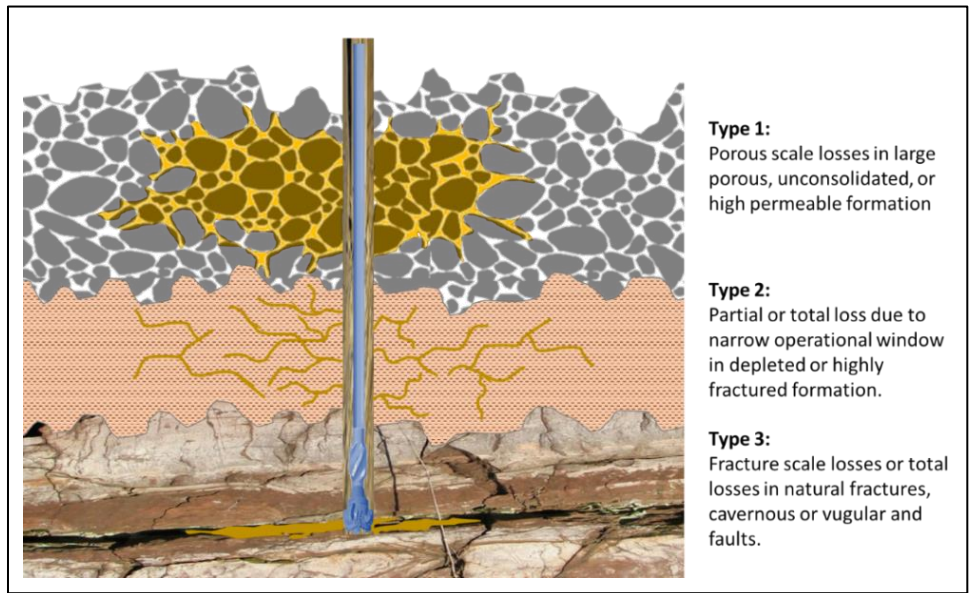


Figure 2. 1: Lost circulation mechanisms.

Ghalambor et al. (2014) stated that the current adopted classification focuses on the mechanisms of lost circulations, which can be categorized into loss to pore throats, loss to induced or natural fractures, and loss to vugs or caverns. For instance, seepage losses are usually encountered in high permeable formations such as sandstone, where large pore throats exist. In

contrast, partial losses are more observed in unconsolidated sands, gravel, or microfractures (Javeri et al. 2011; Brandl et al. 2011). The total losses are associated with large fractures, apertures, and vugular and cavernous formations (Bugbee 1953; Ghalambor et al. 2014).

Narrow operational mud windows make the lost circulation problem more complicated. Usually, it is more likely to exceed the fracture gradient in depleted reservoirs, deepwater wells, deviated wells, and HPHT wells (Zamora et al. 2000; Addis et al. 2001). For example, drilling in-fill wells in depleted reservoirs is usually associated with frequent mud loss incidents because of the significantly decreasing fracture pressure. Fracture pressure decreases due to the drop in pore pressure through the field's long production life. A similar situation is faced in deepwater wells; the density of seawater, which is much lower than rock's density, lowers the overburden pressure and causes lower than usual fracture gradients, which narrow the operational window. Moreover, narrow mud windows are also observed in deviated wells, where loss can occur at the high inclination at a pressure significantly less than the normal fracture gradient (Byrd and Zamora 1988; Salehi and Nygaard 2011).

Identifying the loss mechanism is critical for quick action in the rig site. Usually, the loss profile and mud tank level reflect the loss mechanism. Table 2.1 summarizes the typical profiles of loss rate and pit level for different loss mechanisms. In some situations, where the loss occurs due to exposure to rock with high permeability, the loss rate increases gradually with more exposure to the rocks while drilling is proceeding deeper. The onset points on the profile, which reflects the starting of the loss, are shown for each type. The bit-level or mud tanks also vary with the same trend corresponding to the loss rate. The first type shown in Table 2.1 is the loss due to high permeable formations, where the loss continues to increase steadily after the onset point of the loss. After a while, the loss drops with time, suggesting that the loss occurs at the drill bit. The

loss then reduces gradually as the drilling passes the trouble interval. Beda and Carugo (2001) stated that for loss to highly permeable-rocks, the pore size of the rocks should be at least three times more than the size of the mud solids (Beda and Carugo 2001; Lavrov 2016).

Table 2. 1: Loss rate and mud pit level at different loss mechanisms, modified after (Chilingarian and Vorabutr 1981)

| Loss diagnostic | Highly permeable formation | Natural fracture | Cavernous/vugular formation |
|-----------------|----------------------------|------------------|-----------------------------|
| Loss rate | | | |
| Mud bit level | | | |

On the other hand, the loss mechanism in natural fractures depends on the wellbore pressure and the fracture's hydraulic aperture. In addition, the viscosity of the mud, fluid leak-off through the wall of the fractures, and the filter cake evolution inside the fracture also control the loss severity. It is worth mentioning that the fracture's permeability depends highly on fracture width and the mineralization products inside the fracture. For the fracture to be conductive and causes fluid loss, the fracture width needs to be large enough to provide enough permeability. The loss rate can be very high if there is a connected-fractures matrix with significantly high permeability, which can cause severe fluid loss. According to Dyke et al. (1995), natural fractures cause about 76% of the losses at one major operator (Lavrov 2016; Dyke et al. 1995; Kumar et al. 2011). Table 2.2 summarizes different types of lost circulation mechanisms, the typical formation characteristics, loss rate profiles, and preventive or corrective measures.

Table 2. 2: Loss classifications based on mechanisms and formation characteristics

| Loss classification | Typical formations characteristics | Mechanism | Loss rate profile | Preventive/corrective measures |
|---------------------|--|--|--|--|
| Porous scale | <ul style="list-style-type: none"> ▪ Permeability matrix ▪ Sands ▪ Sandstone ▪ Silt | <ul style="list-style-type: none"> ▪ Starts gradually. ▪ Depends on filter cake permeability | <ul style="list-style-type: none"> ▪ Usually seepage loss, less than 10 bbl/hr ▪ If not controlled may become severe loss (10 - 50 bbl/hr) | <ul style="list-style-type: none"> ▪ Manage ECD ▪ Use loss circulation materials (LCM) ▪ Manage drilling parameters and hole cleaning |
| Fracture scale | <ul style="list-style-type: none"> ▪ Natural fractures ▪ Induced fractures ▪ Fracture network | <ul style="list-style-type: none"> ▪ Depends on fractures size and filter cake inside fractures walls | <ul style="list-style-type: none"> ▪ A significant drop in mud height inside the wellbore ▪ Severe loss ▪ May lead to a total loss. | <ul style="list-style-type: none"> ▪ LCM ▪ Wellbore strengthening ▪ Pill and cement plugs |
| Vuges or caverns | <ul style="list-style-type: none"> ▪ Cavernous formations ▪ Large natural fractures | <ul style="list-style-type: none"> ▪ Mud invasions depend on the size of the vugs and conductivity of the surrounding fractures network | <ul style="list-style-type: none"> ▪ Sudden severe or total loss | <ul style="list-style-type: none"> ▪ Particulate LCM ▪ Crosslinked pills ▪ Cement plugs |
| Abnormal pressure | <ul style="list-style-type: none"> ▪ Subsalt formation ▪ Depleted formation ▪ Deepwater | <ul style="list-style-type: none"> ▪ Occurs due to tensile failure in narrow drilling operational windows | <ul style="list-style-type: none"> ▪ Loss has two stages; first, it starts gradually during fracture creation, then increases abruptly with fracture propagation. | <ul style="list-style-type: none"> ▪ Managed pressure drilling (MPD) ▪ Wellbore strengthening |

Moreover, in the drilling operation, the common classifications and general loss circulation mechanism set the base for considering the other factors and lost circulation mechanisms. Basically, the factors affecting loss circulation can be divided into controlled and uncontrolled factors. The controlled factors represent the drilling operational factors that can be optimized within reasonable limits. These factors include the mud type, mud density and rheology, LCM type and concentration, circulation rate, rotary speed, tripping speed, and annulus back pressure if chock valve is available. The uncontrolled parameters represent the reservoir's pre-existing condition, such as temperature, pressure gradients, rock type, porosity, permeability, and natural fracture

sizes. The effect of these factors on mud loss and how to help in loss prevention is explained in detail in section 2.4.

2.2 Review of Applied Solutions in the Field and Current Gaps

Solving lost circulation reduces many drilling potential problems such as hole instability, differential sticking, and well control issues. A major concern in drilling is the immediate detection of lost circulation events and the post anticipation of potential loss areas to apply appropriate preventive or remedial measures. Effective drilling fluid design and proper selection of remedial actions help quickly regain circulation and avoid amplified drilling costs due to increased NPT. The industry's solution techniques can be classified qualitatively into corrective and preventive methods, depending on whether the action is taken before or after the loss.

2.2.1 Corrective and Preventive Treatments

The corrective treatments are defined as any remedial actions taken after the loss occurs. The aim is to quickly stop the loss and regain drilling fluid circulation to avoid drilling problems and reduce NPT. Corrective treatments include adding conventional plugging materials in a single treatment or a blend of one or more LCM types, spudding LCM pills, or cement plugs, depending on the type and severity of the loss.

The common corrective solutions can be grouped into four methods. The first method is called the waiting method. This method is applied when the loss is minor or seepage. After drilling is stopped and a few stands of the drill string is pulled out above the loss zone while monitoring circulation and pressure. If the loss continues to propagate, a conventional LCMs such as sized calcium carbonate, fibrous and flaky materials, or graphite are used to help seal off the loss area (Luzardo et al. 2015b; Ezeakacha and Salehi 2018). The second method is redesigning the drilling fluid by including plugging materials with the proper size or mixture of LCMs to form a low

permeable mud cake. This method is used when the loss is partial to severe. While applying this method, the mud column level inside the well should be maintained to avoid possible kicks or loss of well control. This third method is the spotting of the LCM pill. The pill is intended to create a physical barrier by filling the void in the lost circulation zone by squeezing an extremely thick material or a mixture of LCMs.

The process of applying the pill may utilize an open-ended drill pipe to inject the pill mixture. Then the pressure is maintained to gently squeeze the pill for a period to ensure pill integrity. The pill should be designed to fill and bridge inside the loss structure rapidly. Many rapid-set LCM pills are available in the industry that can quickly react with mud after being spotted inside the loss zone. The formation of a dense, flexible plug inside the fractures helps quickly resume the drilling operations (Sweatman et al. 2004).

The fourth method in the corrective treatment is cement squeeze or plugs, which should be the last resort if the loss was not contained by the previous techniques or in case of sudden severe or total loss. Treating lost circulation with cement squeezing and plugs is irreversible in many cases; however, it has an advantage over the LCM pill because the pill may fail due to the swab and surge effect during drill strings trips in and out of the hole. Therefore the treatment with cement squeeze and plugs are usually applied in non-producing zones where formation damage is not an issue, and loss is extremely severe (Fidan et al. 2004a).

In both the cement squeeze and cement plug approaches, a cement slurry is placed in the thief zone to isolate it completely. However, there are some differences between these two techniques in terms of operational procedures and cost. The cement squeezing is considered to take less time and cost compared to the cement plug. The process restores the drilling fluid circulation by spotting a cement slurry across the loss zone, waiting on cement to cure, then drill

through the plug. The advantage of cement squeezing is that the cement can be injected through the bit to save the time required for pulling out of the well or using a small diameter tubing called the stringer that can be installed below the drill pipes. Low-pressure formation such as depleted reservoirs are good candidate for this treatment (Luzardo et al. 2015a). On the other hand, the cement plug requires more cement volume and is used when large fractures or caving are encountered. A combination of cement squeeze and plug may be necessary in severe cases, mainly when the loss occurs below the casing shoe (Wojtanowicz and Zhou 2001).

The case study reported by Rahmanifard et al. (2014) is a good example showing attempts to solve loss circulation by the methods explained above while drilling a 12 inches section of an exploration well. They first used less density mud and conventional LCM to stop the loss, then pumped LCM pill (110 bbl mica in 20 lb/bbl), which failed due to the loss severity. Eventually, the loss was cured by pumping a 100 bbl cement slurry with concentration of 137 pcf (Rahmanifard et al. 2014).

Over the last decade, techniques and methods of loss prevention have developed significantly. The urge to develop new prevention and proactive treatment techniques comes from the amount of time and cost lost in solving lost circulations and the subsequent instability and well control problems. The field's practice and experience have proven that preventing the loss in the first place is easier and less expensive than curing them (Magzoub et al. 2020a). Moreover, LCMs, in many cases, fail to restore drilling fluid circulation due to extreme downhole conditions, which will lead to tremendous NPT. The goal of preventive or proactive treatment is to reduce the tendency of loss events by taking actions before the loss. This is achieved by either a set of operational techniques such as manipulating drilling parameters or wellbore strengthening methods.

In drilling rig sites, there are many useful practices used to prevent lost circulation. For example, reducing the mud density, using proper solids handling equipment and ensure hole cleaning to maintain the mud density, and minimizing the equivalent circulating density (ECD). Another effective practice used in the rig site is to slowly run-in drill pipes to avoid surge pressure effects that may cause stability problems and lead to lost circulations (Lavrov 2016). Also, gradual starting on mud pump and drilling fluid circulation, which is called break-circulation, after a long period of static condition reduces the risk of lost circulation, especially in deep wells with long open-hole sections. A successful practice is the addition of proper LCMs to the drilling fluids before entering a known loss zone, which has significantly reduced loss tendency and increased the formation fracture gradients in many reported field applications (El-Sayed et al. 2007; Belyakov et al. 2018).

Although these practices are proven effective in preventing lost circulation in many cases, in some situations, the downhole conditions pose more challenges. For instance, narrow operational drilling windows make it very difficult to manipulate the ECD. In such cases, proactive treatment is highly recommended. The most effective proactive treatment is the method of wellbore strengthening, which can be defined as any technique applied to widen the gap between the pore pressure and the formation fracturing pressure by toughening or strengthening the wellbore (Salehi 2012). In the process, the fractures are sealed and plugged while drilling to increase the formation fracturing pressure. This pressure presents the maximum pressure that the formation can withstand before causing the fracture to initiate or propagate, which is the key parameter in loss mitigation.

In general, wellbore strengthening can be applied in many situations where narrow operational windows limit the use of other methods. For example, in deepwater drilling, depleted

reservoirs with varying fracture gradients and highly fractured formations. In addition to the significant benefit of reducing lost events and enhancing well-control, the wellbore strengthening contributes significantly to NPT reduction (Lavrov 2017) during the cementing stage after drilling, as highlighted by the industry. Sealing the natural and induced fractures while drilling contributed to quick and efficient cementing jobs by reducing the loss of cement slurry.

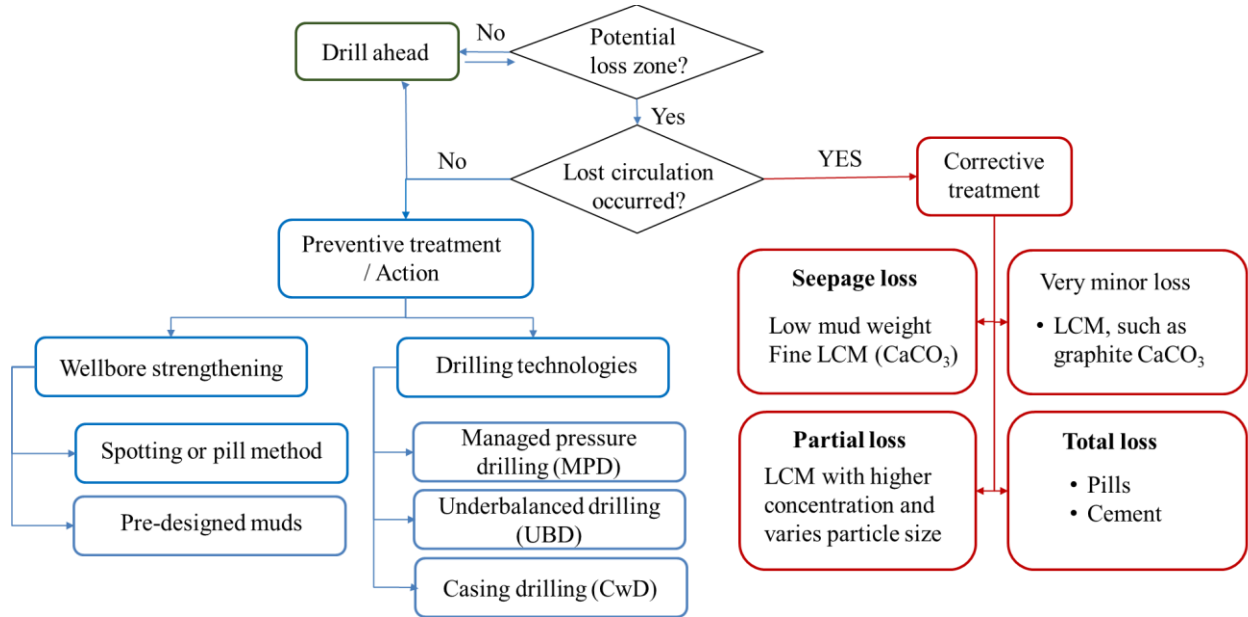


Figure 2. 2: Selection chart of preventive and corrective treatment and methods.

Furthermore, all loss prevention and reduction techniques depend mainly on the drilling fluid and well construction design. Proactive treatment plans should be considered in advance by accurately identifying potential loss intervals, estimating the loss severity, and studying the formations' geological characteristics causing the loss. Therefore, the implementation cycle of wellbore strengthening should start by data collection, knowing the similar loss events from the offset wells, determining fracture dimension, and modeling fracture creation and sealing mechanisms. Based on this information, a proper design of the mud would be prepared in advance.

Several case studies and field deployment experiences reported that a significant enhancement in formation fracturing pressure was achieved, which helped reduce the number of

required casing strings and NPT (Nygaard and Salehi 2011). The various techniques applied in the industry for preventive and corrective measures are summarized in a decision-making flow chart illustrated in Figure 2.2.

2.2.2 Solutions from Drilling Technologies and Techniques

Generally, applied solutions methods can either rely on using plugging materials that are selected and designed based on formation type and loss severity or on drilling technology and techniques, such as casing while drilling (CwD), underbalanced drilling (UBD), and managed pressure drilling (MPD).

Managed pressure drilling (MPD) is one of the most efficient drilling methods used to reduce NPT by reducing the number of unplanned casing strings and safely drill through very narrow operational windows with high lost circulation risk. Unlike UBD, the MPD does not encourage fluids influx into the wellbore. MPD's primary objectives are to mitigate drilling hazards such as lost circulation, stuck pipe, wellbore instability, and well control incidents by increasing operational drilling efficiencies.

According to the definition adopted by the Underbalanced Operations and Managed Pressure Committee (UBD &MPD) of the International Association of Drilling Contractors (IADC), the MPD can be defined as an adaptive and flexible drilling process used to precisely control the pressure profile in the annulus and throughout the wellbore. Overall, the MPD allows quick intervention to react to any observed pressure variation. The MPD can be used in a reactive or proactive approach. In the reactive MPD, the well is planned to be drilled conventionally, and the MPD method and equipment are used as needed when unexpected problems are encountered. On the other hand, in the proactive MPD, the annular pressure profile is actively controlled. The MPD application requires proper personnel training and proper selection of the MPD method to better address the encountered problems.

Recent studies showed that 25 to 33% of all Gulf of Mexico NPT could be reduced using MPD (Malloy 2007), besides several successful cases reported in the literature (Essam et al. 2019; Hollman et al. 2015). The MPD provides a reliable solution to a difficult drilling situation where the driller can navigate through a narrow operational window and avoid many drilling problems and associated costs. However, it is worth mention that these methods are associated with logistics complications. Additional equipment and rig components are required, which may be limited by cost and the rig site area. Moreover, the application may be feasible on offshore wells where seawater is available to be used in the MPD process, unlike onshore wells. Also, proper training is required for the personnel to be familiar with the method and the MPD well control matrix.

Underbalanced drilling (UBD) is one of the earlier drilling techniques used to prevent drilling fluid from causing formation damage and preserve the reservoir for characterization purposes. The Hydrostatic pressure of the mud is intentionally allowed to drop below formation pressure by designing a lighter drilling fluid or adding less dense substances such as air, inert gases, or natural gas. The Influxes from the well are encouraged and controlled by surface containment devices such as rotating control device (RDC), drilling choke manifold (DCM), or multiphase separator (Hannegan 2001). Among the benefits of the UBD that includes, but are not limited to, reduction of formation damage and differential sticking, the UBD is a reliable solution to lost circulation since the hydrostatic pressure is reduced to a level where the loss is not possible.

As an example of UBD application in avoiding lost circulation, the following case studies can be highlighted. Misbah (2010) reported drilling of a horizontal section in Libya. The rock strength properties from core analysis collected from an offset well revealed low formation pressure and high wellbore instability risk. Therefore the UBD was adopted successfully to drill the well to the planned TD of 10767 ft (Misbah 2010). Similarly, 18 UBD horizontal wells have

been drilled in Saih Rawl Field in Oman (Eissa and Al-Harhi 2003). Over the last 40 years, the UBD has been a common practice in the South Texas fields. Reports showed that lost circulation rates were up to 100 gpm; with the help of UBD, the operators successfully mitigated this problem and saved up to \$200,000 in drilling fluid cost only in addition to the reduced NPT (Tangedahl 1996).

This method's shortcoming is due to the many technical limitations, safety and environmental concerns, and the relatively high cost estimated by up to 30 % more than conventional overbalanced drilling (Malloy 2007). The technical limitations include the requirement of additional surface and downhole equipment and skilled operation crew. In addition to the potential wellbore instabilities that resulting from wellbore stress, and high-permeability and fractured reservoir, which is not favorable in UBD due to well control complications (Rehm et al. 2013).

Casing while drilling (CwD) is a technology used to reduce some of the drilling problems associated with open hole exposure time. Reducing the formation exposure time to the mud will reduce lost circulation problems, formation swelling due to filtration, and the NPT by saving casing running time (Pavković et al. 2016; Patel et al. 2019). Besides reducing the open hole exposure time, the casing while drilling has unique filter cake features resulting from plastering or smearing effects. The inherent plastering effect in CwD helps strengthen the wellbore and prevent lost circulations. The plastering effect is caused by the tight clearance between casing and hole, which is usually larger when the drill pipe is used. Karimi et al. (2011) investigated some of the key factors that contributing to the positive effect of CwD on filter cake properties. The authors suggested that the casing to hole diameter ratio be in the range of 0.75 to 0.9, as shown in Figure 2.3. Also, cuttings size with casing drilling was an indicator for successful plastering effect

occurrence; therefore, it is recommended to reduce the length of the drill pipe portion used on top of the non-retrievable casing drilling assembly (Karimi et al. 2011). Naveen and Babu (2014) conducted experiments on the plastering effect on the filter cake properties. The possible reason for the plastering effect was the crushed cuttings in the tight clearance between the casing and wellbore. During drilling, the contact with the filter cake leads to plastering effect and formation of a thin layer but strong enough to prevent mud loss.

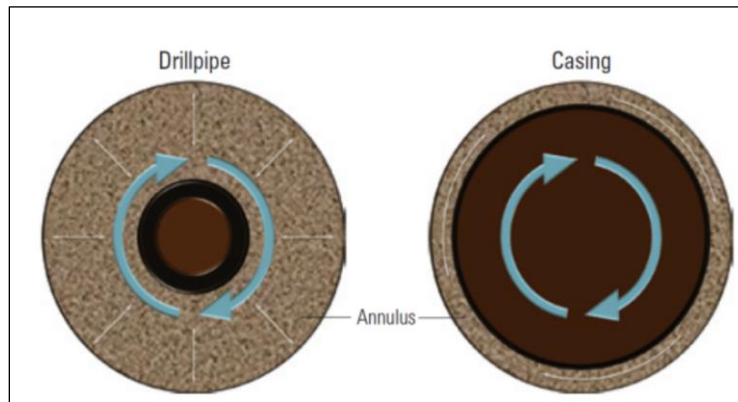


Figure 2. 3: Annular space in regular drilling and casing while drilling contributing to plastering effect (Karimi et al. 2011).

Multiple field case studies documented the significant effect of CwD on enhancing filter cake properties and reducing loss circulation. For example, it was reported that the cutting spearing helped reduce lost circulation in a field in Peru (Lopez Herrera et al. 2010). Also, drilling in a highly permeable section in an oilfield in Colombia was successfully operated without severe loss by understanding the positive effect of filter cake plastering. In addition to several reported cases in Oman (Sánchez and Al-Harthy 2011), Malaysia (Dawson et al. 2010), and Western Australia (Graves and Herrera Gomez 2013), where cutting spearing into the pore hole greatly helped in wellbore strengthening and mud loss prevention. Meza et al. (2017) demonstrated the difference in filter cake properties in conventional drilling and CwD and how it affects lost circulation, especially in weak formations. Their experimental setup was designed to hold a 7” pipe placed eccentrically in a hole with small clearance to touch the wall on the same spot in every rotation.

Figure 2.4a shows the smear and plastering effect on the filter cake cross-sectional view. The mud particles were forced to enter the rock, which helped plug the pores and reduce filtration and filter cake thickness, unlike the filter cake simulated by the conventional drilling shown in Figure 2.4b (Meza et al. 2017).



Figure 2. 4: Cross-sectional view of filter cake during a) conventional drilling and b) casing while drilling (Meza et al. 2017).

2.2.3 Review of LCM Types, Formulations, and Applications

Over the past years, drilling fluids development has offered various smart lost circulation treatments with chemicals and materials designed for specific loss situations and drilling conditions. However, the sealing pressure may become very low if the materials' size and concentration are not appropriately designed. Besides, thermal stability plays a non-negligible factor affecting the performance of LCM. The sealing efficiency depends on the re-opening pressure produced and how quickly the circulation is restored. The following subsections review the available LCM types, including the most recent advance of new smart chemicals. The temperature constraints, the recommended concentrations, and the range of particle size distribution are summarized.

There are many LCMs available for lost circulation treatment and wellbore strengthening. Proper selection of LCM type among various available options requires careful consideration for

formation characteristics, filtration mechanisms, and downhole conditions. In general, LCM should provide sufficient mechanical strength to resist stress from drilling operation and wellbore pressure (Salehi 2012). The LCM should also adapt to downhole environments such as temperature and geochemical attributes (Cook et al. 2016). The LCMs can be classified on many bases; the most used classification is based on the appearance. They are classified as granular, flaky, and fibrous materials, or a blend of two or more (Alsaba et al. 2014). Another classification is based on the treatment method, corrective or preventive treatment, as bridging materials for wellbore strengthening or pills and plugging materials.

Granular LCMs are the most used additives with drilling fluids for lost circulation prevention and treatment. Granular LCMs include organic clay, perlite, calcium carbonate, walnuts, graphite, and gilsonite. The common characteristics of this type of LCM are the wide range of particle size distribution, the large surface area, and resistance to crushing forces. The last property is what makes them a good candidate for wellbore strengthening application. Bridging theories and many researchers have emphasized on the significance of particle size and high hardness provided by the granular LCMs (Lee and Dahi Taleghani 2020).

Flaky and fibrous materials are also important for adequate bridging and sealing of loss zones. The coarse bridging materials lodge into fractures opening, while the fine particles seal the voids in the bridge (Gatlin and Nemir 1961). Flaky materials and fibrous materials are widely used in corrective and preventive treatments due to their flexibility, flat shape, and various sizes. Although most of the flaky and fibrous types of LCM are known to have little or no mechanical strength, they can form mat-like bridges over the face of the permeable formation, which reduces filter cake permeability (Howard and Scott Jr 1951). Using LCM may have some limitations in OBM due to suspension capacity and in drill-in fluids due to formation damage considerations.

More options of LCMs are available to overcome this limitation, such as acid/water-soluble LCMs, which are easy to be removed after drilling by washing and acid treatments (Alsaba et al. 2014). Some downhole conditions and complex situations of lost circulation require using blends of two or more types of LCMs. Several studies revealed that using LCMs mixture increases sealing efficiency to cover a wide range of pore throat sizes and fractures (Al-saba et al. 2014b).

Recent studies were conducted on smart LCMs such as nanoparticles (NP), encapsulated downhole mixed pills, and shape memory polymers (SMP). Mansour et al. (2019) used SMP that can be activated by downhole temperature to restore predesigned shape to seal large fractures (Mansour et al. 2019). NPs are engineered materials in the range of 1–100 nm; they have distinctive properties under a wide range of operating conditions.

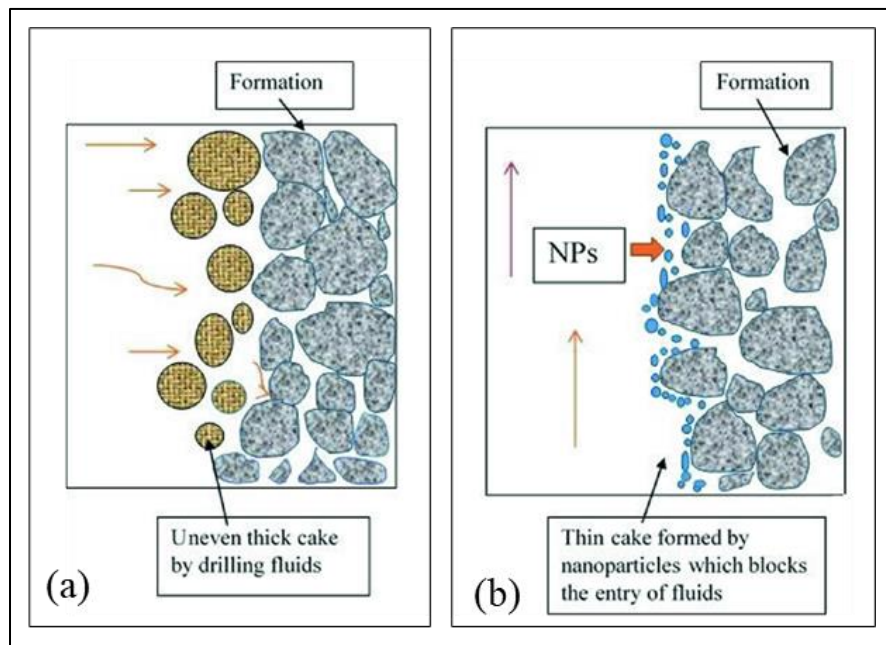


Figure 2. 5: A schematic representation of mud losses while drilling in the case of (a) typical LCM and (b) NPs (Modified from Borisov et al. 2015).

A successful field application reported by Borisov et al. (2015) showed that nanoparticle-based invert emulsion drilling fluids can significantly reduce fluid loss and create a thinner filter cake compared to fluids containing LCMs alone (Borisov et al. 2015). Due to their superior

properties, NP can fill the gaps between the micron-sized particles, which leads to lower permeability and decreased filtrate flux (Figure 2.5) (Seetharaman and Sangwai 2020).

Moreover, synthetic polymers and polymeric gels are used to enhance filtration control and provide higher thermal stability. Most crosslinked polymers used for conformance control in water shutoff applications can be used for fluid loss prevention and wellbore strengthening. In this study, a crosslinked polymer comprising PAM and PEI that can be used in temperatures above 130°C (266°F) were developed. The crosslinked polymers successfully sealed fracture and permeable cores with high sealing pressure up to 1000 psi. Comparing the crosslinked polymer with a conventional LCM formulated by calcium carbonate (55 lb/bbl) and cedar fiber (10 lb/bbl), the crosslinked polymer reduced the mud loss by 80% at 130°C (266°F). Table 2.3 summarizes the broad types and their applications. Information on the table is summarized from (Alsaba et al. 2014; Rafati et al. 2018; Hamza et al. 2019; Mansour et al. 2017).

Table 2. 3: Broad types of LCM and their applications

| Classification | Description | Examples | Application |
|----------------|--|---|--|
| Granular | Variable sizes High crushing resistance\ | Sized calcium carbonate, walnut, nutshell, sized ground marble, | Wellbore strengthening Bridging materials |
| Flaky | Thin flat shape Large surface area No degree of stiffness | Cellophane Cottonseed hulls Mica, corn cobs | Seal permeable formation phase Seal voids may exist in bridging materials Concentrated pills |
| Fibrous | Longs and flexible Various sizes May have a little degree of stiffness | Cedar fiber, nylon fiber, mineral fibers, sawdust, shredded paper, and natural cellulose fiber. | Corrective treatment in seepage loss Preventive treatment Concentrated pills in severe loss |
| Blends of LCMs | Blends of LCM with different sizes and strength | Blends of granular, fibrous, flaky, or enforcing materials such as nanoparticles | Preventive and corrective treatments Wellbore strengthening |
| Nanoparticles | High surface to volume ratio High thermal stability | Silicon Nanoparticles Iron Hydroxide NP copper oxide <i>nanoparticles</i> Calcium Carbonate NP | Reduce filtration Reduce pipe sticking Mitigate formation hydration |

| | | | |
|---------------|---|--|--|
| Polymeric gel | Crosslinked polymers with controlled gelation time | Polyacrylamide crosslinked with polyethyleneimine, aluminum acetate, chromium acetate, or chitosan | Polymeric gel Pills wellbore strengthening |
| Smart LCM | Swellable/Hydratable LCMs combinations Shape programable Encapsulated pills | Shape memory polymers Swellable clays Encapsulated crosslinkable polymers | Preventive and corrective treatments in deepwater wells, HPHT wells, and reactive formation. |

2.2.3.1 Temperature Constraints

Downhole conditions such as temperature and pressure are considered pre-existing factors that must be considered in selecting the proper LCM for designing drilling fluids. In such situations, lost circulation becomes more complicated, especially in large fractures (Saleh et al. 2020). The constraints in selecting effective LCMs stem from the fact that most of the conventional LCMs fail to seal at high temperatures (Lee and Taleghani 2020). Conventional filtration control materials and inhibitors do not function at high temperatures. Materials such as organic or cellulosic substances exhibit high degradation under high-temperature environments. In addition to degradation, mud flocculation occurs at high temperature, causing a negative impact on filtration control and LCM effectiveness. Besides, the high temperature limits the functionality of the commonly used chemical deflocculant. The flocculation tendency increases at high temperatures due to the high alkalinity caused by contamination from formation fluids. In ultra-high temperature formation, the best option is to use thermoset rubbers, ground coal, and mineral fibers. Some researchers suggested adding temperature resistant materials to the drilling fluids such as strata-wool and mineral fibers (Loeppke 1986; Salih and Bilgesu 2017).

A study conducted by Cole et al. (2017) on the lost circulation events occurred in 38 geothermal wells drilled between 2009-2017 in the U.S. provided insight into the challenges faced in high downhole temperature. The study revealed that field treatments were 71%, 69%, and 84% for the seepage, partial, and total loss, respectively. The failure was due to the high temperature

and its impact on the LCM and the base fluid, in addition to the depth and length of the loss intervals (Cole et al. 2017).

Good rheology is essential to maintain the LCM suspension at high temperatures. Deterioration of rheological properties imposes constraints on the LCMs concentration and size. Various thickening agents are added to the drilling fluid to provide the required rheological properties, such as xanthan gum and sepiolite. However, not all these chemicals or clays can function at high temperatures. Echt and Plank (2019) tested the carrying capacity of sepiolite and xanthan gum in the water-based fluids at a temperature ranging from 80°C to 150°C (176°F to 302°F). Results showed that unlike xanthan gum, the sepiolite exhibited excellent suspension up to 150°C (302°F), as shown in Figure 2.6 (Echt and Plank 2019).

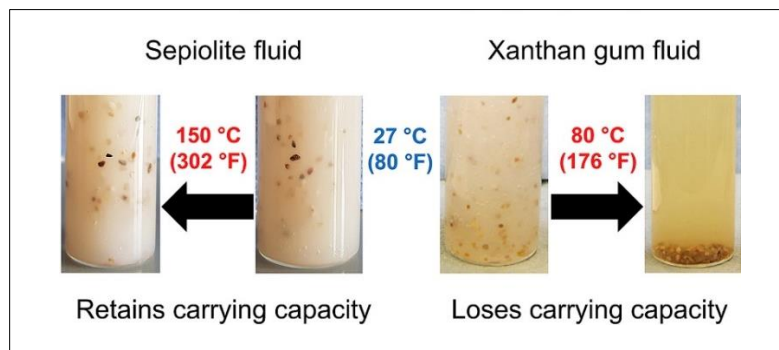


Figure 2. 6: Effect of high temperature on carrying capacity of drilling fluid (Echt and Plank 2019).

Several studies suggested using crosslinked polymers for treating lost circulation at HTHP since crosslinked polymeric gels have high thermal stability. Metcalf et al. (2011) formulated a crosslinked polymer system to solve loss circulation problems encountered in the Permian Basin of West Texas. Their formulation contained a mixture of polymer, LCM, and silicate particles. The field trial showed a 60% reduction in the fluid loss within 9 to 12 hrs., and total circulation was regained in 18 to 24 hrs. In another study, Jian et al. (2019) used crosslinked polymers with an extended gelation time to cure loss at 150°C (300°F) with high sealing pressure up to 1430 psi.

Another factor affecting mud loss is the rotational speed. Studies revealed that it has a significant effect on dynamic filtration in combination with other factors. Ezeakacha and Salehi (2019) conducted an experimental study to characterize the dynamic filtration in permeable cores at a rotational speed varying from 30 rpm to 110 rpm and temperature range from 120 to 240°F (48°C to 115°C). The results showed that LCM concentration and temperature greatly influence the filtration, as shown in Figure 2.7. The notation A, B, and C in the figure refer to LCM concentration, rotary speed, and temperature, respectively. The subscripts 1 and 2 refer to the low and high property level used as boundaries for the sensitivity analysis, as shown in Table 2.4. An interesting finding out of this study is that increasing the temperature from 120°F to 220°F (48°C to 115°C) showed a significant impact on dynamic mud filtration, diminishing the increase of LCM concentration from 30 lb/bbl to 80 lb/bbl. The filtration increased by 23% at elevated temperatures (Ezeakacha and Salehi 2019b).

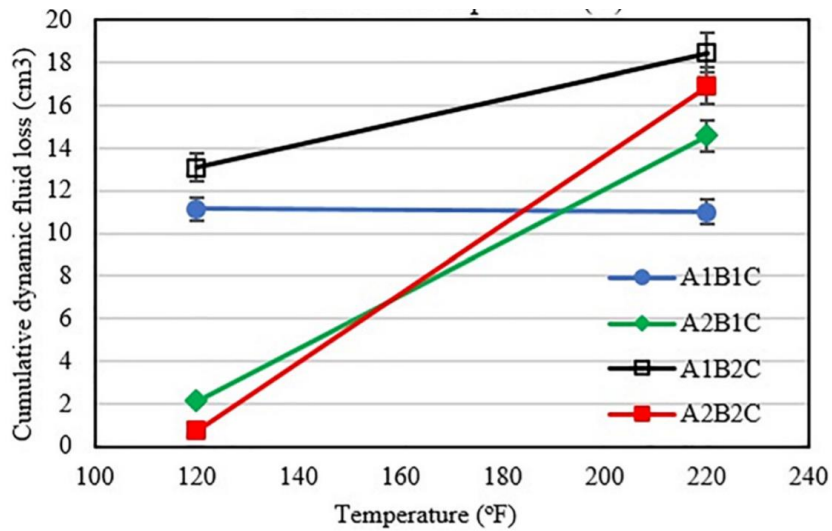


Figure 2. 7: Effect of temperature with LCM concentration on dynamic filtration (Ezeakacha and Salehi 2019b).

Table 2. 4: Boundaries for sensitivity analysis of the three factors affecting mud loss (Ezeakacha and Salehi 2019b)

| Factors | Notation | Low level | High level |
|-------------------|----------|-----------|------------|
| LCM concentration | A | 30 lb/bbl | 80 lb/bbl |

| | | | |
|--------------|---|--------|---------|
| Rotary speed | B | 30 rpm | 110 rpm |
| Temperature | C | 120°F | 220°F |

In conclusion, based on several studies (Wenjun et al. 2014; Thaemlitz et al. 1999; Fink 2015), the following factors should be considered in selecting LCM for high-temperature applications:

1. High thermal stability to avoid degradation and rheology deterioration.
2. Resistance to pollutants such as salts and chemicals, and formation fluids.
3. Environmental impact.

2.2.3.2 *Recommended Particle Size Distribution*

According to API RP 13B-1 (2020); API RP 13B-2 (2018), the LCM should have specific characteristics. For instance, too small particles will pass the fractures and fail to bridge on fracture mouth. Similarly, too large particles will not be able to get into the fracture and seal it. Therefore, proper size distribution is essential for fast and adequate sealing. The theory behind particles' effect was first introduced by Andreasen and Anderson (1930) in what is known as the ideal packing theory (IPT). The IPT refers to the full range of particle size required to seal all voids, including the voids formed during the bridging process. The cumulative filtration fluid (Cum Vol%) is proportional to the particle size diameter by Equation 2.22.

$$Cum Vol\% \propto d^x \dots\dots\dots (2.22)$$

Where x is related to particle size distribution; $x = 1$ when particles are evenly distributed, $x < 1$ when particle distribution is shifted towards the smaller size, and $x > 1$ when the larger size is dominating the distribution.

Abrams' rule suggests the mean particle size of the bridging particles to be equal or slightly greater than 1/3 of the average pore size of the filtration medium. For example, the rule suggests

that for 150 µm porous, the bridging particles should be having a medium particle size of 50 µm (Abrams 1977). More specification to the suitable particle size for an enhanced sealing efficacy was proposed by Vickers et al. (2006), as shown in Table 2.6.

Table 2. 5: Recommended particle size specification with respect to the pore throat size (Vickers and Elkin 2006)

| Particle size of volume % | Recommended specification related to the average size of the pore throat |
|---------------------------|--|
| D90 | Equal to the maximum pore throat |
| D75 | Less than 2/3 of the largest pore throat |
| D50 | Larger or equal to the 1/3 of the mean pore throat |
| D25 | Equal to 1/7 of the mean pore throat |
| D10 | Larger than the smallest pore throat |

The importance of particle size distribution on improving LCM performance to enhance sealing efficiency was emphasized by many researchers (Al-saba et al. 2014a; Aadnøy and Belayneh 2004; Bao et al. 2019; Ezeakacha and Salehi 2019b). Ezeakacha and Salehi (2019) studied different concentrations of LCM and observed a significant effect of particle size and concentration on the dynamic mud loss; however, it could not mask the negative effect of high temperature as discussed in the above section (Ezeakacha and Salehi 2019b). Al-Saba et al. (2014) used slotted discs with different sizes of aperture and fracture tips to evaluate the LCM performance. Based on the results, the authors suggested using blends with a wide range of particles to reduce a fluid loss (Al-saba et al. 2014a). Aadony and Belayneh (2014) emphasized the importance of the wide distribution of particle size in the LCM. The larger particles form the bridge on the fracture mouth, and the smaller particles fill the gaps and stop fluid loss through the bridged particles. Kageson-Loe et al. (2009) demonstrated that for articulated LCM, the finer particles are also crucial for plugging and bridging on fracture opening. As shown in Figure 2.8, the mixture of large and fine particles is necessary to create a tight filter cake and to reduce the fluid leak-off through the fracture walls.

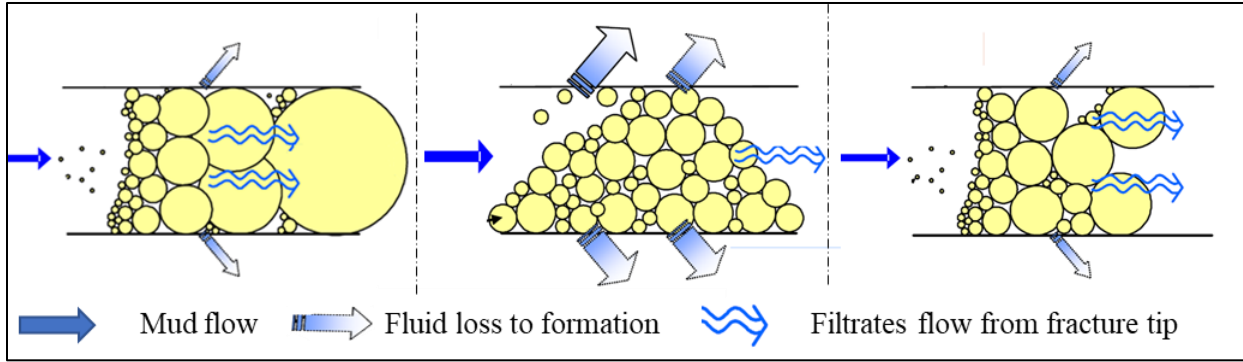
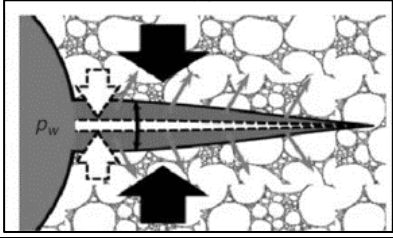
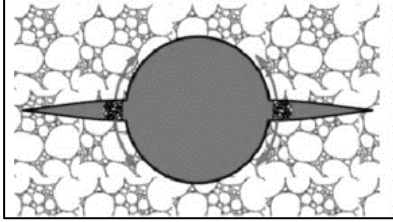
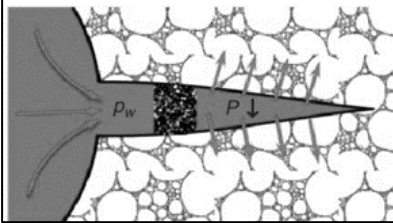
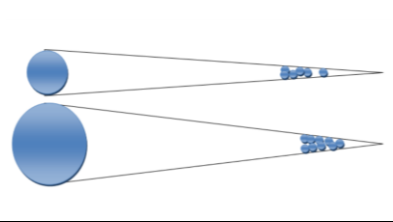


Figure 2. 8: Illustration of the significance of fine and coarse particles on LCM performance (Kageson-Loe et al. 2009).

The LCM particle size also influences the plastering effect, which is important for wellbore strengthening. He et al. (2018) conducted several HPHT filtrations experiments on 16 cores and then used the Brazilian test to quantify rock specimens' strength after the filtration test. Based on the analysis, the particle size distribution was a major factor in wellbore strengthening measurements. The author suggested the D50 of the particles be equal to the mean pore throat size to get the maximum benefit of the plastering effect.

From the above discussion, a proper particle size selection for LCM treatment is crucial. However, according to Dupriest (2005), particle size selection is relatively unimportant when the lost circulation is treated using heavy pills because the sealing mechanism depends on the concentration of heavy, immobile mass that fills and plugs the voids. The author also recommended that particles less than 100 μm be used only for matrix seepage, not for severe loss or fracture treatment. For the pill application, particles of 400 μm showed better performance. Table 2.6 summarizes the importance of particle size selection based on different studies on wellbore strengthening modeling.

Table 2. 6: Importance of particle size in different models of wellbore strengthening (Dupriest 2005)

| Wellbore strengthening model | Strengthening theory | Significance of particle size | Illustration | Author s |
|---------------------------------------|--|-------------------------------|--|----------------------------|
| Fracture Closure Stress (FCS) | Fluid invade the fracture Isolated fracture tip and increases closure stress | Not important |  | (Dupriest 2005) |
| Stress Cage (SC) | The LCM strength support and prop the fracture at the fracture opening. Tangential stress around the wellbore increases | Important |  | (Alberty and McLean 2004a) |
| Fracture Propagation Resistance (FPR) | Fluid not required to invade the fracture Fracture tip is isolated | Important |  | (Mehrabian et al. 2015) |
| 3D poroelastic models | Restoring hoop stress is the main mechanism during fracture sealing. A change in particle size appears to be necessary to seal different sizes of crack mouth Same size particles for sealing the crack tips | Important |  | (Salehi 2012) |

2.3 Implications of Mud Loss and Operational Challenges

2.3.1 Chemical and Geochemical Challenges

Chemical factors refer to the mud's chemical composition, such as LCM and rheology additives, while geochemical factors refer to the formation rock's type and composition. The drilling fluid's ability to stop and prevent mud loss highly depends on the chemical and geochemical factors and the interaction between them. This section summarizes the impact of each of these factors on mud loss.

The chemical influencing factors can be broadly grouped into three aspects, the mud type, the type of rheology additives, and most importantly, the type of bridging materials used for

filtration control. The water-based mud (WBM), oil-based mud (OBM), and aerated mud are the common classifications of mud type. The general composition of OBM is illustrated in Figure 2.9a, in weight percent, excluding weighting agents. OBM consists of 25 to 75 wt.% of aqueous-brine fluids, while the oil phase is dispersed within the aqueous brine phase. Offshore OBM generally contains high saline calcium chloride solution, about 30 wt.%. The filtration control additives in OBM may contain asphalt and gilsonite, and amine clays or lignite products. The WBM, on the other hand, composes of sodium or potassium brine as a continuous phase. The generalized composition is illustrated in Figure 2.9b, showing the typical formulation for onshore and offshore applications. For offshore applications, the WBM usually contains special polymeric additives to control swelling of clays and geochemical complications (Wenger et al. 2004).

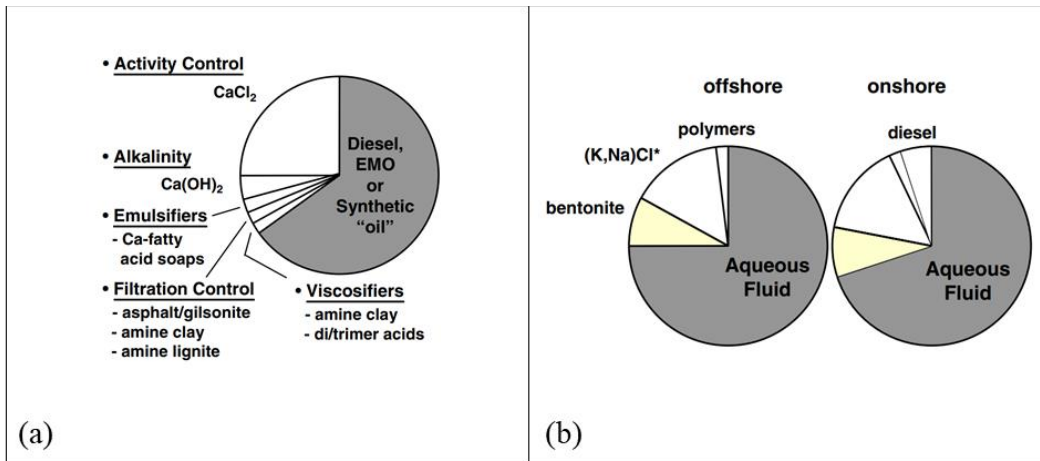


Figure 2. 9: Typical composition of a) OBM and b) WBM, excluding weighting agents (Wenger et al. 2004).

In addition to this broad classification, Zaba and Lyons (1996) summarized the base fluid used for mud formation into fresh-water, inhibited that suppress clay hydration, low-solids, emulsified, and oil-based mud (Zaba and Lyons 1996). The fresh-water muds have pH ranges from 7 to 9.5, and several additives are used, such as clays, dispersants, and organic polymers. The filtration control in this type of mud is based on the rheology and conventional LCMs. The inhibited mud is used to suppress the reactive clays by preventing hydration caused by the mud

filtrate invasion. Examples of these muds are lime, seawater, and gypsum muds (Zaba and Lyons 1996). Many reports from literature show variations in loss control capabilities depending on the mud type. For instance, the OBM usually performs better than WBM, especially at HPHT applications due to the higher thermal stability, in addition, better filtration control performance can be obtained by using the inverted emulsion drilling fluids (Abduo et al. 2016).

Other influencing parameters, such as mud pH and mud and filtrates alkalinity, are essential for colloidal particles such as bentonite to form a compressible filter cake. Hydration of bentonite can significantly diminish the effectiveness of its filtration control. Therefore, some chemicals, such as caustic soda, are added to prehydrate bentonite in freshwater to improve its fluid loss characteristics (Johannes 2012). Additionally, thinners or dispersants are added to enhance fluid-loss control and reduce filter cake thickness by plugging the tiny openings in the filter cake (Darley and Gray 1988a). For example, lignosulfonate is known for enhancing rheology at high temperatures and therefore reduces fluid loss. Ghazali et al. (2018) synthesized A biopolymer tannin-lignosulfonate and used it as a deflocculant to reduce mud gelation at high temperatures. Figure 2.10 shows the enhancement in clay dispersion when deflocculant is used, which prevents the attraction of particles with different charges.

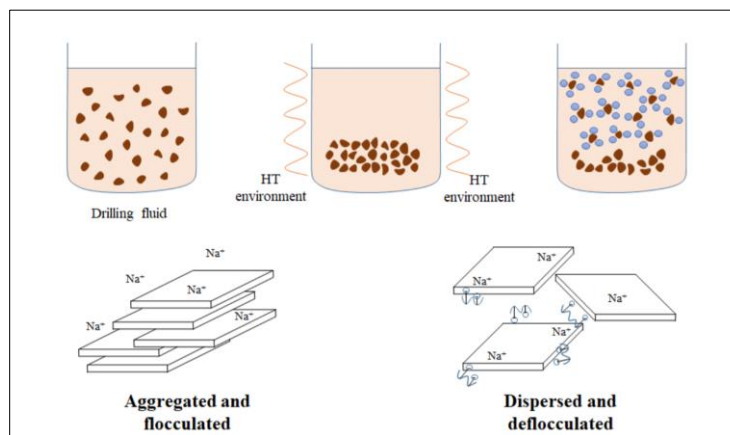


Figure 2. 10: Effect of deflocculant on clay dispersion (Ghazali et al. 2018).

Fluid loss additives or bridging agents can be classified based on a chemical perspective as inert and non-inert particles. The common bridging agents include sized calcium carbonate, mica, nutshell, and fiber (Munoz Jr and Todd 2006). The reaction of non-inert additives with drilling fluid components and formation ions affects the wellbore's fluid properties and stability. For example, when starch is added to a drilling fluid containing chemically bonded ceramic particulates, the starch hydrates into a colloidal suspension, causing fluid gelation and affecting its loss control properties.

The geomechanical factors, on the other hand, are beyond control. It involves lithology and mineral composition, which are considered one of the pre-existing conditions that cannot be controlled. The industry has realized that the mud design and evaluation of dynamic mud filtration should incorporate geochemical factors for good loss circulation prevention practice. Also, the real-time performance of the drilling fluid depends on the geochemical properties of the drilled formation. Therefore, chemical tests should be conducted on the mud and filtrate to monitor any contamination from formation fluids that can affect its performance. The analysis includes various measurements such as alkalinity, lime content, total hardness, methylene blue test, H₂S content, electrical stability, and water activity (Darley and Gray 1988b).

Statistics showed that most lost circulation events occur in permeable sand and induced fractures, particularly in shale formations. Wellbore strengthening can enhance fracture opening and propagation pressure and filter cake plastering to prevent lost circulation (Contreras et al. 2014; Nwaoji 2012; Salehi 2012). The proper design of LCMs particle size helps avoid leaks of mud and enhances fractures propagation resistance. However, the interaction of mud chemicals with rocks and formation fluids may significantly reduce the treatment's effectiveness (Fuh et al. 1992).

Several studies revealed that rock type and lithology significantly affect dynamic mud filtration (Ezeakacha et al. 2017; Ezeakacha et al. 2018; Wenger et al. 2004; Deuel Jr and Holliday 1998). Ezeakacha and Salehi (2018) investigated the impact of rock type and lithology on WBM filtration characteristics. The authors used dynamic HPHT filtration tests to evaluate LCMs performance in different rock types, including Upper Gray sandstone, Michigan sandstone, Indiana limestone, and Austin chalk. The dynamic filtration tests revealed that lithology complexities had a significant impact on the affecting factors of mud loss, such as LCM concentrations. For example, the Upper Grey sandstone exhibited a delayed invasion time and lower filtration profile than the Michigan sandstone, as shown in Figure 2.11 (Ezeakacha et al. 2018).

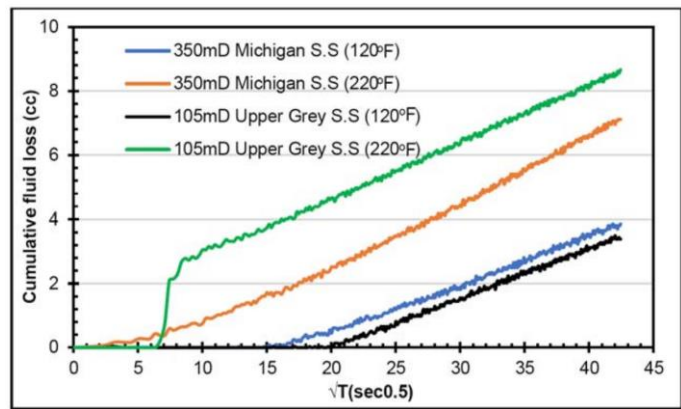


Figure 2. 11: Effect of rock type on dynamic filtration (Ezeakacha et al. 2018).

In another study, Ezeakacha et al. (2017) demonstrated the effect of lithology on mud filtrations and filter cake plastering. The authors studied various mud filtration affecting factors, including permeability and rock mineralogy. The study disclosed that studying dynamic filtration using standard ceramic discs only considering permeability variations is misleading and does not reflect the actual filtration mechanism. Figure 2.12 summarizes their dynamic filtration test on cylindrical cores from Austin chalk and limestone. The accumulative filtration and filtration rate were greatly depending on the type of rock (Ezeakacha, Salehi, and Bi 2017).

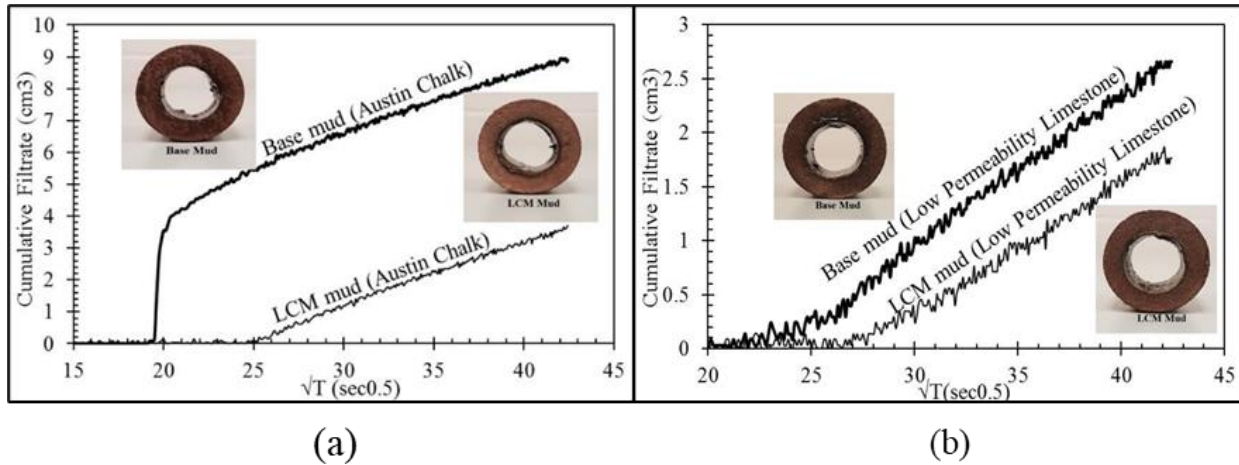


Figure 2. 12: Dynamic filtration using cylindrical cores from a) Austin chalk and b) limestone (Ezeakacha, Salehi, and Bi 2017).

One of the significant concerns in treating loss circulation is the formation damage caused by the LCM and how it varies with different rock types. Salehi et al. (2015) conducted an experimental study to investigate rock type implications on filtration profiles and formation damage. Different formations were tested, including Bandera Brown, Berea Buff, and Michigan sandstone. The mud filtrations results showed that Michigan sandstone exhibited the highest loss, more than 100% higher than Bandera Brown. The bridging particles used in the drilling fluids were visible in the SEM images taken after the filtration test, as shown in Michigan cores in Figure 2.13.

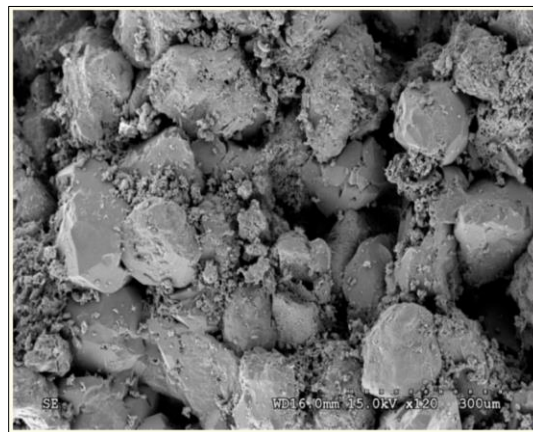


Figure 2. 13: SEM of Michigan core after the filtration test (Salehi et al. 2015).

2.3.2 Thermal and In-situ Stresses Complications Impacting Mud Loss

Lost circulation to fractures is usually the worst to face during drilling. Successful treatment should enhance the near-wellbore hoop-stress and prevent fracture propagation. However, sometimes due to many complications, even a good designed and implemented wellbore strengthening fails to achieve decent fracture gradient improvement. In the beginning, the subsurface rocks before drilling are under a balanced stress condition; such equilibrium is disturbed when a wellbore is created. Drilling alters the stress distribution in the localized area around the wellbore. The absence of rock leads to a redistribution of stress around the borehole. Near-wellbore regions could fail if the stress concentration exceeds the rock's strength (Kang et al. 2009). These stresses can cause micro-fractures, which can propagate and grow if not stabilized and sealed through mechanical wellbore stabilization. Instability may be caused by excessive stress, physicochemical effects, or a combination of both factors, resulting in the failure of the borehole in tension that appears in the form of induced fractures (Darley and Gray 1988b). It is crucial to distinguish these types of induced fractures from the natural ones.

The induced fractures are caused by drilling processes and in-situ conditions resulting from the stress concentrations around the wellbore. They are expected to be confined to a specific part of the borehole wall. This will allow it to have only local penetration near the wellbore that does not help in assisting reservoir drainage since they are likely not connected to reservoir permeability networks. Natural fractures generally transect the entire borehole at arbitrary orientations and sometimes act as the primary reservoir permeability network and likely to contribute to hydrocarbon production; therefore, it is vital to distinguish between those fractures correctly.

Fracture-initiation pressure (FIP) and fracture-propagation pressure (FPP) are essential parameters for preventing and mitigating lost circulation. Overburden stress gradient, formation pore pressure gradient, and Poisson's ratio of rocks are evidenced to be the independent variables

that control fracture pressure gradient (Eaton 1969). For significant fluid loss to occur, a fracture must initiate on an intact wellbore or reopen on a wellbore with pre-existing fractures and then propagate into the far-field region. Wellbore-strengthening operations are designed to increase one or both two pressures (FIP and FPP) to combat lost circulation.

The stress concentration in the near-wellbore vicinity is dominated by the mud density or the equivalent circulating density (ECD), which determines the magnitude of the supporting pressure provided by the static or dynamic fluid pressure during the drilling operation, which helps hole stability. However, this pressure also affects how rapidly fluid pressure penetrates the wellbore wall. In the absence of an efficient filter cake, such as in fractured formations, a rise in a bottom hole pressure may be detrimental to stability. It can also increase differential sticking risk (Pašić et al. 2007).

2.3.3 Wellbore Strengthening

To stop or prevent lost circulation, the wellbore should be protected from fractures initiation or propagation. For that reason, wellbore strengthening techniques enhance the wellbore hoop stress or increase the formation's resistance to fracture propagation. Generally, there are two common hypotheses of how a wellbore can be strengthened: increasing wellbore hoop stress when fractures are sealed. The other is by enhancing fracture propagation pressure by fracture tip isolation with proper LCM (Salehi 2012). The commonly used physical models for wellbore strengthening are the stress cage, fracture closure stress (FCS), and fracture propagation resistance (FPR).

The stress cage models assume fracture bridging occurs close to the wellbore, and fluid filtrates from the fracture walls into the formation. The increase in hoop stress in the stress cage model is assumed due to the compressive forces transferred to the bridging particles at the fracture mouth (Alberty and McLean 2004a). In the FCS model, the fracture must be initiated first, then

bridging particles forced into the fracture. The low permeable plug formed by particles bridging will isolate the fracture tip from wellbore pressure. The fracture tip isolation and increased fracture closure stress will prevent the fracture from reopening (Dupriest 2005). The FPR model, instead of increasing hoop stress, aims to increase the resistance to fracture propagation. This is attained by evaluation of mud cake inside the fracture. A sufficient mud cake built inside the fracture will isolate the tip and prevent further propagation (Morita et al. 1996).

There are several available numerical models for wellbore strengthening to simulate lost circulation due to fracture propagation. However, most of these models assume linear rock elasticity and fail to consider porous features of the formation; therefore, the effect of fluid flow and pore pressure are not considered. (Alberty and McLean 2004b). Salehi (2012) introduced a new numerical three-dimensional model to solve three-dimensional poroelastic models and identifies potential loss zones. Figure 3.9 illustrates the common hypothesis of improving wellbore strength (Mehrabian et al., 2015).

2.3.4 Thermal Complications Affecting Mud Loss

Drilling in HPHT reservoirs or deep water often involves thermal complications that jeopardize fluid loss control. Wellbore strengthening works to enhance hoop stress by propping and plugging natural and induced fractures to prevent its propagation. But thermal stress around the fractures can diminish the hoop stress achieved by the wellbore strengthening effect. When cold mud flows into hot rocks, the large temperature differences between the fluid and the wellbore surrounding rocks alters the state of stress around the natural or drilling-induced fracture. The exposure of surrounding rocks to the cold mud lowers the borehole breakdown pressure (Choi and Tan 1998; Morita et al. 1990)

The study of the rocks' non-isothermal geomechanical properties is usually based on the thermo-poroelasticity, which combines the heat transfer equation with the poroelasticity equations.

Chen and Ewy (2005) used the thermo-poroelastic theory to build a sensitivity analysis model to study the effect of thermal stress on wellbore stability. Their conclusion demonstrated that heat transfer between the wellbore and surrounding rocks decreases the effective hoop stress and reduces fracture gradient. The pore pressure will also change because the coefficient of pore fluid is much larger than the coefficient of formation rocks, particularly in low permeable formations. The difference in the coefficient of thermal expansion of the formation rock and the pore fluids can alter the near-wellbore stresses. This will lead to a thermal-induced deformation of the borehole and the surrounding rocks (Stephansson et al. 2004).

Field reports showed that thermal complications due to temperature variations are essential to be considered in fracture propagation evaluation. Such consideration enhances the wellbore strengthening strategy by considering the thermal impact on different loss prevention methods. Numerous analytical and numerical modeling models are available for analyzing induced thermal stress for a non-isothermal wellbore strengthening evaluation.

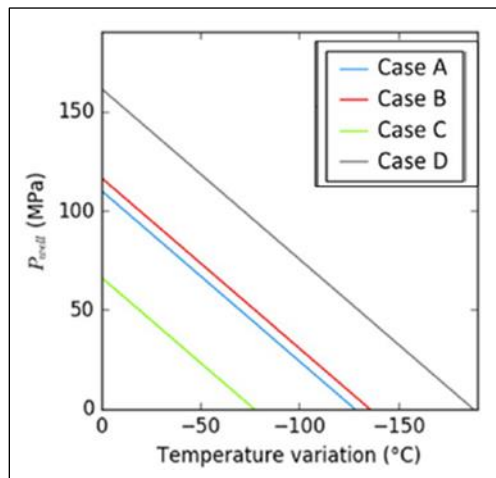


Figure 2. 14: Effect of temperature variations on failure pressure (Peter-Borie et al. 2018).

Peter-Borie et al. (2018) studied the cooling effect on geothermal wells and found that temperature variations resulted in tensile failure in all studied cases. Figure 3.14 shows the

summary of the studied cases and the reduction in failure pressure with respect to the temperature difference between the mud and the surrounding rocks (Peter-Borie et al. 2018).

Finally, many reports from the literature showed that lost circulation events occurred while drilling for no obvious reason related to problematic zone or changes in operational parameters. For example, four deepwater wells in the Gulf of Mexico suffered repetitive loss circulation incidents, and the only possible reason was the significant reduction in mud temperature below formation temperature. Figure 2.15 shows the case on one of these wells, where a clear correlation between mud temperature logs and the record of encountered lost circulation despite the low ECD (Gonzalez et al. 2004).

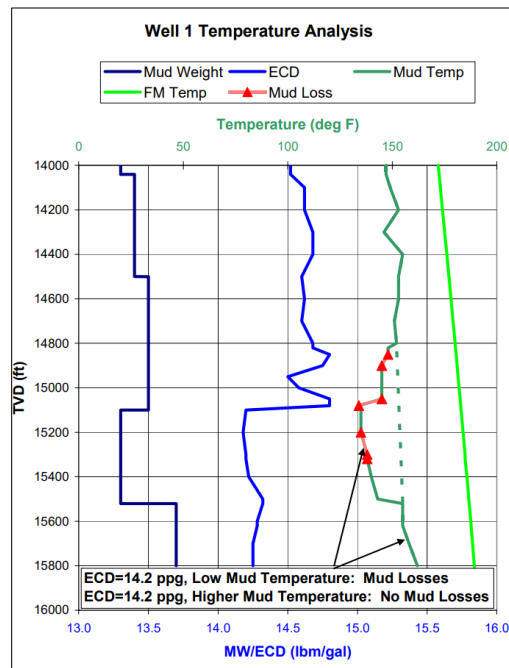


Figure 2. 15: Correlation between mud loss and drop in mud temperature in a deepwater well in the GoM (Gonzalez et al. 2004).

2.4 Effect of Operational Factors on Mud Loss

Operational factors such as rotary speed, mud rate, wellbore geometry, hydrostatic, and bottom hole pressure are the most affecting factors on dynamic mud filtration. From a quantitative

perspective, most of the lost circulation occurs during the well's dynamic state, specifically through drilling-induced fractures (Howard and Scott 1951; Allen et al. 1991; Magzoub et al. 2020a). Among factors affecting mud loss, there are preexisting factors beyond control, and there are factors that we can design and control to prevent or cure loss circulations. The suitable mud formulation and proper drilling operation design are the keys to better loss prevention and lost circulation management. The following sections highlight the effect of the important operational factors on mud loss.

2.4.1 Effect of Mud Rheology on Mud Loss

Rheology of the mud plays a significant role in defining the filtration properties and overall mud efficiency. Rheology's significance is observed on various filtration affecting parameters, such as the fluid capacity to carry LCMs, flow characteristics of fluid invasion into the formation, mud hydraulics, and ECD. Besides, rheology of mud affects rock fracturing, fluid-rock-interaction, and hole cleaning, which directly affects mud density and borehole stability (Khodja et al. 2010; Bohlooli and de Pater 2006).

In the absence of large natural fractures or abnormally pressurized zones, loss prevention is manageable by merely optimizing mud properties and rheology. Drilling operators pay great attention to designing and sustaining good rheological properties to avoid high ECD and fluid loss (Wastu et al. 2019; Igwilo et al. 2019). However, maintaining good rheology is a challenging goal. The drilling fluid rheology usually alternates due to many factors, such as contamination while drilling and thermal degradation (Steffe 1996).

However, the drilling fluid viscosity alternates due to contamination while drilling (Steffe 1996). Therefore, the management of drilling fluid components and rheological characteristics is a challenging process. Such problems can be solved by chemical processing of drilling fluid by various polymers types (Kudaikulova 2015; Kister 1972; Du et al. 2018). Some of these materials,

such as polymers, are considered fluid loss control additives and viscosity enhancers. (Caenn and Chillingar 1996; Hamza et al. 2019). A recent study by Rana et al. (2019) revealed that enhancing mud rheology by adding sodium dodecyl sulfate modified graphene (SDS-Gr) helped to reduce the mud loss by 20% after aging the mud at 150°F (Rana et al. 2019).

Deliberate reduction of rheology to lower the ECD is a common practice. However, field reports showed that insufficient hole cleaning in deviated wells or when drilling in a low rate of penetration (ROP) might increase mud rheology due to accumulation of the larger cuttings in the hole. An operating company reported using an engineered synthetic-base drilling fluid to enhance rheology while drilling into a deepwater reservoir in GoM. As a result of improving mud rheology, specifically maintaining the yield point, the hole cleaning improved, and a 17 ½”-hole was successfully drilled with less ECD and no mud loss (Friedheim 2004). Many authors have emphasized the relation between rheology and mud loss. Therefore, for loss prevention, it is essential to understand the fundamental of rheological models. Sun and Huang (2015) demonstrated that the fluid invasion radius is affected by the fluid flow index (n) of the power law model. The author also concluded that for a wide range of differential pressure, from 5 to 20 mPa, the rheological characteristics governed the variation of fracture length and evolution of mud invasion radius.

Another mud loss influencing parameter affected by rheology is the fluid leak-off, which is a measure of the magnitude of pressure required to force fluid into permeable rock or fracture network. The leak-off is expressed by the deflection on the plot of injected fluid into rock formation versus the pressure obtained from the pressure integrity test (PIT). Lavrov (2016) highlighted rheology's significance to the leak-off through the fracture and the buildup of mud cake inside the fracture. The main factors that dominate mud loss through natural fracture are

drilling fluid rheology, wellbore pressure, and hydraulic aperture of the fracture (Lavrov 2016). Majidi et al. (2010) conducted a quantitative analysis of lost circulation in naturally fractured formations. Their mathematical model based on the Herschel-Bulkley model revealed a distinguished relationship between the rheological properties of the drilling fluid, such as yield stress and shear-thinning viscosity, and the mud loss to fractures, as shown in Figure 2.16.

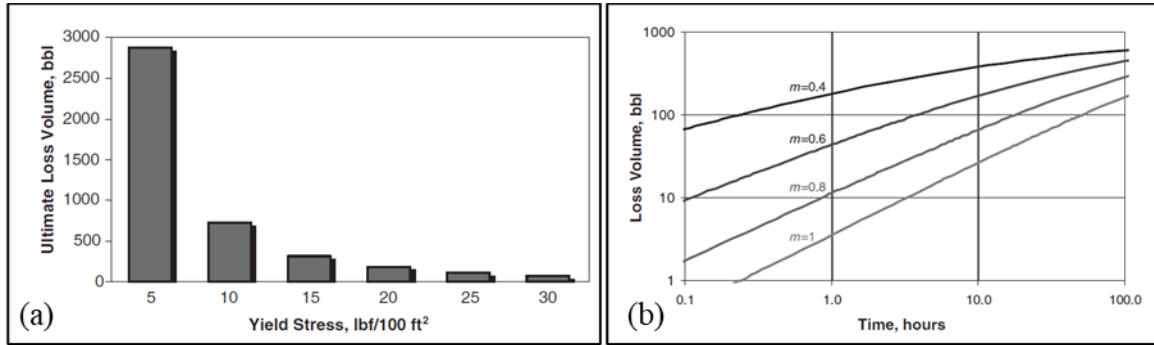


Figure 2. 16: Effect of yield stress on the ultimate volume of losses, b) effect of shear-thinning on mud losses (Majidi et al. 2010).

2.4.2 Effect of Pressure on Mud loss

The drilling window between the formation and fracture pressure is beyond control, while the hydrostatic and the bottom hole pressure are controllable parameters. Care must be taken when designing the drilling fluid to be heavy enough to hold back the formation pore pressure but not so heavy that it causes the formation to fracture, especially at the weak areas such as the casing shoe. Exerting excessive pressure on the formation increases fracture creation tendency, which leads to severe losses. However, several field reports and analysis of small changes in downhole pressure and fracture gradient showed that many lost circulations occur at pressures far below the fracturing pressures. Several actions can be taken to prevent this from happening, such as controlling operational factors, hole cleaning, and ECD to minimize downhole pressure. The ECD is the most important parameter during the dynamic state, especially in depleted reservoirs,

deviated wells, deepwater drilling, and fractured shales. In depleted reservoirs, the drop in pore pressure reduces the total formation stress, which increases the risk of fluid loss.

Minimizing downhole pressure can be obtained by controlling drilling operation factors and following precaution measures. For instance, many wells experience mud losses due to high surge pressures during running in drill pipe because of the limited compressibility of the drilling fluids (Howard and Scott 1951; Majidi et al. 2011). For example, a 450 to 650 psi surge pressure at 7,500 to 10,000 ft is equivalent to a sudden increase in mud density of 1.2 ppg (Goins Jr et al. 1951). Any increases in the ECD put the well at the risk of fracturing and lost circulation if any further surging pressure is exerted. Another important factor causing pressure surges is the starting and stopping of the mud pumps. Rapid starting of mud flow creates a high pressure that may cause mud loss, especially when breaking circulation while the bit is at the bottom of the hole. When downhole pressure increases, the loss occurs, most likely at upper locations where weaker formation cannot withstand that pressure. Accurate modeling of critical annular pressure losses is essential to design proper mud weight, viscosity, and other drilling parameters. Many researchers explained through numerical models that viscous pressure losses caused by dynamic circulation are the main cause for significant downhole pressure and loss circulation (Salehi and Nygaard 2012a; Ozdemirtas et al. 2009; Kostov et al. 2015).

Furthermore, in the absence of proper LCM to wedge the fractures and form a low permeable filter cake, the fluid invasion affects the wellbore status due to penetration of the fluid pressure (Pašić et al. 2007). Figure 2.17 illustrates the mud weight effect on wellbore stresses. Intact well is the case when the wellbore pressure is in balance with the fracture initiation pressure. Then fracture initiates before it propagates with more wellbore pressure.

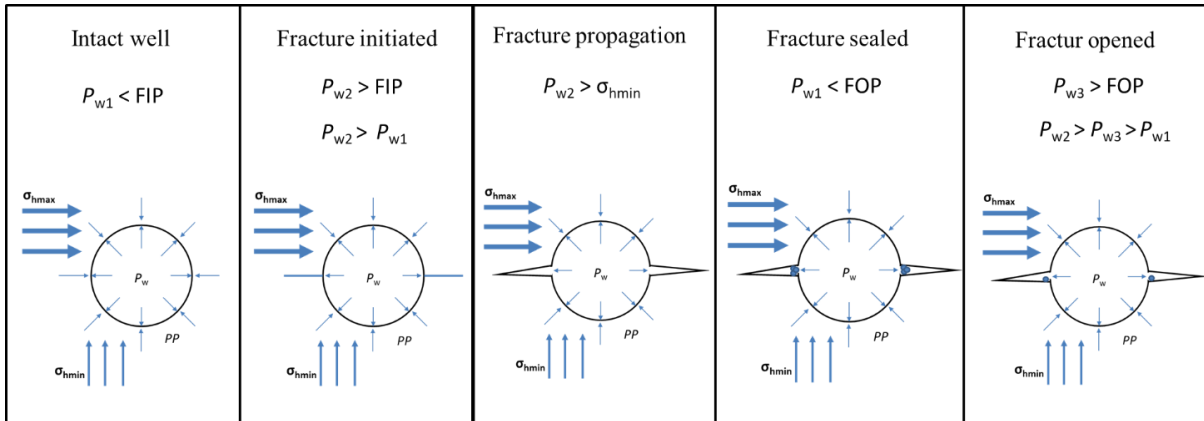


Figure 2. 17: Status of the wellbore with respect to wellbore pressure.

Monitoring pressure and flow behavior inside the wellbore is one technique of identifying the type of losses due to natural fractures or induced fractures. Majidi et al. (2011) conducted a pressure sensitivity analysis to recognize losses due to natural and induced fractures. The outcome of their study provided guidelines for the best practices for loss prevention. Generally, the variation of pressure defines the type and amount of fluid loss. Figure 2.18 compares variation in loss rate with the variation of differential pressure of overbalance drilling in British Petroleum (BP) wells reported by Dyke et al. (1997). It is clearly shown from the data that small changes in pressure have more effect on the loss caused by hydraulic induced fractures and less on the losses to natural fracture (Dyke et al. 1995).

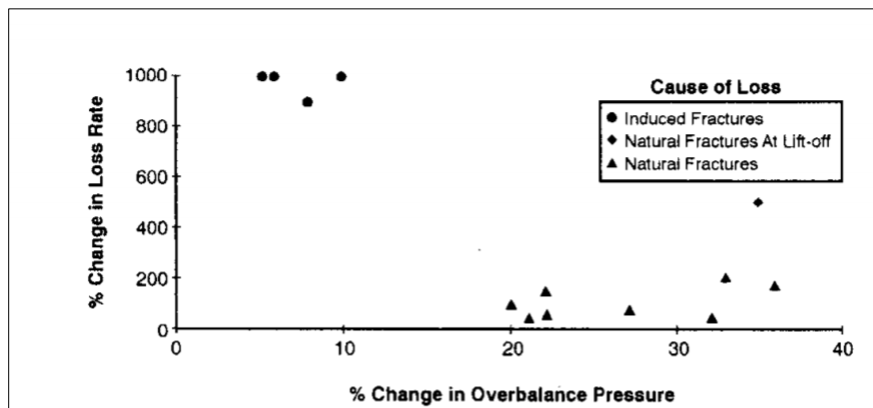


Figure 2. 18: variation in loss rate with the variation of differential pressure of overbalance drilling in BP wells (Dyke et al. 1995).

2.4.3 Effect of Drill Pipe Rotational Speed, Flow Rate, and Wellbore Geometry on Mud Loss

Annular pressure losses depend on the flow regime and the annulus geometry (Haciislamoglu 1994). The mud flow rate in and out of the hole is not only one of the indications of lost circulation but also an important influencing factor. All flow indicators such as pumps speed, fluid velocity, standpipe pressure decrease in case of lost circulation. This situation usually reduces the true vertical height of the hydrostatic column, which increases the risk of taking a kick shortly after the loss occurs. Close monitoring and controlling of drilling operational factors help mitigate the lost circulation.

For instance, the mud flow rate has two opposite effects on the situations leading to excessive pressure in the hole, causing fractures and severe losses. Low flow rates may affect hole cleaning, leading to cutting accumulation in the well, increasing mud density, hydrostatic pressure, and ECD. In contrast, high mud flow rate increases circulating pressure in the annulus and boost the invasion of fluid into the rocks (Lavrov and Tronvoll 2003). In normal conditions, the extra pressure exerted by the friction losses, which causes the ECD to increase, is estimated to be 300 to 500 psi for 10,000 ft. This will add about 0.6 to 1.0 ppg above the static mud gradient (Chaney 1949). The possible mitigation action is to reduce the circulation rate to reduce this annular pressure loss and the resulting ECD.

Furthermore, wellbore geometry impacts mud loss in many ways since it directly affects hole cleaning, wellbore instability, and fracture creation. Most of the borehole instability analyses assume fixed circular borehole geometry and do not consider other variations. The drop in the circulation pressure that causes the ECD to increase depends on the true vertical depth and hole geometry. Well geometry has a significant effect on this situation, especially when drilling a well of 9-7/8", or narrower (Deeg and Wang 2004). The smaller the well is, the smaller the annular

clearance between the drill pipe and the well, which increases the mud velocity and downhole pressure. Annular pressure losses increase as annular clearances decrease (Haciislamoglu 1994).

Another impact of borehole geometry is the required minimum flow rate for proper hole cleaning. Hole geometry increases flow rate and fluid velocity needed to ensure efficient cutting transportation, affecting hole cleaning, mud density, hydrostatic pressure, and ECD (Guo and Liu 2011). Deeg and Wang (2004) studied the effect of changing wellbore geometry on lost circulation control. The authors demonstrated the variation in wellbore strength using two cases: a regular circular borehole with no defects and a borehole intersected with an induced or natural fracture. Changing geometry altered the safe mud window, which required using extremely viscous gel-like materials to strengthen the wellbore and prevent loss circulation (Deeg and Wang 2004).

Due to operational considerations, the operational parameters and mud properties are often difficult to be maintained at a level that can provide sufficient hole cleaning. Therefore, drill pipe rotation and high mud flow rates are the best solution to avoid this condition. However, this will adversely impact lost circulation.

2.4.4 Effect of Temperature on Mud Loss

Pre-existing downhole conditions, such as temperature, are critical factors affecting mud loss. Due to the degradation of additives and properties deterioration, the drilling fluid rheology will severely impact fluid loss through highly permeable or fractured formations (Ezeakacha and Salehi 2018). The temperature effect can be classified into two aspects: the effect on drilling fluid and the effect on the surrounding rocks. At high temperatures, all clays tend to flocculate and lose their filtration control properties (Ghazali et al. 2014; Caenn and Chillingar 1996; Remont et al. 1976).

Selecting proper LCM for high-temperature applications represents a great challenge, especially with large fractures that require plugging material with larger particle size. A major problem facing using such large particles at high temperatures is maintaining good solids

suspension properties (Kulkarni et al. 2016). Magzoub et al. (2020) demonstrated through an experimental study that fractures fail at high temperatures (300°F) when attempting to seal the same size of fractures using the same types and concentrations of LCM that have been successful at low temperatures (Magzoub et al. 2021).

On the other hand, the surrounding rock may experience significant thermally induced stress due to the thermal contraction of the formation rocks. The thermal effect on rocks has been under investigation by many researchers to understand its impact on the stress condition and stability of intact well. However, there is not much progress achieved in the analytical solutions because considering the thermal effect and pore pressure variation requires theoretical background and comprehensive analysis. The numerical solutions also restricted by the complexity of the relationship between heat transfer and pore pressure in the wellbore vicinity.

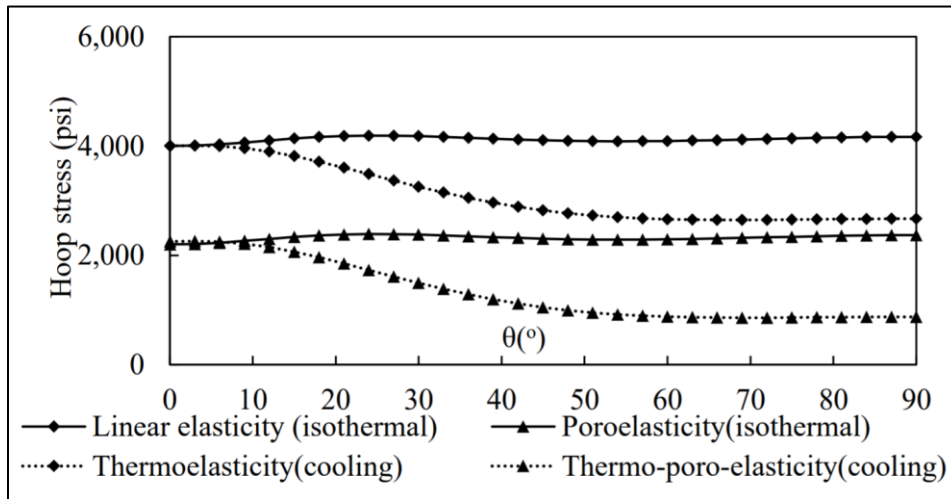


Figure 2. 19: Thermal impact on hoop stress along the wellbore wall (Wang 2018).

Wand (2018) developed a sensitivity analysis to evaluate the significance of induced thermal stress and lost circulation, considering different formation properties and loss conditions. His finding evident that temperature differences between the drilling fluid and the surrounding rocks increase the possibility of fracture propagation during fluid invasion into the rock. Besides

diminishing enhanced hoop stress attained by any wellbore strengthening attempts for loss prevention. Figure 3.14 demonstrates the reduction in hoop stress around the wellbore when the rock is cooled down from 180°F, making it more difficult to arrest the fracture before it propagates.

2.5 Outcomes from Literature Review and Current Research Gap

This chapter reviewed several studies, available data, and background theories required to understand the lost circulation problem. The comprehensive review and study of different mechanisms and affecting factors is essential for developing new formulations for lost circulation treatment. Several factors impacting mud loss and its application in wellbore strengthening have been discussed.

Several major conclusions can be drawn from this theoretical study. For example, the applied solutions in the field are either relying on using plugging materials or on drilling technologies and techniques such as casing while drilling (CwD), underbalanced drilling (UBD), and managed pressure drilling (MPD). Each of these methods has limitations and faces lots of technical and operational challenges. The most critical factor influencing the success of any treatment is the proper selection of materials types, sizes, and concentrations for specific lost circulation cases.

Despite recent technology advances, lost circulation materials still have some limitations as plugging downhole tools due to the large size of the particles required to seal large fractures, pumping difficulties in deep wells, and high temperatures. This exerts an additional load on mud pumps, increases ECD, and sets limitations on bit nozzles size. Large fractures are difficult to be sealed with conventional LCMs such as graphite, sized calcium carbonate, nutshell, and cellulosic fiber. Selecting LCMs type and concentration is vital in naturally fractured and unconventional formations (Al-saba et al. 2014b). Moreover, LCMs fail to regain drilling fluid circulation in many

cases due to the extreme downhole conditions and high loss severity. Therefore, multiple trials of LCM pills or cement plug may be required to continue the drilling operation.

Formation damage is also a big concern in drill-in fluids. As alternative solutions, some drilling technologies are also widely used, such as underbalanced drilling (UBD), managed pressure drilling (MPD), and casing while drilling (CwD). Despite the significant CwD advantages, some challenging and limitations also exist. Many operators do not recommend this for exploration wells. Also, the risk of fatigue problems in casing connections, and the limited flexibility with almost blind drilling where MWD tools and logging while drilling tools (LWD) are unavailable (Pavković et al. 2016; Patel et al. 2019).

Chapter 3: Polymer Gels as Lost Circulation Solution

Since this study focuses on polymer gels as a lost circulation solution, an extensive background study was conducted on the theory and chemistry of crosslinking. This chapter contains a comprehensive review of crosslinked polymers, considering optimization, cleaning, gelation kinetics, and compatibility with drilling fluid formulations. This study is essential for selecting a suitable gel system for lost circulation solution and wellbore strengthening.

3.1 Theory and Chemistry of Crosslinking

Crosslinking changes the physics of the polymers, making them stronger and produce high molecules. The International Union of Pure and Applied Chemistry (IUPAC) defined the crosslinked polymer as a macromolecule formed by chemical or physical reactions involving regions such as functional groups on existing macromolecules (Lambla 1989; Work et al. 2004). The crosslinking of polymers can be through chemical reactions or physical interactions. In chemical crosslinking, the region that works as a functional group can be an atom, a group of atoms, a branch connected by bonds, or a weak chemical interaction. While in physical crosslinking can be entanglements or physical interaction. Chemical crosslinking is a synthetic method in which the polymers are crosslinked through polymerization or post-crosslinking between polymer chains by the crosslinker's reaction with the polymer's reactive groups. The polymerization of the functional groups into the chains is responsible for producing the crosslinked polymer. Moreover, there are interpenetrating polymer networks (IPNs) that cannot be classified as physical or chemical crosslinks. The IPNs compose of two or more chemically crosslinked polymers entangled together in a way that cannot be physically separated from each other, which produces high molecules (Oyama 2015; Gooch 2011; Palsule 2016).

Another classification of the crosslinked polymers gel system, which is also based on the crosslinking process, can be grouped into three categories: the in-situ gels or immature gels, the preformed or mature gel, and the foamed gel. The difference in these three categories is described by the state of the gel and gel formation process. For example, the in-situ gels are immature gel where physical properties require a trigger to change. The trigger can be physical stimulation such as temperature and pH, or chemical reaction. In other words, the in-situ gels can be either thermo-reversible gels, pH-sensitive, or ion-sensitive gels (Swapnil DS et al. 2013; Liu et al. 1999; Makwana et al. 2016). Although these types of gel are widely used, the crosslinked process involves some challenges and drawbacks, such as the difficulties in controlling the gelation time, shear degradation, change in gelation compositions in addition to dilution and contamination, which significantly affect the final gel quality (Bai et al. 2015).

The success of LCM gel treatment depends strongly on the possibility of adjusting its gelation time and its final gel strength (Ghriga et al. 2019). These are essential design factors to address the operational requirements during the injection operation of the in-situ gels. In this study, three chemical crosslinkers, organic, and inorganic were used to crosslink polyacrylamide molecules. The main affecting factors of the in-situ gelation process are discussed.

3.2 The Onset Temperature of Crosslinking

Onset temperature and gelation time of gel formation are the two essential characteristics of the crosslinkers. The onset temperature refers to the temperature at which the thermo-responsive gelation mechanism is triggered, and the transition process starts. There are some analytical solutions to estimate the onset temperature of crosslinking by estimating the polymerization degree (Stockmayer 1944; Flory 1941). The best and most accurate method is through differential scanning calorimetry (DSC). The DSC has been used by many researchers to provides insights

into the crystallization process of polymers. Since the gelation process is similar to the crystallization process, the DSC can be used to study gelation as well. The onset temperature (T_o) can be obtained from the DSC exotherms by finding the peak temperature of the exotherm (Wang et al. 2005). Liu et al. (2016) also used the DSC to determine the onset crosslinking temperature of PAM crosslinked with hexamethylenetetramine + hydroquinone (HMTA- HQ). Figure 3.1 shows the DSC curve of the PAM/HQ system, where a distinguished peak can be observed around 140°C. This peak is because the crosslinked polymer absorbs heat before gel formation and then releases it after gelation (Liu et al. 2016).

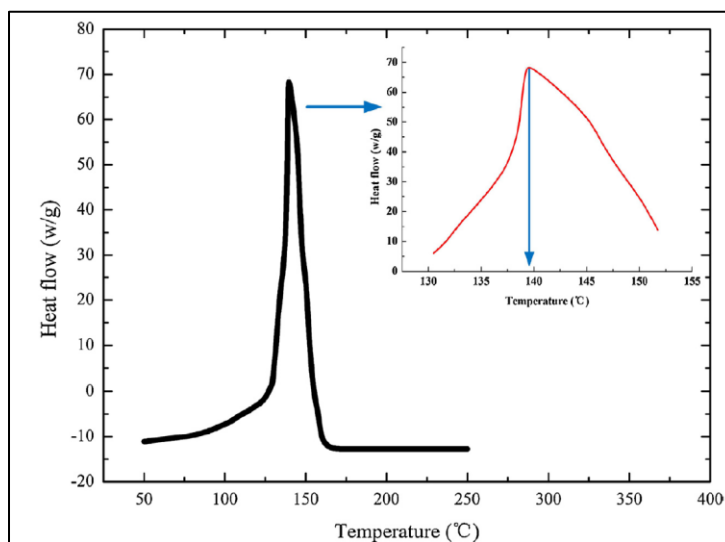


Figure 3. 1: DSC curve of the gel system composed of 0.6 wt.% PAM and 0.6 wt.% crosslinkers (Liu et al. 2016).

Many methods based on rheology measurements were reported in the literature to determine the gelation kinetics of crosslinked polymers. All methods aim to determine the onset temperature and gelation time. For instance, the static shear method gives faster results and accurate determination of the inflection point representing the onset of the gel formation.

In contrast, the dynamic shear method, which is applied using rheometers, gives a more quantitative measurement of the gelation rate (Broseta et al. 2000; Vasquez et al. 2003). The dynamic shear method results provide a direct measurement of the gel strength, which depends

mainly on the gel's elasticity. Therefore, the gelation time can be evaluated by measuring the elastic properties (storage modulus) through dynamic shear testing (ElKarsani et al. 2015a; Mohamed et al. 2015a). The gelation process is a function of the polymer and the crosslinker concentrations, water salinity, temperature, and time. Mohamed et al. (2015b) used DSC to demonstrate salts' effect on PAM gelation mechanisms. The authors concluded that the fractional gelation, a measure of the gel formation, reduces with added salt. For example, in Figure 3.2, the fractional gelation was less when the polymer is crosslinked without salts. Based on the presented results, to achieve 7% of gelation, the process took about 26 min and 36 min when adding 1% NaCl and NH₄Cl, respectively, compared to 15 minutes only when the polymer was pure (Mohamed et al. 2015b).

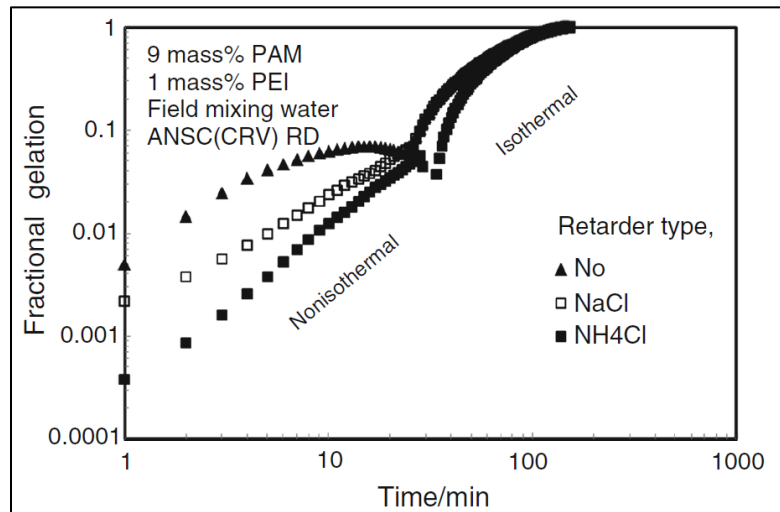


Figure 3. 2: Effect of salts (43.2 g/L) on fractional gelation of emulsified PAM/PEI, 9:1 ratio (Mohamed et al. 2015).

Furthermore, the aqueous medium alkalinity/acidity will also impact the gelation kinetics, as demonstrated by Liu et al. (2016). Figure 3.3 shows a significant reduction in gelation time when pH was decreased from 8 to 4.5. The gelation time decreased from 10.6 hours to 3.2 hours. However, the gel strength was increased from 530 Pa to 620 Pa, which was the initial gel strength at the original pH. The author attributed this alteration in gelation time and gel strength to the acid environment, which promoted the decomposition of the crosslinker and the

hexamethylenetetramine (HMTA) and increased the polymerization reaction. While in the alkaline environment inhibited the decomposition of the HMTA (Liu et al. 2016). However, Wang et al. (2007) have demonstrated that, even in an alkaline environment, the HMTA can decompose and successfully form crosslinked polymer at high temperatures.

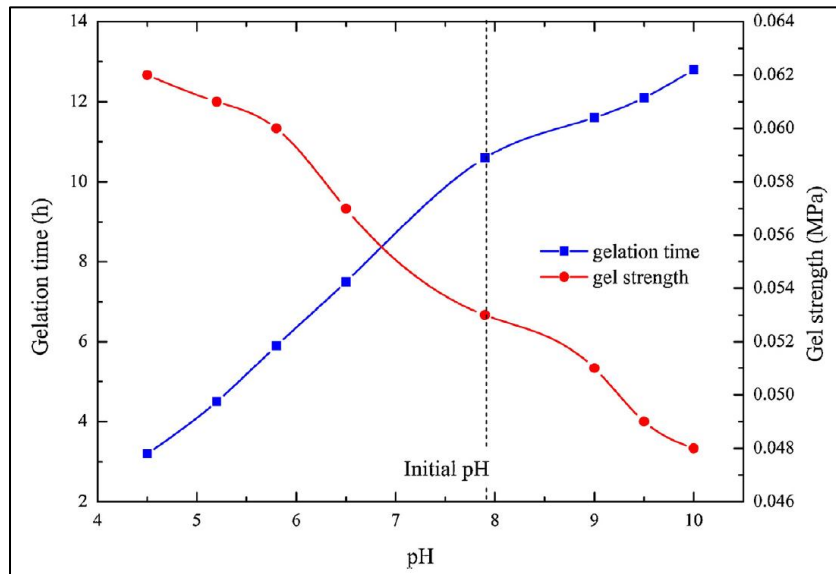


Figure 3. 3: Effect of pH on the gelation process of PAM/PEI gels (Liu et al. 2016).

At a specific temperature and after a predetermined time for gel formation, the gel system will develop. Adequate and designed time is needed for gel formation to avoid the formation of the gel in the pipes during the placement process, especially in high-temperature wells. In other words, PAM/PEI systems tend to slow the gel formation process at lower temperatures and accelerate at high temperatures. To overcome this, treatment of lost circulation at lower depths (lower temperatures) may require quick-curing gels as the time needed to apply the gel and pump it from the surface to the bottom of the well is short. In comparison, lost circulation at high temperatures (deep wells) requires slow gelation to avoid gel formation during the injection. Accurate determination of gelation time is a vital factor in gel placement to determine the time at which a rigid 3-D gel structure is formed.

3.3 Organic and Inorganic Crosslinkers

The classification of organic and inorganic is generally used to describe the origin of the crosslinkers. The common inorganic crosslinkers used in the industry include aluminum (Al^{3+}) and chromium (Cr^{3+}). And the types of organic crosslinkers are countless, including polyethyleneimine, phenol-formaldehyde, and hexamethylenetetramine (Hamza et al. 2019; Sheng 2010). Despite the variety of available crosslinkers, the selection is limited by downhole temperature, stability, and polymer precipitation under harsh conditions, shear degradation, and cost. Organic crosslinkers are more common in the oil and gas industry due to their higher thermal stability (Zolfaghari et al. 2006).

Although the crosslinking mechanism is similar, the response to pH and temperature is completely different. The pre-existing temperature condition governs the selection of the applicable crosslinker. The final gel strength and thermal stability are in favor of organic crosslinkers. Generally, the inorganic crosslinked gels have lower onset temperatures and higher acid tolerance. For example, inorganic crosslinked gel such as chromium acetate gel becomes ineffective at a temperature above 80°C ($\approx 176^{\circ}\text{F}$) (Amir et al. 2019). The inorganic crosslinkers have low thermal stability due to the ionic bonds with the carboxylate groups of polymers. This bond is not as strong as the covalent bond in the organic crosslinkers, which causes lower thermal stability. Additionally, the large number of free amide groups, usually left uncross linked with the limited ionic bonds, increases the degree of degradation of the polymer molecules at higher temperatures (Burns et al. 2008).

Furthermore, inorganic crosslinkers are more prone to precipitations due to the crosslinking of the free carboxylate groups available on the polymer backbone. As an example of this situation, the chromium acetate gel always has a high tendency to precipitate in high alkalinity and high

temperatures. In addition to the downhole conditions, toxicity plays a major role in selecting suitable organic or inorganic crosslinker (Kabir 2001). Therefore, the inorganic crosslinkers are under a lot of research to expand its thermal stability and enhance its gelation control due to environmental and safety issues. Table 3.1 summarizes the main differences between the organic and inorganic crosslinker.

Table 3. 1: Differences between organic and inorganic crosslinkers

| Crosslinker | Type of bond | Examples | Toxicity | Onset temperature | pH | Gelation time without retardation |
|-------------|----------------|--|----------|------------------------|------------|-----------------------------------|
| Organic | Covalent bonds | Polyethyleneimine (PEI) | No | 130°C | 11.2 | 50 min no salts |
| | | phenol-formaldehyde | High | 120°C | 9 | |
| | | hexamethylenetetramine + hydroquinone (HMTA- HQ) | Low | 140°C at original pH=8 | | 10.6 hours at 110°C |
| Inorganic | Ionic bonds | Aluminum acetate | No | 50 to 75°C | 6.2 to 8.5 | 18 to 50 min |
| | | Triamine silicate or Functionalized silica (FS) | No | 130°C | 6 to 7 | 50 min |
| | | Chromium Acetate | No | 50°C | 5.5 | 50 min |

3.4 Gels as Lost Circulation Materials

This section reviews the application of crosslinked polymers in the oil and gas industry, focusing on the drilling application and LCM formulations. The potential application of wellbore strengthening, particularly the acrylamide polymer system, is highlighted. The review also covers the commercially available polymers and crosslinkers and their performance evaluation in HPHT conditions. Technically, the sealing mechanism of the crosslinked polymer depends on their controlled gelation process. The polymer/crosslinker system can be squeezed or circulated inside the wellbore and invade the formation. The fluid then gels and seals off the permeable and fractures, causing the loss. The earliest reported application of crosslinked polymers was for treating high water production zone. A crosslinked PAM was used to plug a highly permeable zone

in a producer well (Paul and Strom 1987). Similarly, the crosslinked polymers were used in drilling as LCM to be injected and crosslinked downhole (in situ gels) to seal loss zones.

The polymeric formulations have been under investigation in many studies. Natural polymers such as carboxymethyl cellulose (CMC) and starch are widely used in drilling fluid formulations as viscosity and loss control additives. Moreover, several fields and laboratory reports revealed crosslinked polymers' applicability in lost circulation treatment (Gibson et al. 2011; Hashmat et al. 2017; Al-Muntasheri et al. 2008). The polymeric gels have great advantages in sealing large fractures that have challenged the conventional granular and fibrous LCM, such as calcium carbonate, graphite, fibers, and LCM blends (Hashmat et al. 2016a). To expand crosslinked polymers' application into wellbore strengthening and formulation of gelling muds, it is needed to understand their rheology, crosslinking process, and gelation control.

The water-soluble polymers are the most used types, such as PAM. The PAM has a wide range of molecular weights and relatively low cost (El-karsani et al. 2014). Various types of water-soluble polymers are also used in drilling formulations, such as partially-hydrolyzed polyacrylamide (PHPA) and tert-butyl acrylate (tBA). These types have demonstrated higher thermal stability; however, they are more costly than the PAM. The chemical structures of different acrylamide-based polymers are shown in Figure 3.4 (Kurenkov et al. 2001; Al-Muntasheri et al. 2008; Omer 2012).

The polymers are crosslinked with various types of organic and inorganic crosslinkers. The commonly used and commercially available types are chromium acetate, ferric acetylacetonate, ammonium ferric oxalate, chitosan, and polyethyleneimine (PEI). However, utilizing many crosslinkers is limited by environmental concerns, especially in offshore drilling (Magzoub et al. 2020a). The less toxic and most used crosslinker is the PEI and chitosan. Both chitosan and PEI

crosslink PAM because of the amino groups on their backbone (El-karsani et al. 2014). The chemical structures of the PEI and chitosan are shown in Figure 3.5 The crosslinked PAM/PEI system forms a gel in a wide temperature range (Zhang et al. 2015; Allison and Purkaple 1988; Reddy et al. 2003).

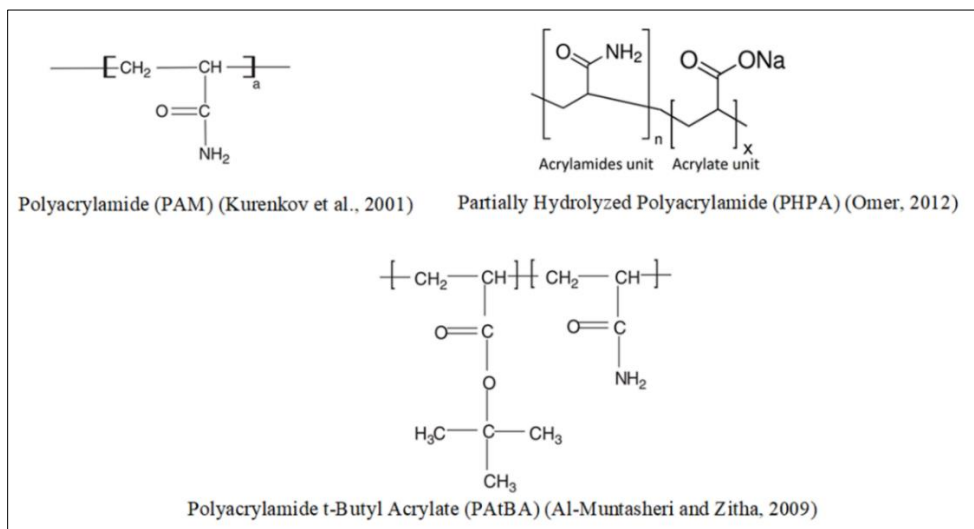


Figure 3. 4: Chemical structures of different types of acrylamide polymers used as LCMs (Kurenkov et al. 2001; Al-Muntasheri et al. 2008; Omer 2012)

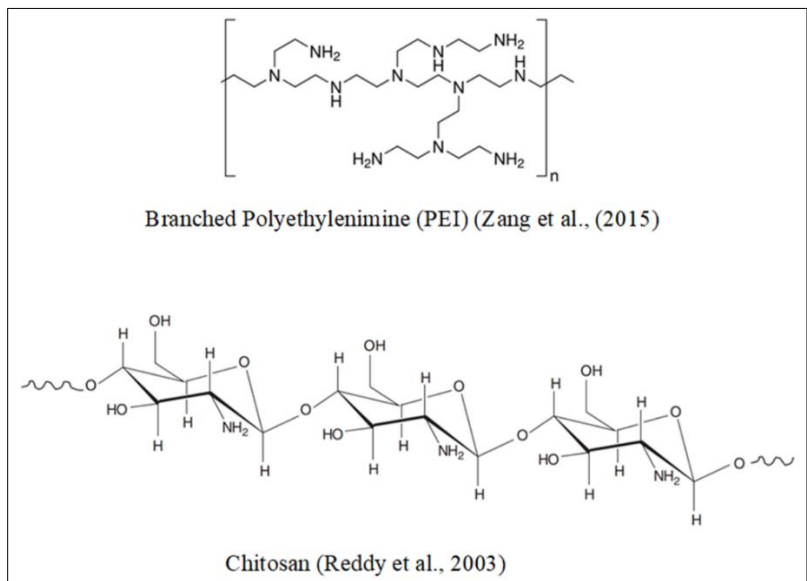


Figure 3. 5: Chemical structure of chitosan and highly branched PEI (Zhang et al. 2015; Reddy et al. 2003)

Until recently, most crosslinked polymers applications were limited to conformance control. The gelling formulations are widely used to seal undesired water zones to minimize

unwanted water production (Hamza et al., 2019). The unique rheological properties and thermal stability encouraged the research on utilizing the crosslinked PAM formulation in LCM applications. The first known application of polymeric fluids in loss prevention backed to 1955, when the Union Oil Co. used hydrolyzed polyacrylamide, having a molecular weight ranging from 50,000 to 400,000 Dalton, to treat lost circulation. However, PAM's concentration was 8 lb/bbl, which is much lower than what was used in this study, up to 27 lb/bbl of PAM (Oldham and Kropa 1955).

In the beginning, despite the high sealing efficiency and thermal stability up to 400°F, but the application of polymeric gels was not very successful due to the presence of divalent cations in lime and gypsum formations; also, polymers did not function well in seawater (Gleason and Szymanski 1986; Shupe 1981). A few years later, modified aqua-soluble copolymers with a high tolerance to electrolytes were developed and successfully deployed (Uhl et al. 1984). Several studies were also reported using synthetic polymers for high-temperature drilling in the North Sea (Plank 1992). Horton et al. (2006) developed a crosslinked polymer by combining vinyl phosphonate co-monomer units into the polymer by copolymerization with the other co-monomers. The authors described a process of injecting the crosslinked polymer gel into the wellbore to form in situ gel and cure severe drilling fluid loss (Horton et al. 2006)

Fidan et al. (2004) developed a crosslinked gelling pill mixed with diesel oil, bentonite, calcium carbonate, and cement. The mixture was successful in sealing large fractures (Fidan et al. 2004b). Hashmat et al. (2017) conducted filtration experiments with a highly permeable core treated with polyacrylamide (0.5wt.%), crosslinked with phenol (0.4 ppb), and formaldehyde (0.37 ppb). The treatment yielded high sealing and no fluid loss. In a recent field case study reported by Fen et al. (2018), acrylamide unites and hydroxyl and carboxyl-based crosslinked system was used

in three wells with a successful regain of total lost circulation. Table 6.2 lists examples of crosslinked polymers used as LCM.

Table 3. 2: Example of polymers and crosslinkers used as LCMs

| Polymer | Crosslinker | Concentration/ ratio | Onset crosslinking temperature | Author |
|--|--|-------------------------|--------------------------------------|-----------------------------|
| Polyacrylamide | Polyethylenimine | 7.5:1:1 | > 130°C | (Magzoub et al. 2020b) |
| Polyacrylamide | Aluminum acetate and nanosilica | 7.5:1:3 | > 130°C | (Shamlooh et al. 2020) |
| Polyacrylamide | Functionalized silica and nanosilica | 7.5:1:3 | > 50°C | (Shamlooh et al., 2020) |
| Hydrolyzed polyacrylamide | Polyethylenimine | 3:1.2 | > 120°C | (Hashmat et al. 2016b) |
| Polyacrylamide | Phenol and formaldehyde | 0.5:0.4 | > 100°C | (Hashmat et al. 2017) |
| Hydrolyzed polyacrylamide | chromic III carboxylate | N/A | > 105°C | (Ghassemzadeh 2011) |
| Polyacrylamide | Zirconium (Zr) | 66:3 | 132 to 232°C | (Al-Muntasheri et al. 2008) |
| Polyacrylamide | Zirconium (Zr) And activator | 3.4:3.7 | 38 to 132°C | (Al-Muntasheri et al. 2008) |
| Hydrophilic polyacrylamide gel (HPG) | Zirconium (Zr) | 0.5:0.4 | 30 to 100°C | (Qiu et al. 2018) |
| HPAM, Xanthan Gum, Guar Gum, TVP, and AMPS | Ethylene diamine tetraacetic acid (EDTA) DTPA: Diethylene triamine pentaacetic acid | 0.43:20 | > 150 | (Kamal et al. 2018) |

Chapter 4: Laboratory Experimental Methods and Machine Learning

This chapter contains a detailed description of the experiments conducted for developing the polymeric gel formulations for lost circulation treatment. The design of experiments, parameters, experimental methods, and laboratory procedures are explained. The details in this section will also cover the Machine Learning (ML) approach introduced in this study for building a rheology prediction model for the designing stage of the polymeric gel in drilling fluids.

4.1 Design of Experiments (DoE)

Different combinations of polymers and crosslinkers were evaluated for potential use as LCM, as discussed in the materials section (section 4.2). The selected gelling polymer system comprising polyacrylamide (PAM), which is widely used in non-LCM applications in the oil industry. Three potential gelling polymer systems were screened. Polyethyleneimine, aluminum acetate, and functionalized silica were used as crosslinkers. Nanosilica addition also was investigated to add more strength and stability to the gelling polymer system. Figure 4.1 shows the workflow prepared to accomplish the objectives of this study.

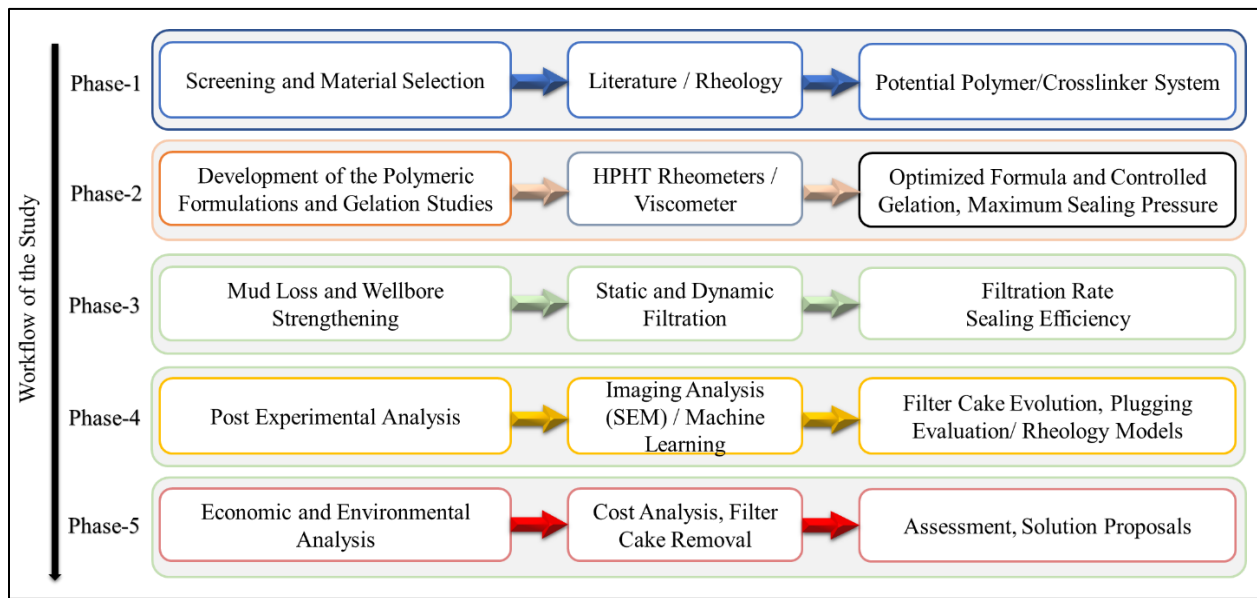


Figure 4. 1: Workflow of the polymeric LCM developing study.

The study considered gelation kinetics, gel strength, and stability in typical drilling mud formulations. The formulation's composition was adjusted to control its gelation process to achieve wellbore stabilization and strengthen the formation under the specified conditions of temperature and pressure at the desired depth.

For the optimization study, the viscosity and gel strength measurements are the main key parameters. For the wellbore strengthening analysis, the static and dynamic mud filtration equipment discussed in this chapter will be utilized, considering the effect of gelation time, temperature, concentration, gel strength, and fracture size. As mentioned in section 1.4, this study aims to develop a flowing polymeric gel and gelling LCM pills. The designing stages depended on material selection and concentration optimization, as discussed in detail in the following sections of this chapter. Figure 4.2 shows the flow chart of the developing process for crosslinked polymer-based mud (gelling mud) and the crosslinked polymer pill (gelling pill).

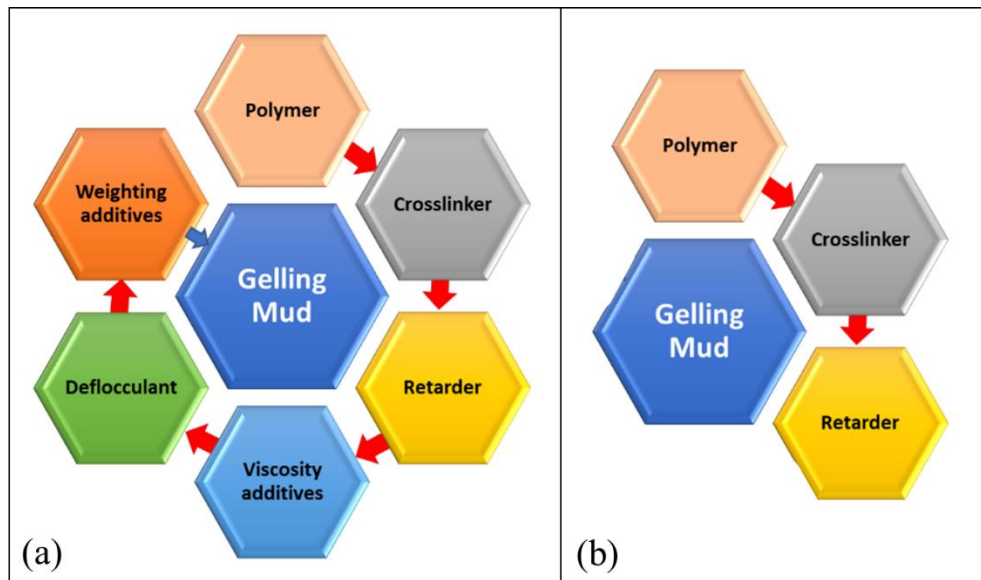


Figure 4. 2: Flow process of the optimization study for the crosslinked polymer.

4.2 Experimental Methods and Laboratory Procedures

4.2.1 Material Selection and Preparation of Polymeric Gel Systems

This study begins with evaluating the potential polyacrylamide to formulate the base fluid of the polymeric mud. The PAM was selected because it is a commonly used water-soluble polymer in the oil and gas industry. Other options considered were the hydrolyzed polyacrylamide (HPAM) and the poly tert-butyl acrylate polymer. However, these polymers have higher thermal stability, but the PAM still suitable for high-temperature applications in addition to the wide range of molecular weights and relatively low cost. Non-ionic Polyacrylamide (PAM) of 12.5 to 20 wt.% concentration was obtained from SNF Floerger Group, France. Three different average molecular weight ranges (Mw) were considered for the screening study, ranging from less than 200,000 Da to more than 1.5 million Da. The viscosity of pure PAM ranges from 70 to 195 mPa.s for the lowest and highest average molecular weight, respectively. The PAM is crosslinked with 33.3 wt.% of highly branched PEI of 750,000 Da average Mw, an example of a commonly used crosslinker in the industry. Since the PEI only works at elevated temperatures, two other crosslinkers were investigated for the low-temperature treatment. The aluminum acetate and functionalized silica. The other additives were barite as a weighting agent, sodium hydroxide to raise the mud's pH, commercial tannin-based deflocculant dispersant called Desco®, and lignite as mud dispersant. Ammonium chloride was also chosen as the retardation agent because it is available, inexpensive, and showed superiority over the other salts.

For comparison purposes, two water-based mud formulations were used. The first one was a basic mud (Ref. Mud#1) containing bentonite as the main viscosity additive. The second and third references muds (Ref. Mud#2 and Ref.Mud#3) were water-based mud having a mud weight of 9.6 ppg, which is typically used in depleted reservoirs to avoid loss circulation. The Ref. Mud#2 and Ref.Mud#3 contains, in addition to bentonite, cedar fiber, or sized calcium carbonate of fine

and coarse particles mixture that was selected as examples of conventional LCMs. The WBM contained 5 lb/bbl cedar fiber or 55 lb/bbl of calcium carbonate with particle size distribution having $d_{10} = 2 \mu\text{m}$, $d_{50} = 15 \mu\text{m}$, and $d_{90} = 100 \mu\text{m}$. The detailed composition of Ref. Mud#1, 2, and 3 are shown in Table 4.1, 4.2, and 4.3, respectively. All materials from commercial suppliers were used as received. The three potential gelling polymers with different molecular weights were screened to determine the appropriate molecular weight for drilling fluid applications. Table 4.4 shows the details of the investigated parameters and components.

Table 4. 1: Composition of Ref.Mud#1 [20 lb/bbl Bentonite]

| Product | lb/bbl | Weight % | Volume % |
|-----------|--------|----------|----------|
| Water | 341.6 | 94.5% | 97.6 |
| Bentonite | 20 | 5.5% | 2.4 |

Table 4. 2: Composition of Ref.Mud#2 [9.6 ppg]

| Product | lb/bbl | Weight % | Volume % |
|--------------------------|--------|----------|----------|
| Water | 265.5 | 65.8 | 75.8 |
| Caustic | 0.5 | 0.12 | 0.14 |
| Bentonite | 20 | 5 | 2.4 |
| Lignite | 4 | 1 | 1.14 |
| Mud deflocculant (Desco) | 4 | 1 | 1.14 |
| Calcium carbonate | 55 | 13.6 | 15.7 |
| Barite | 54.2 | 13.4 | 3.6 |

Table 4. 3: Composition of Ref.Mud#3 [9.6 ppg]

| Product | lb/bbl | Weight % | Volume % |
|--------------------------|--------|----------|----------|
| Water | 322 | 79.8 | 92.2 |
| Caustic | 0.5 | 0.12 | 0.1 |
| Bentonite | 20 | 5 | 2.4 |
| Lignite | 4 | 1 | 0.8 |
| Mud deflocculant (Desco) | 4 | 1 | 0.72 |
| Cedar Fiber | 5 | 1.3 | 0.9 |
| Barite | 47.7 | 11.8 | 3.2 |

Table 4. 4: Details of the investigated component and parameters

| Component | Material | Parameter | Range |
|--------------------|--|---|--|
| Polymer | Polyacrylamide | Molecular weight (Mw)/ Concentration | Mw: 0.2×10^6 to 1.5×10^6 PAM: 5 to 12.5 wt.% |
| Crosslinkers | Polyethylenimine (PEI) Aluminum Acetate (AlAc) Functionalized silica (FNS) | Type/ Concentration | PEI: 0.25 to 1.5 wt.% AlAc: 0.5 to 3 wt.% FNS: 0.5 to 3 wt.% |
| Enforcement | Nanoslica (NS) | Particle size/ Concentration | Size: 8 nm to 85 nm NS: 0.25 to 2 wt. % |
| pH control | Caustic soda | Concentration | Lignite: 0.25 to 1 lb/bbl |
| Viscosity | Bentonite | Concentration/ Addition procedure | Bentonite: 1 to 5 lb/bbl Different addition order |
| Deflocculant | Lignite | Concentration | Lignite: 0.25 to 1 lb/bbl |
| Weighting material | Barite | Concentration | Increasing weight in the range of 9 ppg to 11.5 ppg |

4.2.2 Gel Description According to Sydansk's Codes

During preparation, testing, and optimization of the polymeric gel formulas, the gel structure must be accurately described. There are different codes to describe the condition of the gel. The commonly used codes were suggested by Sydansk (1990). The coding system divides the polymeric gels based on the look, structure, and fluid ability. The gel status is classified into 9 categories, from “A” to “I”. Each letter of the code refers to a specific gel structure and gives an idea about the gel strength. For example, the letter “A” refers to the initial states of the solution where the fluid has the same viscosity as the original polymer solution. The letters “B” to “H” describe the gels ranging from highly flowing to barely deformable if forced to move by gravity while pouring out of a bottle. Table 4.5 describes Sydansk's codes in detail.

Table 4. 5: Sydansk gel strength codes (Sydansk 1990)

| Gel strength code | Gel description |
|-------------------|---|
| A | No detectable gel formed: The gel appears to have the same viscosity as the original polymer solution |

| | |
|---|---|
| B | Highly flowing gel: The gel appears to be only slightly more viscous than the initial polymer solution |
| C | Flowing gel: Most of the gel flows to the bottle cap by gravity upon inversion |
| D | Moderately flowing gel: Only a small portion (5-10%) of the gel does not flow to the bottle by gravity upon inversion (usually characterized as a tonguing gel) |
| E | Barely flowing gel: The gel can barely flow to the bottle cap and/or a significant portion (>15%) of the gel does not flow by gravity upon inversion |
| F | Highly deformable nonflowing gel: The gel does not flow to the bottle cap by gravity upon inversion |
| G | Moderately deformable nonflowing gel: The gel deforms about halfway down the bottle by gravity upon inversion |
| H | Slightly deformable nonflowing gel: Only the gel surface slightly deforms by gravity upon inversion |
| I | Rigid gel: There is no gel surface deformation by gravity upon inversion |

4.2.3 Cores, Filter Disks, and Fractured Disks Preparation

Different types of filter disks were used in the static filtration experiments instead of the filter paper usually used with the API filter press. Carbonate cores were used to prepared filter disks. First, a 2.5 inches coring bit was used to prepare the core from a carbonate bulk, then quarter-inch thick disks were cut. The process of coring and disks preparation is explained in Figure 4.3.

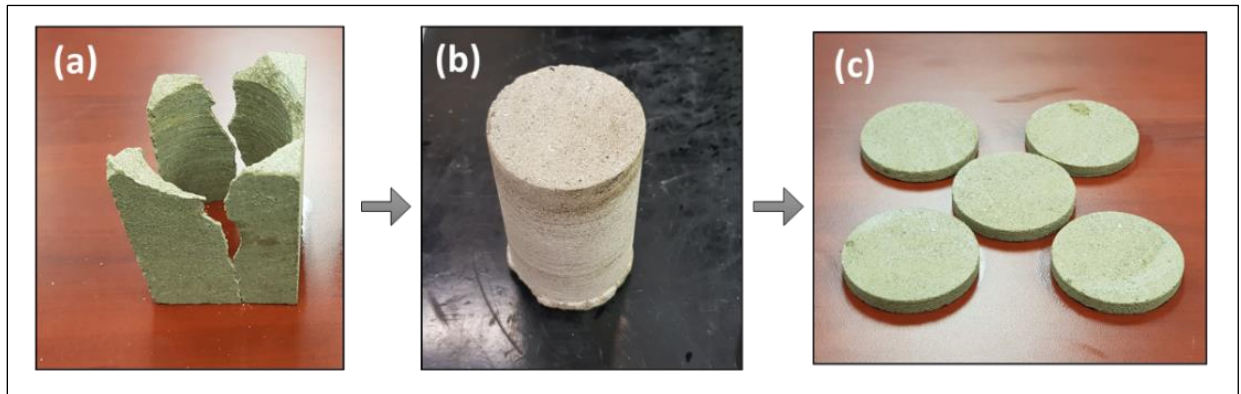
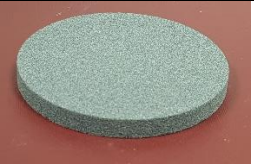



Figure 4. 3: Process of carbonate coring and filter disks preparation, (a) rock after coring, (b) core 2.5 x 3 inches, and (3) disks 2.5 x 0.25 inches.

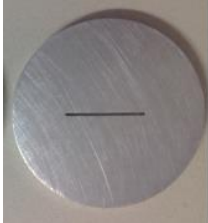
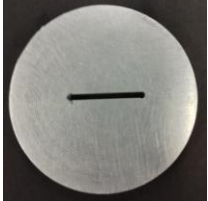
In addition to the carbonate disks, two types of ceramic disks were also used. The ceramic disks were obtained from an international supplier. The two types of ceramic filter disks have two ranges of permeabilities, as detailed in Table 4.6.



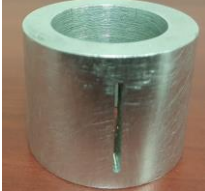
Table 4. 6: Types and properties of used ceramic filter disks

| Ceramic filter disk | Properties | Image |
|---------------------|---|---|
| No#170-53 | Diameter: 2.5" (6.35 cm) Thickness: .25" (0.635 cm) Mean Pore Throat: 50 μ m Permeability: 15 D |  |
| No#170-55 | Diameter: 2.5" (6.35 cm) Thickness: 0.25" (0.635 cm) Mean Pore Throat: 10 μ m Permeability: 775 mD |  |

Moreover, various shapes and fractures with different sizes were fabricated out of aluminum for the static and filtration experiments. Also, for the wellbore strengthening experiment in the dynamic filtration setup, a well-shaped cylindrical aluminum with a 1000 μ m vertical fracture was fabricated. Table 4.7 gives details on the prepared aluminum fractured mediums. The following subsection will show graphically how each filter medium/fractured disks will be used in the static and dynamic filtration setups.

Table 4. 7: Types and properties of used fractured aluminum filter mediums

| Filtration test | Properties | Image |
|-------------------|---|--|
| Static filtration | Diameter: 2.5" (6.35 cm) Thickness: .25" (0.635 cm) Shape: single fracture Fracture width: 1000 μ m Fracture length: 1 inch |  |
| Static filtration | Diameter: 2.5" (6.35 cm) Thickness: .25" (0.635 cm) Shape: single fracture Fracture width: 1000 μ m Fracture length: 1 inch |  |

| | | |
|--------------------|--|--|
| Static filtration | Diameter: 2.5" (6.35 cm) Thickness: .25" (0.635 cm) Shape: single fracture Fracture width: 1000 μ m Fracture length: 1 inch |  |
| Static filtration | Diameter: 2.5" (6.35 cm) Thickness: .25" (0.635 cm) Shape: complex fracture Fracture width: 1000 μ m Fracture length: 1 inch |  |
| Dynamic Filtration | Diameter: 2.5" (6.35 cm) Thickness: .25" (0.635 cm) Shape: vertical radial fracture Fracture width: 1000 μ m Fracture length: 1 inch |  |

4.2.4 Experiments, Apparatus, and Procedures

4.2.4.1 Rheology of Drilling Fluid and Gelling Formulations

A good LCM evaluation study should incorporate a comprehensive rheological analysis for various conditions. In this study, several rheological measurements were designed to provide the necessary information required for screening, optimizing, and developing the crosslinked polymeric LCMs. Three types of instruments were used, the speed dial viscometer, the steady shear high temperature rheometer, and the dynamic shear rheometer. Although all these instruments are rotational viscometers that rely on the same torque measuring concept where the torque is correlated with the viscosity and other parameters, however, each type can conduct certain experiments under different conductions to give specific outcomes.

For instance, the speed dial viscometer is used to obtain apparent viscosity, plastic viscosity, yield point, and API gel strength. The second one is the high-temperature rheometer with concentric cylinder configuration with an option of testing at downhole conditions, which is an essential assessment for degradable LCMs and crosslinked polymers. The third one, the dynamic shear high-temperature rheometer, has a parallel plate configuration (25 mm diameter

and 2 mm gap), capable of testing solid-like materials such as polymeric gels. The parallel plate rheometer also allows testing for dynamic frequencies and strain percentages. The main reason for using this rheometer was for studying the gelation kinetics and gel strength of the crosslinked polymers at elevated temperature and elevated pressure conditions, as detailed in this section.

Four main sets of rheology measurements were designed to optimize the crosslinked polymer in drilling fluids formulations and capture its gelation kinetics.

- i. Drilling fluids rheology measurements including apparent viscosity, plastic viscosity, yield point, and API gel strength.
- ii. Viscosity versus time curves to determine gelation times and onset points.
- iii. Dynamic frequency sweep tests to determine gelation time from storage modulus.
- iv. Dynamic frequency sweep tests to determine ultimate gel strength.

The automated speed dial viscometer was used for testing the drilling fluid rheological parameters. The samples were gradually heated to the desired temperature at 4°F/min under constant rotation of 100 rpm. Then the measurements were conducted at different speeds (3, 6, 100, 200, 300, and 600 rpm) corresponding to shear rates ranging from 5.1 to 1021 s⁻¹. Then the apparent viscosity (AV), plastic viscosity (PV), and yield point (YP) values were calculated. The AV is the viscosity corresponding to a specific shear rate, and according to the API, the AV is defined for the Bingham plastic rheology model as one-half of the dial reading at 600 rpm, which gives a shear rate of 1022 s⁻¹ in the speed dial viscometer. The PV is computed by determining the difference between dial reading at 600 and 300 rpm, which represents the viscosity of the fluid corresponding to an infinite shear rate. The third parameter, which is the YP is determined by the slope of the shear stress versus shear rate based on the Bingham plastic rheology model. From the

speed dial viscometer measurements, the PV is calculated by subtracting the plastic viscosity value from the dial reading at 300 rpm, expressed in pounds per 100 ft².

In the second and third sets of the rheology measurement, the gelation time was determined using two different methods: the viscosity versus time curves and the dynamic frequency sweep test. The viscosity versus time curves is one of the direct and efficient methods for gelation time determination. The apparent viscosity is measured under steady shear for an extended period to detect the point where an abrupt change in viscosity occurs. Before the test, the samples are conditioned under constant shear (170 s^{-1}) and heated gradually until the desired temperature is reached. Various polymeric formulations under different temperatures and pH conditions were tested. The experiments were carried using either the atmospheric speed dial viscometer or the steady shear HPHT rheometer with the concentric cylinder depending on the required temperature of crosslinking. The second type of gelation time experiment was conducted using the HPHT rheometer with the parallel plates by calculating the storage modulus by applying a constant frequency (10 Hz) while fixing the strain percentage to 10%. Like the viscosity versus time, the storage modulus will exhibit a sudden increase in its magnitude when gel formulates, which will directly and accurately give the gelation time.

Finally, in the fourth set of the rheology measurements, the ultimate gel strength was obtained for each sample by conducting frequency sweep tests using the parallel plates HPHT rheometer. During the frequency sweep test, the strain was fixed at 10 %, intentionally selected within the linear viscoelastic region of the weakest polymer sample. The frequency was varied in the range between 0.25 to 100 Hz. The storage modulus (G') and loss modulus (G'') were collected through the test, which are indicators for the solid and liquid phases of the gel before and after the gelation occurs. In other words, the loss modulus (G'') is a measurement of the viscous liquid phase

of the fluid, while the storage modulus represents the elastic behavior of the produced gel and the amount of stored energy in the system. High storage modulus increases the pressure which the gel can withstand before fracture reopens.

4.2.4.2 Static and Dynamic Drilling Fluid Loss and Filtration

Static mud filtration provides information on loss control and LCM performance when drilling is stopped. It can be conducted at low pressure, low temperature (LPLT), or elevated pressure, elevated temperature conditions which is the one used in this study. Various testing methods are available to assess the performance of LCMs under reservoir conditions, using a cell where the bridging materials can be poured and pushed against a filter medium or slotted disk. In this study, the static testing apparatus or the permeability plugging apparatus (PPA) is used. The PPA is a modified high temperature filtration test capable of testing various porous mediums, rock cores, and artificial fractures at pre-determined testing conditions, up to 5000 psi and 500°F. A larger LCM receiver modifies the PPA to handle a larger LCM size to avoid plugging part of the testing apparatus and not the slotted disks.

Figure 4.4 illustrates the PPA schematic with the aluminum disk; also, carbonate cores were used similarly. The fluid is placed inside the PPA cell and pressurized at 1000 psi before being heated to the desired temperature, mainly the onset crosslinking temperature of the polymer. After the sample is conditioned, the flow is encouraged by controlling the top back pressure valve. The progress of filtration with time is recorded for up to 30 minutes. More time was given, if necessary, for the gelation study. The static filtration experiments were conducted under a differential pressure of 500 psi across the disks and different temperature conditions. During the test, and to evaluate the sealing efficiency, the pressure is increased gradually to obtain the maximum sealing and measure the fluid loss volume. The LCM's performance is assessed by the

time taken to develop the plug, if any, the amount of lost fluid, and the maximum sealing pressure. If a sealing pressure of 1000 psi is achieved, the filtrate volume is monitored for another 10 minutes.

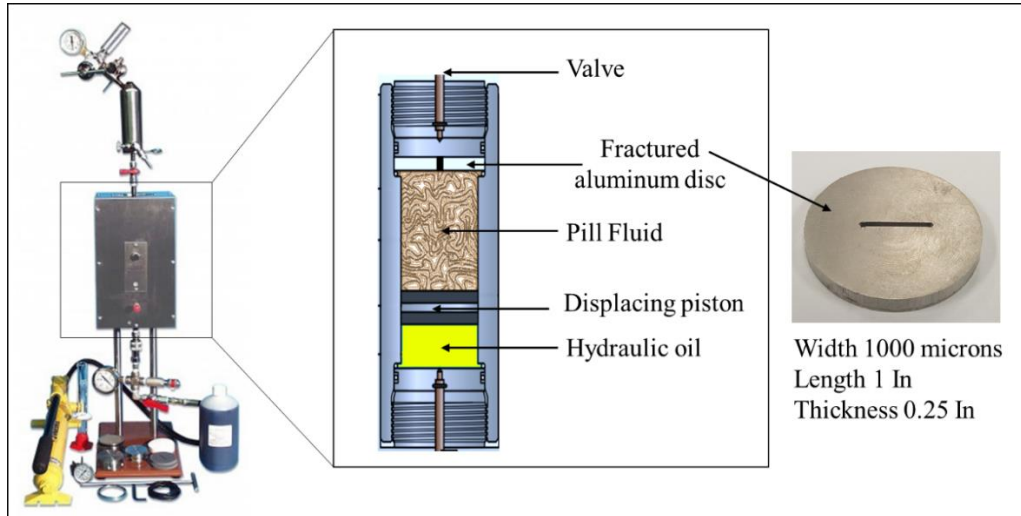


Figure 4. 4: Schematic of the permeability plugging tester (PPA) and the fractured aluminum disk.

Furthermore, a dynamic filtration test was conducted using the dynamic drilling simulator. The dynamic drilling simulator provides a method of mimicking radial filtration under downhole conditions. The one used in this study is the dynamic wellbore strengthening simulators model M2200 shown in Figure 4.5. The rotational shaft has the option of including a drill bit to simulate the drilling operation. At the end of the test, the wellbore strengthening is evaluated by the LCM's maximum sealing pressure and the amount of fluid loss.

The simulator is designed to hold a cylindrical-shaped porous medium and simulates fractures with different sizes and orientations. The testing cylinders' dimensions are 1.51 inches outer diameter, 1-inch inner diameter, and 1.105 inches height. Figure 4.6 shows the fractured cylindrical-shaped aluminum used for this test. A mud volume of 350 cm³ was poured inside the cell, and back pressure was applied before conditioning the sample to the pre-determined temperature. During the experiment, the cylindrical filtration medium was held inside the core

holder, and the rotating shaft is centered through the holder. The filtrates are collected through a hose to an automatic collection system. The collection system is coupled with software handling the testing conditions and data collection as per API standard filtration time recommendations.



Figure 4. 5: M2200 dynamic drilling simulator, modified after (Ezeakacha and Salehi 2019a).

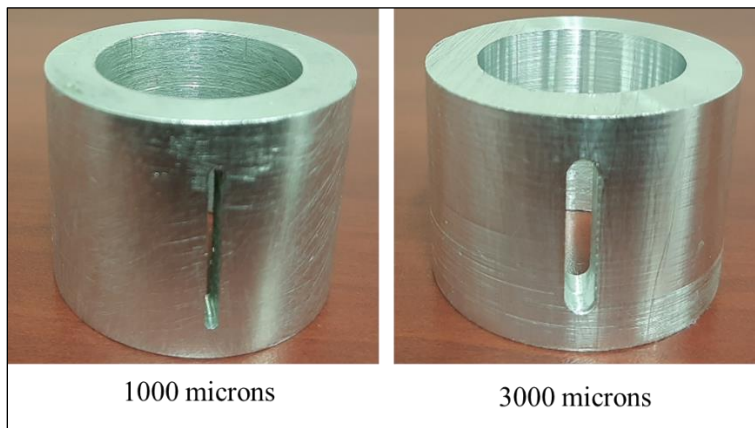


Figure 4. 6: Fractured cylindrical wellbore-shaped aluminum.

4.2.4.3 Post-Experimental Investigations

The post-experimental investigations carried out were the internal and external filter cack evolution examination, filter cake composition analysis, and the status of the gel plug on the fractures. Scanning electron microscope (SEM) images were used to examine the filter cakes, and Energy-Dispersive X-ray (EDX) analysis was used to identify the elemental composition. After

the filtration experiments, the core or aluminum filter disks were examined visually to check the placement of the gel plug. The imaging techniques were included as an essential part of LCM evaluation for two reasons. First, the sealing mechanisms require visualization to define the bridging patterns and pores and fracture filling mechanism. The second is to evaluate the effect of LCM on formation damage.

In this study, the investigation of filter cake evolution was introduced to expand the evaluation of these polymeric gels as LCMs. The goal was to evaluate the invasion of the polymer into the near-wellbore area and the possible risk of formation damage. Moreover, SEM imaging was used to study how crosslinked polymer activates and forms a gel inside the formation's pores. Figure 4.7 shows the process of preparing the cores for the SEM imaging analysis after the filtration experiments. The disks were cut into two halves, then the extra gel is removed from the top, and the filtration direction is marked. The internal filter cake analysis is taken at the indicated spot (a), and the external filter cake is taken from the spot (b), as described in Figure 4.7.

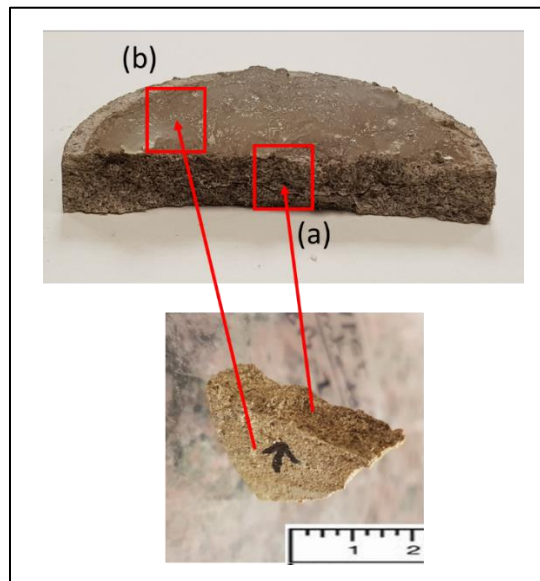


Figure 4. 7: Preparation of filter disks for SEM and EDX post-experimental analysis.

4.2.4.4 *Gel Solubility Test*

After treating the loss zone, the filter cake needs to be cleaned before the production phase to avoid damage and productivity reduction. Also, the cementing job may fail with an insufficient removal of the filter cake. Therefore, part of the LCM evaluation in this study was removing filter cake formed by the polymeric gels. The gel is collected from the filter cake evolved after the static filtration on rock cores and fractured aluminum disks. Then different concentrations of ammonium chloride solutions were prepared for the gel solubility test.

Breaking of the gel was evaluated visually by adding pieces of the gel collected from the filter cake to the ammonium chloride solutions and observing the gel's dissolving with time. Graduated cylinders were used to mark the phase separation and the suspension of the gel after being dissolved. All tests were conducted at atmospheric conditions after the gel is cooled down.

4.2.4.5 *Zeta Potential (ZP)*

The zeta potential is a method of assessing the stability of colloidal crosslinkers in aqueous solutions expressed in millivolts (mV). The magnitude of the zeta potential's absolute value reflects the electric double layer surrounding the particles in the suspended system. High magnitudes, negative or positive voltages indicate high suspension stability. The measurements were conducted at room temperature by using a Nanosizer instrument. Samples were homogenized before diluted to 5 vol.% to make sure it contains enough suspended particles for the measurement. Then the pH of the fluid was adjusted as needed.

4.3 Machine Learning Approach

The application of machine learning (ML) in the design of drilling fluids has recently attracted more attention. This part investigates ML techniques to evaluate the components that control the rheology of crosslinked polymer-based muds. Data science implies using knowledge extracted

through systematic studies by conducting statistical analysis to understand parameters' weight and interference. The machine learning (ML) approach surpasses conventional statistical analysis in many ways; for example, analyzing heterogeneous and unstructured data requires defining the complicated relationship between different entities, which is possible by machine learning (Dhar 2013). The use of the experimental framework, in combination with ML's predictive ability, can be used to develop a preventive strategy for an efficient drilling operation.

In this study, machine learning (ML) was used to develop a framework to identify materials composition based on the desired rheological characteristics. The framework aims to assess the relationship between rheology and mud components for polyacrylamide/crosslinker-based mud. Four different ML algorithms were implemented to model the rheological data for various mud components at different concentrations and testing conditions. These four algorithms include: (a) k-Nearest Neighbor, (b) Random Forest, (c) Gradient Boosting, and (d) Ada-Boosting.

The k-Nearest Neighbor (kNN) model is one of the most common regression models based on the k-nearest neighbors' algorithm. This algorithm can be used in combination with other mathematical rules to test the predictive capability. Apart from other industries, the petroleum industry is frequently implementing kNN algorithms for prediction applications. For example, some studies utilized different machine learning algorithms, including kNN, to predict reservoir fluid properties (Onwuchekwa 2018). The success of this regression model is highly dependent on the distance metrics from the nearest neighbors. After identifying the desired nearest neighbors, the predictive value for input data will be the mean output of the identified samples.

The second algorithm used here is the random forest (RF) algorithm, which is a robust supervised machine learning algorithm, consists of various combinations of decision trees. Sometimes, one decision tree algorithm can produce inaccurate results due to variability and over-

adaptation of the predictions. Thus to overcome this abnormality, a set of decision trees is framed, and the final predictions are produced from the average values of all decision trees (Belyadi et al. 2019). This RF regression model improves individual estimator performance by adopting an ensemble-based combined performance strategy (Dietterich 2000; Breiman 1996). An example of employing RF algorithm prediction applications in the oil and gas industry is predicting the drilling penetration rate from operational and lithology data (Hegde et al. 2015).

Breiman (2001) built a set of decision trees based on nonparametric regression estimation for random forest modeling. A predictor is employed, which consists of a collection of randomized regression trees. The predictor estimate for the regression is defined by the following equation (Breiman 2001):

$$m_{M,n}(\mathbf{X}; \theta_1, \theta_2, \dots, \theta_M, D_n) = \frac{1}{M} \sum_{j=1}^M \sum_{i \in D_n^*(\theta_j)} \frac{1_{X_i \in A_n(x; \theta_j, D_n)} Y_i}{N_n(\mathbf{X}; \theta_j, D_n)} \quad (1)$$

Equation 1 gives the predicted values for the number of trees (j^{th}) at the query point x . The prediction uses the independent random variables of the training sample expressed as D_n , which is related to the variable number (n). The predicted value at (x) is denoted by $m_{M,n}(\mathbf{X}; \theta_1, \theta_2, \dots, \theta_M, D_n)$ where $\theta_1, \theta_2, \dots, \theta_M$ are independent random variables for each query point (x) located at m and n order. These are randomly distributed and independent of the training sample variable (D_n). A_n represents the set of data points selected before tree construction and expressed in the form of a matrix where $A_n(x; \theta_j, D_n)$ denotes the cell containing the query point x . The number (N_n) of the cell that falls into the query point is expressed by the term $N_n(\mathbf{X}; \theta_j, D_n)$. Equation 1 also uses the output data point (Y_i), related to the query point (X_i), to generate the predictions.

The error in RF predictions depends on the correlation between any two nodes in the forest and individual nodes' strength. The higher correlation between nodes leads to a higher error rate,

while greater strength reflects the reduction of error, which is affected by the size of the subset of the variables used in tree building. The central theme of RF is to improve the reduction in the variance of bagging by reducing the correlation between the nodes without a substantial increase in the variance. This can be achieved by growing the nodes through a random selection of the input variables (Breiman 2001). The decision tree can be expanded to its maximum depth using a combination of features from the input parameters. RF also helps rank the features conducive to prediction estimates; however, we have only seven different input parameters. Therefore, we have solely focused on testing the accuracy of the test dataset.

The third algorithm is the Gradient boosting (GB), which is another type of ensemble supervised machine learning program that utilizes an additive model in a forward stage-wise fashion (Rajadurai and Gandhi 2020). Like the RF, the GB also uses decision trees as a fundamental building block for an ensemble of weak models (Friedman 2002). It uses an individual weak complementary regressor in sequence. A new weak learner is constructed to provide maximum correlation with the negative gradient of loss functions at each stage of iterations (Natekin and Knoll 2013). After these loss functions are implemented, a strategy like the artificial neural network is adopted. One of GB's common loss functions is logistic regression, which is the one used in this study (Friedman 2001; Hastie et al. 2009). A decision tree is then used to make a prediction based on a series of rules that consist of different nodes. The difference between prediction and actual values describes the error rate. This error rate is represented as a gradient, which is the partial derivative of the loss function. The gradient is used to minimize the error for the next round of training. The extreme gradient boosting accelerates tree construction and uses a new algorithm for tree searching (Torlay et al. 2017).

Finally, the AdaBoost algorithm was also used. This algorithm is inspired by numerical optimization, and statistical estimation uses a sequence of a simple weighted weak base classifier to construct a strong classifier. In each step, it attempts to find the optimal estimator as per weight distribution. Each estimator's performance defines its weight in the next iteration, and finally, accurate predictors get more weightage (Freund and Schapire 1996; Freund and Shapire 1997).

Figure 4.8 shows the broad framework for the ML approach prepared for this study. The workflow is constructed to automate the process of identifying suitable drilling fluid for field applications. First, the desired rheological properties will be defined for each specific drilling condition. After that, the machine learning models are used to determine the amount of materials required to achieve these rheological properties.

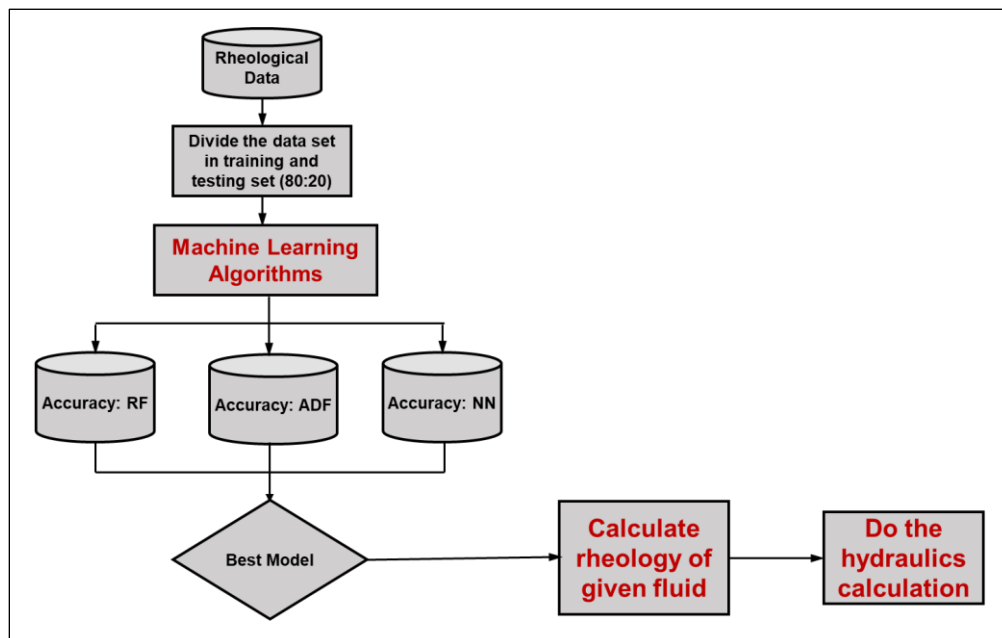


Figure 4. 8: Workflow of the ML study.

The experimental data and rheological properties are used for the training and testing stage to build the ML models. The experimental data is used as input, consisting of materials quantities, temperature, and the rheological properties such as plastic viscosity, apparent viscosity, and yield point. The dataset consisting of 284 data points was randomly split in 80:20 to train and test

different algorithms. Only one crosslinker (PEI) was used in this ML application. In addition to the polymer (PAM) and the crosslinker (PEI), other essential drilling fluids additives, including barite, caustic soda, lignite, cedar fiber, and calcium carbonate, were used. The experimental matrix was designed to investigate the dependency of the rheological properties on each component of the drilling fluid formula. Since the three main contributors to the rheology are the quantities of PAM, PEI, and bentonite, these three components were varied the most in the data set. The effect of other drilling fluid additives was incorporated using an appropriate range of concentrations for each additive. Each parameter was varied individually while keeping others constant at their optimized values. Each recipe was tested at four different temperatures. The machine learning algorithms were then used to evaluate the relationship and the rheology dependency for each fluid based on these established interrelationships. The selected materials and concentration ranges used to build the dataset are described in Table 4.8.

Table 4. 8: Mud component and their range of concentrations

| Component/ Temperature | Concentrations | | | | | | | | lb/ bbl | Weight % |
|---------------------------------------|----------------|------------|--------------|-----|-----|------|-----|------|------------|---------------|
| | 5 | 6 | 7 | 7.5 | 8 | 9 | 10 | 12.5 | | |
| PAM (lb/bbl) | 5 | 6 | 7 | 7.5 | 8 | 9 | 10 | 12.5 | 17 - 44 | 5 - 12.5 |
| PEI wt.% (lb/bbl) | 0 | 0.25 | 0.5 | 0.8 | 1 | 1.25 | 1.5 | | 0.8 - 5 | 0.25 - 1.5 |
| Bentonite wt.% (lb/bbl) | 1 | 2 | 2.5 | 3 | 3.5 | 4 | 5 | | 0 - 5 | 0 - 1.5 |
| Caustic soda (lb/bbl) | 0 | 0.5 | 1 | 1.5 | | | | | 0 - 1.5 | 0 - 0.4 |
| Mud weight (ppg) / Barite (lb/bbl) | 9.5 / 10 | 10 / 54 | 11.5 / 90 | | | | | | 10 - 90 | 2 to 30 |
| Fiber (lb/bbl) | 0 | 5 | 10 | | | | | | 0 - 15 | 3.5 |
| Temperature (°F) | 70 | 120 | 160 | 200 | | | | | | |

Chapter 5: Experimental Results and Discussions

In this chapter, an optimized formulation of flowing gel for loss circulation treatment is described. A screening criterion for selecting the proper range of PAM molecular weight and optimized mud formulation is provided. The results of rheology and stability of mixing with drilling fluids additives are discussed for several combinations of polymers and additives. This chapter also contains the results of the gelation study and sealing efficiency using static and dynamic filtrations experiments and filter cake investigations.

5.1 Optimization of Polymeric Gel Formulation

The most critical design factors of any gel system intended for loss circulation treatment are the rheological properties, the gelation time, the onset temperature, and the final gel strength. Each of these characteristics of the LCM gel system plays a vital role in the treatment process. For example, the system's rheology affects the pumping requirement, friction loss, and annular pressure losses, which affect the ECD. The gelation time, which corresponds to the end of the transition state, directly affects the gel placing process. The goal is to have an optimized gel system that can provide enough time for the gel to be placed into the targeted depth. Furthermore, the gel strength of the final gel gives the sealing pressure and enhances the wellbore strength. A proper amount of polymer, crosslinker, retarders, and mud additives will result in an optimized gel system that can meet the LCM application requirements.

Many researchers conducted screening studies on the polymeric gel system components for various oil and gas industry applications (Trifunoski and Mostofi 2020; Elkatatny et al. 2020; Amir et al. 2018; Reddy 2014). The laboratory results and field experience revealed that suitable rheological properties and gel characteristics could be optimized through various controlling elements. For instance, the polymer works as the primary viscosity builder. The crosslinkers and

pH control agents control the gel strength and onset point, while salts and temperature control gelation rate. Amir et al. (2018) conducted an optimization study of PAM/PEI gels for reservoir conformance control. They concluded that the crosslinked polymer's optimum formulation is 1.5 wt.% of PAM and 0.3 wt.% of PEI. The results presented in Amir et al. (2018) demonstrated the relationship between PAM and PEI concentrations and their gelation time. The authors were able to control the gelation from 10 minutes up to 80 minutes. The following sections explain the optimization and gelation studies conducted in this work to develop the polymer-based drilling fluid formulation using different organic and inorganic crosslinkers.

5.1.1 Rheological Screening of Non-Cross-Linked Polyacrylamide

The rheology of LCM in drilling fluid and LCM pills plays a critical role in the treatment operation and its success. The rheology parameters influence LCM performance since it governs the flow of drilling fluids into the well and through the fractures and porous surrounding rocks. First, the rheological measurements were used to select the most suitable PAM system from the three average molecular weights chosen to prepare the polymer bases fluid. Testing these three polymers at a temperature range from surface temperature up to 205°F (21 to 96°C) gave an idea of the molecular weight range suitable for LCM gel application. The results of viscosity-temperature curves for 10 wt.% solutions prepared with non-crosslinked PAM demonstrated the effect of temperature on the viscosity for the different PAM batches. The results were compared with a typical 9.6 ppg WBM (Ref.Mud#2) containing 55 lb/bbl calcium carbonate as LCM; the complete formulation is given in Table 4.2 in section 4.2.1. Figure 5.1 shows the temperature dependency of the viscosities where similar trends are observed for the three PAM samples; however, the magnitude increases with the molecular weight. The PAM yielded final viscosities of 50, 40, and 24 mPa.s for the high, medium, and low molecular weight polymers, respectively, while the typical mud showed relatively constant viscosity at 40 mPa.s. Based on this result, the medium molecular

weight seems to be the better choice. However, looking at the beginning of the viscosity time curve, the low-temperature viscosities were very high. Therefore, the PAM with a lower molecular weight of 200,000 Da was selected as the best candidate for this study.

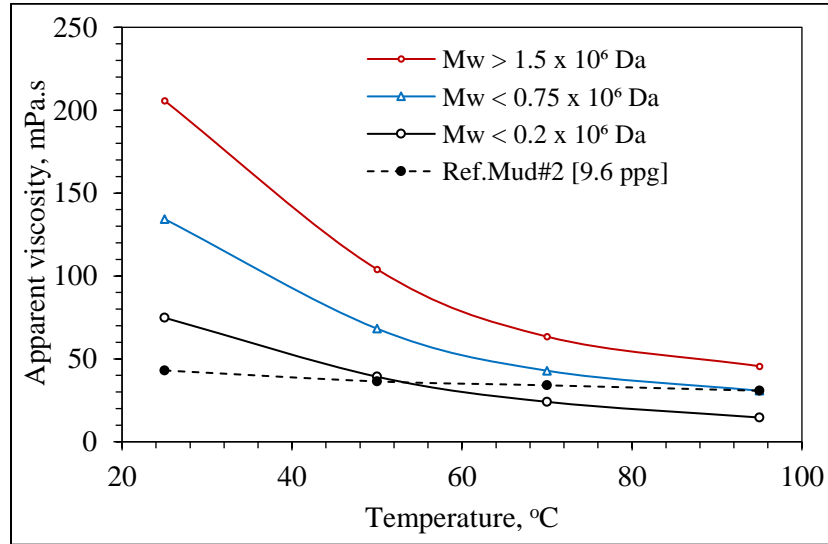


Figure 5. 1: Viscosity versus temperature for PAM samples (10 wt.%) having different molecular weights, compared to the Ref.Mud#2.

Another comparison basis was the plastic viscosity measurement. The results for the three samples, shown in Figure 5.2, agree with the viscosity-temperature results shown above in Figure 5.1. The low molecular weight PAM yielded the most matched viscosities. The high molecular weight samples showed approximately seven times the reference mud's plastic viscosity (Ref. Mud#2). In drilling fluids, suitable plastic viscosity is required to achieve high drilling rates and to avoid pumping difficulties with an increase in energy consumption. The effect of molecular weight is also expected to be more pronounced when the polymer is crosslinked with the PEI, which will develop a very high apparent and plastic viscosity and gel strength at low temperatures. Unless a proper Mw of the PAM is selected, this will result in a non-flexible mud design with minimal additives tolerance and difficulties in the mixing and handling process. Therefore, the polymer with the lower molecular weight is selected for this study for further investigations.

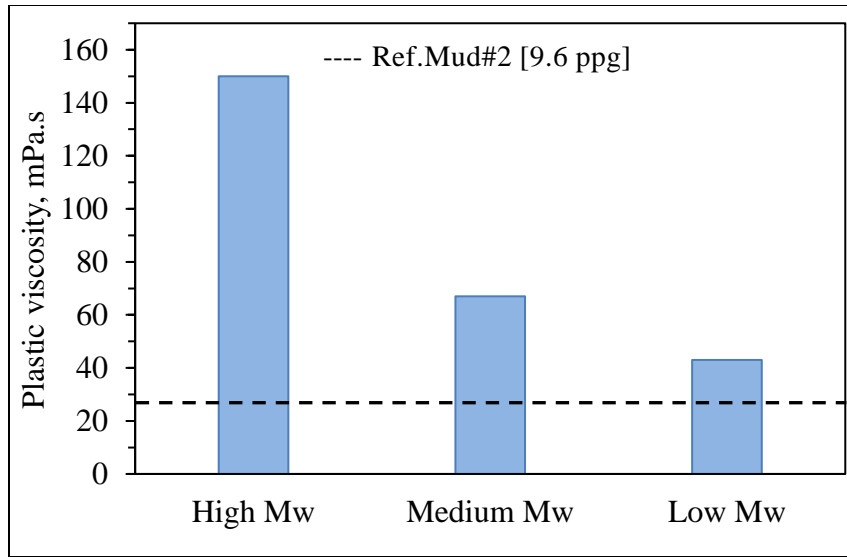


Figure 5. 2: Plastic viscosities of PAM samples (10 wt.%) of different molecular weights, compared to the Ref.Mud#2.

After the polymer system was selected, the optimization was taken to the next step, optimizing the polymer base fluid concentration. Optimization aims to provide reasonable viscosities for the PAM/PEI system and other crosslinkers for drilling fluid application. Besides, optimization aim at minimizing the friction loss and ECD. The gel system was prepared from the selected low molecular PAM in a concentration varied from 5 to 12 wt.% to get the optimum PAM concentration. These concentrations were chosen to represent a wide range of viscosity above and below the typical drilling fluid viscosity. The effect on viscosity was projected through viscosity-time curves measured at shear rates of 170 s^{-1} , as shown in Figure 5.3. A quick conclusion from these measurements is that the polymer gel system's rheology is flexible and easy to control by selecting a proper concentration.

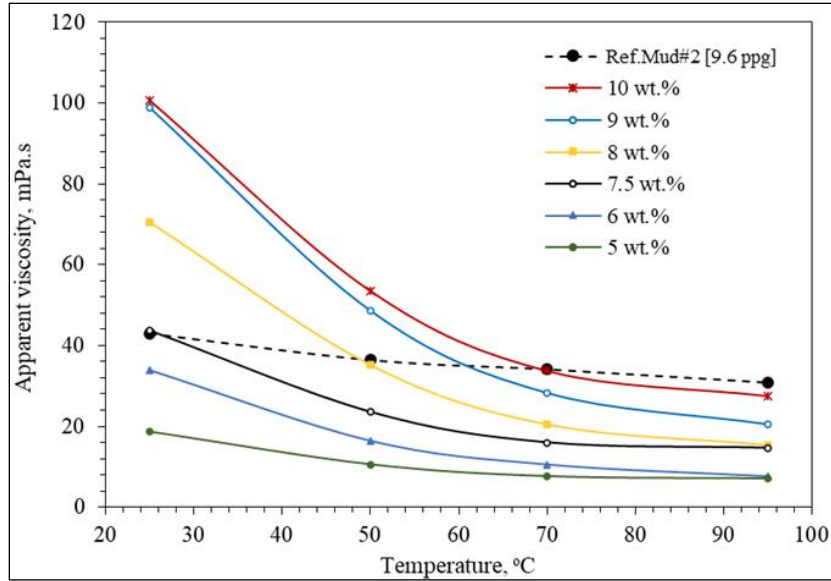


Figure 5. 3: Viscosity versus temperature of the low molecular weight PAM at different concentrations, compared to the Ref.Mud#2.

Figure 5.4 presents the results of apparent viscosity measurements for the same range of concentrations obtained from the viscometer readings at 75°F and 200°F (24°C and 93°C). As demonstrated in the results, the PAM concentration increases the apparent viscosity almost exponentially. This concentration, which represents the initial viscosity before the gel formation, is essential when designing the PAM-based formulas. Also, drilling fluids' viscosity needs to be optimized to avoid hole cleaning problems and at the same time prevent pumping difficulties or lost circulation due to high equivalent circulation density ECD at high viscosities.

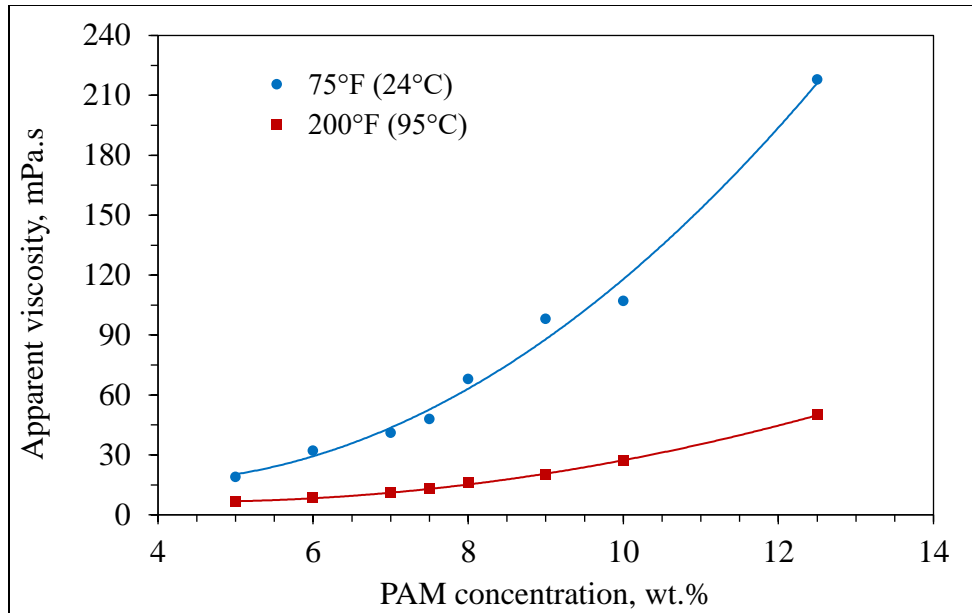
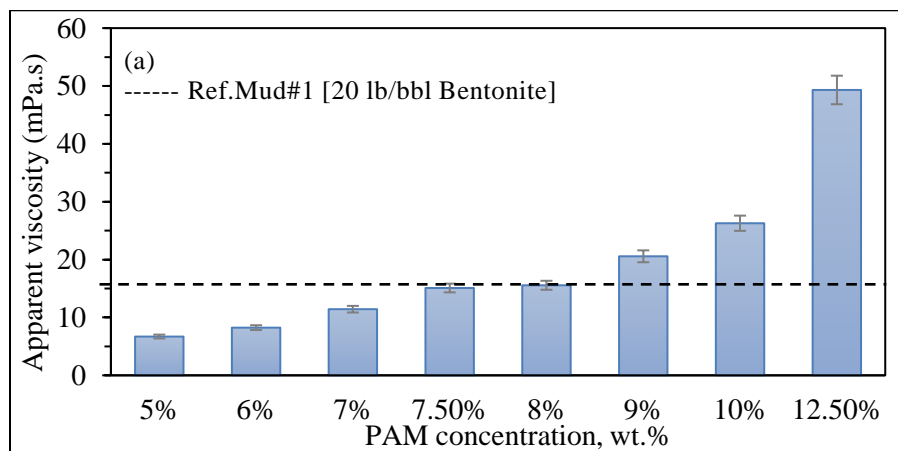


Figure 5. 4: Viscosity of PAM (<math><2 \times 10^5 \text{ Da}</math>) with different concentrations at 75°F and 200°F.

Hence, the apparent viscosity, plastic viscosity, and yield point values were obtained from the viscometer dial readings at 200°F (93°C). The results are compared with the reference basic mud (Ref.Mud#1), as shown in Figure 5.5a, b, and c. For apparent and plastic viscosities, the best matching results were obtained when the PAM concentration of 7.5 wt.% is used. The yield point was very low at all concentrations; however, this will be improved with more additives, as will be shown in the following sections.



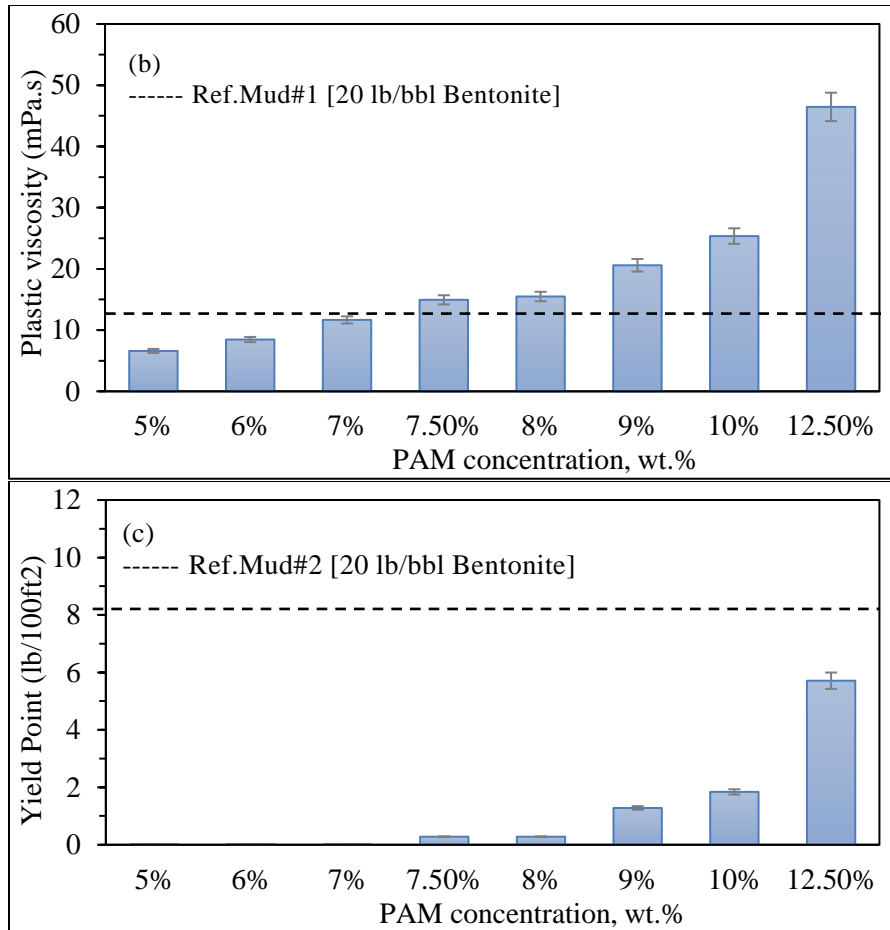


Figure 5. 5: The (a) AV, (b) PV, and (c) YP of the low molecular weight PAM at different concentrations compared with Ref.Mud#1 at 200°F.

5.1.2 Optimization of crosslinkers in the polymeric gel formulation

The next step in the polymeric LCM gel formulation is to crosslink the polymer with the proper amount of the crosslinker. Based on the previously discussed result, the viscosity of PAM solutions is directly influenced by their molecular weight and concentration. The higher concentration accelerates the gelation process, while long chains of the high Mw polymers promote the interactions and lead to more entanglements between the polymer and the crosslinker.

For optimizing the crosslinker concentration, the viscosity versus time curve was used to see how the crosslinker and other drilling fluid components will affect gel formation. One of the main indicators of gelation is the abrupt increase in viscosities. The increase in viscosity over time

will be reflected in the gelation time. The gelation rate is mainly governed by the amount of the crosslinker and the temperature of the formation. However, the crosslinker concentration may be limited by the required final gel strength of the mature gel, where a sufficient amount is needed to form a strong gel. Therefore, at some point, a retarder will be required to extend the gelation time.

A revisit to the screening of PAM molecular weight shows that even at a relatively low concentration of PEI, higher apparent viscosities can be obtained if PAM with a higher molecular weight is used. The effect of molecular weight on viscosity becomes more pronounced in the presence of the crosslinker. Figure 5.6 represents the viscosity results over time for the three screened polymers with low, medium, and high molecular weight. The higher molecular PAM at a constant shear rate (170 s^{-1}) showed higher viscosity magnitude overall viscosity versus time profile. Changing the temperature with time caused two trends; one decaying trend when polymers viscosity degraded with temperature, then an escalating trend after gelation occurs. Reduction in viscosity indicates that the gelation process had not been initiated yet, or the effect of temperature is more dominant than the crosslinking. The starting viscosity was 75, 145, and 200 mPa.s for the low, medium, and high molecular weight PAM, respectively. Then all viscosities decreased due heating effect down to around 30 mPa.s before gelation causes the rapid increase.

The gelation of PAM may occur even at lower than 266°F (130°C). The results showed that when the temperature was kept constant at a temperature relatively lower than the crosslinking activation temperature, the onset temperature. The gelation occurred when samples were given enough time, about 90 minutes. After the temperature was kept constant, the rate of gelation and viscosity was highly dependent on the molecular weight of the PAM. Based on these results, the crosslinked PAM with high Mw ($>1.5 \times 10^6 \text{ Da}$) yielded a very high apparent viscosity equal to more than three times the viscosity developed by the PAM of the lowest Mw. Therefore, for

suitable polymeric gel mud, the PAM with low Mw is recommended to ensure more flexibility. The high molecular weight may be used for LCM pills in very limited concentrations.

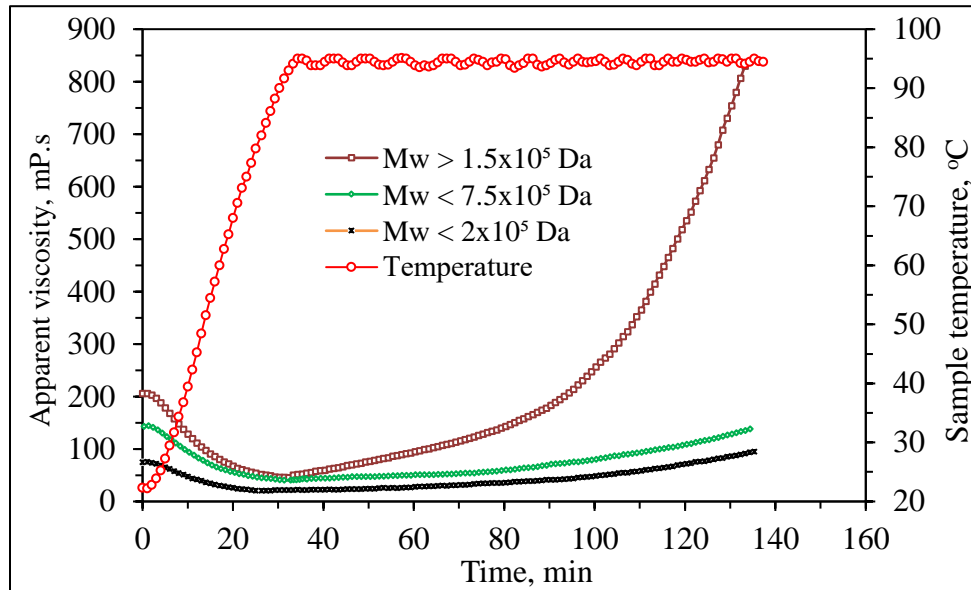


Figure 5. 6: Impact of PAM molecular weight on gelation kinetics on Salt-free water.

The following section of the results explains the development of the crosslinked polymer-based LCMs and LCM pills using different crosslinkers. The PAM with the 0.2×10^6 Da molecular weight was used in each gel formulation with other crosslinkers, the aluminum acetate, and the functionalized silica. The goal was to achieve higher gel strength with the minimum concentration of crosslinkers. This optimization serves two ultimate purposes, first provides enough gel strength for the sealing of high permeable rocks and fractured formations. The second maintains the rheological properties of the flowing gel system within an acceptable range for simple pumping requirements. Moreover, optimization of crosslinkers concentrations will keep the cost of the mud loss treatment as low as possible.

5.2 Development of Crosslinked PAM/PEI-Based Pill

Polyethylenimine (PEI) was used to crosslink the low molecular weight PAM selected from the above rheological screening study. The PAM/PEI systems are known for their wide applications

in enhanced oil production applications to shut-off highly productive water zones. The strong gel and the exceptional rheological properties allow for flexible drilling fluid formulation. This optimization study provides a rheological method for screening the crosslinked PAM/PEI-based LCM for drilling formulation to be used for corrective and preventive loss circulation treatments. Comparative analysis of rheology of crosslinked PAM with typical water-based drilling fluids formulation and proper mixing procedures is provided. The results of this optimization study can be used as a reliable tool for designing PAM/PEI-based pills and drilling fluids.

Various tests were conducted for different PEI concentrations to assess the impact of the PAM/PEI ratio on PAM crosslinking and resulted rheology. The PAM concentration was fixed at 10 wt.%, and the PEI concentration was varied from 0 to 1 wt.%. Measurements were recorded right after the sample reached 200°F (93°C) while the mixture was flowing, at the time before the gelation process impact the results. First, the 30-minute API gel strength was measured. The results presented in Figure 5.7 showed that the gelation process was taking place as reflected in the increase of gel strength with time. The 10 sec, 10 min, and 30 min API gel strength for PEI concentrations (0.0, 0.25, 0.75, 0.5, and 1.0 wt.%) prepared in distilled water show the high impact of the PEI concentration. A substantial increase in gel strength occurred as more than 280% increase was obtained in the 30 min gelation when PEI concentration increased by 50%. At the end of the test, a rigid mature gel was observed.

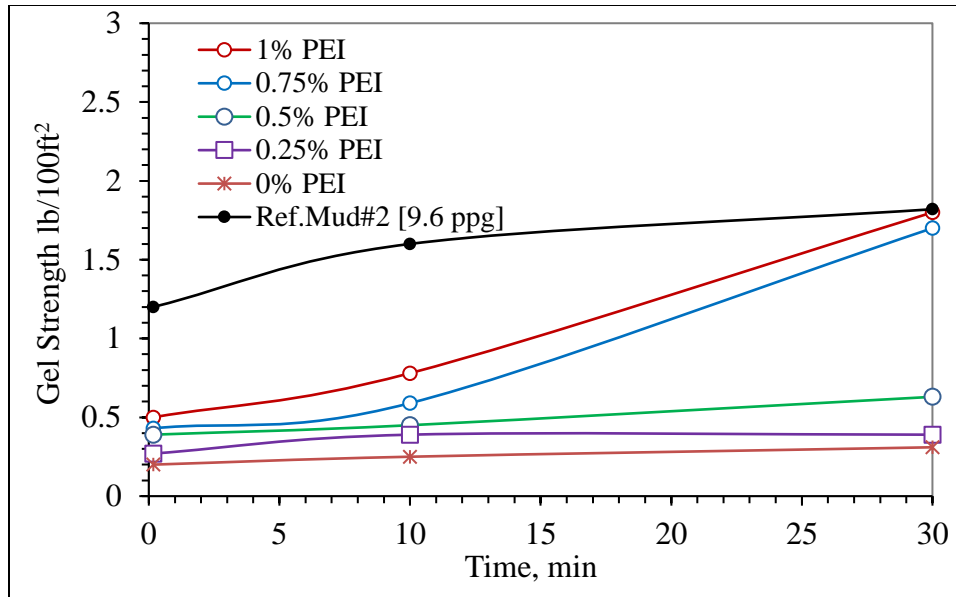


Figure 5. 7: Effect of crosslinking with PEI on gel strength of 10 wt.% PAM compared with Ref.Mud#2 at 200°F.

Furthermore, the effect of PEI concentration on AV, PV, and YP was investigated. The measurements at 200°F (93°C) revealed the same conclusion that PEI has little impact on the rheology of the flowing gel. The AV, PV, and YP measurements shown in Figure 5.8 reveal that the viscosity of the PAM solution exhibited a slight increase with PEI addition. This little impact indicates that PEI is a gel strength controlling parameter rather than a viscosity modifier since the viscosity only increased by less than 50% with a 100% increasing in PEI. However, in comparison with the water-based reference mud (Ref.Mud#1), the PAM/PEI system rheology is still competent. Also, the yield point increased but still below the reference value, as shown in Figure 5.8c.

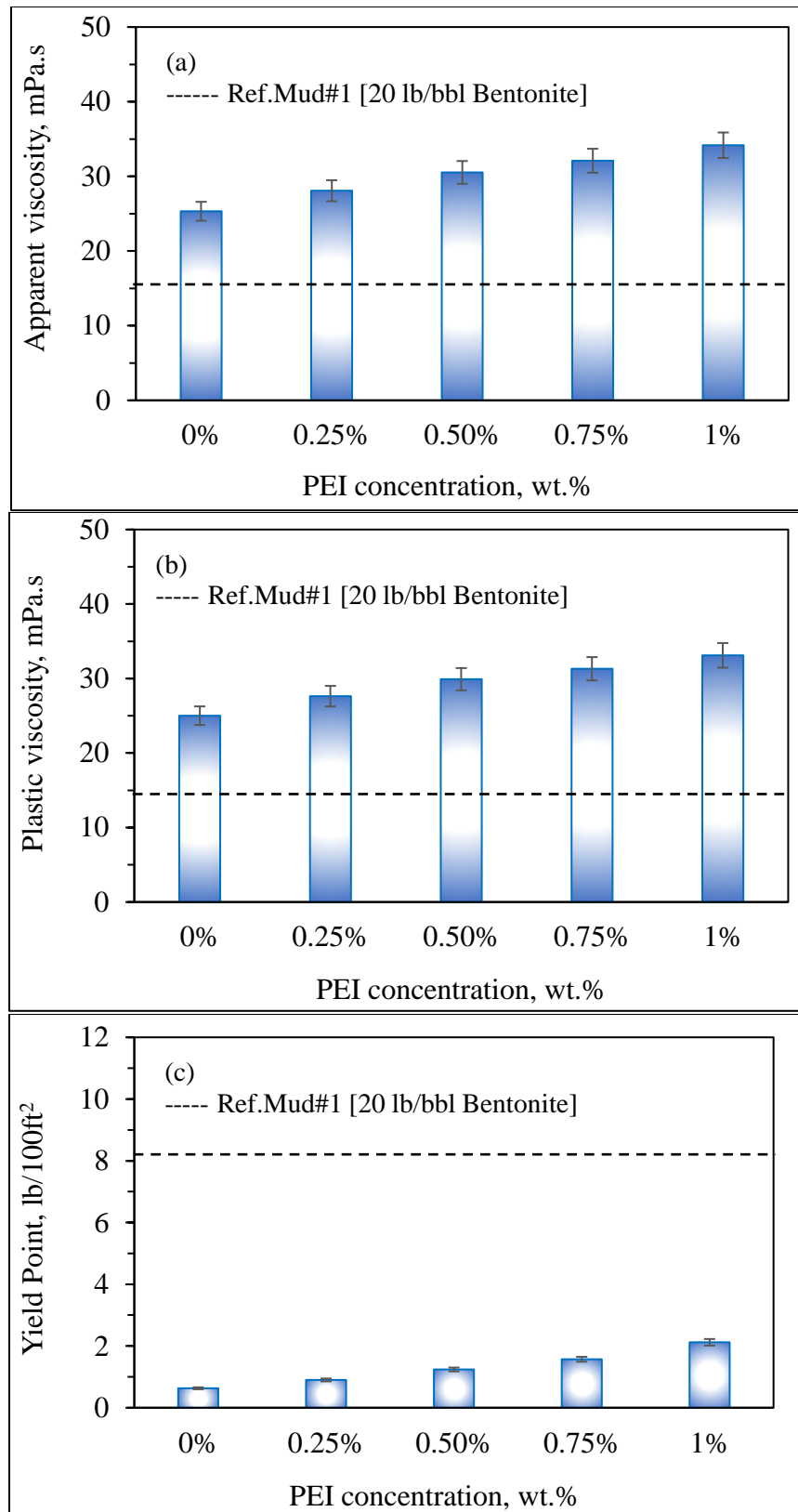


Figure 5. 8: Effect of crosslinking with PEI on AV, PV, and YP of 10 wt.% PAM compared with Ref.Mud#1 at 200°F (93°C).

The previously presented results explained the effect on PEI in the downhole condition, but the mixing and injection process takes place on the surface. Similarly, the PEI concentration showed less influence on the crosslinked PAM viscosity in surface conditions, as shown in Figure 5.9. Increasing PEI concentration by 100% only increased the system viscosity by 10% for measurement at 75°F (24°C) and is even less at higher temperatures. Again, the PEI concentration effect is more significant in the gel strength.

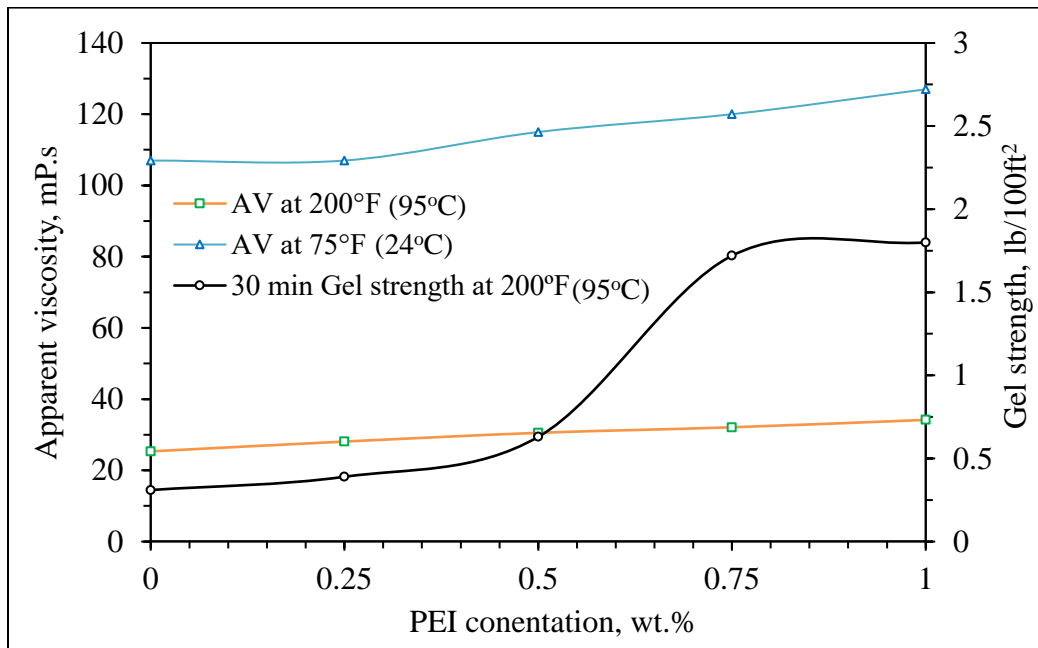


Figure 5. 9: Effect of PEI concentration on AV, PV, and Gel strength.

Since the gelation process is time-dependent; therefore, viscosity versus time curves was also used in the optimization study of the PEI in the crosslinked PAM fluid. The PAM concentration was fixed at 10 wt.% by varying PEI concentration from 0 to 1 wt.%. The measurements were recorded during the graduate heating process and after the sample reached 200°F (93°C). Before reaching the on-set temperature of gelation, the PAM/PEI system was flowing. Figure 5.10a shows the time-dependent viscosity of PAM/PEI samples with different PEI concentrations (0.0 to 1.0 wt.%). The measurements were taken under a constant shear rate of

170.3 s⁻¹, while temperature gradually increased until 200°F (93°C), then kept steady. The heating is meant to reflect the gradual increase in fluid temperature while injected into the well. During the first period, while the temperature was ramped up, the apparent viscosity of PAM/PEI fluids decreased considerably from values higher than 120 mPa.s to less than 40 mPa.s. Once the temperature is kept constant, resembling that the polymeric gel has invaded the formation, the viscosity will start to build up because of the gelation process. Another observation is that the high concentration of PEI reduced the gelation time by increasing the PAM molecules' crosslinking chance, as reflected in the viscosity, which increased exponentially with time, as shown in Figure 5.10b.

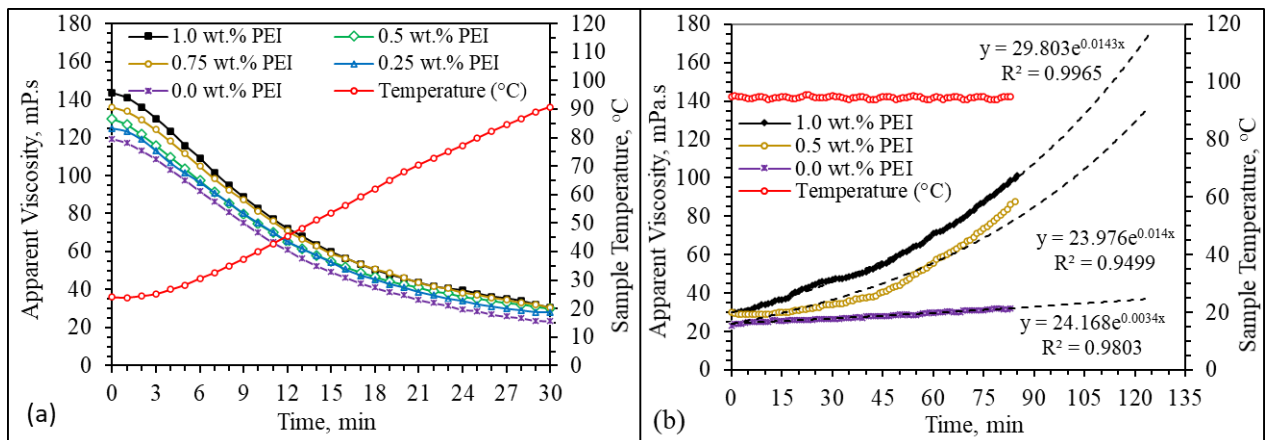


Figure 5. 10: Effect of PEI concentration on the viscosity of 7.5 wt.% PAM (a) before, and (b) after gelation starts.

As concluded from the above results, no more than 1% of PEI should be used because influence in viscosities and gel strength is insignificant beyond that. Also, the apparent viscosity was increased by less than 35% when PEI was doubled, as shown earlier in Figure 5.9. This finding was in agreement with many other reported studies where no more than 1% of PEI was recommended to give the optimal gel strength (Tessarolli et al. 2019). The extended test on fixed temperature and shear rate showed the gelation time with respect to PEI concentration. The PEI was optimized to give the maximum gel strength required for fracture sealing.

Furthermore, the dynamic shear experiments by the HPHT rheometer were used to measure the storage modulus (G') to determine the maximum gel strength that can be attained with the 1% PEI. The loss modulus also shows how the fluid is changing from liquid to solid phase. The measurements were conducted for the optimized PAM/PEI ratio (7.5:1) and yielded 540 Pa (Figure 5.11). This value was validated by the fracture sealing experiments and was more than enough for maintaining the integrity of the seal under differential pressures up to 1000 psi.

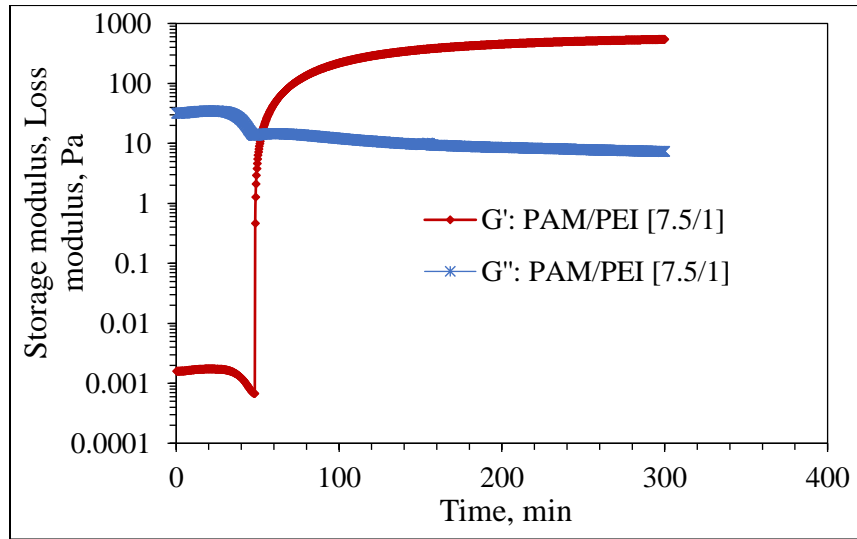


Figure 5. 11: Dynamic shear experiment for a) optimized PAM/PEI system.

5.3 Development of Crosslinked PAM/PEI-Based Mud

From the preceding results, it was observed that the viscosity of the PAM-based fluid deteriorates as temperature increases (see Figure 5.10). Therefore, small quantities of bentonite (1 to 5 lb/bbl or 0.25 to 1.24 wt.%) were added to the optimized formula (PAM/PEI [7.5 wt.%,1]) to improve its rheology, especially at elevated temperatures. The viscosity was measured at the shear rate of 170 s^{-1} , equivalent to 100 rpm in the automated speed dial viscometer. Figure 5.12 shows the measurements of viscosities at 70, 120, 160, and 200°F. There was a noticeable improvement in the viscosity of the PAM/PEI solutions with bentonite addition. For example, the viscosity of the PAM at 200°F (93°C) was doubled three times by adding 5 lb/bbl of bentonite. Measurements at

all temperature ranges conclude that the bentonite amount of 2.5 to 3.5 lb/bbl can be used to improve crosslinked PAM/PEI rheology.

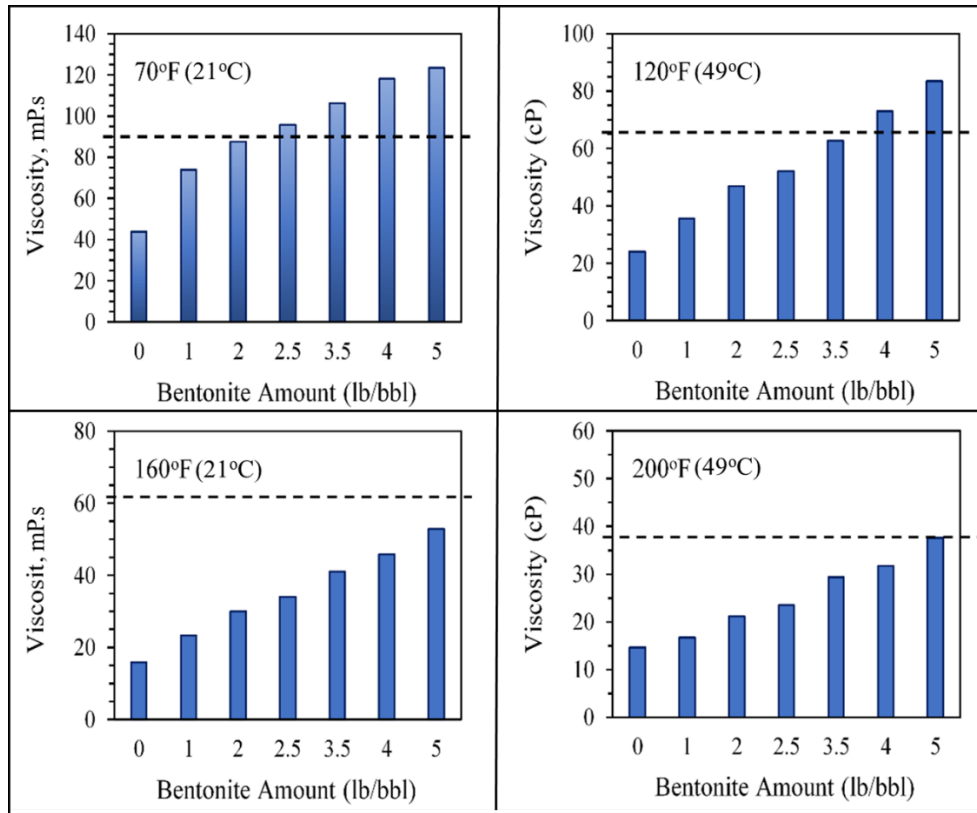


Figure 5. 12: Effect of bentonite on PAM/PEI [7.5:1] viscosity compared with the Ref.Mud#2 (indicated by the slotted lines).

Another benefit of introducing bentonite to the formula is to enhance the gel strength and plastic viscosity to improve the carrying capacity and hole cleaning capability of the polymer-based mud. The effect of bentonite was visible when API gel strength was measured with bentonite compared to Ref.Mud#1 and Ref.Mud#2, as shown in Figure 5.12. The PAM/PEI-based fluid stands alone showed low gel strength, especially before activating the gelation process. Therefore, a small amount of bentonite provides better properties and maintains good solids and cuttings suspension. With the addition of 5.0 lb/bbl of bentonite, the gel strength of the PAM/PEI fluid improved from 1.7 to 5.8 lb/100ft² compared to 5.6 lb/100ft² for the reference mud (Ref.Mud#1). Bentonite optimization, shown in Figure 5.13 showed good results at 2.5 lb/bbl of bentonite.

Similarly, the amount of 3.5 lb/bbl of bentonite in Figure 5.13 can better result in gel strength. However, with time, the crosslinking process is expected to improve the gel strength; however, 2.5 lb/bbl is still an optimized amount.

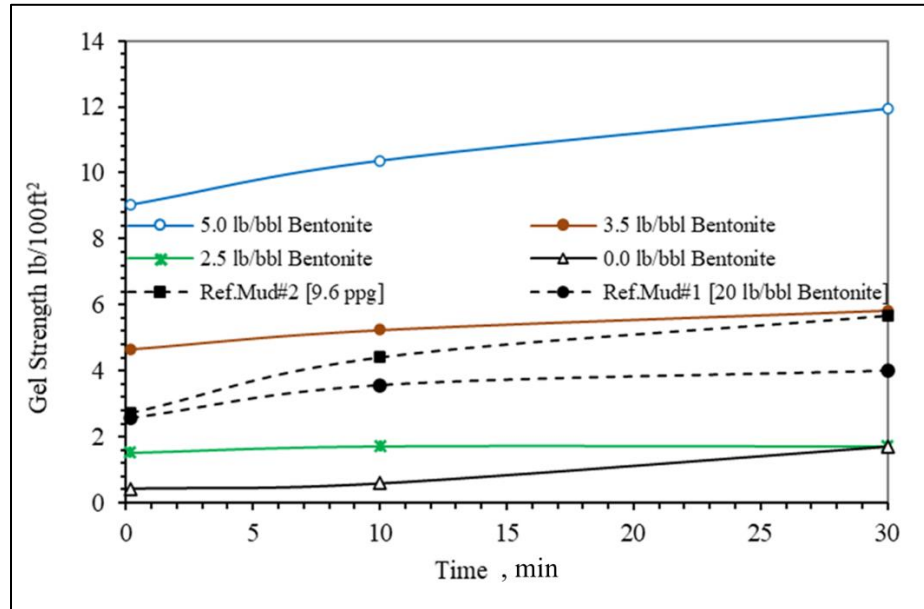


Figure 5. 13: Effect of bentonite on gel strength of 7.5 wt.% PAM/PEI compared with Ref.Mud#1 and Ref.Mud#2.

During the mixing and preparation stage, it was critical to investigate the impact of the mixing method on the stability and rheology of the polymeric formulation. The mixing order is crucial for most of the drilling fluid additives. In polymers and clays, the stability and mixture properties are highly dependent on the mixing order. Generally, if polymers are mixed first and bentonite added later, this will affect the hydration of bentonite, and it will not mix properly. The stability may also be affected by the type of PAM. Flocculation of fine colloidal particles such as bentonite may occur when cationic PAM is used due to the presence of charges [19, 20]. Although the PAM used in this study is non-ionic, some flocculation was still observed due to hydrogen bonding. However, the proper order of adding the materials and high mixing speed can solve this problem, as shown in the following section.

Different mixing orders of polymer and bentonite were tested. The amounts of bentonite were selected based on the previous rheological screening as 2.5, 3.5, and 5 lb/bbl, and the samples were prepared using distilled water with 7.5 wt.% PAM and 1 wt.% PEI.

Two different mixing orders were assessed. In the first method, bentonite was added first and slowly to the distilled water, then mixed at a speed of 5000 rpm using a high-speed mud mixer for 20 minutes before adding then PAM to the suspension followed by the PEI. The mixture was stirred for 5 minutes before testing. In the second method, the PAM and PEI were added first to the distilled water and mixed well for 5 minutes to form a 7.5 wt.% PAM/PEI solution. Then bentonite was introduced, and the mixture was mixed at high speed of 5000 rpm for 20 minutes. The measurements of viscosity versus temperature for three selected bentonite concentrations prepared by the two mixing methods are shown in Figures 6.14 and Figures 6.15. From the results, it was clear that the order of mixing has a great impact on rheology. The values of viscosity had reduced significantly when PAM/PEI was added first before bentonite is well dispersed, as shown in Figures 6.14. Overall, the viscosity versus temperature profile decreased by more than 23%, 33%, and 33% for the samples containing 2.5, 3.5, and 5 wt.% of bentonites, respectively.

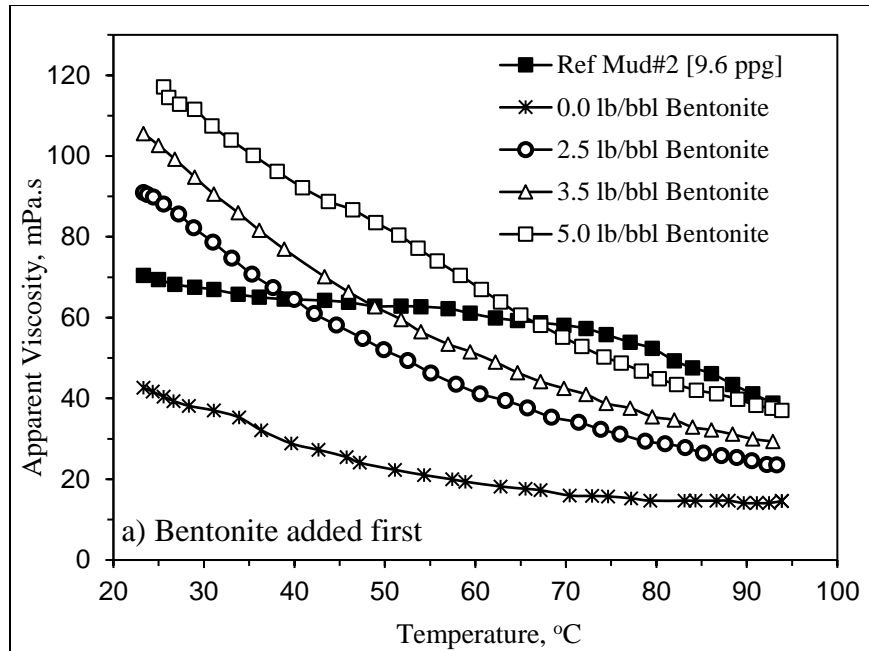


Figure 5. 14: Effect of mixing order on the viscosity of the PAM/PEI mud when Bentonite is added first.

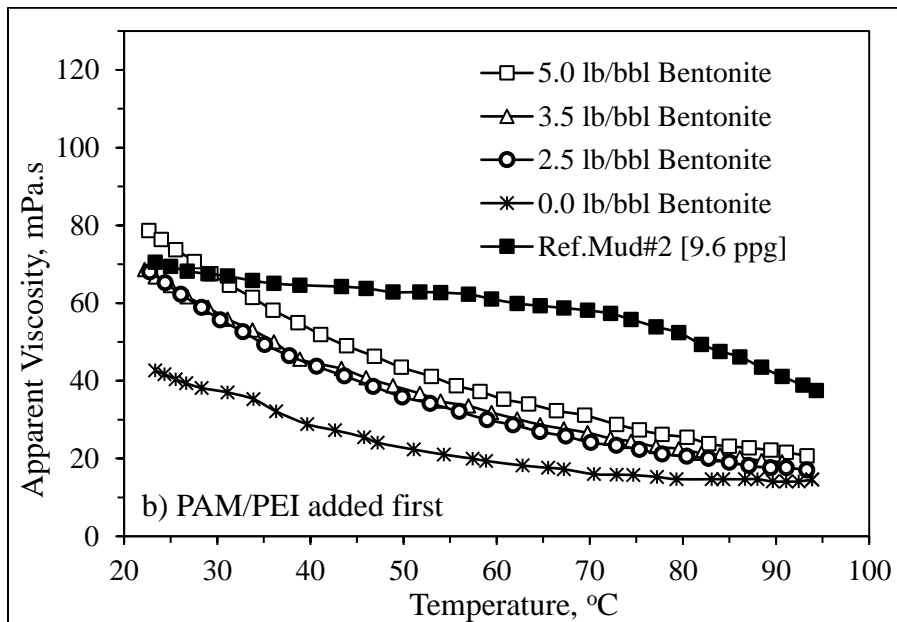


Figure 5. 15: Effect of mixing order on the viscosity of the PAM/PEI mud when PAM/PEI is added first.

Another observation on stability was recorded; when bentonite was dispersed first, the mixture was more stable, in addition to an increase in pH value from 7 to 10. Samples prepared with the "bentonite added first" method were stable for more than 14 days and showed good

swelling with aging and no separation. The sample prepared by the "PAM added first" method exhibited flocculation and particle separation within the first hour after being mixed. The same stability test was conducted using barite. Although the mixing method with barite did not affect the rheology, however, the stability was noticeably affected, and quick settling of barite was observed. This can conclude that for better stability and suspension, the barite and other drilling fluid additives should be added to a mixture of mud prepared by the “bentonite added first” method.

Finally, the crosslinked polymer-based mud (PBM) was designed using the optimized PAM/PEI system of 7.5 wt.% PAM, 1 wt.% PEI, 2.5 and 3.5 lb/bbl bentonite, caustic soda, lignite, and barite, as shown in Table 5.1. The selected mud weight was 9.6 ppg as an example of a moderate low mud weight commonly used in depleted reservoirs and low fracture gradient formations to avoid loss circulation. Figures 6.16 and 6.17 show the comparison of viscosity for the water-based mud (Ref. Mud#2) and the polymer-based mud (PBM) with and without bentonite. For muds preparation, caustic soda, deflocculant agent (Desco®), and dispersant are added, in addition to barite to increase the mud weight to 9.6 ppg (see Table 4.2 and 4.3). The rheological properties were measured at 120°F (50°C) and 200°F (93°C). These two temperatures were selected according to API recommended practice for the laboratory testing of drilling fluids for rheology and stability evaluation API RP 13B-2 (2018).

Table 5. 1: Composition of the polymer-based mud (PBM-2.5, 9.6 ppg)

| Component | lb/bbl | Weight % | Volume % |
|------------------|---------------|-----------------|-----------------|
| Water | 312.3 | 77.4 | 89.8 |
| Bentonite | 3.5 | 0.87 | 0.42 |
| PAM | 25.6 | 6.3 | 4.8 |
| PEI | 3.4 | 0.85 | 0.95 |
| Barite | 58.3 | 14.4 | 3.89 |

Figure 5.16 shows the measured apparent and plastic viscosities and yield points at 120°F (49°C). The optimized polymer-based mud showed enhanced values higher than the previous basic PAM/PEI system. Because in the mixing with mud additives, the plastic viscosity and yield point have improved due to the addition of more dispersed solids inside the PAM/PEI. This improvement was more evident when samples were tested at elevated temperature (200°F), the polymer-based mud rheology parameters did not deteriorate with heating and sustained the required rheological properties, as shown in Figure 5.17.

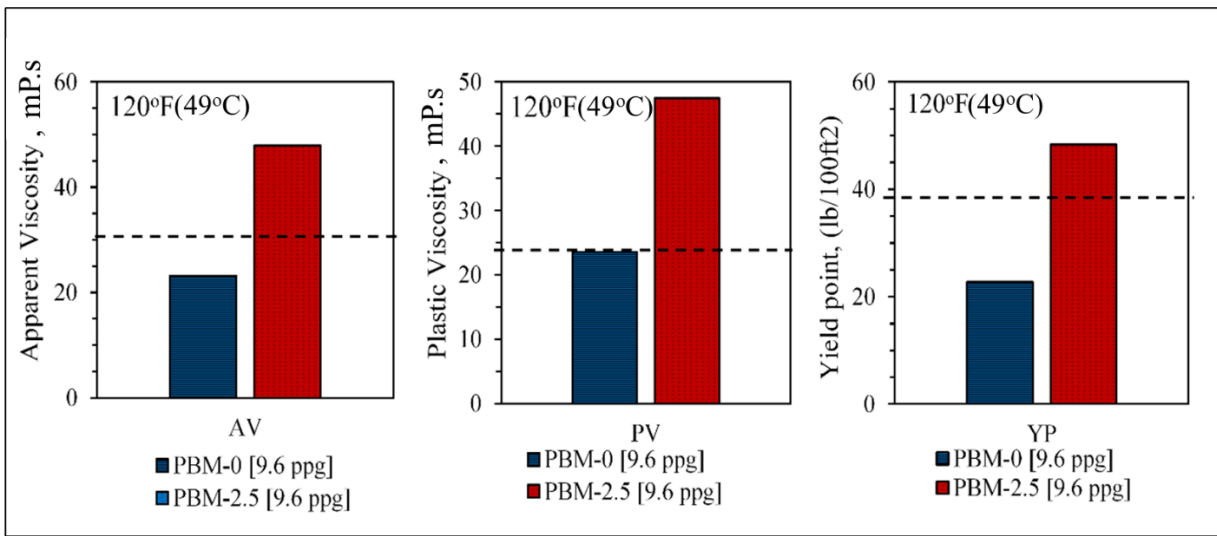


Figure 5. 16: AV, PV, and YP of the optimized polymer-based mud at 120°F compared with Ref. Mud#2 (illustrated by the slotted line).

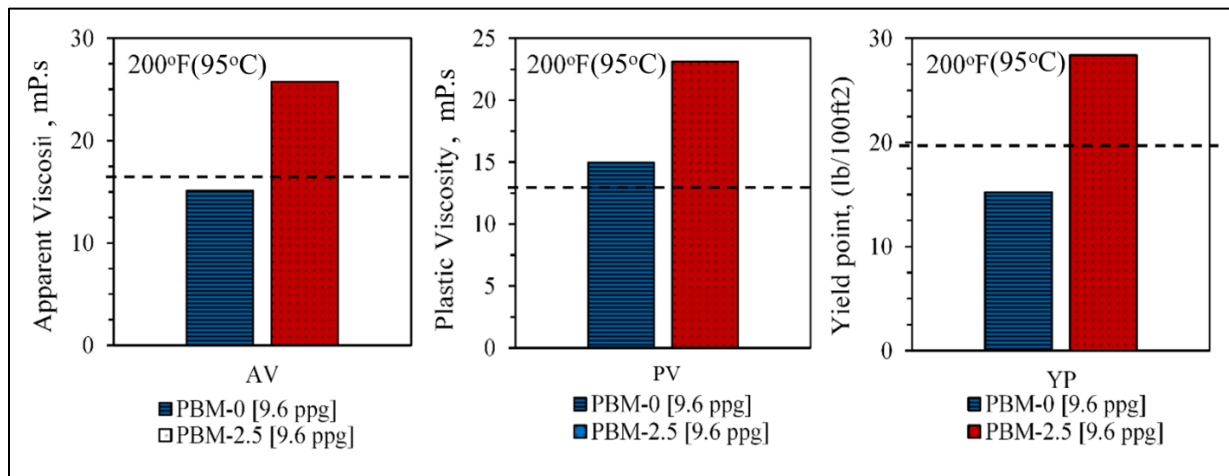


Figure 5. 17: AV, PV, and YP of the optimized polymer-based mud at 200°F compared with Ref.Mud#2 (illustrated by the slotted line).

5.4 Development of Crosslinked PAM/AlAc-Based Pill

The polymeric LCM pill formulated with aluminum acetate as a crosslinker was prepared by mixing the PAM with the proper amount of aluminum acetate to produce a pumpable and gelation-controlled fluid. For the optimization study, the various concentration of aluminum acetate was added to the 7.5 wt.% PAM to make the gel, and several rheological measurements were conducted. The first set of experiments were the gel strength or storage modulus (G'), which reflects the solid-like behavior of the gel and quantifies the maturity of the rigid gel. The G' was extracted from the dynamic frequency sweep test, and the final value is considered the gel strength. Figure 5.18 illustrates the final gel strength for PAM samples with varying crosslinker concentrations (AlAc) from 1 to 5 wt.%, at a fixed temperature of 130°C (266°F) without pH alterations. The gel strength appears to increase with AlAc addition until 3 wt.%, then no significant change was observed.

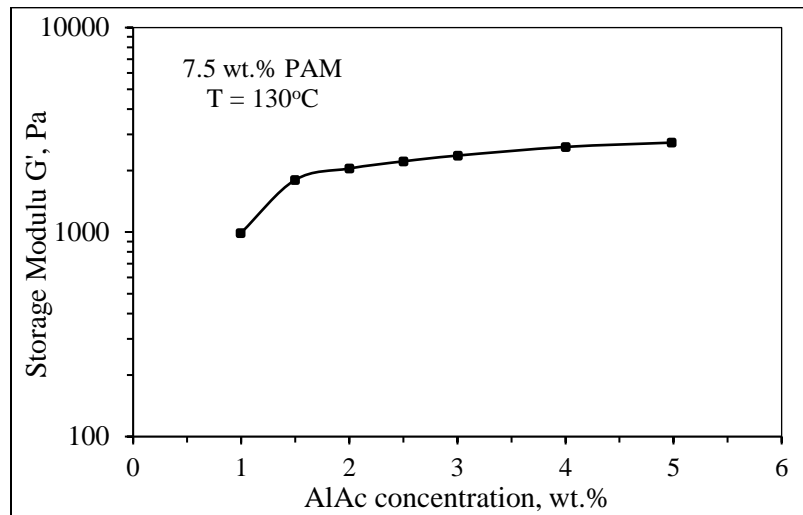


Figure 5. 18: Effect of aluminum acetate (AlAc) on storage modulus of 7.5 wt.% PAM.

The final gel strength is an indicator of the maturity of the produced gel at the end of the gelation process. Still, the AlAc concentration showed an effect that cannot be ignored on the gelation time. The PAM/AlAc pill sealing capability really on both the gelation time and final gel

strength, which should be optimized. A set of gelation experiments were conducted for varying concentrations of AlAc to investigate its effect. During this gelation experiment, the polymer's gel strength is monitored for a prolonged period under constant frequency (10 Hz) and constant temperature (50°C). As shown in Figure 5.19, increasing the concentration of AlAc from 1 to 3 wt.% reduces gelation time from 40 minutes to few minutes, almost instantly at high concentrations. This will cause trouble in the mixing and pumping process during drilling operations. To delay this process, reducing the AlAc concentration is not an option as concluded from the final gel strength measurements since it directly reduces the strength of the gel, which will reduce its sealing capability. Therefore, in the gelation study section, a proper retardation treatment will be implemented to control the gelation process of the PAM/AlAc pill.

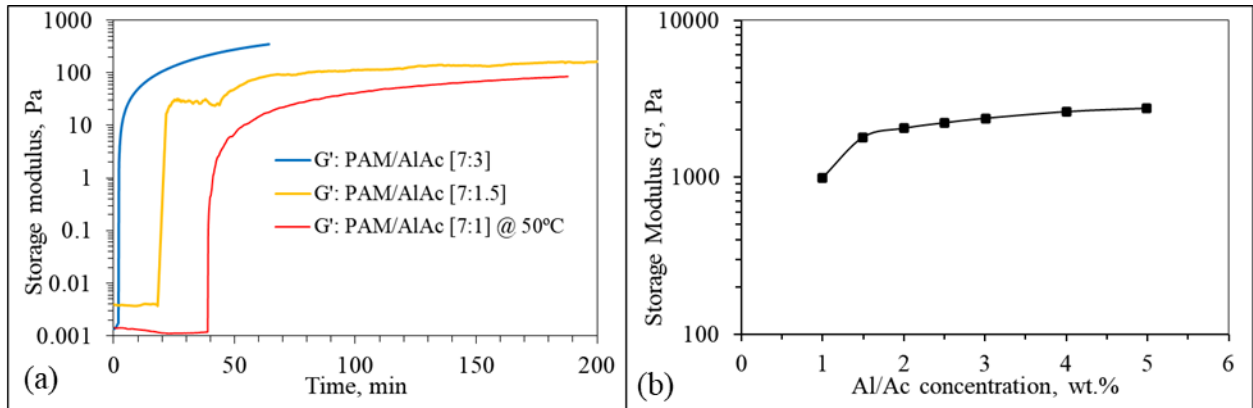


Figure 5. 19: (a) gelation of PAM/AlAc with time at different concentrations, and (b) Effect of AlAc concentration on the final gel strength (storage modulus).

The effect of AlAc amount on gelation is also noticed in the viscosity versus time curves. Figure 5.20 shows the impact of gelation on the viscosity readings for the PAM/AlAc fluid while the shear rate was kept constant at 170 s^{-1} . Simultaneously, the temperature was increased gradually at approximately $2^\circ\text{C}/\text{min}$ until the targeted temperature is reached, then kept constant for the rest of the test duration. The viscosity versus time curves was used to investigate the effect of the AlAc on PAM crosslinking at different concentrations. The viscosity profile had two

prominent trends. During the gradual temperature ramp-up, the viscosity of PAM/AlAc fluid remained almost constant, which indicates that gelation did not occur yet.

Later at temperatures higher than 50°C (122°F), viscosity started to increase instantly from less than 50 mPa.s to more than 1000 mPa.s because of the gelation process. The mature rigid gel was observed in the measuring cylinder of the viscometer, as shown in Figure 5.21. The major finding from the viscosity versus time curves of the gelation process is that a minimum of 1 wt.% of AlAc is required to produce a crosslinked gel with PAM solutions. Therefore, the optimized PAM/AlAc formula is recommended to be 7.5 to 1 to achieve both appropriate viscosity during the flowing period and rigid gel at the end of the gelation process.

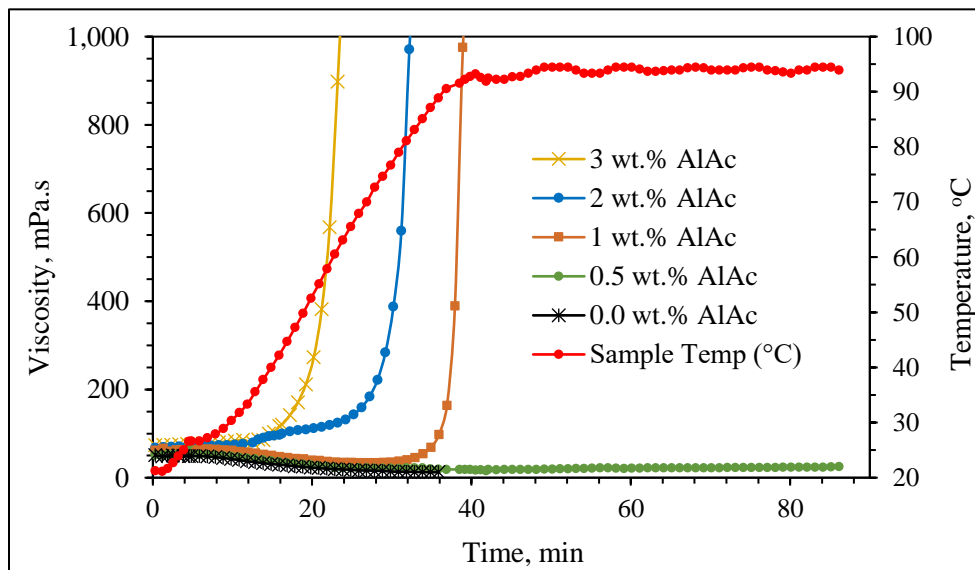


Figure 5. 20: Effect of AlAc concentration on the apparent viscosity.



Figure 5. 21: Figure Gel formation on the rotating viscometer pop during the gradual heating.

Moreover, since the rheology of an LCM pill is a key parameter that influences the performance of loss treatment and governs the flow of fluids into the well and inside the fractures, more investigations were conducted. Viscosity measurements were performed to evaluate the performance of the PAM/AlAc pill for both low and elevated temperature applications. Figure 5.22 shows the results of viscosity measurements conducted over shear rates range from 5 to 1020 s^{-1} at 200°F (93°C). The result of PAM/AlAc fluid is illustrated in comparison with the Ref.Mud#2 containing calcium carbonate and Ref.Mud#3 containing cedar fiber. The complete formulations are detailed in Table 4.2 and 4.3. All fluids exhibited a shear thinning behavior; however, the influence of shearing on PAM/AlAc fluid was insignificant.

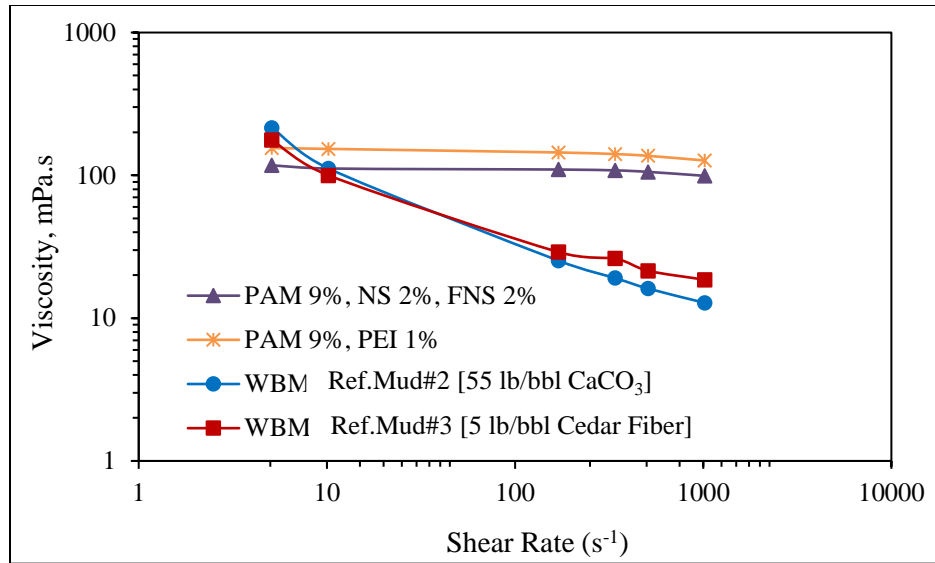


Figure 5. 22: Viscosity measurements at room temperature.

Similarly, the rheological parameters will be affected by gel formation. Figures 6.23a and b show the effect of gelation on the apparent viscosity and plastic viscosity at room temperature. From these results, the increase in viscosity seems to be linear with the AlAc concentration. Therefore, the minimum optimum amount should depend on the minimum amount necessary for gelation. This optimal concentration was obtained by the viscosity-time curve shown earlier in Figure 5.19a and found to be 1 to 3 wt. %.

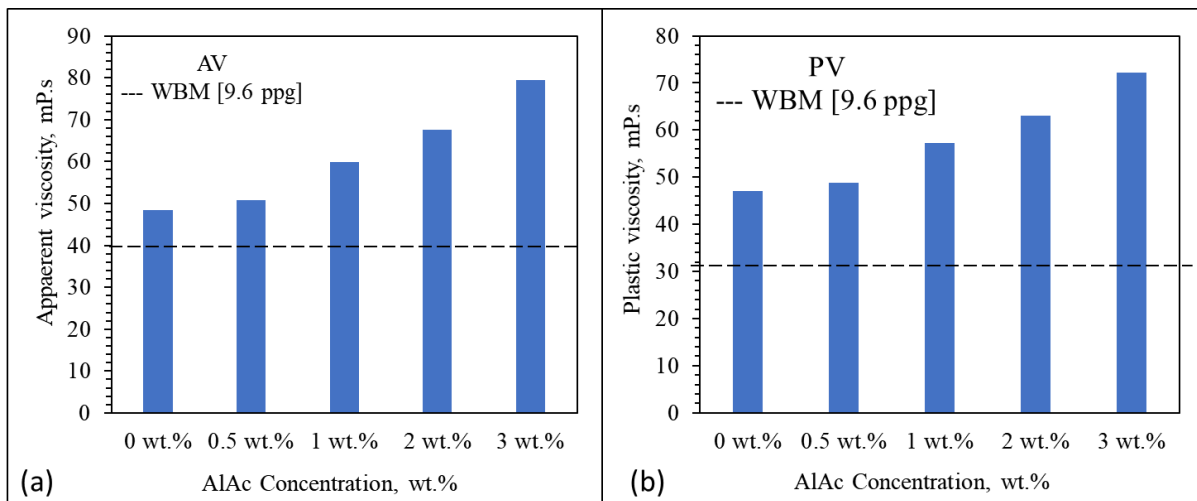


Figure 5. 23: Effect of AlAc concentration on (a) apparent viscosity and (b) plastic viscosity of 7.5 wt.% PAM.

While the AlAc has succeeded in crosslinking the polyacrylamide and produce a firm gel, it failed to sustain its suspension stability at low temperatures. Before gelation occurs, phase separation was observed. The AlAc, which has a particle size of around 10 μm showed severe settling reached 100% in 10 minutes. Therefore, nanosilica of 50 nm was introduced into the system to enhance its stability. The addition of nanosilica in concentrations 1 to 2 wt.% provided better stability to the system since it is expected to give a better particle size distribution with the AlAc. The AlAc particles have a high settling rate and low suspension stability, as demonstrated by the zeta potential measurement, as shown in the gelation study discussed in section 5.6.2. Moreover, the physical observation supported the hypothesis of the effect of nanosilica on the AlAc suspension stability. Figure 5.24 shows the observed phase separation before nanosilica addition.

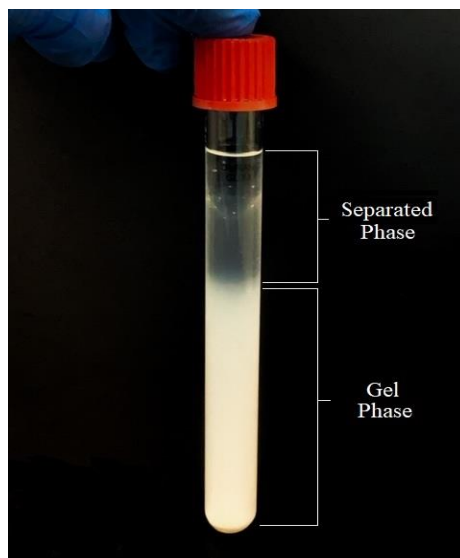


Figure 5. 24: Phase separation without nanosilica observed in PAM/AlAc [7.5:3].

From a rheology perspective, the nanosilica showed a minor effect on the rheological properties of the PAM/AlAc when small quantities are used, up to 2 wt.%. Figure 5.25 shows the results of viscometer measurements conducted at 25°C. All rheological properties remained almost the same when nanosilica concentration was below 2 wt.%; however, beyond this concentration,

the PAM/AlAc fluid exhibited a sharp drop in rheology by 75%. The shear viscosity also exhibited a shear thinning behavior with a more pronounced influence of shearing on PAM/AlAc fluid when more nanosilica was used. The bottom line here that the nanosilica did not significantly affect the PAM/AlAc rheology. The viscosity increased slightly from 56 to 61 mPa.s with 2 wt.% of nanosilica, which was important to enhance the dispersion of the AlAc in PAM.

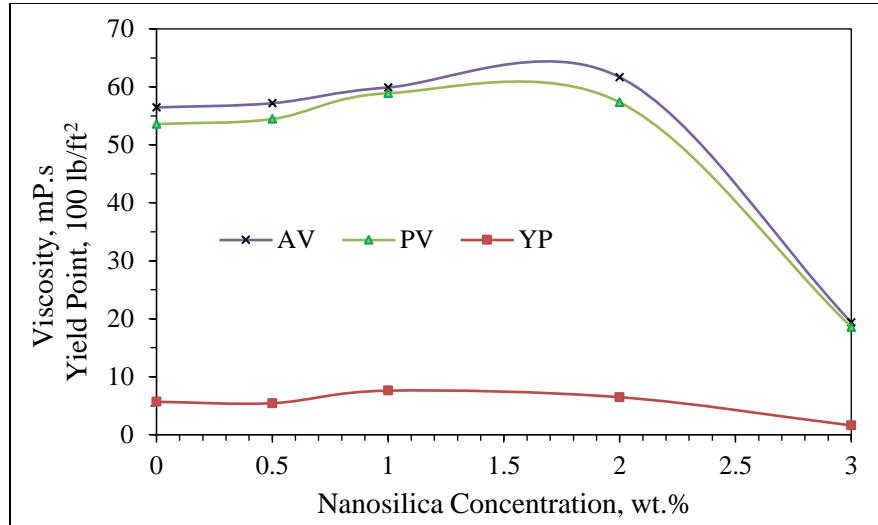


Figure 5. 25: Effect of nanosilica concentration on the AV, PV, and YP of PAM/AlAc [7.5:3].

Table 5.2 summarizes the effect of nanosilica addition on stability and viscosity of the PAM/AlAc crosslinked polymer system. It was clear that a minimum of 1 wt.% of nanosilica is required to ensure no phase separation in the system before gelation. Also, phase separation will reduce the final gel strength of the produced gel and therefore reduces its fracture sealing efficiency. Finally, it is important to highlight that excessive addition of nanosilica is not recommended, not only because it might reduce the viscosity but also due to economic perspectives. Therefore, 1 to 2wt.% of nanosilica is considered as an adequate amount to ensure optimum stability, gel strength, and viscosity of the gel.

Table 5. 2: Effect of Nanosilica on viscosity and phase separation of PAM/AlAc system

| System | Viscosity (mPa.S) | Phase separation |
|-------------------------------|-------------------|------------------|
| 7.5% PAM + 1% AlAc + 0% NS | 60 | 100% |
| 7.5% PAM + 1% AlAc + 0.5 % NS | 63 | 40% |
| 7.5% PAM + 1% AlAc + 1% NS | 65 | 0% |
| 7.5% PAM + 1% AlAc + 2% NS | 70 | 0% |

5.5 Development of Crosslinked PAM/FNS-Based Pill

The second inorganic crosslinker used to crosslink the selected PAM with a low molecular weight (0.2×10^6 Da) is the triamine functionalized silica (FNS). The PAM/FNS gel was prepared by mixing FNS in concentrations from 0.1 to 2 wt.% in a 9 wt.% PAM solution. The gel formation was highly dependent on the FNS concentration. No gel was observed in a concentration below 0.5 wt.%, while high to barely flowing gel formed in concentrations from 0.5 wt.% to 2 wt.%. Although triamine functionalized silica (FNS) has been able to crosslink PAM but it is clear from the observation that settling of silica is an issue. The settling behavior can be attributed to the micro size of the functionalized silica ($> 40 \mu\text{m}$) and the high concentration used. However, the amount of silica that remained suspended was enough to crosslink the polymer but produced a weak gel.

The FNS failed, stands alone, to achieve the same gel strength achieved by the PEI, as shown from the results discussed in earlier sections. The PAM/FNS gel strength is between 1000-2000 Pa when PAM is 9 wt.%, as shown in Figure 5.26. Thus, nanosilica was introduced to the system to enhance both the stability of the particles and the physical strength of the gel. In the beginning, the proper size of nanosilica needed to be defined. Figure 5.26 shows that the final gel strength from the dynamic frequency sweep changes with respect to NS concentration and size. Also, there is a local maximum at 2 wt.% at most NS concentrations, and the maximum value resulted from nanosilica of 50 nm.

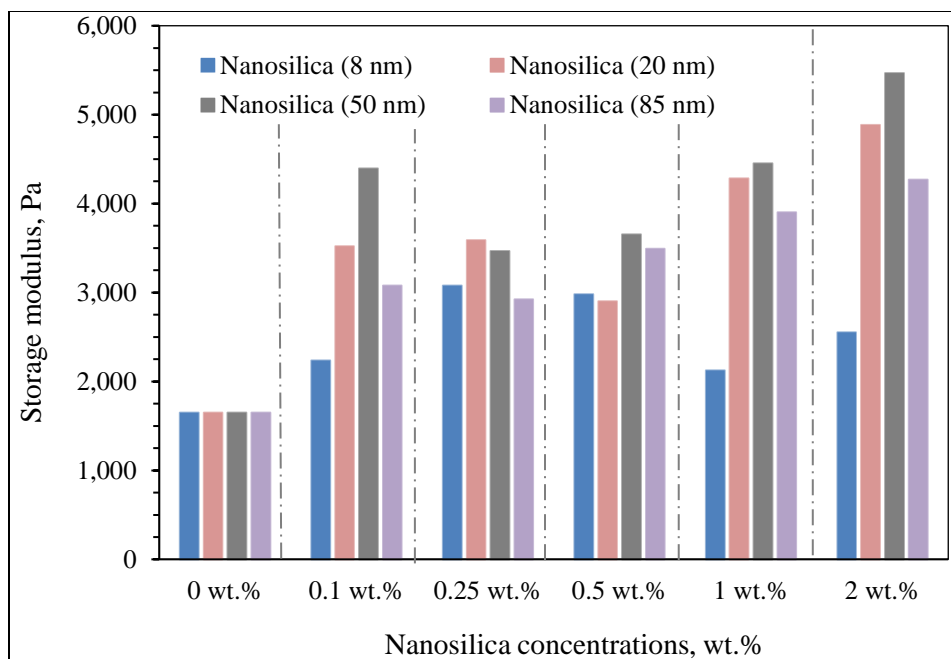


Figure 5. 26: Final gel strength of PAM/FNS with different NS concentrations and sizes.

The increase in gel strength after adding nanosilica can be explained by the adsorption of PAM into the surface of nanosilica by the silanol group and carboxyl via hydrogen bonding. However, the decrease in storage modulus at low concentrations suggests that the interaction between NS and FNS initially inhibits slightly the crosslinking reaction, which leads to producing of a weaker gel. However, after a certain limit, the effect of physical reinforcement overwhelms this effect which results in an increase in the gel strength upon the addition of more NS. Figure 5.27 shows a schematic illustration of the effect of nanosilica size on the PAM adsorption and network structure of the reinforced composite PAM/FNS/NS. A similar mechanism was reported by Chen et al. (2018) using 28.6 nm silica (Chen et al. 2018).

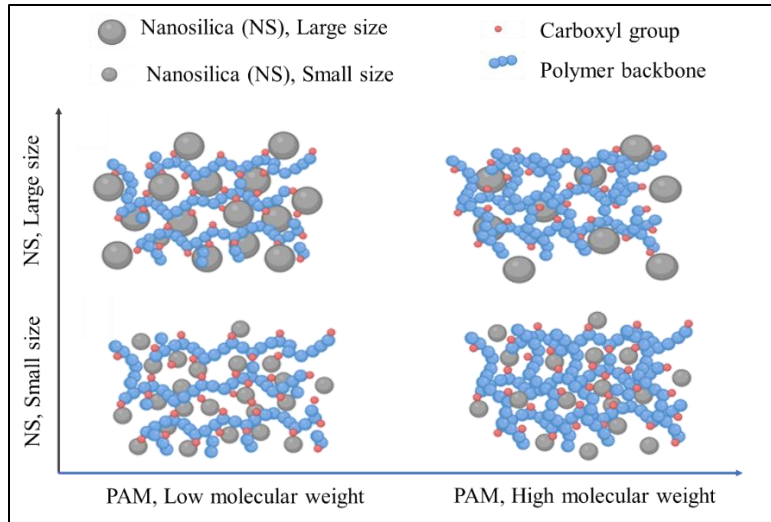


Figure 5. 27: Schematic illustration of the dispersion with respect to the size of nanosilica and molecular weight of the PAM.

For polymeric gel used as LCM, the fluid is required to have moderate low viscosity at the surface to facilitate the pumping of fluid into the well and to have high injectivity. Figure 5.28 shows viscosity measurements at different shear ranging from 0.1 to 1000 s^{-1} using the viscometer at room temperature. The results show that for the same PAM concentration of 9 wt.% the PAM/NS/FNS system has lower viscosity compared to the PAM/PEI; however, it is a bit higher than Ref.Mud# 2 and 3.

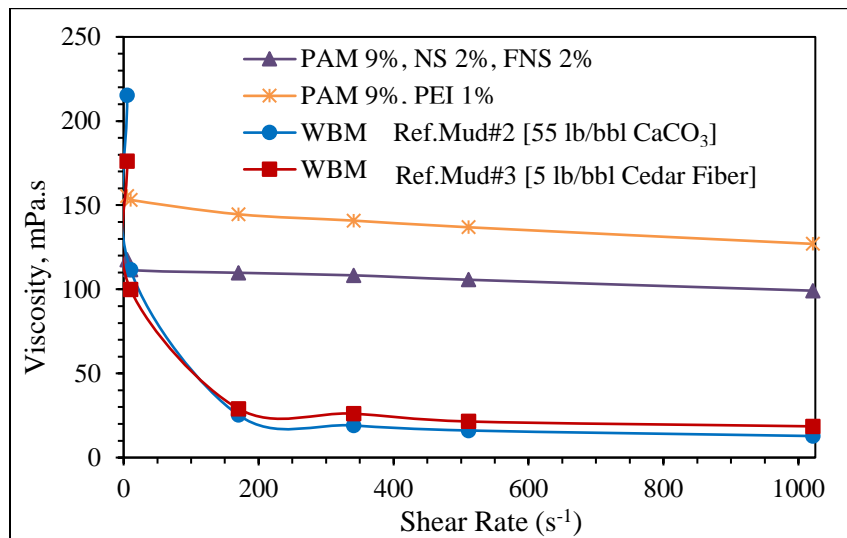


Figure 5. 28: Viscosity measurements at room temperature.

5.6 Study of Gelation Kinetics of Polymeric Gel Formulations

The injection of a polymeric gel into a well is a critical process that requires careful design of rheology and gelation time. In a good gel treatment job, the gel should keep its flowing characteristics until reaching the targeted depth where the gelation process should take place. If the gel rheological properties and gelation process was not carefully designed to match the downhole temperature and time to reach the targeted depth, the gelation might occur in the drill string. The gelation time depends on the viscosity measurement over time, which accordingly defines the gelation time as the time required to reach an inflection point on the viscosity versus time curve (Hardy et al. 1998). Under insight of this fact, the gelation process of the PAM with different crosslinkers used in this study was investigated under possible downhole conditions of temperature, salinity, pH, and time required to reach the target. Among various available approaches for gelation time determination (Broseta et al. 2000; Vasquez et al. 2003), the steady shear method provides a fast and accurate conclusion. The gelation time is obtained by detecting the point where the viscosity exhibits a sharp increase. The point is considered the onset of the gel temperature, and the time when it occurs is the gelation time. The second method is based on the results of the dynamic shear, which also gives a quantitative estimation of the gelation rate. The following subsections discuss in detail the gelation's most influencing parameters of each crosslinker.

5.6.1 Study of Gelation Kinetics of PAM/PEI Based-Mud and Pill

Rheology experiments were conducted to investigate crosslinking of PAM-based drilling fluid to understand their gelation formation process and determine their gel strength. The goal is to define the maximum gel strength, which is obtained by using the HPHT rheometer. From the results of the dynamic shear, the gel strength was taken as the maximum value of the storage modulus (G'). For each crosslinked gel, the viscoelastic region was considered to avoid the destruction of the gel

structure; therefore, the tests were conducted within 10% strain under a constant frequency of 10 Hz. After determining the maximum gel strength, the gelation time was determined by the automatic speed dial viscometer and the HPHT rheometer from the viscosity-time curves while ramping up the temperature. The gelation process was monitored for the crosslinked polymer with and without retardation agent (NH_4CL).

Figure 5.29a and b show the viscosity of PAM/PEI [7.5:1] at two different temperatures (95 and 130°C) obtained over an extended testing period of 150 minutes at a constant shear rate (170 s^{-1}). At low temperatures below 200°F (93°C), the polymer took a longer time to crosslink, indicated by the linear and slow increase in viscosity. The gelation rate was governed by the temperature, which reflected on the system's viscosity. Figure 5.29b, shows a sharp increase in viscosity at (266°F), which is the onset temperature of PAM gels; therefore, delaying the gelation rate should be considered when PAM/PEI-based LCM is utilized in deep wells or where high temperature is expected.

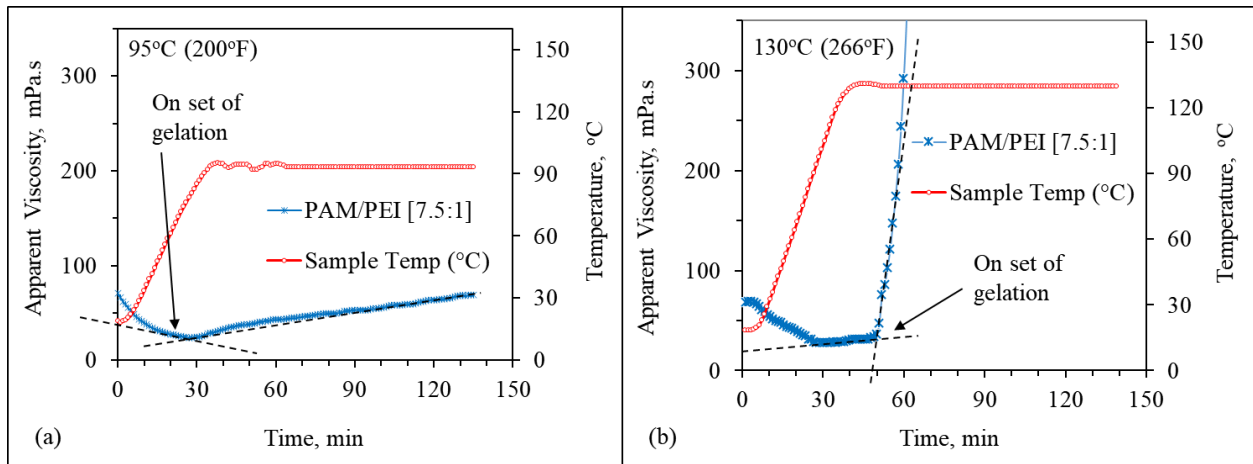


Figure 5. 29: Effect of temperature on gelation of PAM/PEI [7.5:1], (a) at 200°F, and (b) at 266°F.

The gelation rate can also be affected by the amount of crosslinker available in the system. The PEI concentration has a significant effect on gelation time, as will be shown from the viscosity-time curves for different concentrations of PEI. Using excessive PEI amount may lead

to rapid gel formation because it will provide more free functioning groups that can increase the chances of the PAM to crosslink. However, the minimum PEI concentration is always limited by the maximum gel strength. A sufficient PEI concentration is necessary to form a strong gel. For optimizing the PEI concentration, several viscosity experiments were conducted for various PEI concentrations. The PEI had slightly changed the viscosity versus time as shown in Figure 5.30a; when PEI concentration was less than 1 wt.%, then a sudden sharp increase from 30 to over 500 mPa.s was observed. Further, the gelation time was extracted from viscosity profiles for each PEI concentration, and a power model was used to fit the data, as shown in Figure 5.30b.

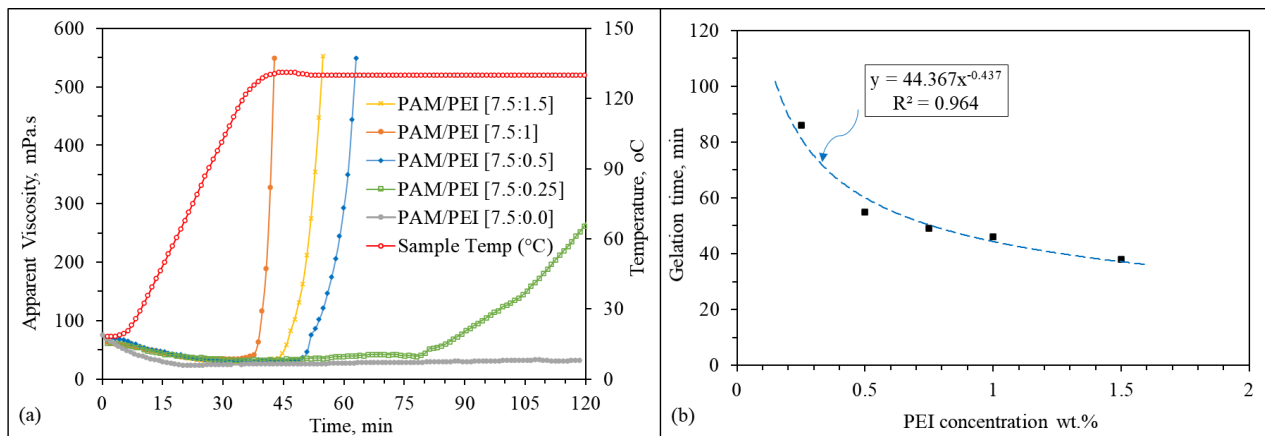


Figure 5. 30: (a) viscosity versus time with gelation by different PEI concentration, and (b) effect on gelation time.

5.6.1.1 Retardation with Ammonium Chloride (NH4Cl)

The previous analysis did not consider controlling the gelation rate, only PAM/PEI was used, and the gelation time was about 50 minutes. This time will define the gel formation responding to the background temperature. For specific depth and temperature, a suitable gelation time will be required to prevent the gel from forming in the pipes and during the placement process, especially for high-temperature wells. In the opposite scenario, PAM/PEI gels tend to slow their gelation rate at low temperatures. To account for this, designing the gel formulas for lost circulation treatment at low depths (low temperatures) should consider fast curing gels because the time taken to reach

the loss zone is short. Quite the opposite, gel intended to treat loss at high temperatures or deep wells should incorporate retardation agents to allow for more time to reach the loss zone. The precise determination of gelation time is critical.

Considering the above discussion, the effect of NH_4Cl on gelation rate was investigated using the viscosity over time measurements at constant temperature and PAM concentration. Two concentrations of PEI (0.5 and 1 wt.%) were considered to reflect the response of different PEI concentrations to the hindering effect of the retarder (NH_4Cl). The amount of NH_4Cl was varied from 0 to 5 wt.%, as shown in Figures 6.31 and 6.32. The viscosity of pure PAM/PEI rapidly increased, while the samples containing NH_4Cl exhibited a lower increasing rate due to the slower gelation rate.

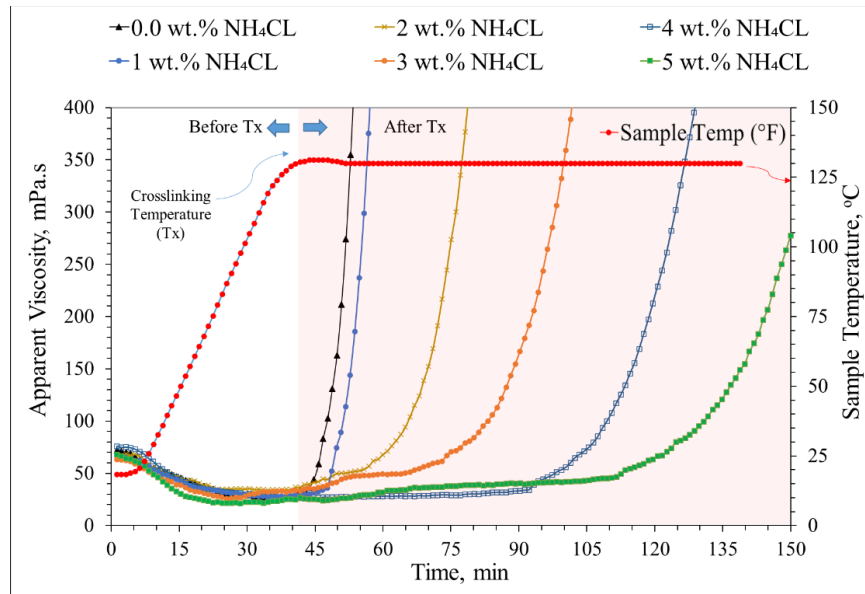


Figure 5. 31: Viscosity evolution of pure PAM/PEI [7.5:1] gel and PAM/PEI gels containing NH_4Cl up to 5 wt.%.

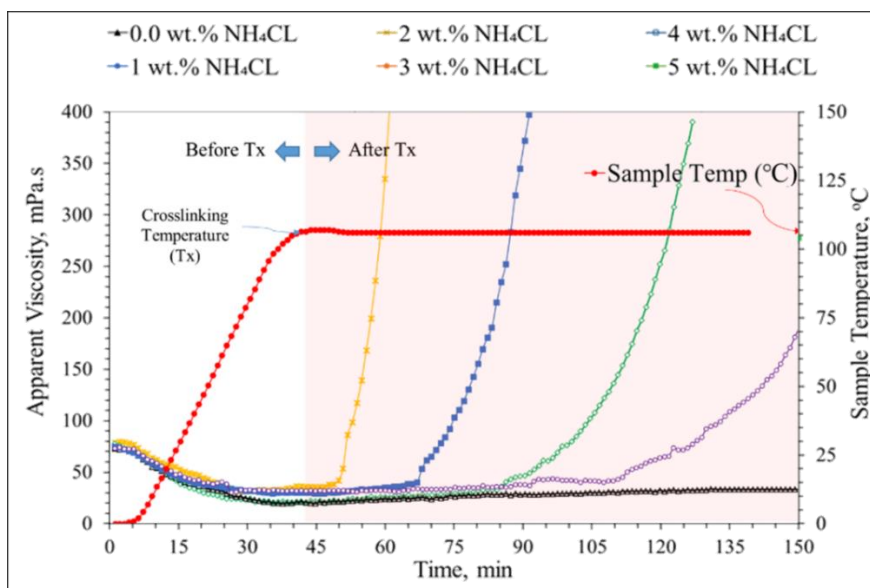


Figure 5.32: Viscosity evolution of pure PAM/PEI [7.5:0.5] gel and PAM/PEI gels containing NH₄Cl up to 5 wt.%.

From the results of various NH₄Cl concentrations and the two PEI concentrations, the gelation time was extracted and plotted in Figure 5.32. The relationship between gelation time and the amount of NH₄Cl for the two PEI concentrations was linear. However, the viscosity data for the lower PEI concentration did not show any gel when 4 wt.% NH₄Cl was used. This was due to the limitation of the time. However, still, it can be extrapolated to cover for the unseen data. Also, this correlation can be used to obtain the proper amount of the NH₄Cl required to reduce the gelation rate enough for the placement process. Overall, for the time needed to place the PAM/PEI [7.5:1] gel, up to two hours can be attained with no more than 5 wt.% of NH₄Cl.

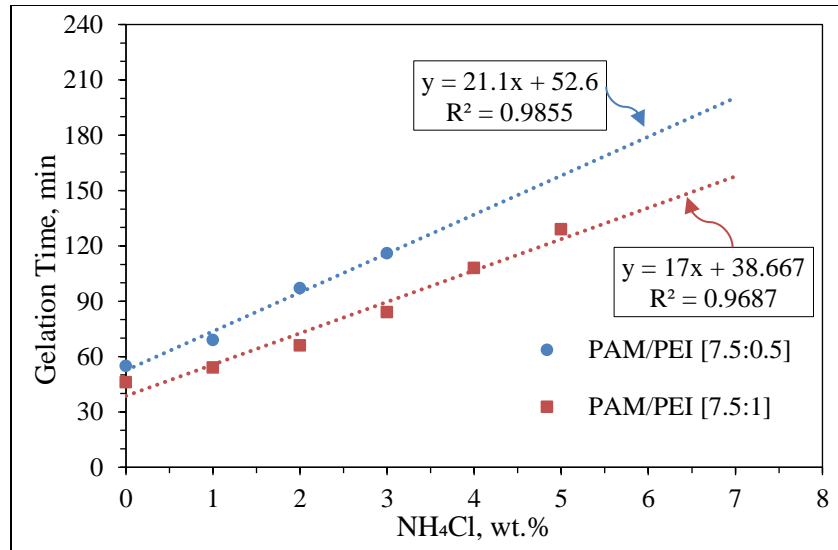


Figure 5.33: Gelation time of PAM/PEI containing NH₄Cl from viscosity evaluation.

5.6.1.2 Effect of drilling fluid additives on gelation and gel strength using G' and G''

Evaluate the interaction of polymers and crosslinker with the drilling fluid additives is essential for the proper preparation of gelation polymer-based LCMs. In this subsection, the polymeric matrix was interacted with various mud components to evaluate the alteration in the polymer gelation process. For example, bentonite is the common component in the water-based drilling mud and is known for its PAM interactions which may hinder the crosslinking process. The rheology results for the PAM/PEI [7.5:1] presented in Figure 5.34 showed that adding bentonite in small amounts (0 to 2.5 lb/bbl) caused insignificant alteration in gelation time. The gelation point decreased slightly from 78.5 to 76.5 minutes. Also, the storage modulus was impacted by bentonite addition and decreased by 18% when 2.5 lb/bbl was added.

Further addition of bentonite up to 5 lb/bbl was investigated, and the results were presented in Figure 5.34a. The higher concentration of bentonite caused a significant reduction in gel strength from 550 Pa to 88 Pa and delayed the gelation time. The gelation time increased from 50 minutes to 221 minutes. Although equilibrium was not achieved at the end of the test, the conclusion on gel strength reduction was evident from the massive decrease in the gel strength.

The alteration of the gelation process was believed to be due to the physical interaction between polymeric matrix and bentonite particles. Similar to the earlier discussed results on the effect of the mixing method on bentonite and PAM viscosity, the mixing method impacted the storage modulus of the produced gel. When bentonite was dispersed first before the polymer addition, the crosslinking of the polymer was enhanced.

Besides, studied literature reports revealed that clays positively affect the crosslinked polymers and increase their gel strength (Bhattacharyya and Ray 2015; Haraguchi and Takehisa 2002). Based on the results presented in this study, the reinforcing effect of bentonite depends on the mixing procedures. Still, the positives charges in bentonite will occupy some of the free amine groups in the crosslinker, which could weaken the gel if a high dose of bentonite is used. Moreover, several studies reported a high adsorption tendency of PAM to bentonite particles (Shaikh et al. 2018). Consequently, bentonite can reduce the number of polymer chains available for crosslinking, which justifies the drop in the storage modulus, as shown in Figure 5.34b.

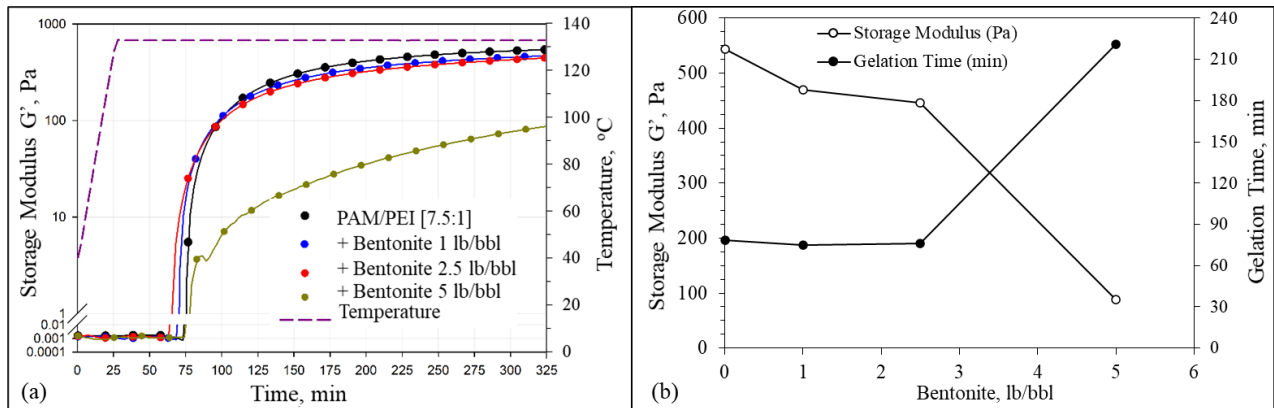


Figure 5. 34: Effect of bentonite concentration on (a) gelation process and (b) gelation time and storage modulus of PAM/PEI [7.5:1] at 130°C.

Another important component of drilling fluid is the barite. Three samples of PAM/PEI-based mud were prepared with barite content to increase the density from 9.5 to 10.5 and 11.5 ppg to investigate the effect of barite. The results presented in Figure 5.35a reveals that barite reduces

the storage models (G') similarly to bentonite as it acts as a barrier that hinders the crosslinking reaction. However, by examining the gelation kinetics, an observation can be withdrawn that a small amount of barite has barely altered the gelation time and the final gel strength, as summarized in Figure 5.35b. At a higher mud weight (11.5 ppg), where a significant quantity of barite was added, the gelation time was delayed to more than 100 minutes, and the gel strength dropped by 35%, down to 350 Pa.

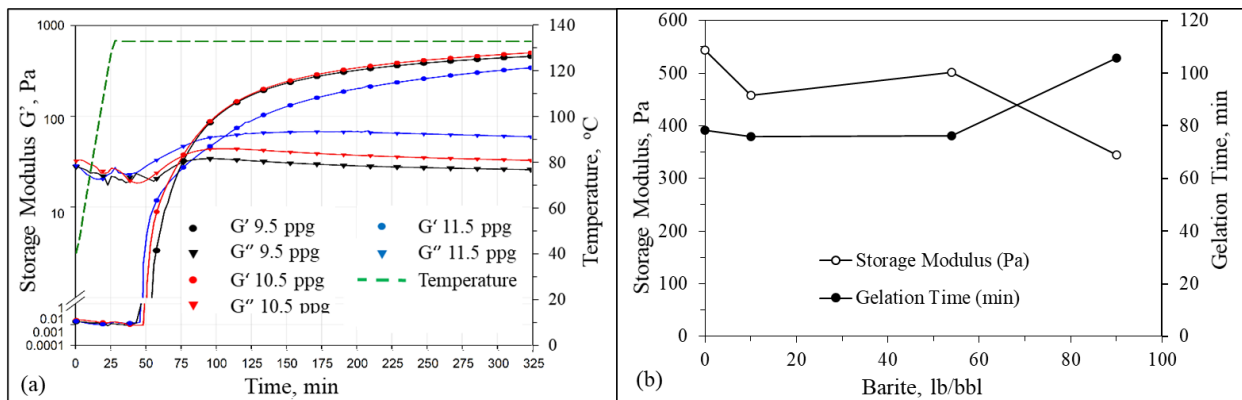


Figure 5. 35: Mud weight effect on (a) the gelation process with time, and (b) gelation time and final storage modulus of PAM/PEI [7.5:1].

Figure 5.36 summarizes the results of gelation experiments for the various PAM/PEI formulas investigated in this study. Overall, all additives had negatively impacted the gel strength and caused a delay in the gelation rate. Two different approaches were used to investigate the drilling fluid compatibility with the gelling polymer, considering two possible scenarios where the polymeric LCM can be applied in the field. The first approach is when the polymeric LCM is used in the beginning as a proactive treatment. In this case, the polymer-based mud will be prepared from the proper concentration of polymers, crosslinkers, retarders, and other additives to attain a specific density, pH, or rheological properties. The second approach is accounting for the case where the polymer is used as a corrective intervention solution. In this case, the optimized polymeric formulation of 7.5 wt.% PAM and 1 wt.% PEI was mixed with the water-based mud

(Ref.Mud#2) at different ratios. This will simulate when the PAM/PEI formula is added as a liquid directly to the existing drilling fluid system to cure the lost circulation. The ratio of the polymeric formulation to WBM was varied from [5:5] to [9:1].

The results showed that the crosslinked polymer-based mud (PBM) ratio, less than 0.9 failed to produce gel since the polymers were diluted. Besides, the different additives proved to be hindering materials were in a significant amount in the system. A more concentrated PAM/PEI formula can achieve gelation at low mixing ratios with the WBM. At the mixing ratio of [9:1], the delay in gelation time was insignificant, but the gel had a storage modulus of 268 Pa with a reduction of 50% from the pure PAM/PEI. In addition to the negative effect of bentonite and barite, plus the impact of adding lignite and caustic soda was more pronounced. The PAM/PEI system showed little tolerance up to 0.5 lb/bbl for each additive, where no gel was produced beyond this concentration. The alteration was believed to be due to the high increase in the alkalinity of the system ($\text{pH} > 13$), where the polymers are no longer crosslinkable.

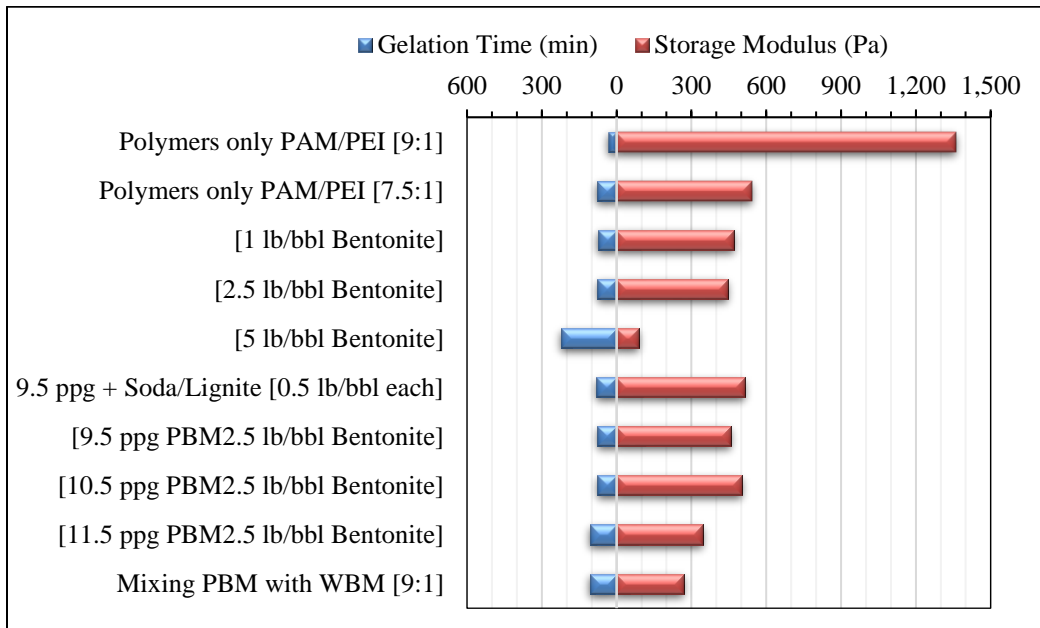


Figure 5. 36: Summary of the gelation behavior of the different PAM/PEI based systems.

5.6.2 Study of Gelation Kinetics of PAM/AlAc Based-Pill

The Crosslinking mechanism of AlAc is similar to the PEI, but the response to pH and temperature is completely different. Figure 5.37 shows gelation experiments conducted at 3 different temperatures (25, 50, and 65°C) and under a constant frequency of 10 Hz for extended periods. As illustrated in Figure 5.37a, the gelation experiments showed when the abrupt change in gel strength occurred. In addition to the final gel strength represented by the peak of the storage modulus. In Figure 5.37b, the variation in loss modulus, which reflects the viscous part of the fluid, increases with temperature by 50% and 100% at 50°C and 65°C, respectively. Based on this presented result, the temperature has a significant positive effect on gel strength, gelation time, and viscosity of the PAM/AlAc. This can be advantageous in shallow depths application for loss circulation treatment; however, care must be taken to avoid uncontrolled gelation due to the limited gelation time.

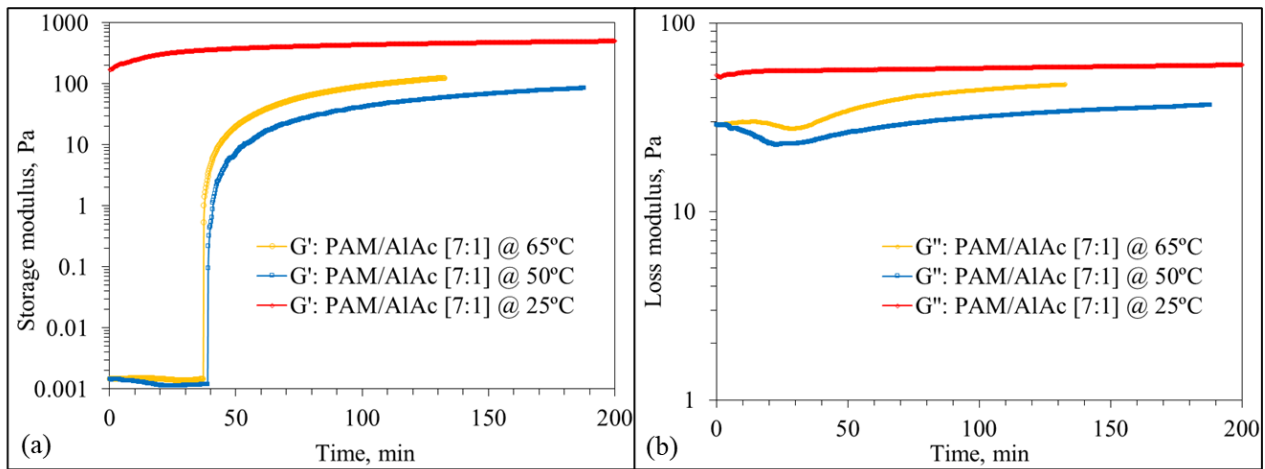


Figure 5. 37: Effect of temperature and time on PAM/AlAc (7:1) (a) storage modulus and (b) loss modulus.

In addition to the temperature effect, the PAM/AlAc was found to be more sensitive to the small changes in pH as shown from the gelation experiments conducted at very close two pH values (4.1 and 4.6). The pH showed a reversed gelation triggering effect, where the slight increase of pH from 4.1 to 4.6 delayed the gelation from 50 to 80 minutes, as shown from the change in

storage modulus (Figure 5.38) and the gelation point indicated by the overlapping of the storage and loss modulus.

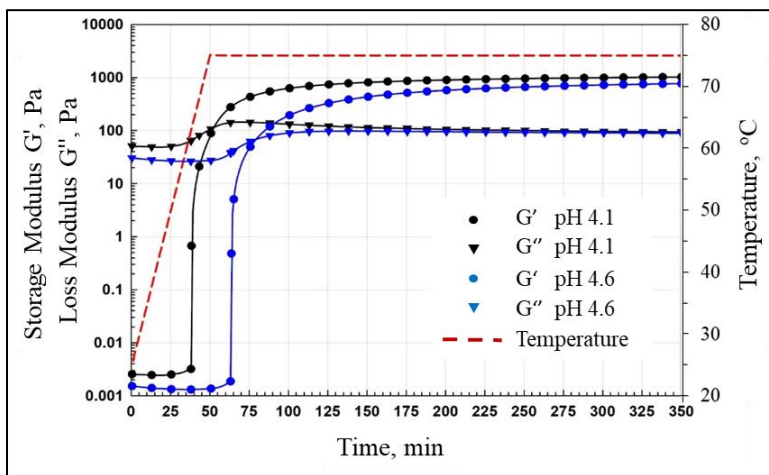


Figure 5.38: Gelation profile of PAM/AlAc system.

Besides the obvious delaying of the gelation process at high pH values and rapid gelling at low values, the pH also affects the viscoelastic behavior of the PAM/AlAc system. That was clearly observed from the dynamic frequency sweep conducted for different pH values ranging from 3.5 to 8.45 at 50°C for frequencies ranging from 1 to 100 Hz. Figure 5.39 shows a high reduction in gel strength with the increasing alkalinity. Moreover, the alkaline condition decreased the stability of AlAc suspension in the polymer system. A separation phase was observed when the pH was increased. The effect of pH on stability was also proved by measuring the zeta potential (ZP) presented in Figure 5.40. When ZP approaches zero, this means the suspension is becoming more unstable. Therefore, a conclusion can be drawn that the gelation rate, stability, and gel strength decrease with the pH. In Figure 5.39b also the strengthening effect of NS can be observed as higher gel strength was attained with the addition of 2 wt.% NS to the PAM/AlAc, at similar pH conditions.

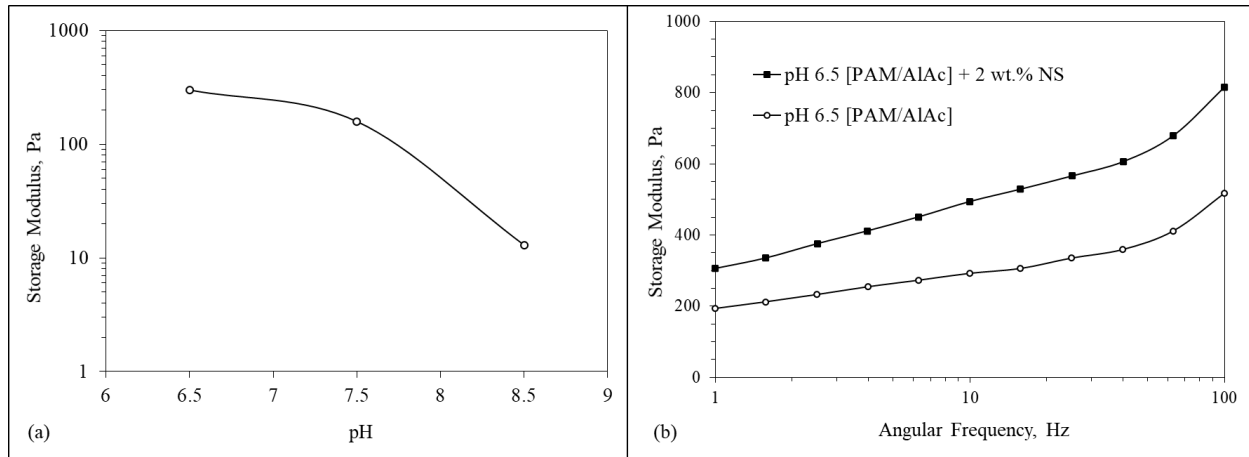


Figure 5.39: Effect of pH and nanosilica on (a) storage modulus of PAM/AlAc, and (b) frequency Sweep of PAM/Alac [9:3].

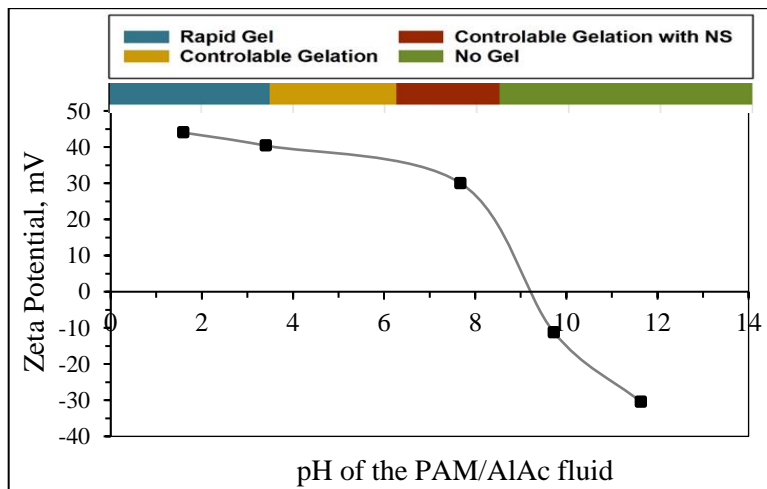


Figure 5.40: Effect of pH on gelation formation and stability indicated by the zeta potential.

From the gelation experiments results, it can be observed that the original gelation time of the PAM/Al/Ac system is about 18 minutes. The time is obtained from the intercept of the two tangents of the viscosity profile before and after the inflection point, as shown in Figure 5.41a. This time window might not be enough to prepare the gel and pump it through the drill string to reach the depth of the loss. Ammonium chloride (NH_4Cl) in concentrations of 2.5 to 10 wt.% was used to extend this flowing period of the gel. Figure 5.41b shows the results of gelation with the presence of NH_4Cl . The gelation time was expanded with retardation, which delayed the gelation process, as shown in Figure 5.42, where the inflection points shifted with more NH_4Cl .

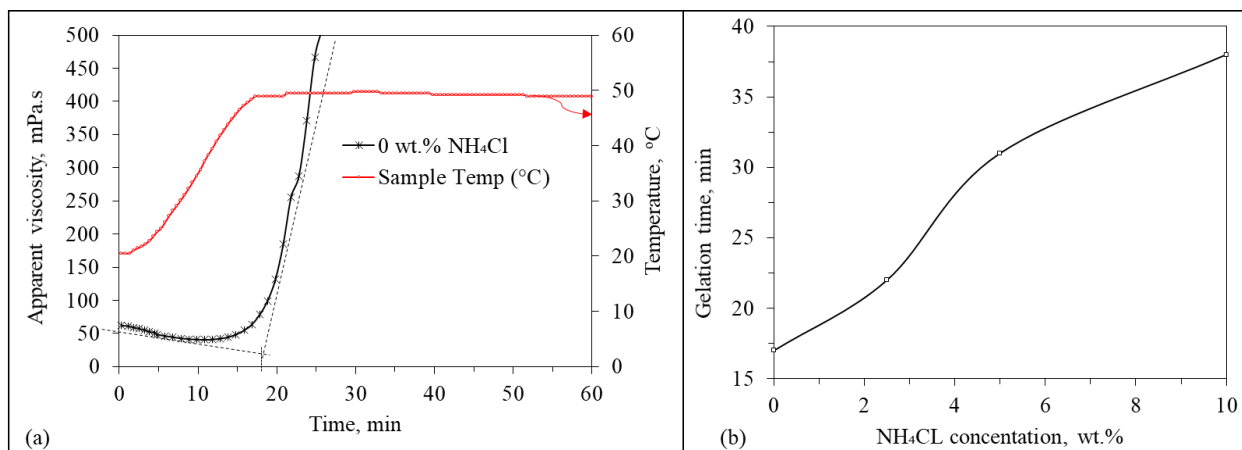


Figure 5. 41: (a) Gelation time estimation for PAM/AlAc without NH_4Cl retardation, and (b) with retardation effect.

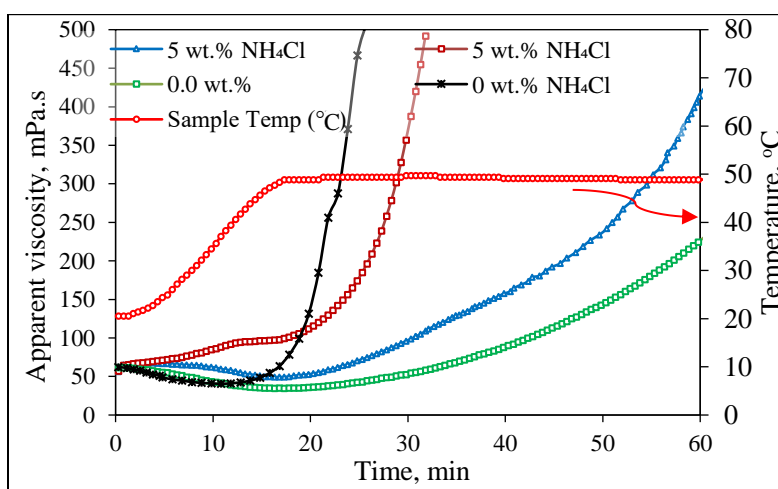


Figure 5. 42: Effect of NH_4Cl concentration on the gelation process with time.

5.6.3 Study of Gelation Kinetics of PAM/FNS Based-Pill

The PAM/FNS gel also showed significant pH and temperature dependency in addition to the strengthening benefits of the nanosilica. One way to increase the gel strength and the stability of the FNS in the polymer system was by controlling the amount of the nanosilica. Figure 5.43 shows that adding nanosilica improves the gel strength of the PAM/FNS system consistently. In the beginning, the storage modulus reduced from 1900 Pa at 1 wt. % NS to 1542 and 1868 Pa for 1.5 and 2 wt. %, respectively. However, after that, the gel strength sharply increased when more nanosilica was added. A high value of 9013 Pa was obtained at 6 wt.% NS, which is about 374 %

greater than the storage modulus at 1 wt. % NS and about 13 times stronger than the gel formed without nanosilica at the same PAM/FNS concentrations.

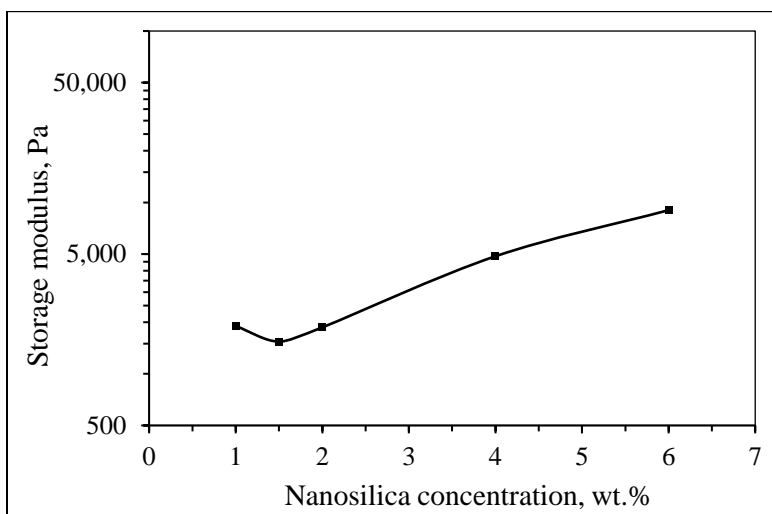


Figure 5. 43: Effect of adding 50 nm of nanosilica at different concentrations on the gel strength of 9 wt. % PAM crosslinked by 2 wt. % FNS.

On the other hand, the NS addition helped to increase the stability of the gel, which prevents settling of the crosslinker (FNS), which was another reason for forming a stronger gel. Figure 5.44 shows the zeta potential (ZP) measurement for nanosilica ranging from 8 nm to 85 nm. This result shows high negative ZP with nanosilica of 50 nm, which agrees with the dynamic frequency sweep results where 50 nm gave the highest final gel strength.

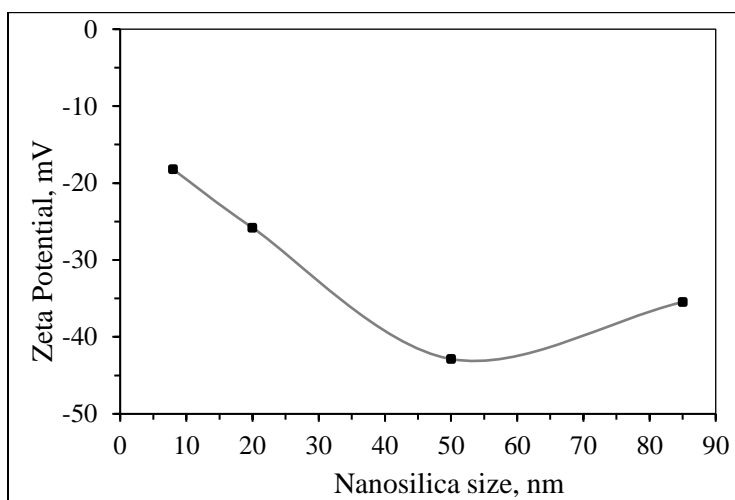


Figure 5. 44: Effect of nanosilica particle size on zeta potential of PAM/FNS solution.

Table 5.3 shows the Sydansk code of different gels formed after crosslinking 9 wt. % PAM by FNS at various concentrations before and after adding nanosilica. At low concentrations, settling behavior was not much affected, whereas 2 wt. % nanosilica completely inhibited the settling and strengthened of the composed gel.

Table 5. 3: Sydansk code of the formed gels using TAS only to crosslink PAM and silica settling

| PAM wt. % | FNS wt. % | NS wt. % | Sydansk Code | Silica Settling |
|-----------|-----------|----------|--------------------------------------|-----------------|
| 9 | 0.1 | 0 | A: No gel | No |
| 9 | 0.5 | 0 | B: Highly flowing gel | No |
| 9 | 1 | 0 | C: Flowing gel | Yes |
| 9 | 2 | 0 | E: Barely flowing gel | Yes |
| 9 | 2 | 0.5 | F: Highly deformable non flowing gel | Yes |
| 9 | 2 | 2 | I: Rigid gel | No |

5.7 Drilling Fluid Filtration and Wellbore Strengthening Experiments

This section summarizes the performance evaluation of the developed formulations of crosslinked polymer-based mud and pills as loss circulation treatment and wellbore strengthening methods. The polymeric LCM's main objective is to stop further invasions of drilling fluids into formations through fractures and high permeability. For example, the PAM/PEI-based mud can be used as a preventive treatment to drill trouble zone. In contrast, LCM pills developed by PAM/PEI, PAM/AlAc, and PAM/FNS can be used to treat minor to severe or total loss by completely seal loss zones which allows drilling to continue safely. Establishing a rigid gel inside the pores and fractures can provide high sealing pressure. The following sections of the results show the efficiency of each developed crosslinked polymeric gel formulations in treating loss circulation by several static and dynamic drilling fluid filtration and wellbore strengthening experiments conducted in various porous and fractured mediums.

5.7.1 Pore-Scale Static Drilling Fluids Filtration

The experiments of pore-scale drilling fluid filtration are intended to evaluate the capability of the polymeric gels and polymer-based mud to stop mud loss. The filtration tests were conducted using the permeability plugging tester with ceramic filter disks having two different permeabilities, 775 mD and 15 D. Effect of temperature and gelation time were considered. The results are compared with the performance of a typical water-based drilling fluid containing 55 lb/bbl calcium carbonate as LCM (Ref.Mud#2). The results are reported as accumulative filtration volume versus square root of time for 30 minutes. Also, the maximum pressure that can be maintained without further loss is considered as the sealing pressure. The following two subsections describe the results of static filtration using crosslinked polymer-based mud (PBM) and polymeric LCM pills.

5.7.1.1 Static Filtration in Ceramic Filter Disks

The developed polymer-based mud (PBM), prepared based on the screening and optimizations study, was used to conduct the static drilling fluid filtration experiments. The mud formulation is listed in Table 5.1. in section 5.3. The PBM contains 7.5 wt.% PAM, 1 wt.% PEI, 2.5 lb/bbl bentonite, and barite as a weighting agent to prepare 9.6 ppg, which will be referred to as PBM-2.5. The filtration test conducted using the permeability plugging tester showed the superiority of the PBM in elevated temperature in comparison with the regular WBM with calcium carbonate. Figure 5.45 shows the results of filtration tests for the calcium carbonate at 75 and 205°F (24 and 93°C). The calcium carbonate failed to control fluid loss at elevated temperatures. These findings agree with previous published experimental work by Ezeakacha et al. (2017). They concluded on their testing of several LCM that calcium carbonate is not a good LCM at elevated temperature as many other conventional LCMs (Ezeakacha et al. 2017).

On the other hand, the proposed PBM-2.5 showed a reduction in the filtrate volume by 80%. This performance is because the crosslinked polymer, when invading the porous or

unconsolidated formation, will form a strong gel and plug it efficiently. The mud cake developed on the ceramic filter disk is shown in Figure 5.46. The calcium carbonate mud developed about 4.4 cm cake thickness while the PBM-25 formed a thin layer on the surface of the disc, about 2 cm. This is another advantage since thick mud cakes increase the potential of pipes sticking.

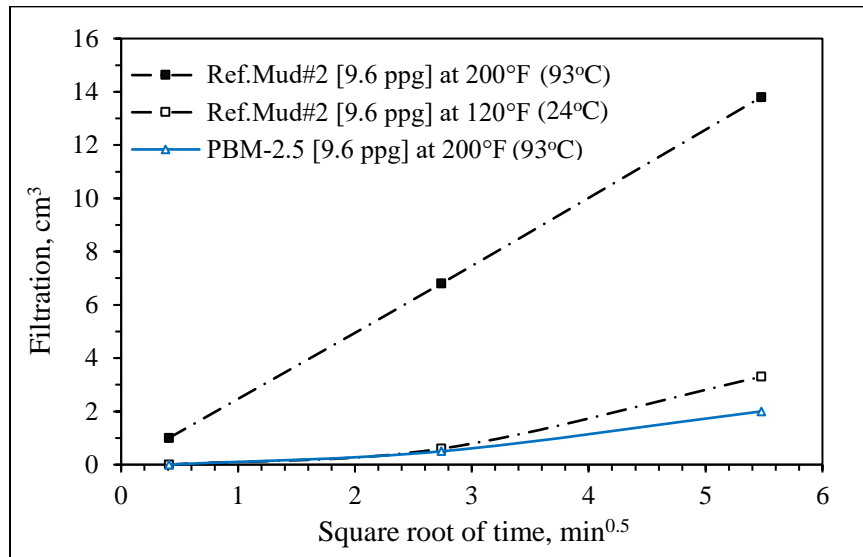


Figure 5. 45: Comparison of filtration control performance of the PBM-2.5 and Ref.Mud#2.



Figure 5. 46: Filter cake on the ceramic disc, calcium carbonate (left), and PBM-25 (right).

Another performance evaluation with static drilling fluid filtration experiments was also conducted using PAM/PEI pills. The filtration control evaluation results of the WBM containing calcium carbonate and filtration profile of the PAM/PEI pill are shown in Figure 5.47. Filtration experiments were conducted under 500 psi differential pressure using the two ceramic filter disks described in the figure. The PAM/PEI formula stopped filtration through both types of disks in a few minutes and peaked at 2 to 5.5 cc for both disks with different permeabilities (755 mD and 15

D). As the gelation process takes place when the temperature of the fluid reaches the gel onset temperature (266°F), the filtration stopped immediately as the fluid rheology increased. The WBM, however, exhibited a progressive filtration over time because of the high-temperature effect and the deterioration in mud properties with heating. One interesting observation is that the total loss in the disk with higher permeability was slightly less than the loss in the lower permeability. This is unusual for conventional LCMs, but for the gel, this is attributed to the mechanism of sealing. The gel needs high injectivity at the beginning to be able to invade the pores from the sealing gel inside, which makes a strong plug with higher sealing pressure. The process takes more time to establish the sealing in the lower permeability disk. As shown in Figure 5.47, the filtration stopped 4 minutes later than in the high permeability case.

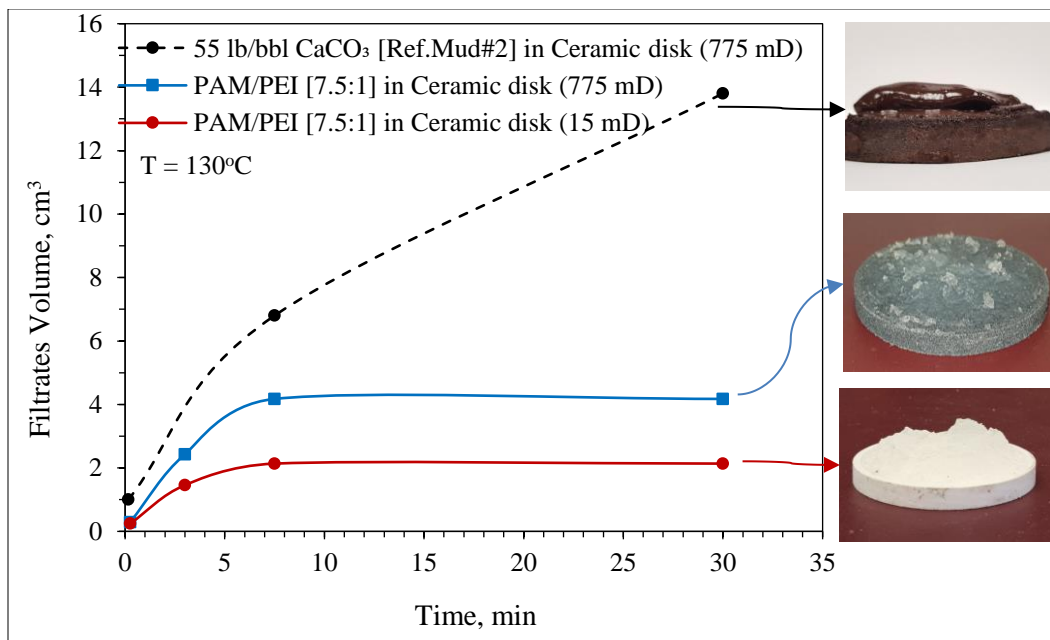


Figure 5. 47: Results of static filtration with ceramic filter disks using PAM/PEI pill and Ref.Mud#2.

5.7.1.2 Static Filtration in Carbonate

Carbonate formations usually have natural fractures that cause lost circulation. The purpose of this part of the experiments is to evaluate the performance of the polymeric gels in sealing micro-fractures in carbonate formation. The PAM/PEI formula in its flowing state and the WBM

(Ref.Mud#2) were designed to have the same rheological behavior. The difference is that the WBM contains various solids particles, as shown in Tables 4.2 and 4.3, and sized calcium carbonate (CaCO_3) as primary LCM. On the other hand, the PAM/PEI main sealing mechanism is its gelling property attained at the preset onset temperature (130°C). Both fluids have apparent viscosities from 15 to 20 mPa.s at 130°F .

The results of the WBM and the PAM/PEI filtration in carbonate cores are shown in Figure 5.48. Filtration experiments were conducted under 500 psi differential pressure and 130°C . The PAM/PEI formula stopped filtration through the carbonate core instantly after 3 minutes with a total loss of only 1 cm^3 . It outperformed the WBM performance due to forming a high-strength gel inside the fracture network of the carbonate under elevated temperature. On the other hand, the WBM, which relies on calcium carbonate, exhibited a very sudden severe loss of about 25 cm^3 , and the loss continued at a high rate till the end of the test. The total loss with the calcium carbonate at elevated temperature was 42 cm^3 compared to the 5.4 cm^3 collected at low temperature presented in Figure 5.45 from the previous section. The temperature negatively affected the performance of the calcium carbonate while improving the performance of the gel.

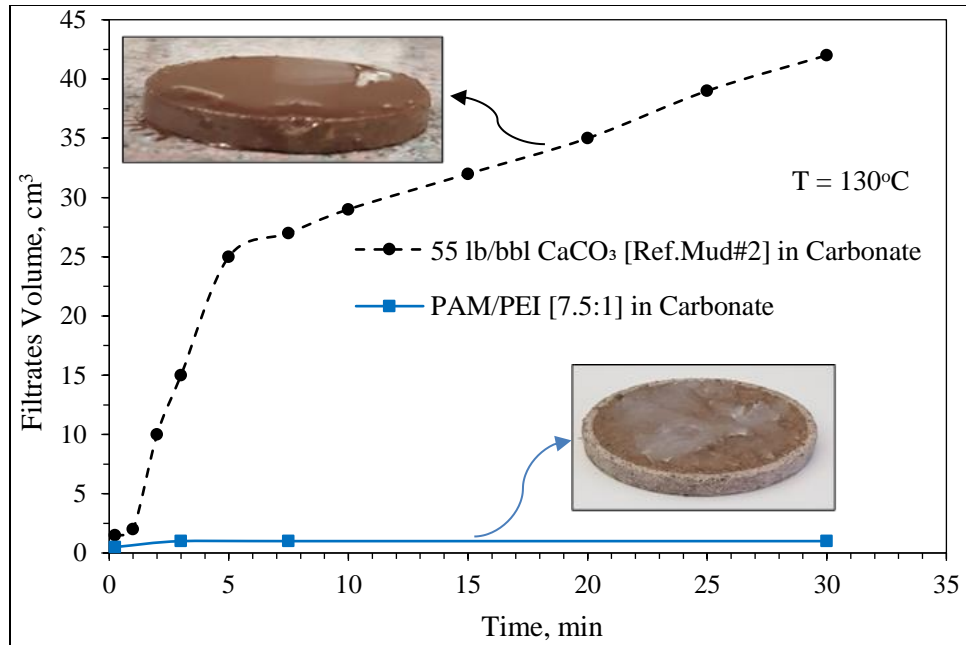


Figure 5. 48: Filtrates volume by PAM/PEI and WBM Ref.Mud#2 from the static filtration experiments in carbonate cores.

The discussed above case simulated the base case where pure PAM/PEI is used as a pill. However, in real drilling, there is contamination from the WBM and wellbore fluids, which will affect the crosslinking process of the polymer. Based on the gelation study discussed in section 5.6, bentonite significantly impacts both rheology and gelation kinetics. The effect of bentonite on filtration was observed in the results of the static filtration in carbonate cores for the PAM/PEI containing 3.5 lb/bbl bentonite shown in Figure 5.49. Figure 5.50 shows the summary of cumulative filtration volumes and sealing pressure from the pore-scale static filtration experiments. Generally, the cumulative filtration volume at the end of each static filtration experiment was directly related to the maximum sealing pressure achieved by the sealing.

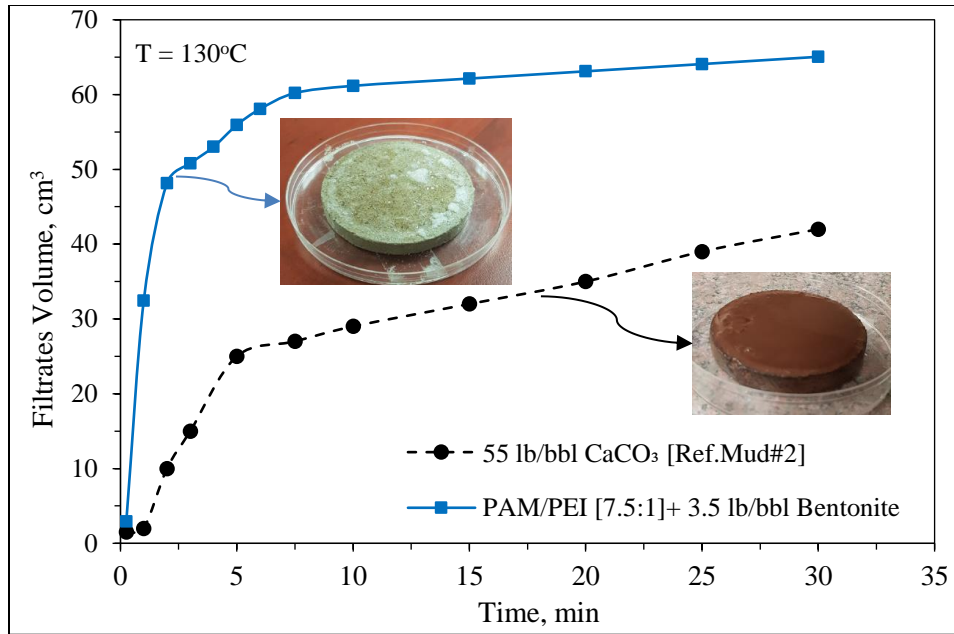


Figure 5. 49: Effect of bentonite on filtration volume of PAM/PEI compared with WBM (Ref.Mud#2) in carbonate cores.

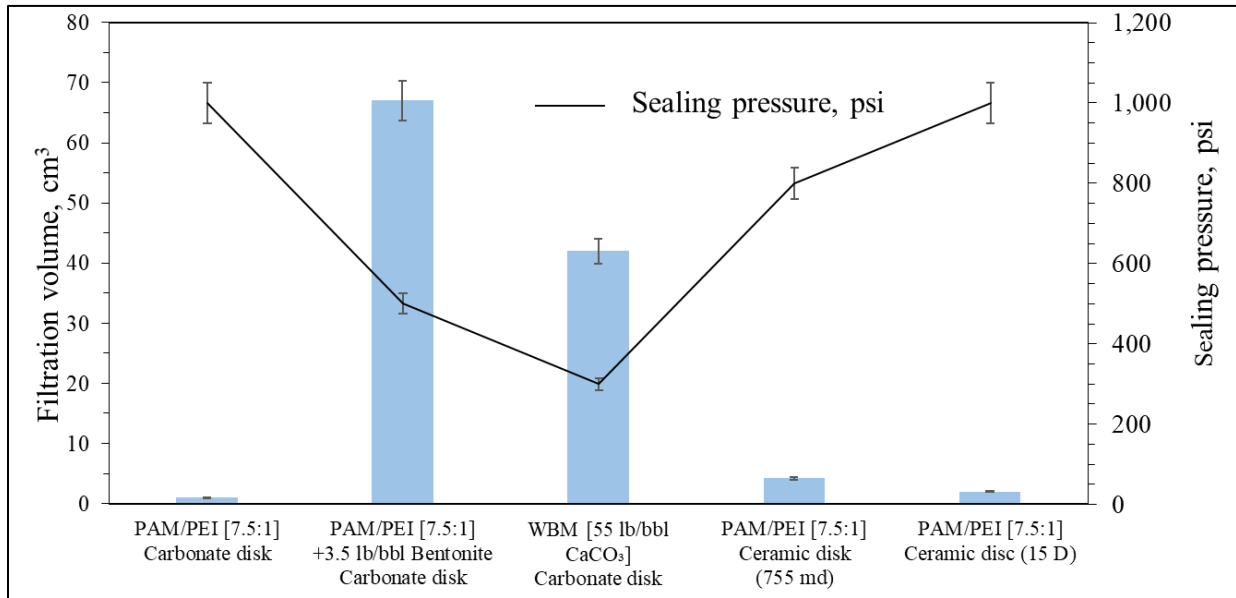


Figure 5. 50: Summary of cumulative filtration volumes and sealing pressure from pore-scale static filtration experiments.

5.7.2 Fracture-Scale Static Drilling Fluids Filtration

5.7.2.1 Fractures sealing with different polymeric gels

The results of fracture-scale static filtration using crosslinked polymer-based mud (PBM) are shown in Figure 5.51. The PBM was formulated with PAM/PEI as detailed in Table 5.1 in section

5.3. The gelling mud developed a strong plug inside the fracture, as shown in the image attached to Figure 5.51. There was a noticeable delay in achieving the sealing, which was attributed to two possible conditions. First, the fracture is larger than the pores of porous filter disks, which take longer to seal. Secondly, bentonite and barite in the PAM/PEI-based mud cause a delay in the gelation process, as explained earlier in the gelation study section 5.6. Although this delay, the sealing was eventually achieved, and filtration peaked at 28 cm³ after 30 minutes. The test was extended to 20 minutes to eliminate the low gelation rate effect, and no flow was observed.

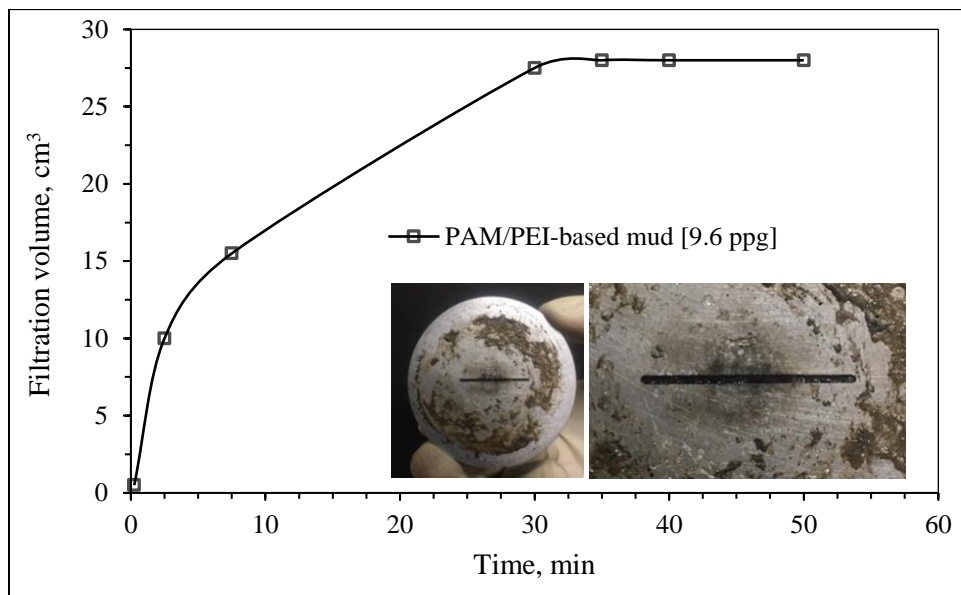


Figure 5. 51: Fracture-scale filtration by the PAM/PEI-based mud.

Figure 5.52 summarizes cumulative loss volumes and the attained maximum sealing pressure for various conducted tests. The polymeric formulations with PEI, AlAc, and FNS all succeeded in stopping loss at 130°C (266°F). The slight variations in the performance are due to the different gelation times, which reflected clearly on the sealing pressure. The pure PAM/PEI at a high concentration of PAM (9 wt.%) showed similar performance to the 7.5 wt.% PAM since they both have the same PEI concentrations; they developed a sealing gel following the same kinetics. Comparing calcium carbonate and cedar fiber revealed that calcium carbonate fails in

sealing fractures while cedar fiber successfully stopped the loss. Figure 5.53 shows the images of fractured aluminum disks after the static filtration experiments with the different formulations used in this study. Like the filtration volume and sealing pressure, the performance was reflected on the fractured disks' physical appearance after the experiments. The polymeric gels established strong plugs inside the fractures.

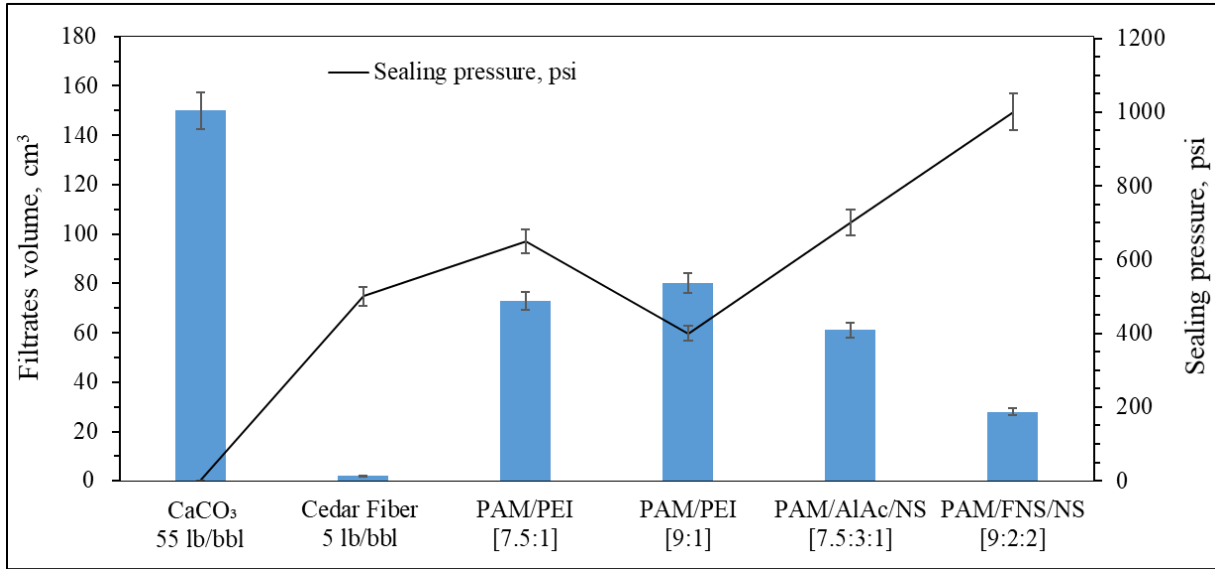


Figure 5. 52: Summary of cumulative loss volume and sealing pressure from the fractured scale static filtration experiments.

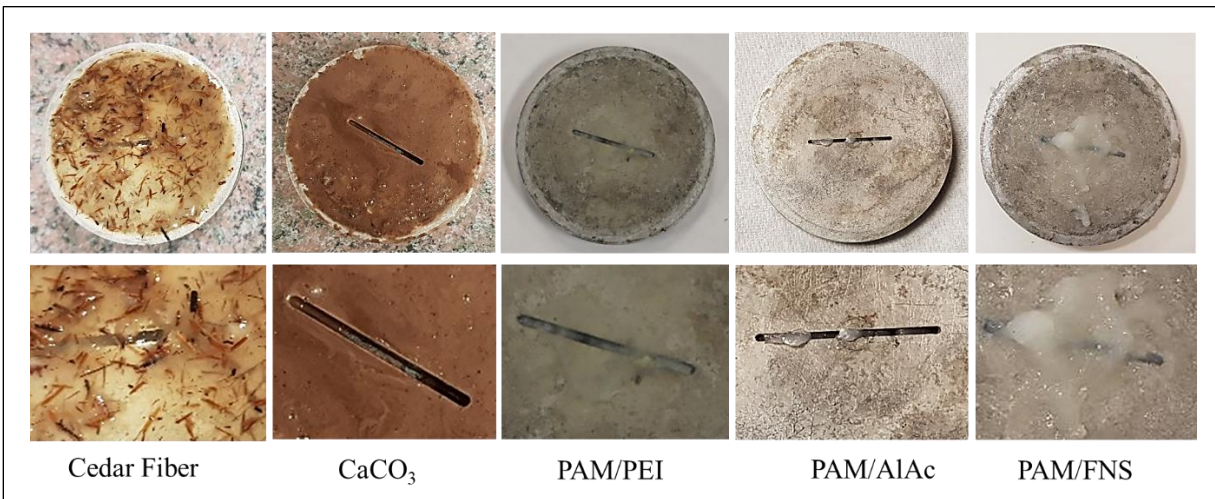


Figure 5. 53: Images of 1000 microns fractures after static filtration experiment with different formulations.

5.7.2.2 Effect of Fracture's Shape and Size

One of the critical factors in any loss circulation treatment is the proper understanding of fracture characteristics. The shape and fracture size define the selection criteria of the LCM types, size, and concentrations. Polymeric gel LCM reduces the limitation in material selection, where one formulation can work for multiple fractures with various shapes and sizes. In this subsection of the results, several experiments of fracture-scale static filtration were conducted using PAM crosslinked with PEI, AlAc, and FNS. Figure 5.54 shows the sealing of a complex fracture with PAM/FNS pill, and Figure 5.55 shows the sealing of fractures having different sizes, 1000, 2000, and 3000 microns. All experiments yielded similar results, which conclude that the polymeric gels' sealing mechanism does not depend on the size or shape of fractures. The most important parameter is to properly design the composition to control the gelation time and gel strength.



Figure 5. 54: Sealing of a complex fracture with PAM/FNS pill.

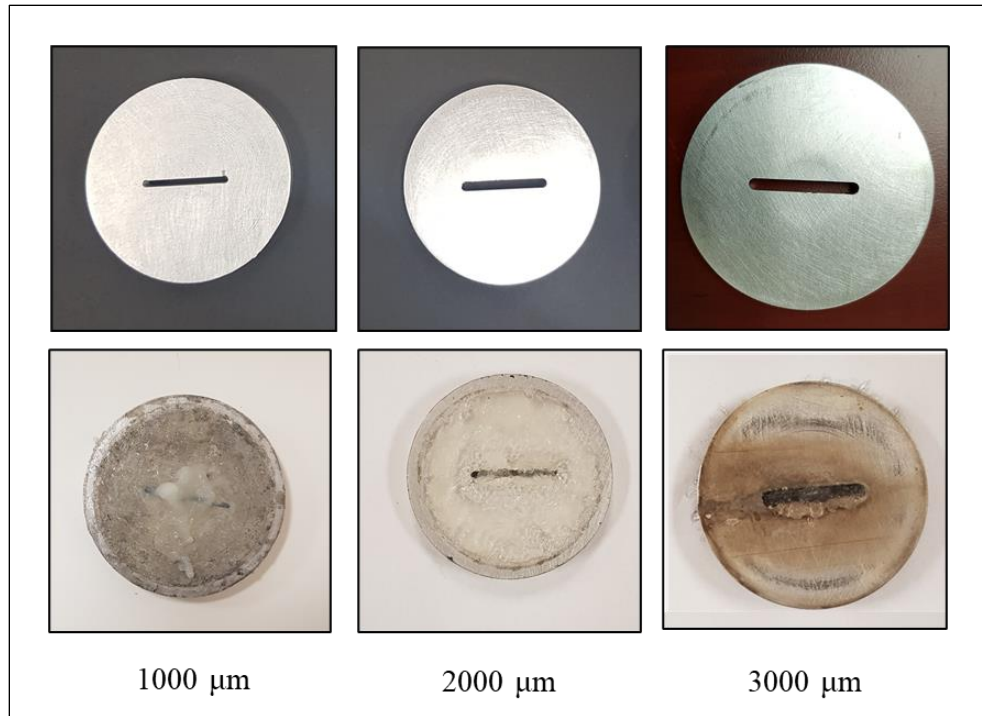


Figure 5. 55: Sealing of fractures of different sizes with PAM/PEI pill.

5.7.2.3 Effect of Temperature on Polymer-Based LCMs

The gelation process, which controls the flow status of the gel and its viscosity, is mainly governed by the temperature and the concentration of polymers, crosslinkers, and retarders. In this study, the effect of temperature was investigated by conducting several static filtrations using 1000 μm fracture for an extended time instead of 30 minutes. All filtration tests were started after waiting on the gel for 20 minutes to activate the gelation process and eliminate the gelation time effect. The extended test time also proves that the pill keeps its integrity, and the fractures or loss zones in the well will remain sealed enough for the drilling process to be safely continued.

Figure 5.56 shows the results for the PAM/PEI and PAM/FNS pills. The two temperatures selected were the low temperature, where the gel is in the flowing state and when under downhole temperature matches the onset temperature of gelation (130°C). The effect of temperature was evident in the cumulative volume and the injectivity of both crosslinked polymers. The gels tend to have high injectivity at the beginning at low temperatures or before the gelation temperature is

reached, then the flow stops completely at a time less than 2 minutes for the PAM/FNS pill and 10 minutes for the PAM/PEI pills.

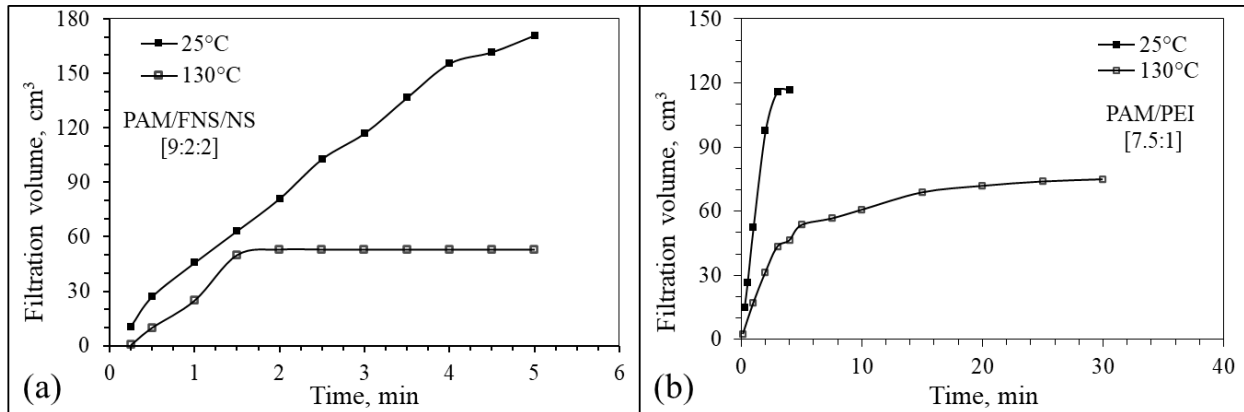


Figure 5.56: Effect of temperature on the cumulative loss of (a) PAM/FNS and (b) PAM/PEI pill by static filtration experiments in 1000 microns fracture.

For the PAM/AlAc gels, the fracture sealing experiments were conducted at three different temperatures, 25°C, 50°C, and 130°C, while the pressure kept constant at 1000 psi. The progress of filtrates volume with time and the maximum sealing pressure were used as performance indicators. The temperature range was selected to reflect the operational conditions in the field. For instance, the 25°C was tested to simulate the surface mixing and preparation or the injectivity before gelation occurs. The results showed high injectivity through the fracture at surface temperatures. After the fluid is injected into the well, its temperature gradually increased until it reached the gel onset temperature, 50°C for the AlAc.

Figure 5.57 shows the sealing experiment results at 50°C and 130°C to test sealing efficiency at a more comprehensive temperature range. Testing at higher temperatures was intended to expand the temperature window of the PAM/AlAc pill. The results presented in Figure 5.57 showed that both experiments at elevated temperatures have similar filtration trends. In the beginning, the filtration rate was 3 cc/min, and then after 3 minutes, the gelation process achieved about a 50% reduction in the filtration rate to 1.6 cc/min. The filtration then continued at a

sustained rate of about 80% less until the fracture was wholly sealed in 30 minutes. The polymeric gel held sealing pressure up to 700 psi and 2000 psi with no flow when experiments were conducted at 50°C and 130°C, respectively. The conclusion that can be withdrawn here is that temperature has a positive effect on sealing efficiency. The polymers usually have high thermal stability, and the ultimate gel strength increases with temperature. Figure 10 shows the artificially fractured aluminum discs wholly packed with the polymeric gel. The pill held the pressure across the fracture for more than 30 minutes, which was the total time of the experiment.

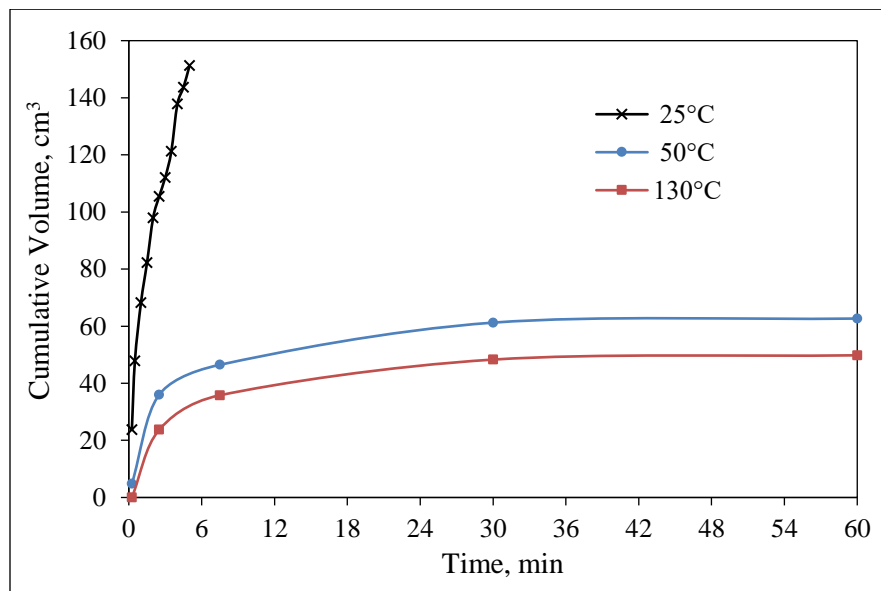


Figure 5. 57: Effect of temperature on the cumulative loss of PAM/AlAc pill by static filtration experiments in 1000 microns fracture.

5.7.2.4 Effect of Gelation time Polymer-Based LSM

The gelation time should be considered to remediate severe drilling fluid loss. The mature polymeric gel can form an efficient sealing material inside the fracture to stop lost circulation when both conditions are met, the gelation time and the onset of the gelation temperature. Figure 5.58 shows an experimental investigation of the effect of waiting time on gel curing and the mud loss treatment using PAM/PEI pills. The mud loss was collected at 266°F (130°C) using PPA equipped with an aluminum disk holding a 1000 μm fracture. Three different waiting times were given to

the PAM/PEI formula before starting the test. In the no waiting case, the PAM/PEI pill required about 15 minutes to stop the mud loss, compared to 5 and 4 minutes for a waiting time of 60 minutes and 120 minutes, respectively. However, the cumulative mud loss was higher by 150%. This agrees with the previous rheological investigation of the gelation time by the viscosity over time curves. The pure PAM/PEI gel required about 14 minutes to start the gelation process.

The sensitivity of time on the cumulative mud loss and the maximum sealing pressure that the polymeric gel pill can achieve can be recognized from the results illustrated in Figure 5.58. As shown in the results, with no waiting time, the gel will escape the fractures until its viscosity gradually increases due to the gelation process. The fluid then will cease to flow as the gelation process is taking place to form a rigid gel and permanently plug the fracture. The sealing pressure (Figure 5.59) is also affected by the time given to the gel to mature since the gel strength of the gel is time dependent as well. With enough time for the gelation process to complete, the sealing pressure has been able to hold up to 2000 psi compared to 400 psi at the beginning of the pill placement. Given that, the setting time for the gel needs to be designed carefully to stop lost circulation by using proper retardation to delay the gelation just enough for the fluid to reach the targeted depth.

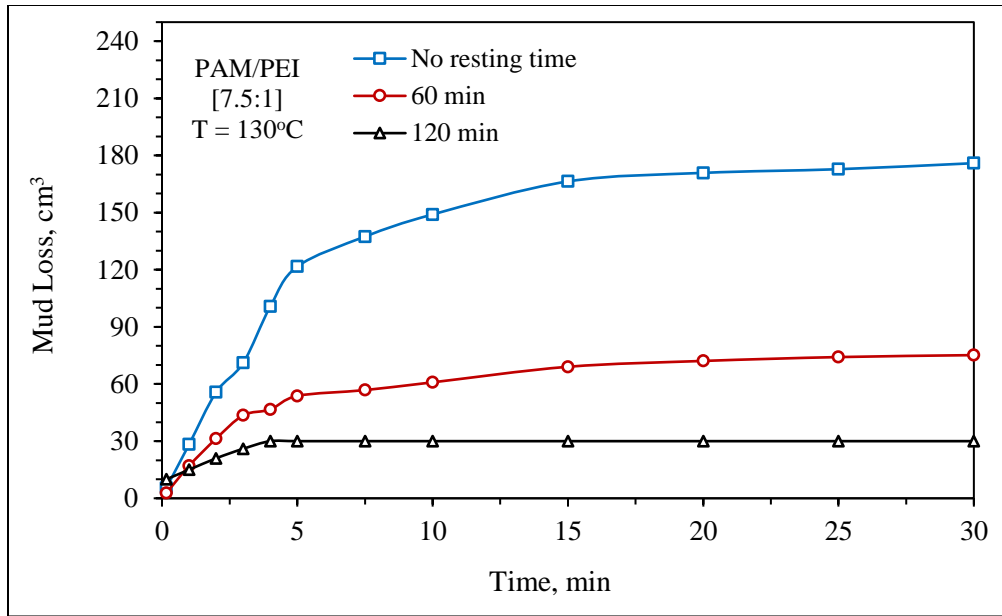


Figure 5.58: Mud loss versus time at different gelation times using PPA with 1000-micron fractured disc.

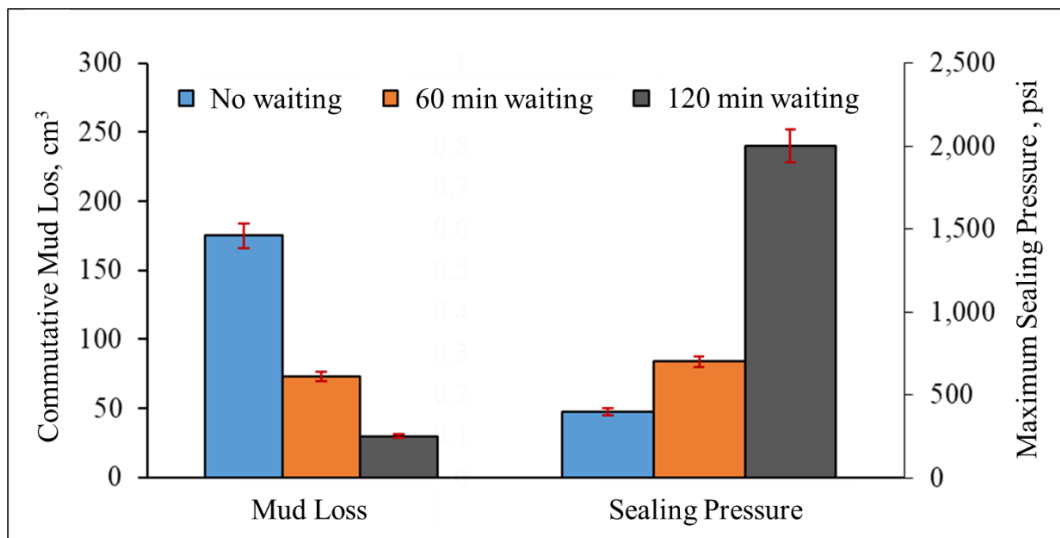


Figure 5.59: Cumulative mud and maximum sealing pressure using PPA with 1000-micron fractured disc.

5.7.3 Fracture-Scale Dynamic Drilling Fluids Filtration

This section shows the loss profile from the dynamic drilling fluid filtration experiment using the dynamic drilling simulator (E2200). The cumulative dynamic fluid loss is plotted against the time in minutes from zero to 30 minutes. The sample selected for this test was the optimized PAM/PEI formula in a ratio of 7.5:1 and used to seal a 1000 μm vertical fracture. The temperature testing conditions also was selected to allow for crosslinking of the polymer at 130°C, tested under 300

psi differential pressure, while 100 rpm rotational speed was applied.

During the test, the data acquisition system (DAQS) was used to collect the filtrates every five seconds, which will accurately capture the spurt loss. Figure 5.60 shows the filtration profile of the PAM/PEI for 30 minutes. Overall, the loss rate was $0.073 \text{ cm}^3/\text{min}$ with a cumulative loss of 5.5 cm^3 . Compared to static filtration results, there is a noticeable delay in the filtration; this can be called breakthrough time. The breakthrough time can be defined as the time required for a considerable amount of loss to occur, which is also expressed as the spurt loss. In static filtration, this takes about 15 seconds. In dynamic filtration, it takes more time due to the flow characteristics and the time required to establish the sealing in the dynamic conditions. For this dynamic filtration experiment, the PAM/PEI breakthrough was 1.6 minutes, as shown in Figure 5.60. The filtration then continued at a low rate ($0.06 \text{ cm}^3/\text{min}$), which is expected to cease complexly after the gel fills the fracture and solidates. After the experiment is completed, the aluminum cylinder was retrieved to examine the plugging visually. Figure 5.61 shows how the 1000 microns vertical fracture is wholly sealed with the gel.

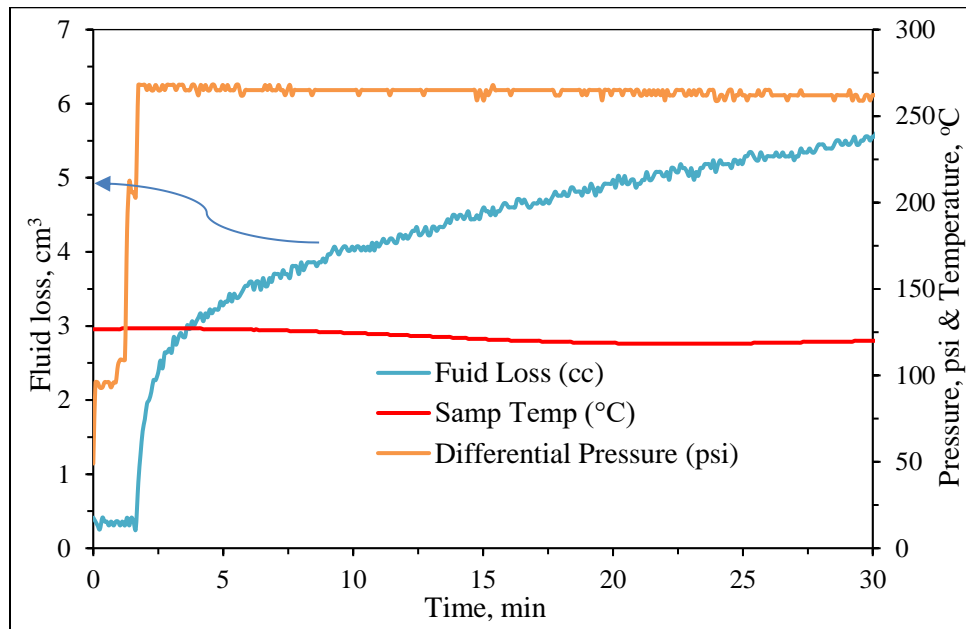


Figure 5. 60: Dynamic fluid loss profiles for PAM/PEI [7.5:1] in 1000 μm vertical fracture.

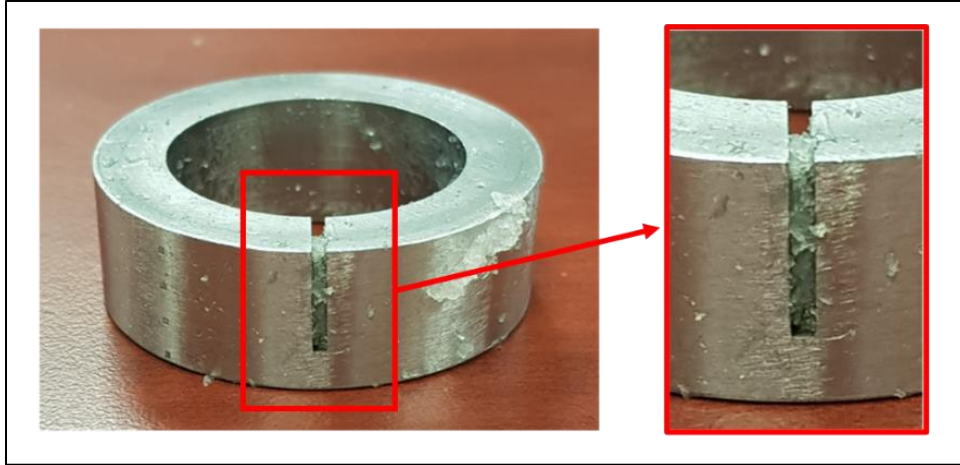


Figure 5. 61: 1000 μm sealed with PAM/PEI gel in dynamic filtration experiment.

5.8 Investigation of Filter Cake Evolution

In this research, it was essential to study the evaluation of filter cake resulting from filtration of the crosslinked polymers. To the best of the author's knowledge, no previous studies considered filter cake investigation and formation damage assessment for the crosslinked polymers. One of the hypotheses of this study was that the gelling LCMs should minimize the probability of formation damage. It eliminates the need for large granular LCMs to plug larger fractures. The filter cake was examined after static filtration experiments to verify this assumption. The filter disks cut from carbonate rocks and ceramic disks were used in the filtration experiments. The polymeric fluids and the reference WBM were encouraged to filtrate through the filter disks before retrieving the disk and examine the filter cake. The internal and external filter cakes were investigated. The visual inspection of the external filter cake showed that the PAM/PEI fluid formed a thin wavy surface with a uniform structure. Figure 5.62 compares the external filter cake of PAM/PEI [7.5:1] fluid compared to mud cake created with the Ref.Mud#2 containing calcium carbonate. Different filter disks showed similar filter cake shapes, and cake thickness was about 2 to 4 mm for all samples.

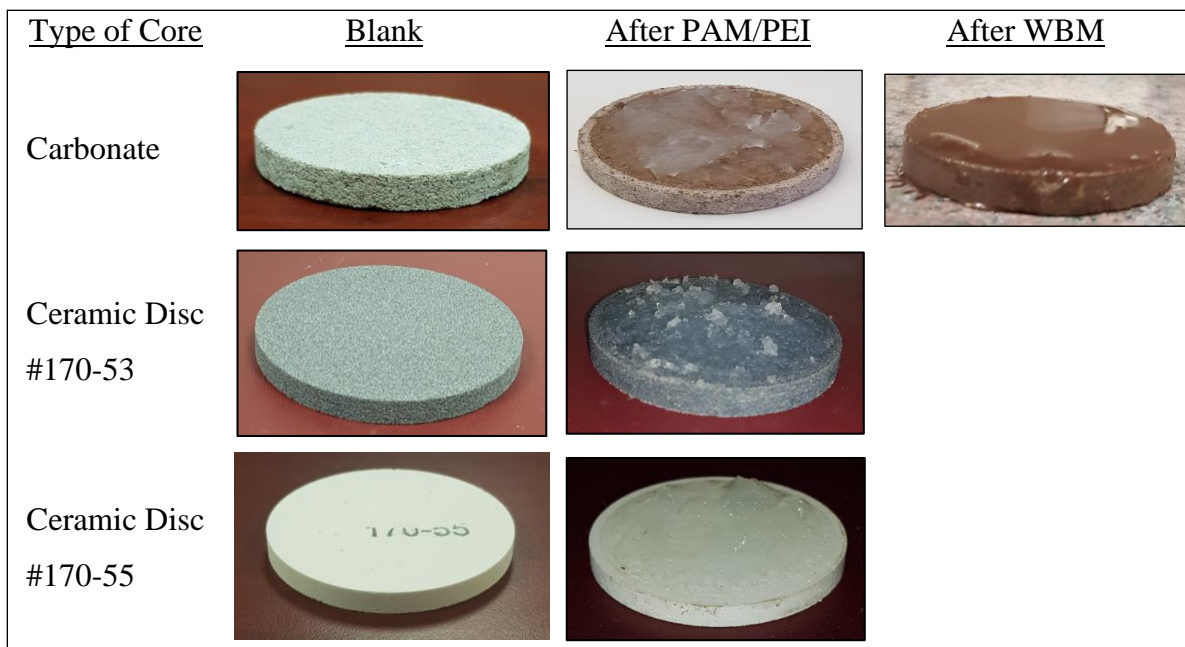


Figure 5. 62: External filter cake formation on different filter disks.

5.8.1 Evolution of the Internal Filter Cake

Figure 5.63 describes the SEM images of the internal filter cake taken from the cross-sectional side of the carbonate filter disk as explained in the methodology section. The results presented show the internal filter cake for the PEI-crosslinked PAM and the calcium carbonate mud. A control sample of carbonate is also presented, which shows clean open pores, as marked in Figure 5.63a. The carbonate grains showed different sizes, varying from 5 to 30 μm with many visible, connected voids. Figure 5.63b and c describe the cross-sectional side of the carbonate filter disk after polymer and calcium carbonate mud invasion. The calcium carbonate and other particulates within the WBM penetrated the carbonate pores and filled its void spaces, as illustrated in the SEM images shown in Figure 5.63b. The images show a uniform distribution of the calcium carbonate particulates inside carbonate core voids which created an internal filter cake with relatively high permeability indicated by the high filtration rate.

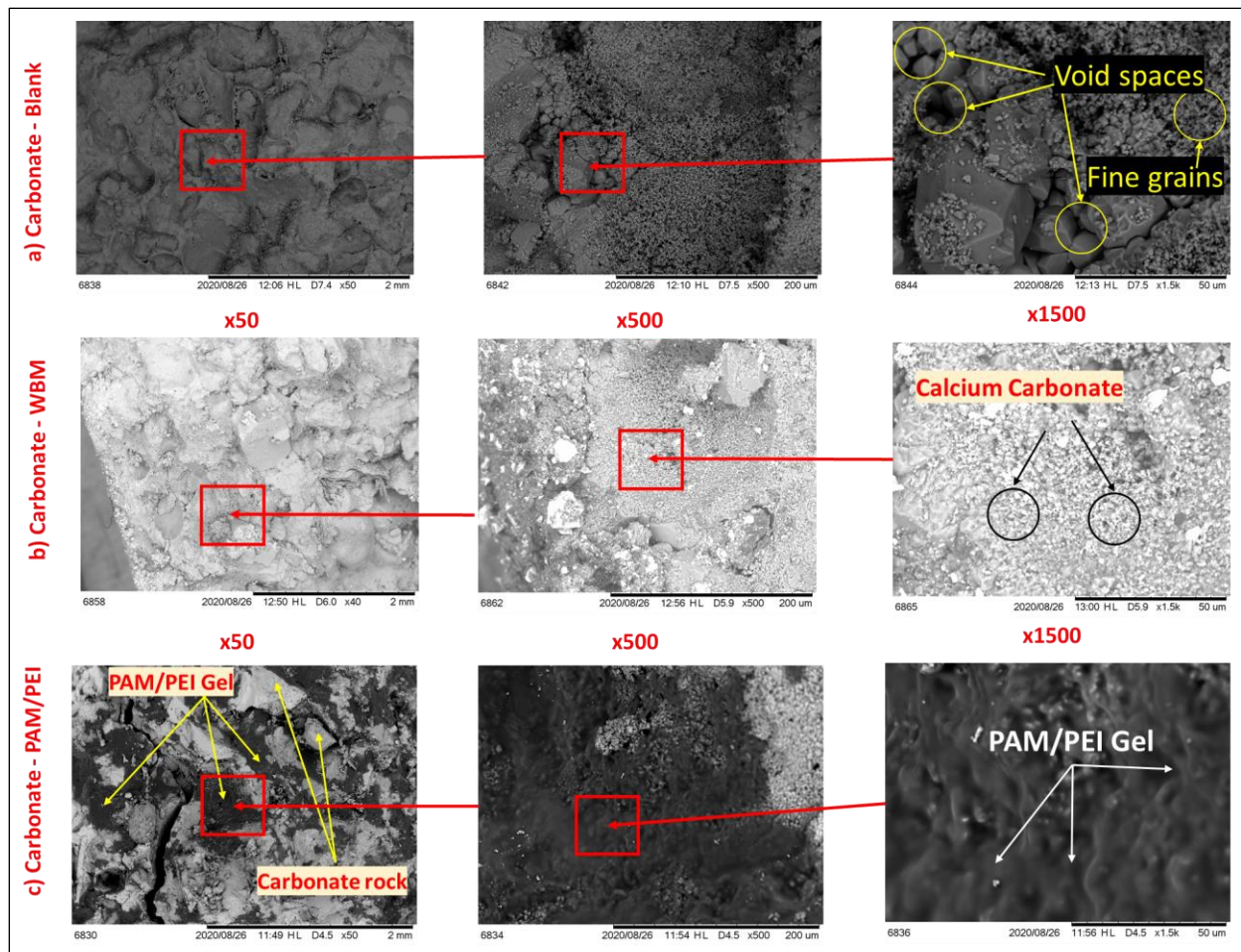


Figure 5.63: SEM images for the (a) carbonate blank core and the internal filter cake after the PPA test with (b) WBM and (c) PAM/PEI.

In the other case, the PAM/PEI gel barely invaded the carbonate disk. A uniform paste-like surface was observed inside the pores. The shape and structure of the PAM/PEI internal filter cake explained their sealing mechanisms; the gels displayed a thick surface and tidy structural shape. The filtration stopped because, unlike calcium carbonate, no open pores in the crosslinked polymer gel's micrographs, as visualized in Figure 5.63c. The black areas in the SEM images are attributed to the high atomic number of the PAM. Based on this microscopic examination, the PAM/PEI had plugged all open voids in the carbonate and sealed it entirely.

Furthermore, Energy-Dispersive X-ray (EDX) analysis was conducted to quantify the internal filter cake composition for the three above samples. The result of the analysis is presented in Figure 5.64. The majority of elements are carbon (C) and calcium (Ca) which is typical for carbonate cores, close to 90 wt.%. The other detected elements were the minerals that exist in the WBM additives. This analysis concludes that in the carbonate core sample where PAM/PEI was used, the carbon content was higher by 100%, and calcium was less by 50%, which means that pores are covered with the gel. The high carbon content in the cores invaded by PAM/PEI was because PAM monomers are primarily composed of carbon and hydrogen, as shown in their chemical structure; $(C_3H_5NO)_n$. The EDX results agree with the SEM images' conclusion, which showed that carbonate pores were filled with the crosslinked gel.

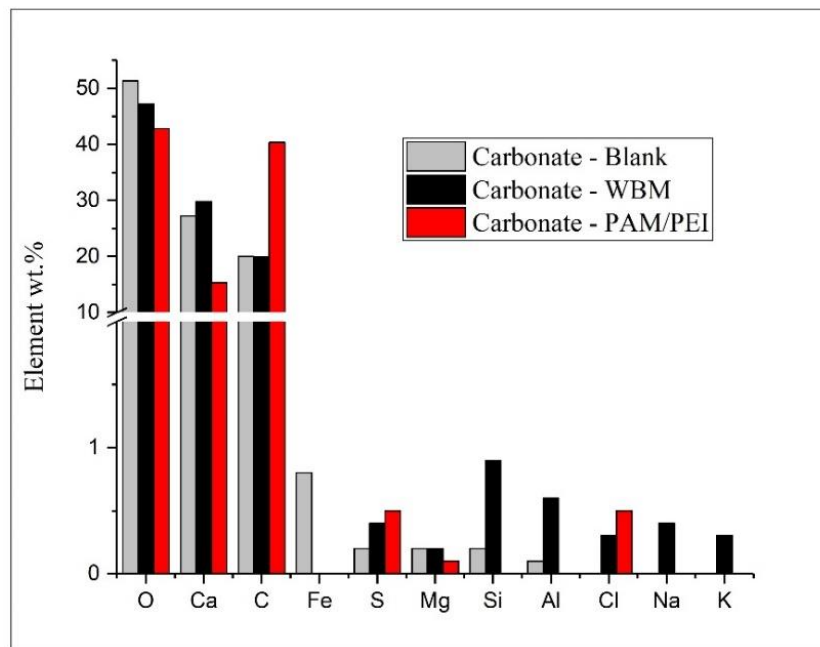


Figure 5. 64: EDX analysis of the internal filter cake forming in carbonate by WBM and PAM/PEI.

More analysis of filtration of PAM/PEI was conducted in ceramic filter disks having two different pore throat sizes and permeability. The purpose was to see how permeability will affect the invasion of the gel into the cores. Figure 5.65 describes the SEM images taken after the static

filtration tests. As described in the microscopic images, the comparison between before and after PAM invasion clearly shows that void spaces are filled with the gel, pointed by the arrows.

Additionally, the color of the images indicates the gel's density inside the pores since more polymers darken the image due to the high atomic number. Examining both filter disk images; one can observe that the permeability had affected the invasion of the gel. The internal filter cake was more visible, having dark color in the filter disk with higher permeability (#170-53 with 15 D). However, PAM/PEI fluid successfully stopped filtration in both tests and plugged the pores of both disks with a slight change in the time when the total sealing was achieved. The low permeability disk took three more minutes, as discussed earlier in this dissertation in section 5.7.1.

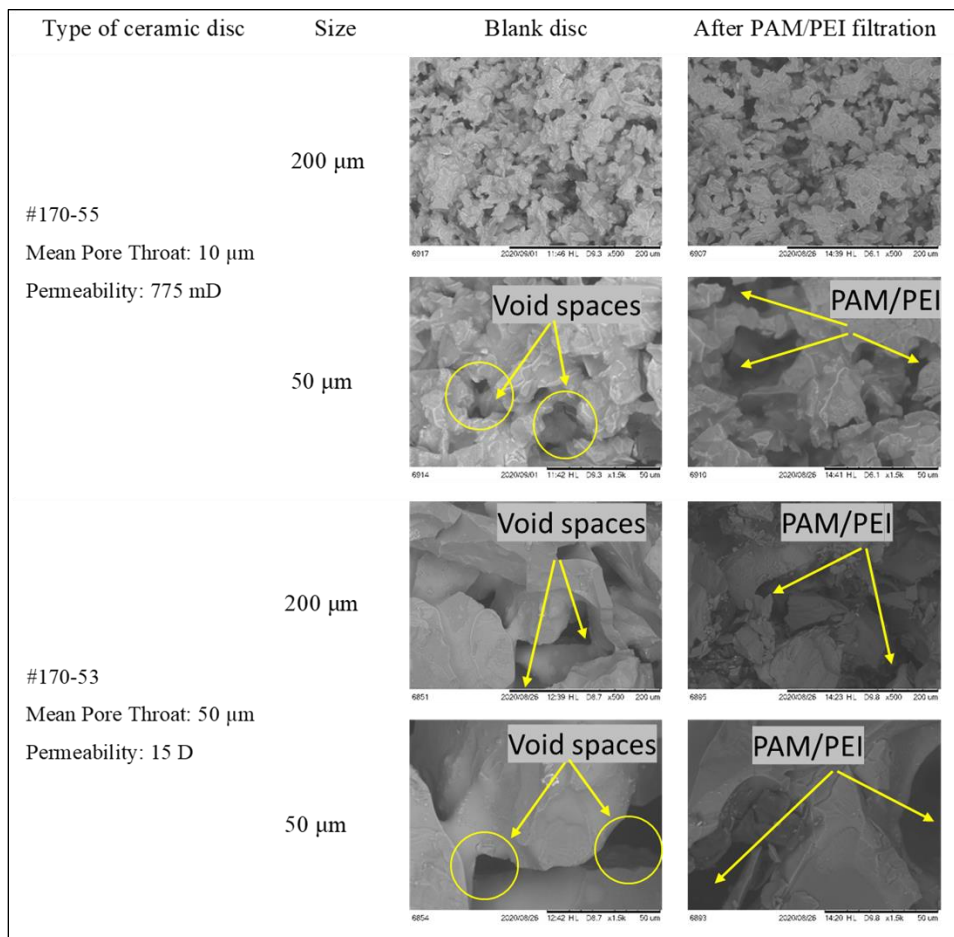


Figure 5. 65: SEM images for the internal filter on ceramic filter disks #170-53 and #170-55 before and after PPA test with PAM/PEI.

5.8.2 Formation Damage and Secondary Filtration

Potential formation damage that may occur was also investigated using SEM images. The spectrum of SEM was selected in two areas to explore the deeper invasion. One point was close to the filtration side, and the other one was close to the exit side. The areas of interest are indicated by the arrows shown in Figure 5.66. The images were grouped into two sections. The top three ones describe the disk area close to the filtration direction, which explores the internal filter cake. The other three images on the bottom of the figure show the deeper invasion after the fluid passes through the internal filter cake. The other three images on the bottom of the figure show the deeper invasion after the fluid passes through the internal filter cake.

The 1500 times magnification shows that the pores of the calcium carbonate within the WBM filled these pores, leaving many spaces between its granular particulates, which allowed for further filtration. As described in the bottom set of SEM images in Figure 5.66, the fine particles of CaCO_3 passed through the internal filter cake and reached deeper in the carbonate disk. With more pressure exerted on the disk, more fine particulates will invade the core. If these particulates were not removed later with a method of filter cake removals, it will significantly reduce formation permeability and impair the productivity of the well.

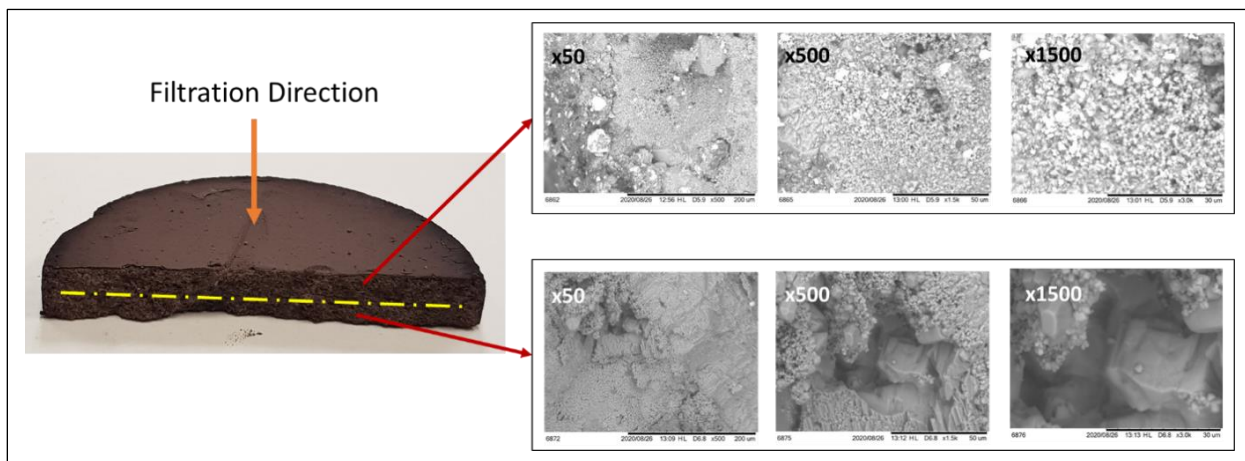


Figure 5. 66: SEM images for the invasion of WBM filtrates inside carbonate disk.

On the other hand, The PAM/PEI internal mud cake did not penetrate deep inside the core; only about 0.125 inches was affected, as shown in Figure 5.67. The top three SEM images in Figure 5.67 show thick polymer gel covering all carbonate pores and sealing it entirely with a thick layer of high strength gel and very low permeability indicated by the filtration results. The bottom set of SEM images shows clear open pores with no visible traces of polymer. This suggests that the resulting internal filter cake from PAM/PEI formula is limited to small areas near the wellbore, which will reduce the contamination of the reservoir and causes less formation damage.

The process mainly depends on the rheological properties and injectivity of the polymer fluid. The injectivity of PAM/PEI fluid will depend on the initial permeability of the rocks in the vicinity of the wellbore, which governs the depth of invasion. Later, when the crosslinked polymer activates, a mature gel will form inside the formation, sealing the pores entirely and preventing a further invasion. After sealing off the loss zone with PAM/PEI gel, the drilling can be resumed.

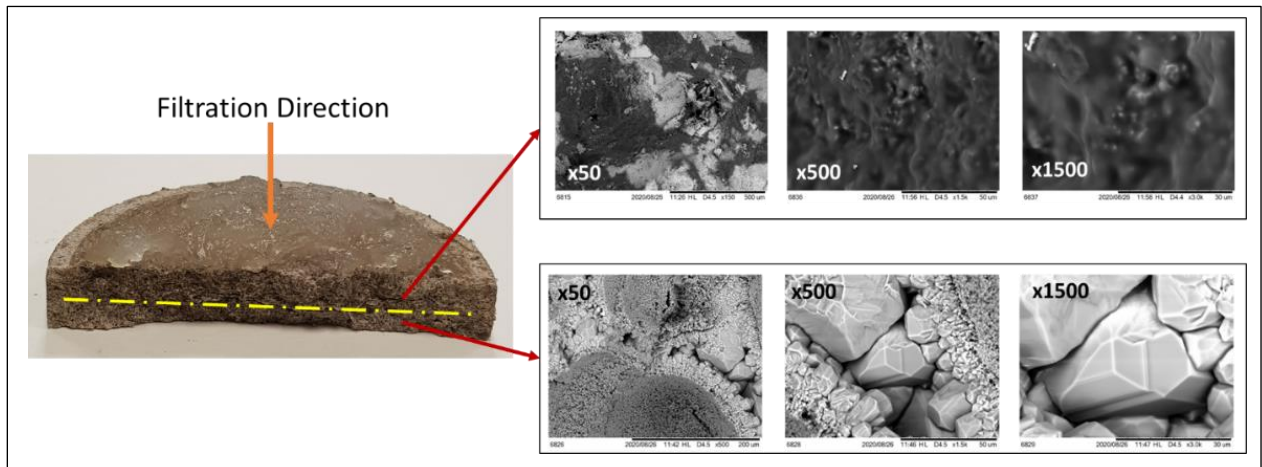


Figure 5. 67: SEM images for the invasion of PAM/PEI filtrates inside carbonate disk.

Chapter 6: Machine Learning Analysis Results and Discussion

In this chapter, the results from the machine learning modeling and rheology data prediction work will be presented. First, the tuning of the model results will be presented for the ML model that was built, as explained in section 4.3. then the prediction performance of models will be discussed.

6.1 Modeling and Tuning of Models Parameters

The accuracy of each used algorithm can be enhanced by tuning and adjusting the parameters of the models. In the k-Nearest Neighbor (KNN) algorithm, the tuning process was conducted in steps. First, a simple model using the KNN algorithm was generated, and the available data set was used to train the model. The input parameters were the concentrations of different components, and the output was the apparent and plastic viscosity. The parameters of interest in the KNN algorithms were the weight, algorithm, leaf size, power parameter, and metrics. A uniform weight was adopted, and an auto algorithm selection was implemented. The power parameters and leaf size were set to 2 and 30, respectively. For the metrics, the Standard Euclidean distance metrics were selected. The maximum accuracies for apparent and plastic viscosity predictions were 67.8% and 77.9%, respectively.

Since the number of the nearest neighbors governs the accuracy of the kNN algorithm, the number of nearest neighbors was varied accordingly to explore the behavior of the algorithm. The prediction accuracy had changed significantly with the change in the nearest neighbors, as illustrated in Figure 6. 1. The combination that yielded the maximum prediction accuracy was determined to 3 closest neighbors sampling for plastic and apparent viscosity.

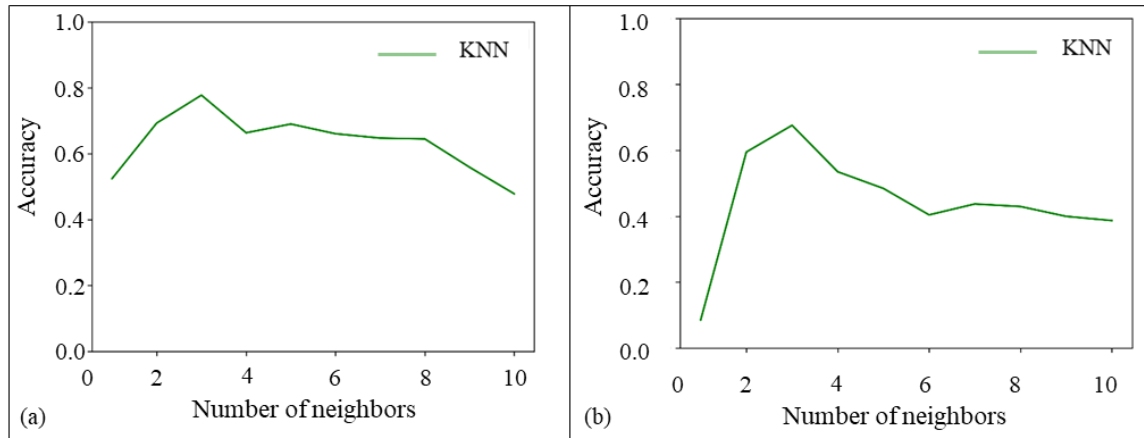


Figure 6. 1: Accuracy of the kNN algorithm regarding the number of nearest neighbors for (a) plastic viscosity and (b) apparent viscosity.

For the Random Forest (RF), the mean square error was used to determine the quality of split and reduction of the variant. The nodes were set to expand until all leaves have less than two samples or all leaves are pure. The minimum number of samples for establishing the leaf node and weight fraction of the total weights were considered 1 and 0, respectively. The RF model was based on all six components of the data set, which are the different inputs that contribute to the rheology of the formula. These various inputs were used to be as features in the model. The main parameter in the RF is the number of trees. In this tuning stage, the number of trees was varied from 0 to 100. Figures 4 present the effect of changing the number of trees on the accuracy of the prediction for apparent and plastic viscosity. The accuracy increases seem to increase with the number of trees up to 20. However, after 13 trees for apparent viscosity and 22 trees for plastic viscosity, the accuracy did not change much, as shown in Figure 6. 2a and b. The maximum accuracies with the RF were 60.6% and 87.9% for the apparent and plastic viscosity, respectively.

The tuning of parameters was also conducted for the Gradient Boosting (GB) algorithm using the least-squares regression to optimize the loss function. The learning rate for shrinkage contribution from each tree was 0.1. The quality of splitting the data set into a training set and testing set was estimated by the mean squared error. The main attribution used for testing the

performance of the model was the number of boosting stages since they are directly impacting the performance of the model. Therefore, the number of boosting stages and the accuracy of the test data were determined and presented in Figure 6.3. The accuracy increases with the increase in the boosting stages until it reached a stable peak of around 20 iterations. The maximum accuracy GP algorithm for apparent and plastic viscosity was 74.3 and 90.7, respectively.

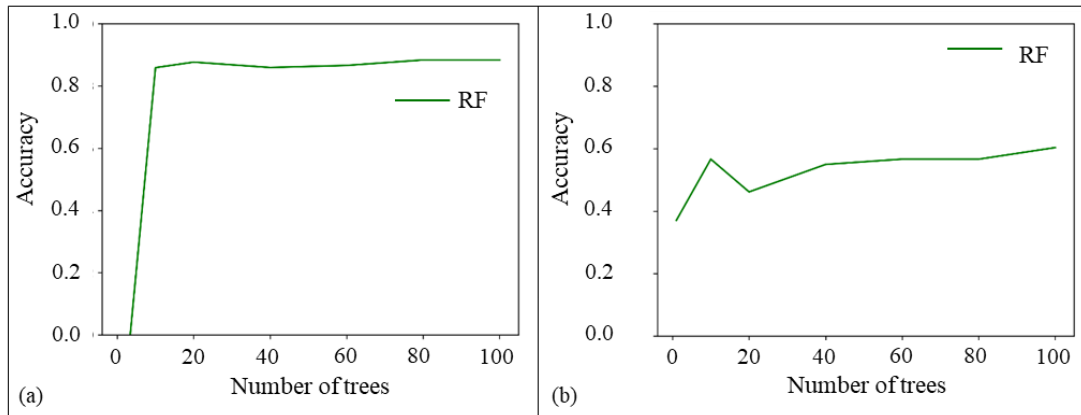


Figure 6. 2: Random Forest classification accuracy vs. the number of trees for (a) plastic viscosity and (b) apparent viscosity.

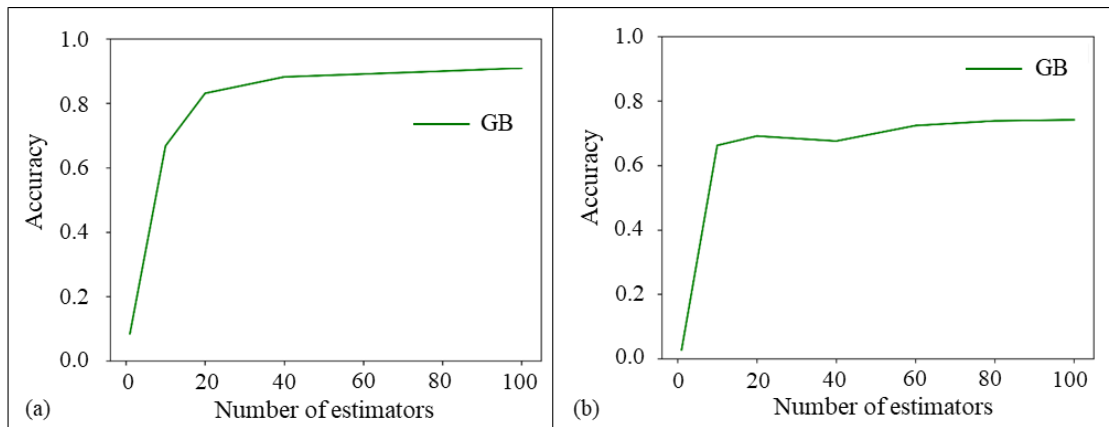


Figure 6. 3: The test dataset accuracy corresponding to the number of boosting stages for Gradient Boosting algorithm for (a) plastic viscosity and (b) apparent viscosity.

The last tuned algorithm in this study was the AdaBoost (AB) algorithm. In this model, the main tuning parameters were the based estimator, number of estimators, learning rate, loss, and random state. The considered base estimator and learning rate were 3 and 1, respectively. The number of estimators was varied in the form of boosting stages. The AdaBoost algorithm's

performance depends on the iterative steps, which improves estimators' performance with the boosting stage. Therefore, the algorithm was tested corresponding to the increase in the boosting stage. Results indicated that the maximum accuracy is obtained around 25 boosting stages. The maximum accuracy was 74.3% and 88.5% for apparent and plastic viscosity, respectively, as shown in Figure 6.4.

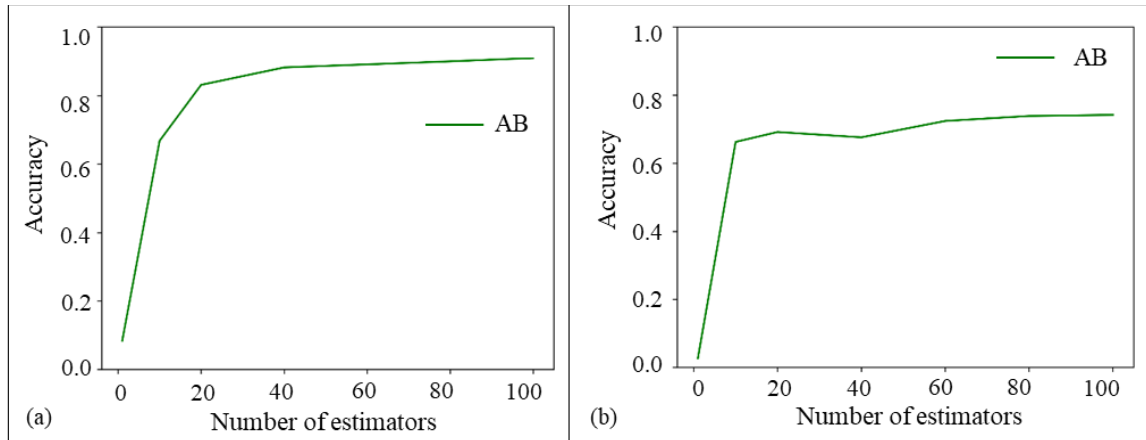


Figure 6. 4: Accuracy in the prediction of plastic viscosity and apparent viscosity using AdaBoosting algorithm.

6.2 Performance and Accuracy of Predictions

Reliable predictions of rheological data can be obtained for other systems of PAM/PEI and mud additives by using different algorithms. Figure 6.5 compares the predicted values of the testing data set with actual values using the four algorithms tested in this study for the high shear rate values. It can be assumed that the overall predictive capability of gradient boosting is higher than any other algorithm for plastic and apparent viscosity. However, AdaBoost's performance in predicting a higher range of plastic and apparent viscosity trumps other algorithms' performance. Applying the same methodology for the low shear rate data was challenging. The prediction performance reduced significantly, and the predicted values differed from the actual values shown in Figure 6.6. The efficiency of these algorithms was evaluated based on a randomly selected training and testing dataset with a ratio of 20:80. For both viscosity values, each algorithm was

executed 20 times, and statistical analysis was conducted. Table 5.4 shows the overall result for each algorithm for the high shear rate data.

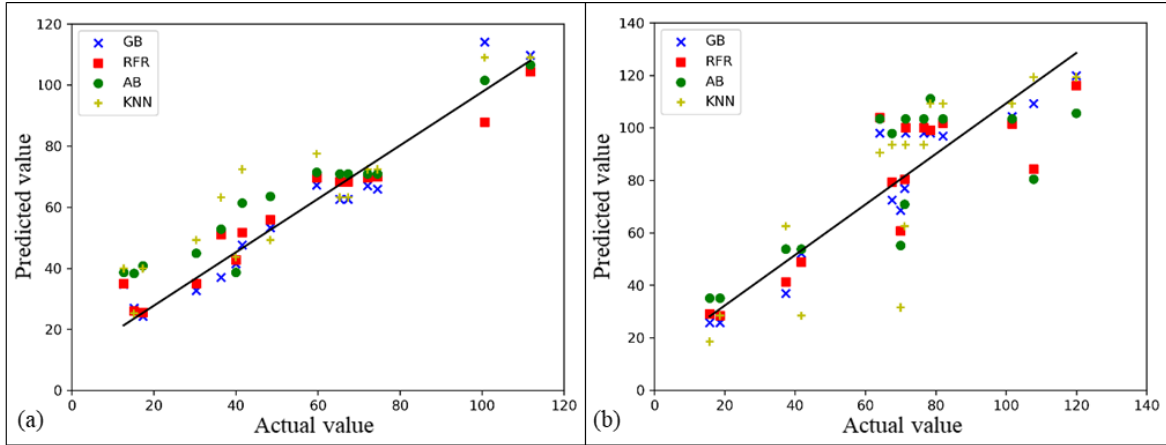


Figure 6. 5: Predicted Vs. Actual values of (a) PV and (b) AV of the testing dataset for different algorithms at high shear rate.

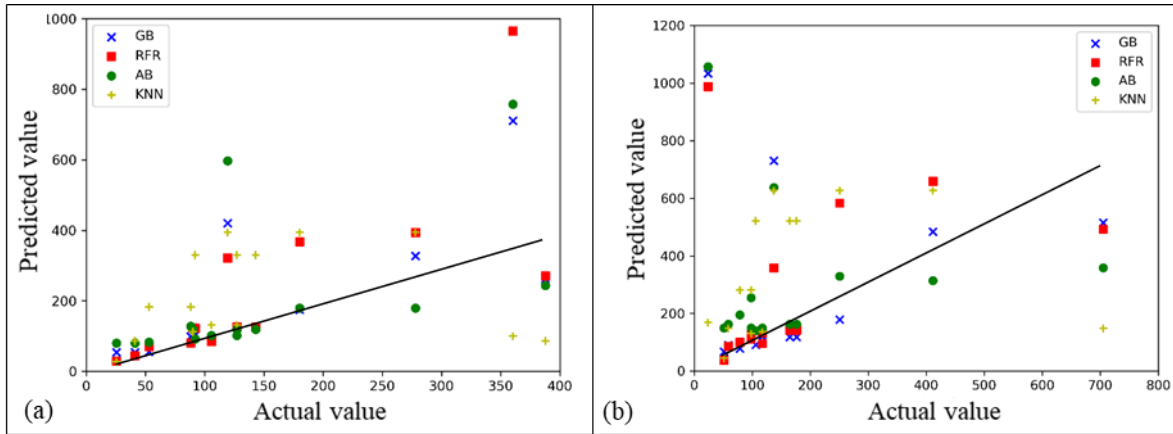


Figure 6. 6: Predicted Vs. Actual values of AV at (a) 6 rpm (10 s^{-1}) and (b) at 3 rpm (5 s^{-1}) of the testing dataset for different algorithms.

Table 6. 1: Performance of algorithms in predicting plastic and apparent viscosity (R^2)

| Algorithms | Performance | |
|--------------------|-------------------|--------------------|
| | Plastic Viscosity | Apparent Viscosity |
| k-Nearest Neighbor | 0.69 | 0.48 |
| Random Forest | 0.88 | 0.60 |
| Gradient Boosting | 0.89 | 0.74 |
| AdaBoosting | 0.75 | 0.37 |

Chapter 7: Environmental Impacts, Economic Feasibility, and Case Studies

7.1 Environmental Impact Assessment

The previous chapters emphasized the significance of types and properties of drilling fluid, type of LCM, and their concentrations for a successful drilling operation. To take it even further for field application, the evaluation of drilling fluid performance should also consider compliance with public concerns, technical requirements, and regulations. Evaluating the impact of drilling fluids impact on health, safety, and environment (HSE) is as important as their performance in the drilling operation. Basically, there is no ideal drilling fluid with zero impact on the environment and can fulfill all industry requirements. Therefore, there is always room for research and development of new formulations.

HSE concerns are crucial aspects of drilling fluid formulation. The impact is mainly due to the disposal of waste such as drilling fluids, chemicals, additives, and drilling cuttings, in addition to the mixing and treatment process (Ogeleka and Tudararo-Aherobo 2011). For instance, in offshore drilling, when fluid is dumped into the sea, the degree of environmental impact depends on water depth, amount of disposed of materials, and the drilling fluid type (Melton et al. 2004). The common assessment of the potential environmental impact of materials is their toxicity (Onwukwe and Nwakaudu 2012). The toxicity associated with the drilling operations can be attributed to three mechanisms, chemistry of mud components, storage and disposal practices, and chemistry of drilled rocks (Khodja, Khodja-Saber, et al. 2010).

According to the United States Environmental Protection Agency (US-EPA), measuring the drilling fluid's degree of toxicity and its impact on the environment is conducted by the Mysid shrimp bioassay test. The toxicity test is a protocol for recording the mean mortality percentages of mysid shrimp for varying concentrations of mud sediments in seawater, as per the National

Pollutant Discharge Elimination System (NPDES 2001). The Organization for Economic Co-operation and Development (OECD) established a bioassay testing protocol that involves preparing solutions of mud sediment in seawater in different concentrations varies from 31.25 to 500 mg/L. The shrimps are placed inside the treatment tanks, and observations are made every 24 hrs. The common observations are irritability, broken appendages, erratic movement, and mortality percentage (Ogeleka and Tudararo-Aherobo 2011; OECD 2004).

In this study, crosslinked polyacrylamide-based mud and LCM comprising organic and inorganic crosslinkers were developed. The organic crosslinker is the polyethyleneimine (PEI), and the inorganic crosslinkers are the aluminum acetate and functionalized silica. The main component of the developed gelling mud is the polyacrylamide in concentrations of 7.5 to 10 wt.%. The PAM is a macromolecule produced by the polymerization of acrylamide and acrylic acid, as shown in Figure 7.1.

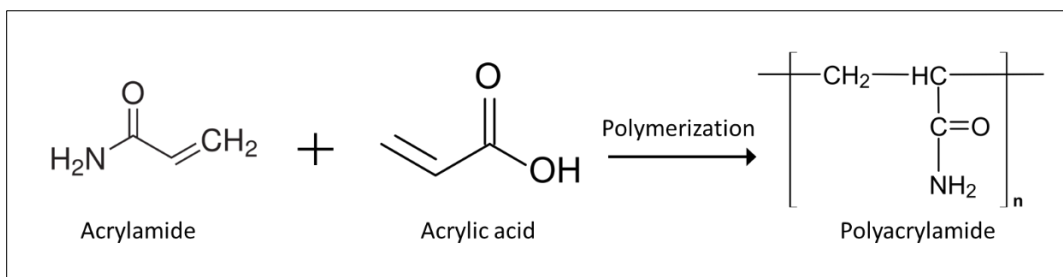


Figure 7. 1: Polymerization of acrylamide with acrylic acid.

The produced polymer has large molecules that cannot penetrate the membrane of aquatic organisms or microorganisms; therefore, it is considered nontoxic (Berndt et al. 1991). However, commercial PAM contains residuals acrylamide monomer that can adversely impact the environment (Seybold 1994). According to the Registration, Evaluation, Authorization, and Restriction of Chemicals (REACH), the PAM is classified as carcinogenic category 1B and mutagenic category 1B substance, which refers to “presumed human carcinogens” (Bradley 2008). Some states in the US specify the acceptable exposure level of acrylamide by 0.2 micrograms per

day (Cowan et al. 2014). European regulations limit the maximum acrylamide allowed in water by 0.1 $\mu\text{g/l}$ (Blondel et al. 1998). Many studies evaluated the biodegradation of acrylamide in the environment (Shanker et al. 1990; Shukor et al. 2009; Labahn et al. 2010). Overall, the results showed that acrylamide's microbial degradation is widespread in various environments, such as soil, sediments, and water. Therefore, the flocculated compounds resulting from acrylamide are not expected to persist in the environment.

Another major concern regarding the developed crosslinked drilling fluid is the corrosion effect on the drill pipe. A recent study conducted by Dong et al. (2019) investigated PAM's impact on the corrosion behavior of N80 steel, which is commonly used in drill pipes and casing. The author used weight-loss analysis and electrochemical tests to simulate the downhole environment in the presence of H_2S and CO_2 . The study revealed that PAM penetrates the N80 steel surface and forms a protective layer that prevents contact between the solution and the steel. Moreover, high PAM concentration increases the pH and promotes the ionization of H_2S . Figure 7.2 shows PAM's effect on the corrosion mechanism of N80 steel in the presence of H_2S and CO_2 . The PAM dissolves the corrosive gases into (HS^-) and (HCO_3^-) (Dong et al. 2020).

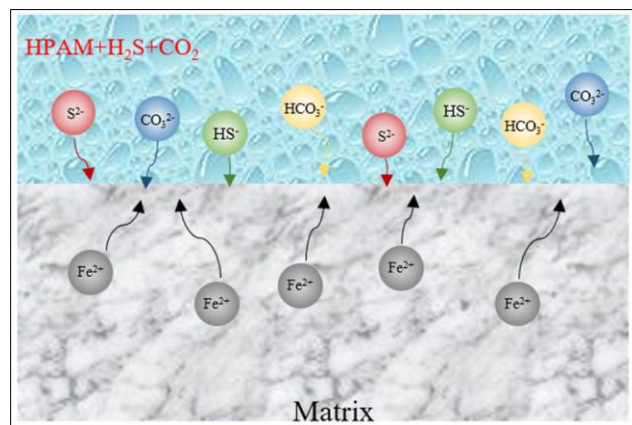


Figure 7. 2: Effect of polyacrylamide/ H_2S / CO_2 on the corrosion mechanism of N80 steel (Dong et al. 2020).

The second major component in the developed polymer-based drilling fluids is the crosslinkers. The first organic crosslinker, the PEI, is a water-soluble cationic polymer with a broad

molecular weight range. The one used in this study is a highly branched PEI with a molecular weight of 750,000 Da. The PEI is considered an environmentally friendly additive in drilling fluid, commonly used as a shale inhibitor (Guancheng et al. 2016). The PEI is widely used in bioengineering, wastewater treatment industry (Wong et al. 2019), and as a catalyst (Park and Kim 2015).

The crosslinked PEI polymers, particularly PAM/PEI gel, are widely used for water shut-off application in temporary plugging of water zone in producer wells as an environmentally friendly crosslinker as an alternative to chromium acetate (ElKarsani et al. 2015b). Moreover, the good HSE record of PEI promoted its wide application in medical applications such as drug and gene delivery systems (Song et al. 2018).

The inorganic crosslinkers (AlAc and FNS) were used in this study to expand the application of the developed gelling formulation for a wider temperature range. The aluminum (Al^{+3}) is an insoluble mineral; the acetate form of the aluminum is prepared by mixing Al with acetic acid and acetic anhydride (Downs 1993). High percentages of aluminum may exhibit toxic effects on the environment. The aluminum toxicity is due to the high reactivity of the $(\text{Al}(\text{H}_2\text{O})_6)^{3+}$ ion. Hydrolysis of this ion in presence can lead to the formation of a toxic form of monomers, $\text{Al}(\text{H}_2\text{O})_5(\text{OH})^{2+}$ and $\text{Al}(\text{H}_2\text{O})_4(\text{OH})_2^+$ (Thomas et al. 1991). On the other hand, nanosilica and functionalized silica also have a minimal environmental impact. They have been used intensively for shale inhibition as an alternative to conventional inhibitors in WBM (Boul et al. 2017; Saleh and Ibrahim 2019)

7.2 Gel Cleaning and Filter Cake Removal

Cleaning of polymeric gel is the filter cake removal process from the wellbore wall after drilling. It is not only crucial for drill-in fluids for oil and gas production but also for successful primary cementing. The conventional drilling fluids usually contain acid-soluble or water-soluble

particulate solids bridging agents. Removal treatment involves using acids and oxidizers. The acid is used to degrade the inorganic portion of the filter cake, while the oxidizer is used for the organic portion (Munoz Jr 2009).

In this study, the developed gelling mud contains polyacrylamide crosslinked with organic and organic crosslinkers. These types of gels have been used widely in water shut-off and permeability alteration in produced wells. The difference between water shut-off and LCM application is the required gel's time to hold its strength. In water shut-off applications, the gel should be stable for a prolonged time. The period extends from months to years. However, in drilling, LCM's filter cake should be removable immediately after the section is drilled.

The crosslinked polyacrylamide polymer is known for its high stability at high temperature of 150°C (302°F), as reported by many researchers and filed case studies. A producer well in West Texas was treated with 625 bbl of polyacrylamide crosslinked with phenol and formaldehyde to shut off water zones and reduce water cut. The treatment succeeded in reducing water production from over 1200 bbl/day to 350 bbl/day. The gel was stable for more than 54 months at a temperature of 110°C (230°F) (Moradi-Araghi et al. 1993a). Chromium acetate crosslinked PAM was also survived two years of aging under 104°C (220°F) (Moradi-Araghi et al. 1993b). Hardy et al. (1999) claimed using organically crosslinked acrylamide and t-butyl acrylate (PA_tBA) to seal the water zone in a well in the North Sea that was completed in naturally fractured chalk formation. The well was successfully put into production with reduced water cut through the life of the well. Several laboratory studies also showed stability of PAM/PEI crosslinked polymers at temperatures above 150°F (302°F) (Al-Muntasheri et al. 2008; Mohamed et al. 2018)

From the above discussion, filter cake removal with crosslinked polymer gel is different from the conventional treatment techniques and requires special considerations. The major concern

is the high stability and high strength of the mature gel. Another challenge is due to the filtration process. The polymer concentration within the filter cake is higher than the initially used concentration in the system. This fact was highlighted by Reddy et al. (2014); the author observed that due to fluid leak-off, the polymer concentration in the formed filter cake was several times higher than the original concentration.

Very few studies were conducted in gel breaking since the common application is intended to keep it for an extended period. The thermal stability of the gel can be broken by three mechanisms, the rupture of polymer chains, the breakage of crosslinker chains, and hydrolysis of polymer. The breaking reaction depends on polymer and breaker concentrations, temperature, and pH. Kihara et al. (2019) treated a crosslinked acryloylhydrazine polymer with a sodium hypochlorite solution. The crosslinked polymer dissolved in water due to de-crosslinking via oxidative degradation.

Sarwar et al. (2011) studied the effectiveness of different oxidizers such as sodium peroxide, calcium peroxide, sodium persulfate, and ammonium persulfate. The author evaluated the breaking of supermolecule polymers at a temperature ranging from 75°F to 300°F (24 to 150°C). All used breakers removed the polymers up to 93% at low temperature and varying performance at high temperature. The persulfate oxidizers did not function well in temperatures higher than 60°C (140°F). The author also highlighted that using galactomannans enzyme (carbohydrate residue and D-galactose) enhances the breaking process with less breaker concentration. Some researchers suggested using encapsulated persulfate to overcome their temperature limits, but it was expensive, and degradation takes a long time (Patil et al. 2013).

In a similar study, Hanes et al. (2006) proposed an alternative for the persulfate oxidizers; the author suggested de-crosslinking the gel by competing for the crosslinker using poly aspartate

and polysuccinimide in the system. An experimental evaluation of the proposed breaker was conducted by Reddy et al. (2013) on a zirconium crosslinked guar polymer. After the invasion on 5-micron discs, the filter cake analysis showed that poly aspartate de-crosslinked the gel and completely prevent filter cake buildup on the disk. Gunawan et al. (2012) developed a bio breaker consisting of non-enzyme-based chemicals, while the breaker's chemistry was not disclosed. However, the author claimed that the breaker functions in a temperature range from 79°C to 107°C (175°F to 225°F) and under alkaline conditions.

Since organic and inorganic crosslinkers were used in this study, the dissolving in salts solutions is recommended to give the best cleaning results. As an example, the ammonium chloride (NH_4Cl) was evaluated under different concentrations to break the gel. The solubility of aluminum acetate crosslinked polyacrylamide (PAM/AlAc) was tested in a solution of ammonium chloride with two different concentrations (5 wt.% and 10 wt.%) at room temperature. The gel was cooled down after complete gelation in 30 minutes at 50°C (122°F). A controlled sample was submersed in distilled water (0 wt.% NH_4Cl); the observation showed immediate and complete dissolving of the gel in the 10 wt.% ammonium chloride solution. The 5 wt.% solution also dissolved the gel in less than 2 minutes, while the gel settled down in the distilled water without been dissolved; the observations are shown in Figure 7.3.

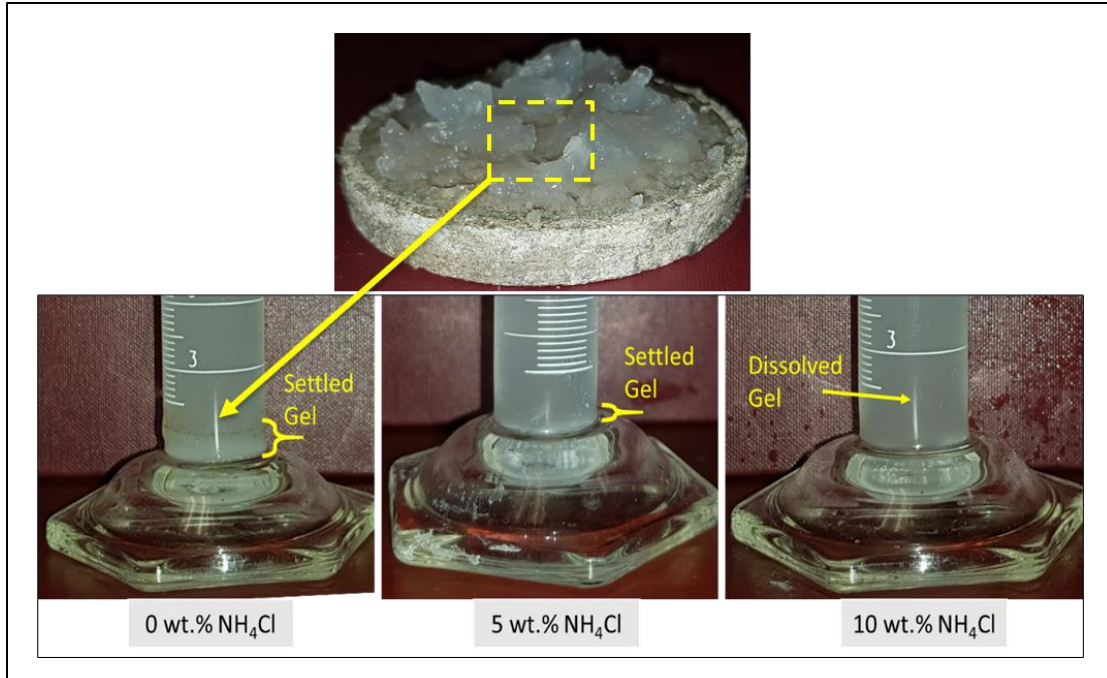


Figure 7. 3: Observation on gel dissolving using ammonium chloride (NH_4Cl).

7.3 Economic Feasibility Analysis: Case Studies

7.3.1 Cost Analysis

Lost circulation is a costly problem due to the loss of expensive drilling fluid and the additional NPT spent regaining the circulation. In addition to the performance evaluation and environmental aspects, the cost plays a vital role in selecting the LCM types and treatments method. Based on industry data published in response to a Notice of Data Availability (NODA) issued by the US Environmental Protection Agency (EPA), the cost of WBM, OBM, and SBM is 45 \$/bbl, 75 \$/bbl, and 200 \$/bbl, respectively. More recently published reports indicate that the OBM and SBM cost 70 to 90 \$/bbl. The EPA expects the cost of the SBM to become around 160 to 300 \$/bbl because of the need for high functioning drilling fluid to meet the industry requirement and regulations and to drill in challenging downhole environments (Johnston and Rubin 2000; Ali et al. 2020)

This research serves as a guide for developing novel, cost-effective drilling fluids. The cost analysis compares crosslinked polymer-based mud and the gelling pill developed in this study as

lost circulation treatment with the conventional and currently available solutions. The pricing list used for this analysis (Table 7.1) was averaged from different commercial suppliers. The data on the current formulations of lost circulation treatment used in the industry were collected from an international drilling company. The costs of commercial formulations were compared with the formulation developed depending on the type of treatment and the loss severity. Figure 7.4 shows the costs of crosslinked polymer-based formulas compared with a typical WBM containing CaCO₃ at the recommended concentration (55 lb/bbl) in proactive treatment (Ezeakacha and Salehi 2019b). Figure 7.5 compares the concentrated pills used in the oil field with the developed gelling pills prepared by PAM and the three different crosslinkers with the optimized concentrations. Appendix A contains cost analysis, including the optimized PAM/PEI-based mud proposed by this study and the composition of the commercial pills and WBM.

Table 7. 1: Pricing list and range of concentrations of the developed gelling mud and pill

| Component | lb/bbl | Price (\$/lb) |
|-------------------|---------|---------------|
| PAM | 17 - 44 | 0.68 |
| PEI | 0.8 - 5 | 1.13 |
| Caustic soda | 0 - 1.5 | 0.14 |
| Bentonite | 0 - 5 | 0.14 |
| Calcium Carbonate | 0 - 55 | 0.16 |
| Fiber | 0 - 15 | 0.2 |
| Barite | 10 - 90 | 2.3 |

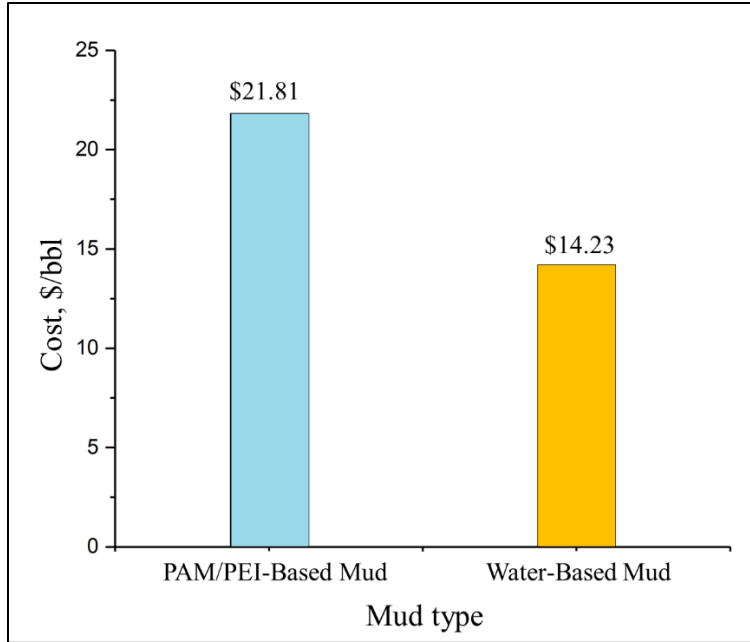


Figure 7. 4: Cost of PAM/PEI-based mud in comparison with a typical WBM.

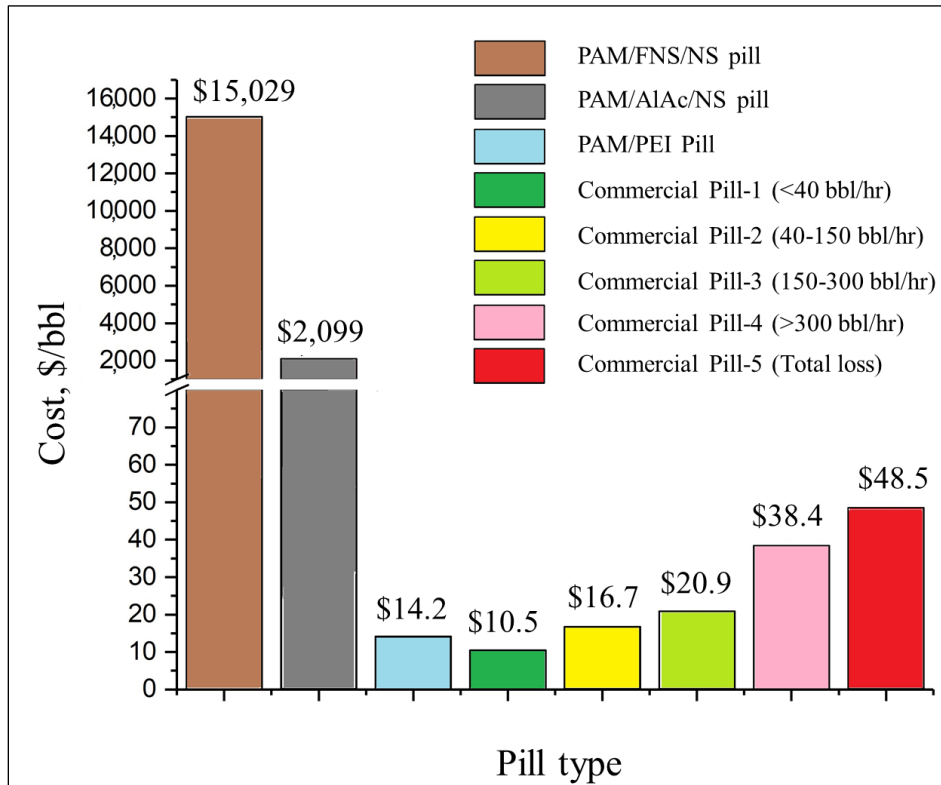


Figure 7. 5: Cost of gelling PAM/PEI based LCM in comparison with commercial pills.

7.3.2 Case Studies

7.3.2.1 Description of Case Studies

The two case studies of interest are two wells located in the Gulf of Mexico within the Mississippi Canyon. According to a survey by major drilling contractors and operators, the annual non-productive time costs on a high-tech platform in the Gulf of Mexico can exceed \$120 million, and \$24 million of that is due to drilling problems, mostly lost circulations. The two wells of the case studies were designated as Well-A and Well-B, both drilled in the Mississippi Canyon field. The average water depth is 2000 ft (610 m). The geological structure in these wells is mostly interbedded sandstone and shale (Mannon 2013). Several previous statistics also revealed that lost circulation tendency increases in some formations because of the lithology. For example, a study conducted by Rosenberg and Gala (2012) on NPT reported in 30 wells drilling in GoM showed that 29% of mud loss was associated with loose sand, shale, limestone, and depleted sand formation. In well A, 11,986 ft of shale and 564 ft of sand were drilled. Well B drilled through 18,271 ft of shale and 1,518 ft of sand. The sand was unconsolidated and depleted with a low-pressure gradient due to the long life of production from the field, which complicated the drilling fluid program.

Another situation in these two wells was the overestimation of the fracture gradient from pore pressure analysis. The mud weight density used to drill the main hole in both wells varied from 12.5 to 13.5 ppg, which was within the operational mud window according to the pre-drill pore pressure analysis. However, frequent kicks and loss circulation events occurred, which increased the NPT and cost of these two wells. Figures 7.6 and 7.7 show the performance plot of Well-A and well-B. Both wells experienced trouble and spend a lot of time on unplanned activities

due to lost circulation problems. The primary cause of the frequent loss event was the depleted sand and salt diapir.

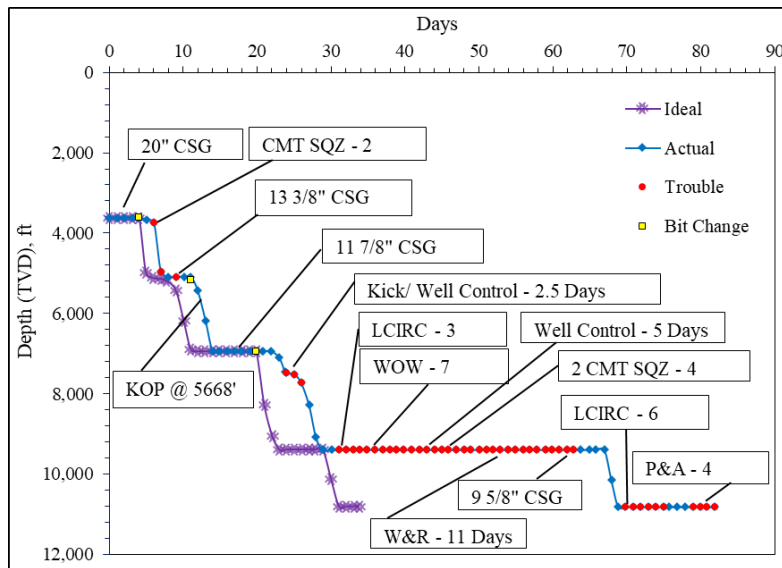


Figure 7. 6: Well-A performance plot, after (Mannon 2013).

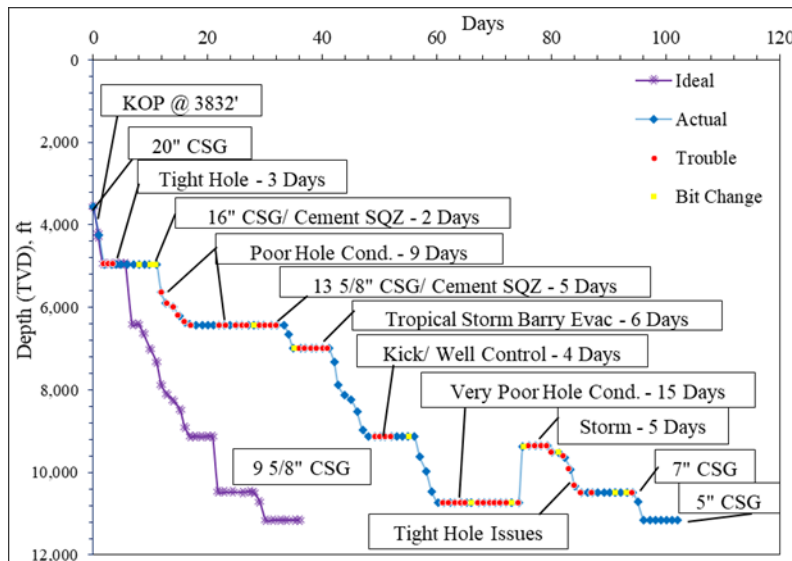


Figure 7. 7: Well-B performance plot, after (Mannon 2013).

The drilling time of both wells shifted from the planned ideal case. Well-A was drilled in 82 days instead of 34 days, while Well-B was drilled in 106 days instead of 36 days. However, many other situations such as weather, casing, and cementing problem have contributed to the extra days in the actual performance, but the lost circulation and poor hole conditions caused the

major portion of the NPT. Figure 7.8 shows the share of each NPT event. Poor hole condition caused 23% of the NPT in Well A and 50% in Well-B, and lost circulation caused about 19% of NPT in both wells.

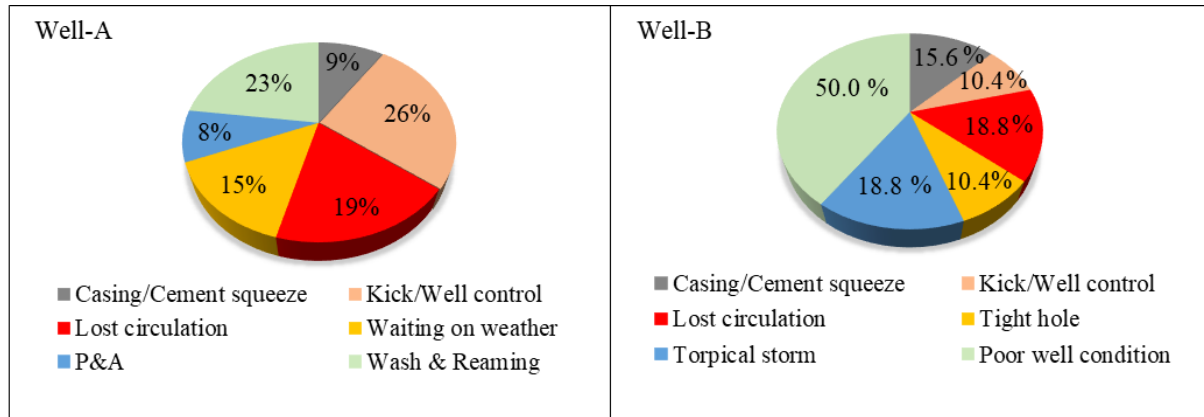


Figure 7. 8: Events contributed to NPT in Well-A and Well-B, data from (Mannon 2013).

7.3.2.2 Attempted Remedial Actions

The well programs were planned according to the pre-drill pore pressure analysis, which dedicated a safe mud weight to be around 12.5 ppg. Still, well-B experienced a kick at 9850 ft TVD with a mud weight of 12.5 ppg, and they had to increase the density to 13 ppg to kill the well and mitigate the loss of well control. This case resulted in a lost circulation situation, and they had to use a liner to avoid it. A lost circulation also occurred at a higher depth at 9400 ft TVD while preparing the 9 5/8” casing. The attempted solution was to spot squeeze LCM pills and cement to stop the losses. The attempt succeeded, and the casing was installed, but it cost the rig 19 days. Another major loss occurred in Well-3 at 10735 ft TVD due to a low-pressure gradient. The efforts to solve the loss were unsuccessful, and the well had to be plugged, cemented, and sidetracked, which caused another 15 days of NPT.

Well-A also experienced lost circulation in shallow depths due to high mud weight (12.9 ppg). The solution involved using casing and liners. Cement squeeze LCM pills were used several times, however at a depth around 10850 ft TVD, the bit entered depleted sand that was producing

for nearly 5 years before Well-A was drilled. The mud weight was reduced to 12.3 but still exceeded the sand fracture gradient, and severe loss occurred, which could not be cured, and eventually, the well was plugged and abandoned.

7.3.2.3 Proposed Solution

Based on the reported drilling performance for the two wells, the two main problems were the depleted sand and the inaccuracies in the estimation of fracture gradient at some depths. The loss was both at shallow depths as 1000 ft TVD and in deep intervals as 10,700 ft TVD. These two situations match perfectly with the range of applications discussed in the results sections of this dissertation. Two possible scenarios for applying crosslinked polymer LCM can be recommended based on the results presented in this research.

The first proposed solution is utilizing a flowing polymeric-based drilling fluid comprising PAM and PEI for proactive treatment to drill risky sections where there are uncertainties in fracture gradients. Figure 7.9 can be used to formulate the base fluid, and the average value can be selected, for example, 7.5 wt.% PAM can work for all intervals in both wells. Other additives based on the pressure gradient can be added as explained in Table 5.1 in section 5.3 to prepare a 12.5 ppg mud. The cost of such mud will be 21.8 \$/bbl, based on the cost analysis presented in section 7.3.1. However, this cost is a little bit higher than the price of the water-based mud (14.2 \$/bbl) but utilizing this proactive treatment will strengthen the loose sand in the depleted formations and prevent lost circulation events. The ultimate benefit of using the developed crosslinked polymer-based mud will be the huge reduction in the NPT by up to 9 days in Well-A and 19 days in well B, which will cover the cost of the mud and save a lot of rig day.

The second proposed solution is using a gelling LCM pill. This will solve the severe lost circulation in Well-A that led to plugging and abandonment action after 83 days. Based on the

optimization and gelation study conducted in this research, the optimal candidate is the aluminum acetate crosslinked polymer. The aluminum acetate can make crosslinked polymer at a temperature less than 200°F (90°C) with gelation time ranging from 20 minutes to 50 minutes, depending on the downhole temperature. Successful single treatment of spotting the developed gelling pill is believed to save up to 19 days in well-B spend in the casing and sidetracking and save Well-A from plugging and abandonment.

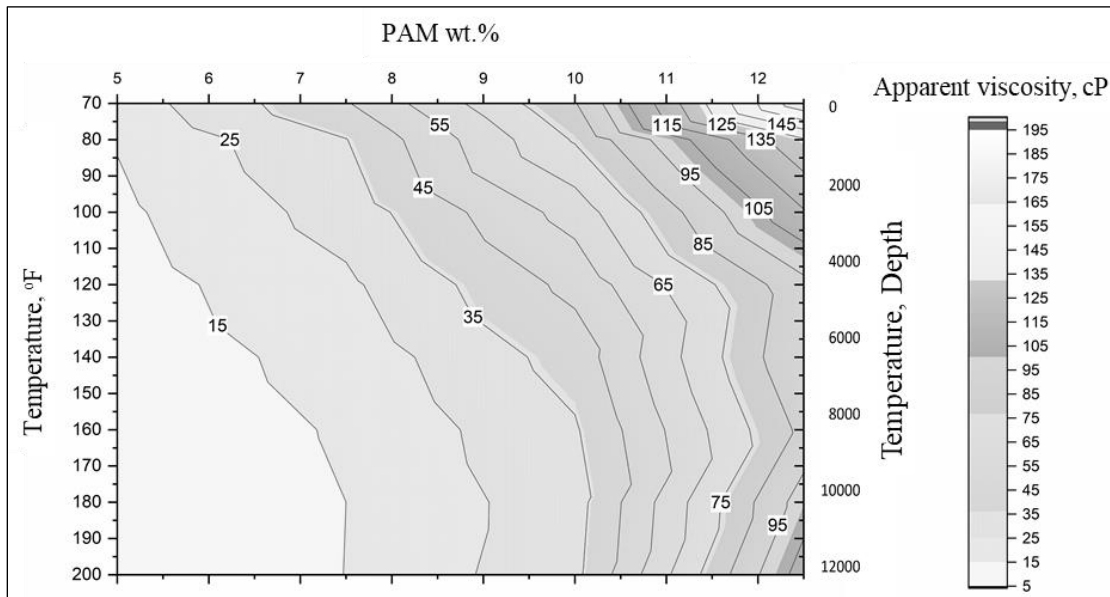


Figure 7. 9: Design chart for lost circulation at different depths and temperatures.

Chapter 8: Summary, Conclusions, and Recommendations

8.1 Summary

This dissertation addressed the lost circulation problem that rises in narrow operational drilling windows encountered in unconsolidated formations, naturally fractured and depleted reservoirs, or abnormal pressure intervals. Drilling in such risky intervals has created the need for wellbore strengthening technologies and innovative lost circulation materials. This study investigated different essential factors for developing novel formulations for lost circulation treatment comprising organic and inorganic crosslinkers and gel controlling agents. Several factors impacting the performance of these gelling LCMs have been discussed and experimentally investigated using pore-scale and fracture-scale filtration tests in static and dynamic conditions. The study also included cost analysis and an evaluation of environmental impacts, and an assessment of filter cake evolution and potential formation damages. A machine learning approach was adopted to build validated models to predict rheological properties and provide a materials screening tool for preparing polymeric formulas for quick field intervention.

8.2 Conclusions

The utilization of crosslinked polymers in drilling fluid formulations can solve various lost circulation problems where the operational and pre-existing downhole conditions limit conventional LCMs. The following conclusions have been drawn based on the results and observations:

1. The most critical design factors of any gel system intended for loss circulation treatment are the rheological properties, gelation time, onset temperature, and the final gel strength. The sealing efficiency depends on the accurate adjustment of the polymer gelation process under different downhole conditions.

2. Lost circulation at high temperatures requires slow gelling systems to avoid gelation during the injection process.
3. The PAM with a low range of molecular weight (2×10^5) at appropriate concentrations of 7.5 to 9 wt.% is the optimal candidate for drilling fluid applications. The amount of crosslinkers is not recommended to be more than 1 wt.% for PEI, 2 wt.% for FNS, and 3 wt.% for the AlAc, to avoid fast gelation.
4. The PEI and the FNS crosslink the PAM only at elevated temperatures above 130°C (266°F), however, at temperature less than 90°C (195°F); viscosity may increase due to the changes in viscoelastic properties of the polymer and crosslinker with heating.
5. The AlAc was capable of crosslinking the PAM at temperatures starting from 50°C (122°F), making it a good candidate for treating lost circulation at shallow depths.
6. Nanosilica of 50 nm in small concentrations (1 to 2 wt.%) increased the stability of the AlAc and FNS suspension in PAM solutions, with a slight increase in viscosities by 5 to 10%. These crosslinkers are controllable, and without nanosilica they were able to form a strong gel; however, phase separation from 40% to 100% was observed when the nanosilica was reduced to less than 1%.
7. The system of PAM/AlAc has a gelation time of around 50 minutes at a temperature of 75°C, making it suitable for near-wellbore fractures plugging. The AlAc has the widest pH window of applicability.
8. Bentonite in small quantities has no significant effect on the performance of the PAM/PEI system. It accelerates the gelation by 25%; however, excessive concentration delays the gelation process by 100% and reduces the final gel strength by 70%. All investigated additives showed a similar delay in gelation from 50 minutes to more than 3 hours.

9. The Energy Dispersive X-Ray Analysis (EDX) showed that the PAM/PEI gels filled the carbonates' pores and formed a uniform internal filter cake. However, the internal filter cake formed by PAM/PEI gel was limited to a small area near the filter disks. This will reduce deep invasion and isolate reservoir fluids which cause less formation damage.
10. Static filtration experiments showed an 80% reduction of filtration volume when tested with the PAM/PEI-based drilling fluid in filter disks cut from carbonate core.
11. All polymeric formulas showed high sealing pressure, up to 1000 psi, and were able to stop fluid loss in few minutes independent of the size and shape of the fractures.
12. Based on the machine learning modeling, the Gradient Boosting performed significantly better than other algorithms, including k-Nearest Neighbor, Random Forest, and AdaBoosting. The Gradient Boosting algorithm's accuracy was 91 and 74% for plastic viscosity (PV) and apparent viscosity (AV), respectively.
13. The cost of water-based mud was estimated to be \$14.23 \$/bbl, which is around \$7 cheaper than the PAM/PEI-based mud (21.81 \$/bbl). However, this cost is still considered competitive to the average prices of water-based mud because it can be compensated by the cost of NPT saved with the PAM/PEI-based mud.

8.3 Recommendations

Based on the results, findings, and conclusions presented in this study, recommendations for future research in this area have been made. These recommendations include but not limited to:

1. Some of the gaps in the knowledge of polymeric gels application as LCM can be filled by investigating the interactions, compatibility, alteration of gelation kinetics of the polymer system considering other types of drilling fluids such as OBM and SBM.
2. Using seawater as a retarder to delay the gelation in offshore drilling is a cost-effective option instead of ammonium chloride.

3. For more options of retardation agents, calcium and sodium salts can be used, besides the formation water, after careful analysis and optimization studies.
4. Results showed that bentonite was needed in the polymer-based mud formula to enhance its rheology; however, it adversely impacted gel strength. Therefore, an optimization study is recommended, in addition to looking for other reinforcement additives. Also, the crosslinker amount can be increased to compensate for the gel strength reduction.
5. Filter cake removal for crosslinked polymer gel is different from the conventional treatment techniques and requires special considerations and more investigations to find effective cleaning methods.
6. Based on the preliminary results, organic crosslinkers are recommended for deep wells because they have high crosslinking onset temperature, while inorganic crosslinkers are recommended for shallow wells.
7. In real-time drilling, careful estimation of required injection time and correlating it with depth and temperature of the loss zone are highly recommended for a successful placing of the gel.
8. The rheology data at the low shear rate were challenging, although the prediction performance was poor; still, some good predictions were obtained at the low values of viscosities where low concentrations of mud additives were used. Increasing the size of the data set is expected to improve the performance of the model.
9. Considering environmental-friendly crosslinkers such as chitosan, acetate, amino-acetate, nitrate-based crosslinker, and other polymers such as tert-butyl acrylate (tBA) will introduce more potential crosslinked polymers, especially in offshore applications.

Nomenclature

Acronyms

| | |
|------|--|
| AdaB | Ada-Boosting |
| AV | Apparent Viscosity |
| AMPS | 2-acrylamido-2-methylpropane sulfonic acid |
| bbbl | barrel |
| CMC | carboxy-methyl cellulose |
| CwD | casing while drilling |
| DCM | drilling choke manifold |
| DSC | differential scanning calorimetry |
| DTPA | Diethylene triamine penta acetic acid |
| ECD | equivalent circulating density |
| EDTA | Ethylene diamine tetra acetic acid |
| EOR | enhanced oil recovery applications |
| EPA | environmental protection agency |
| FCS | fracture closure stress |
| FIP | fracture initiation pressure |
| FPP | fracture propagation pressure |
| FPR | fracture propagation resistance |
| FNS | functionalized silica |
| GB | Gradient Boosting |
| GoM | Gulf of Mexico |
| gpm | gallons per minute |

| | |
|--------|---|
| HMTA | hexamethylenetetramine |
| HPAM | hydrolyzed polyacrylamide |
| HPG | hydrophilic polyacrylamide gel |
| HPHT | high-pressure high-temperature |
| HQ | hydroquinone |
| IADC | the international association of drilling contractors |
| IPNs | the interpenetrating polymer networks |
| IPT | ideal packing theory |
| IUPAC | the international union of pure and applied chemistry |
| KNN | K-Nearest Neighbor |
| lb | pound |
| lb/bbl | Pound per barrel |
| LCM | lost circulation materials |
| LPLT | low pressure low temperature |
| LWD | logging while drilling tools |
| ML | Machine Learning |
| MPD | managed pressure drilling |
| MPP | mandarin peels powder |
| MWD | measure while drilling |
| NODA | notice of data availability |
| NPs | nanoparticles |
| NPT | non-productive time |
| N-S | Navier-Stokes |

| | |
|--------|---|
| OBM | oil-based mud |
| OECD | Organization for Economic Co-operation and Development |
| PAC | polyanionic cellulose |
| PAM | polyacrylamide |
| pcf | pound per cubic foot |
| PDAC | polydiethyl diallyl ammonium chloride |
| PEI | polyethyleneimine |
| PHPA | partially-hydrolyzed polyacrylamide |
| PIT | pressure integrity test |
| PPA | permeability plugging apparatus |
| PPDA | polypentadienamamide |
| ppg | pound per gallon |
| PV | Plastic Viscosity |
| RDC | rotating control device |
| REACH | registration, evaluation, authorization, and restriction of chemicals |
| RF | Random Forest |
| ROP | rate of penetration |
| rpm | rotation per minute |
| SBM | synthetic-based mud |
| SDS-Gr | sodium dodecyl sulphate- modified graphene |
| tBA | tert-butyl acrylate |
| TVP | thermo viscosifying polymers |
| UBD | under blanked drilling |

| | |
|--------|---|
| US-EPA | the United States Environmental Protection Agency |
| WBM | water-based mud |
| WS | wellbore strengthening |
| ZP | zeta potential |

Symbols

| | |
|-----------------|---|
| A | Nodes in Random Forest Regression |
| D_n | training sample of independent random variables |
| f | Fanning friction factor |
| j^{th} | Family tree |
| k | permeability |
| mn | predicted values |
| N_n | number of nodes |
| P | pressure |
| Pa | pascal |
| T_o | onset temperature |

Greek Symbols

| | |
|---------------|-------------------------------------|
| ε | roughness height (m) |
| θ | independent random variable |
| γ | shear rate at cake surface [1/sec] |
| μ | apparent viscosity (cp) |

References

- API RP 96, Recommended Practice for Deepwater Well Design and Construction*, first edition, 2013. Washington, DC: API.
- Aadnøy, Bernt S and Belayneh, Mesfin. 2004. Elasto-plastic fracturing model for wellbore stability using non-penetrating fluids. *Journal of Petroleum Science and Engineering* **45** (3-4): 179-192.
- Abdulbaki, Mazen, Huh, Chun, Sepehrnoori, Kamy, Delshad, Mojdeh, and Varavei, Abdoljalil. 2014. A critical review on use of polymer microgels for conformance control purposes. *Journal of Petroleum Science and Engineering* **122**: 741-753. <http://www.sciencedirect.com/science/article/pii/S0920410514002307>.
- Abduo, M. I., Dahab, A. S., Abuseda, Hesham, AbdulAziz, Abdulaziz M., and Elhossieny, M. S. 2016. Comparative study of using Water-Based mud containing Multiwall Carbon Nanotubes versus Oil-Based mud in HPHT fields. *Egyptian Journal of Petroleum* **25** (4): 459-464. <http://www.sciencedirect.com/science/article/pii/S1110062115300325>.
- Abrams, Albert. 1977. Mud design to minimize rock impairment due to particle invasion. *Journal of petroleum technology* **29** (05): 586-592.
- Addis, M. A., Cauley, M. B., and Kuyken, C. 2001. Brent In-Fill Drilling Programme: Lost Circulation Associated With Drilling Depleted Reservoirs. Paper presented at the SPE/IADC Drilling Conference, Amsterdam, Netherlands, 2001/1/1/. SPE. <https://doi.org/10.2118/67741-MS>.
- Al-Muntasheri, Ghaithan A., Nasr-El-Din, Hisham A., and Zitha, Pacelli L. J. 2008. Gelation Kinetics and Performance Evaluation of an Organically Crosslinked Gel at High Temperature and Pressure. *SPE Journal* **13** (03): 337-345. <https://doi.org/10.2118/104071-PA>.
- Al-saba, Mortadha T, Nygaard, Runar, Saasen, Arild, and Nes, Olav-Magnar. 2014a. Lost circulation materials capability of sealing wide fractures. *Proc.*, SPE Deepwater Drilling and Completions Conference.
- Al-saba, Mortadha T., Nygaard, Runar, Saasen, Arild, and Nes, Olav-Magnar. 2014b. Lost Circulation Materials Capability of Sealing Wide Fractures. Paper presented at the SPE

- Deepwater Drilling and Completions Conference, Galveston, Texas, USA, 2014/9/10/. SPE. <https://doi.org/10.2118/170285-MS>.
- Alberty, Mark W and McLean, Michael R. 2004a. A physical model for stress cages. *Proc.*, SPE annual technical conference and exhibition.
- Alberty, Mark W. and McLean, Michael R. 2004b. A Physical Model for Stress Cages. Paper presented at the SPE Annual Technical Conference and Exhibition, Houston, Texas, 2004/1/1/. SPE. <https://doi.org/10.2118/90493-MS>.
- Ali, Muhammad, Jarni, Husna Hayati, Aftab, Adnan, Ismail, Abdul Razak, Saady, Noori M Cata, Sahito, Muhammad Faraz, Keshavarz, Alireza, Iglauer, Stefan, and Sarmadivaleh, Mohammad. 2020. Nanomaterial-based drilling fluids for exploitation of unconventional reservoirs: A review. *Energies* **13** (13): 3417.
- Allen, David, Auzeais, Francois, Dussan, Elizabeth, Goode, Peter, Ramakrishnan, TS, Schwartz, Larry, Wilkinson, D, Fordham, Edmund, Hammond, Paul, and Williams, Russ. 1991. Invasion revisited. *Schlumberger Oilfield Review* **3** (3): 10-23.
- Allison, Joe D and Purkale, Jerry D. 1988. *Reducing permeability of highly permeable zones in underground formations*, Google Patents (Reprint).
- Alsaba, Mortadha, Nygaard, Runar, Hareland, Geir, and Contreras, O. 2014. Review of lost circulation materials and treatments with an updated classification. *Proc.*, AADE National Technical Conference and Exhibition, Houston, TX1-9.
- Amir, Zulhelmi, Mohd Saaid, Ismail, and Mohamed Jan, Badrul. 2018. An Optimization Study of Polyacrylamide-Polyethylenimine-Based Polymer Gel for High Temperature Reservoir Conformance Control. *International Journal of Polymer Science* **2018**.
- Amir, Zulhelmi, Said, Ismail Mohd, and Jan, Badrul Mohamed. 2019. In situ organically cross-linked polymer gel for high-temperature reservoir conformance control: A review. *Polymers for Advanced Technologies* **30** (1): 13-39.
- API, RP. 2009. 13I, Recommended Practice for Laboratory Testing of Drilling Fluids. *Washington, DC, USA: API*.
- Bai, Baojun, Zhou, Jia, and Yin, Mingfei. 2015. A comprehensive review of polyacrylamide polymer gels for conformance control. *Petroleum exploration and development* **42** (4): 525-532.

- Bao, Dan, Qiu, Zhengsong, Zhao, Xin, Zhong, Hanyi, Chen, Jiayu, and Liu, Junyi. 2019. Experimental investigation of sealing ability of lost circulation materials using the test apparatus with long fracture slot. *Journal of Petroleum Science and Engineering* **183**: 106396. <http://www.sciencedirect.com/science/article/pii/S0920410519308174>.
- Beda, G and Carugo, C. 2001. Use of mud microloss analysis while drilling to improve the formation evaluation in fractured reservoir. *Proc.*, SPE Annual Technical Conference and Exhibition.
- Belyadi, Hoss, McCallum, Scott, Silva, Felipe, Carroll, Oana, Weiman, Sam, and Smith, Malcolm. 2019. Production Prediction Using Multi-Output Supervised Machine Learning ML. *Proc.*, SPE Eastern Regional Meeting.
- Belyakov, Andrey, Panov, Maksim, Shirokov, Ilya, and Silko, Nikita. 2018. First Application of Fiber Based LCM in Srednebotuobinskoe Oilfield, Russia. Paper presented at the SPE Russian Petroleum Technology Conference, Moscow, Russia, 2018/10/15/. SPE. <https://doi.org/10.2118/191506-18RPTC-MS>.
- Berndt, WO, Bergfeld, WF, Boutwell, RK, Carlton, WW, Hoffmann, DK, Schroeter, AL, and Shank, RC. 1991. Final report on the safety assessment of polyacrylamide. *Journal of the American College of Toxicology* **10** (1): 193-203.
- Bhattacharyya, Ruma and Ray, Samit Kumar. 2015. Removal of congo red and methyl violet from water using nano clay filled composite hydrogels of poly acrylic acid and polyethylene glycol. *Chemical Engineering Journal* **260**: 269-283.
- Blondel, Jean, Sinnott, Richard, and Svensson, Palle. 1998. *People and Parliament in the European Union: participation, democracy, and legitimacy*: Oxford University Press.
- Bohlooli, B. and de Pater, C. J. 2006. Experimental study on hydraulic fracturing of soft rocks: Influence of fluid rheology and confining stress. *Journal of Petroleum Science and Engineering* **53** (1): 1-12. <http://www.sciencedirect.com/science/article/pii/S0920410506000210>.
- Borisov, Alexey S., Husein, Maen, and Hareland, Geir. 2015. *journal article*. A field application of nanoparticle-based invert emulsion drilling fluids. *Journal of Nanoparticle Research* **17** (8): 340. <https://doi.org/10.1007/s11051-015-3143-x>.

- Boul, Peter J, Reddy, BR, Zhang, Jilin, and Thaemlitz, Carl. 2017. Functionalized nanosilicas as shale inhibitors in water-based drilling fluids. *SPE Drilling & Completion* **32** (02): 121-130.
- Bradley, Kieran St Clair. 2008. Halfway house: The 2006 comitology reforms and the European Parliament. *West European Politics* **31** (4): 837-854.
- Brandl, A, Bray, WS, and Molaei, F. 2011. Curing lost circulation issues and strengthening weak formations with a sealing fluid for improved zonal isolation of wellbores. *Proc.*, Australian Geothermal Energy Conference, Melbourne.
- Breiman, Leo. 1996. Stacked regressions. *Machine learning* **24** (1): 49-64.
- Breiman, Leo. 2001. Random forests. *Machine learning* **45** (1): 5-32.
- Broseta, D, Marquer, O, Blin, N, and Zaitoun, A. 2000. Rheological screening of low-molecular-weight polyacrylamide/chromium (III) acetate water shutoff gels. *Proc.*, SPE/DOE improved oil recovery symposium.
- Bugbee, J. M. 1953. Lost Circulation-A Major Problem in Exploration and Development. Paper presented at the Drilling and Production Practice, New York, New York, 1953/1/1/. API. <https://doi.org/>.
- Burns, Lyle D, McCool, C Stanley, Willhite, G Paul, Burns, Michael, Oglesby, Kenneth D, and Glass, James. 2008. New generation silicate gel system for casing repairs and water shutoff. *Proc.*, SPE Symposium on Improved Oil Recovery.
- Byrd, Bob and Zamora, Mario. 1988. Fluids are key in drilling highly deviated wells. *Pet Eng Int;(United States)* **60** (2).
- Caenn, Ryen and Chillingar, George V. 1996. Drilling fluids: State of the art. *Journal of Petroleum Science and Engineering* **14** (3-4): 221-230.
- Chaney, PE. 1949. Abnormal pressures and lost circulation. *Proc.*, Drilling and production practice.
- Chen, Guizhong and Ewy, Russell T. 2005. Thermoporoelastic effect on wellbore stability. *SPE Journal* **10** (02): 121-129.
- Chen, Lifeng, Wang, Jinjie, Yu, Long, Zhang, Quan, Fu, Meilong, Zhao, Zhongcong, and Zuo, Jiaqi. 2018. Experimental Investigation on the Nanosilica-Reinforcing Polyacrylamide/Polyethylenimine Hydrogel for Water Shutoff Treatment. *Energy & Fuels* **32** (6): 6650-6656. <https://doi.org/10.1021/acs.energyfuels.8b00840>.

- Choi, S. K. and Tan, C. P. 1998. Modelling of Effects of Drilling Fluid Temperature on Wellbore Stability. Paper presented at the SPE/ISRM Rock Mechanics in Petroleum Engineering, Trondheim, Norway, 1998/1/1/. SPE. <https://doi.org/10.2118/47304-MS>.
- Cole, Patrick, Young, Katherine R, Doke, Clayton, Duncan, Neel, and Eustes, Bill. 2017. Geothermal Drilling: A Baseline Study of Nonproductive Time Related to Lost Circulation, National Renewable Energy Lab.(NREL), Golden, CO (United States).
- Contreras, Oscar, Hareland, Geir, Husein, Maen, Nygaard, Runar, and Alsaba, Mortadha. 2014. Wellbore strengthening in sandstones by means of nanoparticle-based drilling fluids. *Proc.*, SPE deepwater drilling and completions conference.
- Cook, John, Guo, Quan, Way, Paul, Bailey, Louise, and Friedheim, Jim. 2016. The role of filtercake in wellbore strengthening. *Proc.*, IADC/SPE drilling conference and exhibition.
- Cowan, Dallas M, Kingsbury, Tony, Perez, Angela L, Woods, Tyler A, Kovoichich, Michael, Hill, Denise S, Madl, Amy K, and Paustenbach, Dennis J. 2014. Evaluation of the California Safer Consumer Products Regulation and the impact on consumers and product manufacturers. *Regulatory Toxicology and Pharmacology* **68** (1): 23-40.
- Darley, HCH and Gray, George R. 1988a. Introduction to Drilling Fluids. *Compos Prop Drill Complet Fluids*: 1-37.
- Darley, Henry CH and Gray, George R. 1988b. *Composition and properties of drilling and completion fluids*: Gulf Professional Publishing.
- Dawson, Graeme, Buchan, Andrew, Kardani, Ilen, Harris, Andrew, Wercholuk, Lonnie, Khazali, Khairul Amir, Sisson, Keith, Halim, Abdul, and Hermawan, Heru. 2010. Directional Casing While Drilling (DCwD) Heralds a Step Change in Drilling Efficiency from a Producing Platform. Paper presented at the Offshore Technology Conference, Houston, Texas, USA, 2010/1/1/. OTC. <https://doi.org/10.4043/20880-MS>.
- Deeg, WFJ and Wang, H. 2004. Changing borehole geometry and lost-circulation control. *Proc.*, Gulf Rocks 2004, the 6th North America Rock Mechanics Symposium (NARMS).
- Deuel Jr, LE and Holliday, GH. 1998. Geochemical partitioning of metals in spent drilling fluid solids.
- Dhar, Vasant. 2013. Data science and prediction. *Communications of the ACM* **56** (12): 64-73.
- Dietterich, Thomas G. 2000. Ensemble methods in machine learning. *Proc.*, International workshop on multiple classifier systems 1-15.

- Dong, Baojun, Zeng, Dezhi, Yu, Zhiming, Zhang, Haixin, Yu, Huiyong, Tian, Gang, and Yi, Yonggang. 2020. Role of polyacrylamide concentration on corrosion behavior of N80 steel in the HPAM/H₂S/CO₂ environment. *Materials and Corrosion* **71** (4): 526-536.
- Downs, Anthony John. 1993. *Chemistry of aluminium, gallium, indium and thallium*: Springer Science & Business Media.
- Du, Hui, Wang, Gui, Deng, Guicai, and Cao, Cheng. 2018. Modelling the effect of mudstone cuttings on rheological properties of KCl/Polymer water-based drilling fluid. *Journal of Petroleum Science and Engineering* **170**: 422-429.
- Dupriest, Fred E. 2005. Fracture closure stress (FCS) and lost returns practices. *Proc.*, SPE/IADC drilling conference.
- Dyke, CG, Wu, Bailin, and Milton-Taylor, David. 1995. Advances in characterising natural fracture permeability from mud log data. *SPE Formation Evaluation* **10** (03): 160-166.
- Eaton, Ben A. 1969. Fracture gradient prediction and its application in oilfield operations. *Journal of petroleum technology* **21** (10): 1,353-1,360.
- Echt, Timon and Plank, Johann. 2019. An improved test protocol for high temperature carrying capacity of drilling fluids exemplified on a sepiolite mud. *Journal of Natural Gas Science and Engineering* **70**: 102964. <http://www.sciencedirect.com/science/article/pii/S1875510019302161>.
- Eissa, Walid and Al-Harthi, S. 2003. Under Balanced Drilling Building the Future for PDO. Paper presented at the SPE/IADC Middle East Drilling Technology Conference and Exhibition, Abu Dhabi, United Arab Emirates, 2003/1/1/. SPE. <https://doi.org/10.2118/85317-MS>.
- El-karsani, Khalid Saad M., Al-Muntasheri, Ghaithan A., and Hussein, Ibnelwaleed A. 2014. Polymer Systems for Water Shutoff and Profile Modification: A Review Over the Last Decade. *SPE-182266-PA* **19** (01): 135-149. <https://doi.org/10.2118/163100-PA>.
- El-Sayed, Mahmoud, Ezz, Ahmad, Aziz, Moataz, and Waheed, Syed Arshad. 2007. Successes in Curing Massive Lost Circulation Problems with a New Expansive LCM. Paper presented at the SPE/IADC Middle East Drilling and Technology Conference, Cairo, Egypt, 2007/1/1/. SPE. <https://doi.org/10.2118/108290-MS>.
- ElKarsani, Khalid S. M., Al-Muntasheri, Ghaithan A., Sultan, Abdulla S., and Hussein, Ibnelwaleed A. 2015a. Performance of PAM/PEI gel system for water shut-off in high temperature reservoirs: Laboratory study. *Journal of Applied Polymer Science* **132** (17).

- ElKarsani, Khalid SM, Al-Muntasheri, Ghaithan A, Sultan, Abdulla S, and Hussein, Ibelwaleed A. 2015b. Performance of PAM/PEI gel system for water shut-off in high temperature reservoirs: Laboratory study. *Journal of Applied Polymer Science* **132** (17).
- Elkatatny, Salaheldin, Gamal, Hany, Ahmed, Abdulmalek, Sarmah, Pranjal, Sangaru, Shiv, and Alohaly, Maryam. 2020. A Novel Solution for Severe Loss Prevention While Drilling Deep Wells. *Sustainability* **12** (4): 1339.
- Essam, Wael, Scarborough, Christopher, Wilson, Nick, Shimi, Ahmed, Santos, Helio, Hannam, Jason, Catak, Erdem, Lancaster, Jay, Gooding, Neil, and Baan, Robert. 2019. Operator's First Application of MPD in Deepwater GoM Delivers Top Quartile Well. Paper presented at the IADC/SPE Managed Pressure Drilling and Underbalanced Operations Conference and Exhibition, Amsterdam, The Netherlands, 2019/4/8/. SPE. <https://doi.org/10.2118/194549-MS>.
- Ezeakacha, C. P., Salehi, S., and Hayatdavoudi, A. 2017. Experimental Study of Drilling Fluid's Filtration and Mud Cake Evolution in Sandstone Formations. *Journal of Energy Resources Technology* **139** (2). <https://doi.org/10.1115/1.4035425>.
- Ezeakacha, Chinedum Peter and Salehi, Saeed. 2018. Experimental and statistical investigation of drilling fluids loss in porous media—part 1. *Journal of Natural Gas Science and Engineering* **51**: 104-115. <http://www.sciencedirect.com/science/article/pii/S1875510017304948>.
- Ezeakacha, Chinedum Peter and Salehi, Saeed. 2019a. Experimental and statistical investigation of drilling fluid loss in porous media: Part 2 (Fractures). *Journal of Natural Gas Science and Engineering* **65**: 257-266. <http://www.sciencedirect.com/science/article/pii/S1875510019300617>.
- Ezeakacha, Chinedum Peter and Salehi, Saeed. 2019b. A holistic approach to characterize mud loss using dynamic mud filtration data. *Journal of Energy Resources Technology* **141** (7).
- Ezeakacha, Chinedum Peter, Salehi, Saeed, and Bi, Hongfeng. 2017. How does rock type and lithology affect drilling fluid's filtration and plastering. *Proc.*, AADE National Technical Conference and Exhibition, Houston Texas.
- Ezeakacha, CP, Salehi, S, Ghalambor, A, and Bi, H. 2018. Investigating Impact of Rock Type and Lithology on Mud Invasion and Formation Damage. *Proc.*, SPE International Conference and Exhibition on Formation Damage Control.

- Fan, Xiangyu, Zhao, Pengfei, Zhang, Qiangui, Zhang, Ting, Zhu, Kui, and Zhou, Chenghua. 2018. A Polymer Plugging Gel for the Fractured Strata and Its Application. *Materials* **11** (5): 856. <http://www.mdpi.com/1996-1944/11/5/856>.
- Fidan, E, Babadagli, T, and Kuru, E. 2004a. Use of cement as lost-circulation material: best practices. *Proc.*, Canadian international petroleum conference.
- Fidan, E., Babadagli, T., and Kuru, E. 2004b. Use of Cement as Lost-Circulation Material: Best Practices. Paper presented at the Canadian International Petroleum Conference, Calgary, Alberta, 2004/1/1/. PETSOC. <https://doi.org/10.2118/2004-090>.
- Fink, Johannes. 2015. *Petroleum engineer's guide to oil field chemicals and fluids*: Gulf Professional Publishing.
- Flory, Paul J. 1941. Molecular size distribution in three dimensional polymers. I. Gelation. *Journal of the American Chemical Society* **63** (11): 3083-3090.
- Freund, Y and Shapire, R. 1997. A decision-theoretic generalization of on-line learning and an application to boosting. *J Comput Syst Sci* **55**: 119-139.
- Freund, Yoav and Schapire, Robert E. 1996. Experiments with a new boosting algorithm. *Proc.*, icml148-156.
- Friedheim, Jim. 2004. Flat rheology mud shows promise in deepwater GOM trials. *Offshore (Conroe, Tex)* **64** (6).
- Friedman, Jerome H. 2001. Greedy function approximation: a gradient boosting machine. *Annals of statistics*: 1189-1232.
- Friedman, Jerome H. 2002. Stochastic gradient boosting. *Computational statistics & data analysis* **38** (4): 367-378.
- Fuh, Giin-Fa, Morita, Nobuo, Boyd, PA, and McGoffin, SJ. 1992. A new approach to preventing lost circulation while drilling. *Proc.*, SPE annual technical conference and exhibition.
- Gatlin, Carl and Nemir, Charles E. 1961. Some effects of size distribution on particle bridging in lost circulation and filtration tests. *Journal of Petroleum Technology* **13** (06): 575-578.
- Ghalambor, Ali, Salehi, Saeed, Shahri, Mojtaba P., and Karimi, Moji. 2014. Integrated Workflow for Lost Circulation Prediction. Paper presented at the SPE International Symposium and Exhibition on Formation Damage Control, Lafayette, Louisiana, USA, 2014/2/26/. SPE. <https://doi.org/10.2118/168123-MS>.
- Ghassemzadeh, Jaleh. 2011. *Lost circulation material for oilfield use*, Google Patents (Reprint).

- Ghazali, NA, Mohd, TAT, Alias, N, Shahrudin, MZ, Sauki, A, and Maliki, MBF. 2014. The Effects of Temperature on Rheology Properties and Filtrate after Using Lemongrass as Lost Circulation Materials for Oil Based Drilling Mud. *Proc., Advanced Materials Research* 243-247.
- Ghazali, Nurul Aimi, Naganawa, Shigemi, and Masuda, Yoshihiro. 2018. Feasibility study of tannin-lignosulfonate drilling fluid system for drilling geothermal prospect. *Proc., Proceedings of the 43rd Workshop on Geothermal Reservoir Engineering*, Stanford University, Stanford, CA, USA 12-14.
- Ghriga, Mohammed Abdelfetah, Grassl, Bruno, Gareche, Mourad, Khodja, Mohamed, Lebouachera, Seif El Islam, Andreu, Nathalie, and Drouiche, Nadjib. 2019. Review of recent advances in polyethylenimine crosslinked polymer gels used for conformance control applications. *Polymer Bulletin*: 1-29.
- Gibson, Jacob, Javora, Paul H., and Adkins, Mike. 2011. Pre-Cross-Linked Pills Provide Efficient and Consistent Fluid Loss Control. Paper presented at the SPE European Formation Damage Conference, Noordwijk, The Netherlands, 2011/1/1/. SPE. <https://doi.org/10.2118/144213-MS>.
- Gleason, Patricia A and Szymanski, Chester D. 1986. *Fluid loss control agents for drilling fluids containing divalent cations*, Google Patents (Reprint).
- Goins Jr, WG, Weichert, JP, Burba Jr, JL, Dawson Jr, DD, and Teplitz, AJ. 1951. Down-the-hole pressure surges and their effect on loss of circulation. *Proc., Drilling and Production Practice*.
- Gonzalez, Manuel Eduardo, Bloys, James Benjamin, Lofton, John E, Pepin, Gregory Paul, Schmidt, Joseph H, Naquin, Carey John, Ellis, Scot Thomas, and Laursen, Patrick E. 2004. Increasing effective fracture gradients by managing wellbore temperatures. *Proc., IADC/SPE Drilling Conference*.
- Gooch, Jan W. 2011. Chemical Cross-Linking. In *Encyclopedic Dictionary of Polymers*, ed. Jan W. Gooch, 881-881. New York, NY: Springer New York.
- Graves, Kyle S. and Herrera Gomez, Delimar Cristobal. 2013. Casing While Drilling Utilizing Rotary Steerable Technology in the Stag Field-Offshore Australia. Paper presented at the SPE Annual Technical Conference and Exhibition, New Orleans, Louisiana, USA, 2013/9/30/. SPE. <https://doi.org/10.2118/166166-MS>.

- Guancheng, Jiang, Yourong, Qi, Yuxiu, An, Xianbin, Huang, and Yanjun, Ren. 2016. Polyethyleneimine as shale inhibitor in drilling fluid. *Applied Clay Science* **127-128**: 70-77. <http://www.sciencedirect.com/science/article/pii/S016913171630165X>.
- Gunawan, Stanley, Armstrong, Charles D, and Qu, Qi. 2012. Universal Breakers with Broad Polymer Specificity for Use in Alkaline, High-Temperature Fracturing Fluids. *Proc.*, SPE Annual Technical Conference and Exhibition.
- Guo, Boyun and Liu, Gefei. 2011. *Applied drilling circulation systems: hydraulics, calculations and models*: Gulf Professional Publishing.
- Haciislamoglu, Mustafa. 1994. Practical pressure loss predictions in realistic annular geometries. *Proc.*, SPE Annual Technical Conference and Exhibition.
- Hamza, Ahmed, Shamlooh, Mohamed, Hussein, Ibelwaleed A., Nasser, Mustafa, and Salehi, Saeed. 2019. Polymeric formulations used for loss circulation materials and wellbore strengthening applications in oil and gas wells: A review. *Journal of Petroleum Science and Engineering* **180**: 197-214. <http://www.sciencedirect.com/science/article/pii/S0920410519304760>.
- Hanes, Robert E, Weaver, Jimmie D, and Slabaugh, Billy F. 2006. *Methods and compositions for reducing the viscosity of treatment fluids*, Google Patents (Reprint).
- Hannegan, Don M. 2001. Underbalanced Operations Continue Offshore Movement. *Proc.*, SPE/ICoTA Coiled Tubing Roundtable.
- Haraguchi, Kazutoshi and Takehisa, Toru. 2002. Nanocomposite hydrogels: A unique organic–inorganic network structure with extraordinary mechanical, optical, and swelling/deswelling properties. *Advanced materials* **14** (16): 1120-1124.
- Hardy, Mary, Botermans, Wouter, and Smith, Phil. 1998. New organically crosslinked polymer system provides competent propagation at high temperature in conformance treatments. *paper SPE* **39690**: 19-22.
- Hashmat, M. D., Sultan, Abdullah S., Rahman, Saifur, and Hussain, S. M. Shakil. 2016a. Crosslinked Polymeric Gels as Loss Circulation Materials: An Experimental Study. Paper presented at the SPE Kingdom of Saudi Arabia Annual Technical Symposium and Exhibition, Dammam, Saudi Arabia, 2016/4/25/. SPE. <https://doi.org/10.2118/182740-MS>.

- Hashmat, M. D., Sultan, Abdullah S., Rahman, Saifur, Hussain, S. M. Shakil, and Ali, Shaikh Asrof. 2017. Flowing Gels for Loss Circulation Prevention. Paper presented at the SPE Kingdom of Saudi Arabia Annual Technical Symposium and Exhibition, Dammam, Saudi Arabia, 2017/6/1/. SPE. <https://doi.org/10.2118/188103-MS>.
- Hashmat, MD, Sultan, Abdullah S, Rahman, Saifur, and Hussain, SM. 2016b. Crosslinked polymeric gels as loss circulation materials: An experimental study. *Proc.*, SPE Kingdom of Saudi Arabia Annual Technical Symposium and Exhibition.
- Hastie, Trevor, Tibshirani, Robert, and Friedman, Jerome. 2009. *The elements of statistical learning: data mining, inference, and prediction*: Springer Science & Business Media.
- He, Wenhao, Hayatdavoudi, Asadollah, Chen, Keyong, Sawant, Kaustubh, Zhang, Qin, and Zhang, Chi. 2019. Enhancement of Plastering Effect on Strengthening Wellbore by Optimizing Particle Size Distribution of Wellbore Strengthening Materials. *Journal of Energy Resources Technology* **141** (12). <https://doi.org/10.1115/1.4043785>.
- Hegde, Chiranth, Wallace, Scott, and Gray, Ken. 2015. Using trees, bagging, and random forests to predict rate of penetration during drilling. *Proc.*, SPE Middle East Intelligent Oil and Gas Conference and Exhibition.
- Hollman, Landon, Haq, Inam, Christenson, Clayton, Silva, Thiago Pinheiro da, Fayed, Mohamed Idris Ben, Thorn, Nigel, and Geldof, Wilco. 2015. Developing a MPD Operation Matrix – Case History. Paper presented at the SPE/IADC Drilling Conference and Exhibition, London, England, UK, 2015/3/17/. SPE. <https://doi.org/10.2118/173094-MS>.
- Horton, Robert L, Prasek, Bethicia, Growcock, Frederick B, Vian, John W, and Ivan, Catalin D. 2006. *Prevention and treatment of lost circulation with crosslinked polymer material*, Google Patents (Reprint).
- Howard, George C and Scott Jr, PP. 1951. An analysis and the control of lost circulation. *Journal of Petroleum Technology* **3** (06): 171-182.
- Howard, George C. and Scott, P. P., Jr. 1951. An Analysis and the Control of Lost Circulation. *SPE-1218-0014-JPT* **3** (06): 171-182. <https://doi.org/10.2118/951171-G>.
- Igwilo, Kevin C, Okoro, Emeka E, Ohia, Princewill N, Adenubi, Solomon A, Okoli, Nnanna, and Adebayo, Temilade. 2019. Effect of Mud Weight on Hole Cleaning During Oil and Gas Drilling Operations Effective Drilling Approach. *The Open Petroleum Engineering Journal* **12** (1).

- Javeri, Saket Mahesh, Haindade, Zishaan Muhamad Wajid, and Jere, Chaitanya Bhalchandra. 2011. Mitigating Loss Circulation And Differential Sticking Problems Using Silicon Nanoparticles. Paper presented at the SPE/IADC Middle East Drilling Technology Conference and Exhibition, Muscat, Oman, 2011/1/1/. SPE. <https://doi.org/10.2118/145840-MS>.
- Johannes, KF. 2012. *Petroleum engineer's guide to oil field chemicals and fluids*, Oxford: Gulf Professional Publishing (Reprint).
- Johnston, CA and Rubin, M. 2000. Development document for final effluent limitations guidelines and standards for synthetic-based drilling fluids and other non-aqueous drilling fluids in the oil and gas extraction point source category. *Tech Rep*.
- Kabir, AH. 2001. Chemical water & gas shutoff technology-An overview. *Proc.*, SPE Asia Pacific Improved Oil Recovery Conference.
- Kageson-Loe, Nils M., Sanders, Mark W., Growcock, Fred, Taugbøl, Knut, Horsrud, Per, Singelstad, Arne V., and Omland, Tor Henry. 2009. Particulate-based loss-prevention material--the secrets of fracture sealing revealed! *SPE drilling & completion* **24** (04): 581-589. <https://www.researchgate.net/publication/254527684>
- Kamal, Muhammad Shahzad, Mohammed, Marwan, Mahmoud, Mohamed, and Elkatatny, Salaheldin. 2018. Development of chelating agent-based polymeric gel system for hydraulic fracturing. *Energies* **11** (7): 1663.
- Kang, Yongfeng, Yu, Mengjiao, Miska, Stefan Z, and Takach, Nicholas. 2009. Wellbore stability: a critical review and introduction to DEM. *Proc.*, SPE Annual Technical Conference and Exhibition.
- Karimi, Moji, Moellendick, Timothy Eric, and Holt, Calvin. 2011. Plastering Effect of Casing Drilling; a Qualitative Analysis of Pipe Size Contribution. Paper presented at the SPE Annual Technical Conference and Exhibition, Denver, Colorado, USA, 2011/1/1/. SPE. <https://doi.org/10.2118/147102-MS>.
- Khodja, Mohamed, Canselier, Jean Paul, Bergaya, Faiza, Fourar, Karim, Khodja, Malika, Cohaut, Nathalie, and Benmounah, Abdelbaki. 2010. Shale problems and water-based drilling fluid optimisation in the Hassi Messaoud Algerian oil field. *Applied Clay Science* **49** (4): 383-393. <http://www.sciencedirect.com/science/article/pii/S0169131710001705>.

- Khodja, Mohamed, Khodja-Saber, Malika, Canselier, Jean Paul, Cohaut, Nathalie, and Bergaya, Faïza. 2010. Drilling fluid technology: performances and environmental considerations. *Products and services; from R&D to final solutions*: 227-256.
- Kihara, Nobuhiro, Yanaze, Kazuya, Yokoyama, Satoshi, and Kaneko, Moe. 2019. Dissolution of a transparent cross-linked polymer monolith in water by oxidative de-crosslinking. *Polymer Journal* **51** (10): 1007-1013.
- Kiran, Raj, Teodoriu, Catalin, Dadmohammadi, Younas, Nygaard, Runar, Wood, David, Mokhtari, Mehdi, and Salehi, Saeed. 2017. Identification and evaluation of well integrity and causes of failure of well integrity barriers (A review). *Journal of Natural Gas Science and Engineering* **45**: 511-526.
- Kister, EG. 1972. Chemical processing of the drilling fluids. *M: Nedra* **392**.
- Kostov, Nikolay, Ning, Jing, Gosavi, Shekhar V, Gupta, Piyush, Kulkarni, Kaustubh, and Sanz, Pablo. 2015. Advanced drilling induced fracture modeling for wellbore integrity prediction. *Proc.*, SPE annual technical conference and exhibition.
- Kudaikulova, G. 2015. Rheology of drilling muds. *Proc.*, Journal of Physics: Conference Series 1, 012008.
- Kulkarni, Sandeep D., Savari, Sharath, Gupta, Nivika, and Whitfill, Don. 2016. Designing Lost Circulation Material LCM Pills for High Temperature Applications. Paper presented at the SPE Deepwater Drilling and Completions Conference, Galveston, Texas, USA, 2016/9/14/. SPE. <https://doi.org/10.2118/180309-MS>.
- Kumar, A, Savari, Sh, Jamison, DE, and Whitfill, D. 2011. Application of fiber laden pill for controlling lost circulation in natural fractures. *Proc.*, AADE national technical conference and exhibition, Houston, Texas, USA12-14.
- Kurenkov, V. F., Hartan, H. G., and Lobanov, F. I. 2001. Alkaline Hydrolysis of Polyacrylamide. *Russian Journal of Applied Chemistry* **74** (4): 543-554. <https://doi.org/10.1023/A:1012786826774>.
- Labahn, K. Stephanie, C. Fisher, Jenny, A. Robleto, Eduardo, H. Young, Michael, and P. Moser, Duane. 2010. Microbially mediated aerobic and anaerobic degradation of acrylamide in a western United States irrigation canal. *Journal of environmental quality* **39** (5): 1563-1569.
- Lambla, Morand. 1989. Reactive processing of thermoplastic polymers.

- Lavrov, A and Tronvoll, J. 2003. Mud loss into a single fracture during drilling of petroleum wells: Modeling approach. *Proc., Development and Application of Discontinuous Modelling for Rock Engineering: Proceedings of the 6th International Conference ICADD-6, Trondheim, Norway, 5–8 October 2003* 189-198.
- Lavrov, Alexandre. 2016. *Lost circulation: mechanisms and solutions*: Gulf professional publishing.
- Lavrov, Alexandre. 2017. Lost Circulation in Primary Well Cementing. *Energy Procedia* **114**: 5182-5192. <http://www.sciencedirect.com/science/article/pii/S1876610217318738>.
- Lee, Lu and Dahi Taleghani, Arash. 2020. Simulating Fracture Sealing by Granular LCM Particles in Geothermal Drilling. *Energies* **13** (18): 4878.
- Lee, Lu and Taleghani, Arash Dahi. 2020. Looking at Fracture Sealing Mechanisms by Granular LCM at Elevated Temperatures.
- Liu, Y, Bai, B, and Li, Y. 1999. Research on preformed gel grains for water shutoff and profile control. *Oil Drilling & Production Technology* **21** (3): 65-68.
- Liu, Yifei, Dai, Caili, Wang, Kai, Zhao, Mingwei, Zhao, Guang, Yang, Shuai, Yan, Zhihu, and You, Qing. 2016. New insights into the hydroquinone (HQ)–hexamethylenetetramine (HMTA) gel system for water shut-off treatment in high temperature reservoirs. *Journal of industrial and engineering chemistry* **35**: 20-28.
- Loeppke, Glen. 1986. Evaluating candidate lost circulation materials for geothermal drilling, Sandia National Labs., Albuquerque, NM (USA).
- Lopez Herrera, Edwin Alfredo, Bonilla, Pablo Antonio, and Rincón, Javier Adolfo. 2010. Casing Drilling Application With Rotary Steerable and Triple Combo in New Deviated Wells in La Cira Infantas Field. Paper presented at the SPE Annual Technical Conference and Exhibition, Florence, Italy, 2010/1/1/. SPE. <https://doi.org/10.2118/134586-MS>.
- Luzardo, J, Oliveira, EP, Derks, PWJ, Nascimento, R Vega, Gramatges, A Perez, Valle, R, Pantano, I Gianoglio, Sbaglia, F, and Inderberg, K. 2015a. Alternative lost circulation material for depleted reservoirs. *Proc., OTC Brasil*.
- Luzardo, J., Oliveira, E. P., Derks, P. W. J., Nascimento, R. Vega, Gramatges, A. Perez, Valle, R., Pantano, I. Gianoglio, Sbaglia, F., and Inderberg, K. 2015b. Alternative Lost Circulation Material for Depleted Reservoirs. Paper presented at the OTC Brasil, Rio de Janeiro, Brazil, 2015/10/27/. OTC. <https://doi.org/10.4043/26188-MS>.

- Magzoub, Musaab I, Salehi, Saeed, Hussein, Ibelwaleed A, and Nasser, Mustafa S. 2020a. Loss circulation in drilling and well construction: The significance of applications of crosslinked polymers in wellbore strengthening: A review. *Journal of Petroleum Science and Engineering* **185**: 106653.
- Magzoub, Musaab Ibrahim, Salehi, Saeed, Hussein, Ibelwaleed Ali, and Nasser, Mustafa Saleh. 2020b. A Comprehensive Rheological Study for a Flowing Polymer-Based Drilling Fluid Used for Wellbore Strengthening. *Proc.*, SPE International Conference and Exhibition on Formation Damage Control.
- Magzoub, Musaab, Salehi, Saeed, Li, Guoqiang, Fan, Jizhou, and Teodoriu, Catalin. 2021. Loss circulation prevention in geothermal drilling by shape memory polymer. *Geothermics* **89**: 101943.
- Majidi, Reza, Miska, Stefan, Thompson, Leslie G, Yu, Mengjiao, and Zhang, Jianguo. 2010. Quantitative analysis of mud losses in naturally fractured reservoirs: the effect of rheology. *SPE Drilling & Completion* **25** (04): 509-517.
- Majidi, Reza, Miska, Stefan, and Zhang, Jianguo. 2011. Fingerprint of Mud Losses into Natural and Induced Fractures. Paper presented at the SPE European Formation Damage Conference, Noordwijk, The Netherlands, 2011/1/1/. SPE. <https://doi.org/10.2118/143854-MS>.
- Makwana, SB, Patel, VA, and Parmar, SJ. 2016. Development and characterization of in-situ gel for ophthalmic formulation containing ciprofloxacin hydrochloride. *Results in pharmaceutical sciences* **6**: 1-6.
- Malloy, Kenneth P. 2007. Managed pressure drilling-: What is it anyway?: Managed pressure drilling. *World oil* **228** (3).
- Mannon Jr, Timothy Patrick. 2013. *Best Practices for Mudweight Window Generation and Accuracy Assessment Between Seismic Based Pore Pressure Prediction Methodologies for a Near-salt Field in Mississippi Canyon, Gulf of Mexico*.
- Mansour, Ahmed Khaled, Taleghani, Arash Dahi, and Li, Guoqiang. 2017. Smart lost circulation materials for wellbore strengthening. *Proc.*, 51st US Rock Mechanics/Geomechanics Symposium.

- Mansour, Ahmed, Taleghani, Arash Dahi, Salehi, Saeed, Li, Guoqiang, and Ezeakacha, C. 2019. Smart lost circulation materials for productive zones. *Journal of Petroleum Exploration and Production Technology* **9** (1): 281-296.
- Mehrabian, Amin, Jamison, Dale E., and Teodorescu, Sorin Gabriel. 2015. Geomechanics of Lost-Circulation Events and Wellbore-Strengthening Operations. *SPE Journal* **20** (06): 1305-1316. <https://doi.org/10.2118/174088-PA>.
- Melton, HR, Smith, JP, Mairs, HL, Bernier, RF, Garland, E, Glickman, AH, Jones, FV, Ray, JP, Thomas, D, and Campbell, JA. 2004. Environmental aspects of the use and disposal of non aqueous drilling fluids associated with offshore oil & gas operations. *Proc.*, SPE International Conference on Health, Safety, and Environment in Oil and Gas Exploration and Production.
- Metcalf, Arthur Steven, Lopez, Enrique, and Martinez-Guedry, John Dustin. 2011. Case histories: Overcoming lost circulation during drilling and primary cementing operations using an environmentally preferred system. *Proc.*, SPE Production and Operations Symposium.
- Meza, Oscar Grijalva, Yaqoob, Tanveer, Bello, Opeyemi, Boulakhrif, Faissal, Holzmann, Javier, and Oppelt, Joachim. 2017. Combined Investigation of Effects of Contact Stresses, Pore Size and Rotary Dynamics on Mud Plastering in Prevention of Lost Circulation in Weak Zones during Casing Drilling. Paper presented at the Abu Dhabi International Petroleum Exhibition & Conference, Abu Dhabi, UAE, 2017/11/13/. SPE. <https://doi.org/10.2118/188182-MS>.
- Misbah, Biltayib. 2010. First Under-Balanced Drilling Experience in AGOCO Sarir Field. Paper presented at the SPE/IADC Managed Pressure Drilling and Underbalanced Operations Conference and Exhibition, Kuala Lumpur, Malaysia, 2010/1/1/. SPE. <https://doi.org/10.2118/130562-MS>.
- Mohamed, Abdelhalim I. A., Hussein, Ibnelwaleed A., Sultan, Abdullah S., El-Karsani, Khalid S. M., and Al-Muntasheri, Ghaitan A. 2015a. DSC investigation of the gelation kinetics of emulsified PAM/PEI system. *Journal of Thermal Analysis and Calorimetry* **122** (3): 1117-1123.
- Mohamed, Abdelhalim IA, Hussein, Ibnelwaleed A, Sultan, Abdullah S, and Al-Muntasheri, Ghaitan A. 2018. Gelation of emulsified polyacrylamide/polyethylenimine under high-

- temperature, high-salinity conditions: rheological investigation. *Industrial & Engineering Chemistry Research* **57** (36): 12278-12287.
- Mohamed, Abdelhalim IA, Hussein, Ibelwaleed A, Sultan, Abdullah S, El-Karsani, Khalid SM, and Al-Muntasheri, Ghaithan A. 2015b. DSC investigation of the gelation kinetics of emulsified PAM/PEI system. *Journal of Thermal Analysis and Calorimetry* **122** (3): 1117-1123.
- Moradi-Araghi, A, Bjornson, G, and Doe, PH. 1993a. Thermally stable gels for near-wellbore permeability contrast corrections. *SPE Advanced Technology Series* **1** (01): 140-145.
- Moradi-Araghi, A., Bjornson, G., and Doe, P. H. 1993b. Thermally Stable Gels for Near-Wellbore Permeability Contrast Corrections. *SPE Advanced Technology Series* **1** (01): 140-145. <https://doi.org/10.2118/18500-PA>.
- Morita, N, Fuh, G-F, and Black, AD. 1996. Borehole breakdown pressure with drilling fluids—II. Semi-analytical solution to predict borehole breakdown pressure. *Proc., International journal of rock mechanics and mining sciences & geomechanics abstracts*1, 53-69.
- Morita, N., Black, A. D., and Guh, G. F. 1990. Theory of Lost Circulation Pressure. Paper presented at the SPE Annual Technical Conference and Exhibition, New Orleans, Louisiana, 1990/1/1/. SPE. <https://doi.org/10.2118/20409-MS>.
- Munoz Jr, Trinidad. 2009. *In-situ filter cake degradation compositions and methods of use in subterranean formations*, Google Patents (Reprint).
- Munoz Jr, Trinidad and Todd, Bradley L. 2006. *Treatment fluids comprising starch and ceramic particulate bridging agents and methods of using these fluids to provide fluid loss control*, Google Patents (Reprint).
- Natekin, Alexey and Knoll, Alois. 2013. Gradient boosting machines, a tutorial. *Frontiers in neurorobotics* **7**: 21.
- Naveen, V. and Babu, Vinay. 2014. Experimental Study of Plastering Effect During Casing While Drilling. Paper presented at the Abu Dhabi International Petroleum Exhibition and Conference, Abu Dhabi, UAE, 2014/11/10/. SPE. <https://doi.org/10.2118/171997-MS>.
- NPDES, USEPA. 2001. Final NPDES general permit for new and existing sources and new dischargers in the offshore subcategory of the oil and gas extraction category for the Western Portion of the Outer Continental Shelf of the Gulf of Mexico (GMG290000).(66 FR 65209). *Federal Register* **66**.

- Nwaoji, Charles Okeibuno. 2012. *Wellbore strengthening-nano-particle drilling fluid experimental design using hydraulic fracture apparatus*, Graduate Studies.
- Nygaard, R and Salehi, SA. 2011. Critical review of wellbore strengthening: physical model and field deployment. *Proc.*, AADE National Technical Conference and Exhibition, Houston, No. AADE-11-NTCE-24.
- OECD, Guideline. 2004. *Sediment-Water Chironomid Toxicity Test Using Spiked Sediment*: Paris, France: Organisation for Economic Co-operation and Development (Reprint).
- Ogeleka, DF and Tudararo-Aherobo, LE. 2011. Short-term toxicity of oil-based drilling fluid to the brackish-water shrimp *Palaemonetes africanus*. *African Journal of Aquatic Science* **36** (1): 109-112.
- Oldham, Wilbur N and Kropa, Edward L. 1955. *Drilling muds*, Google Patents (Reprint).
- Omer, Mohammed. 2012. EVALUATION OF POLYMERIC MATERIALS AS LOSS CIRCULATION AGENTS IN SHALLOW ZONES.
- Onwuchekwa, Chukwuma. 2018. Application of Machine Learning Ideas to Reservoir Fluid Properties Estimation. *Proc.*, SPE Nigeria Annual International Conference and Exhibition.
- Onwukwe, SI and Nwakaudu, MS. 2012. Drilling wastes generation and management approach. *International Journal of Environmental Science and Development* **3** (3): 252.
- Oyama, Toshiyuki. 2015. Cross-Linked Polymer Synthesis. In *Encyclopedia of Polymeric Nanomaterials*, ed. Shiro Kobayashi and Klaus Müllen, 496-505. Berlin, Heidelberg: Springer Berlin Heidelberg.
- Ozdemirtas, Mert, Babadagli, Tayfun, and Kuru, Ergun. 2009. Experimental and numerical investigations of borehole ballooning in rough fractures. *SPE Drilling & Completion* **24** (02): 256-265.
- Palsule, Sanjay. 2016. *Polymers and Polymeric Composites: A Reference Series*: Springer.
- Park, Jiyoung and Kim, Seok. 2015. Electrochemical analysis of polyethyleneimine-conductive carbon black supports for Pt-Pd electrocatalysts. *Journal of nanoscience and nanotechnology* **15** (2): 1610-1613.
- Pašić, Borivoje, Gaurina Međimurec, Nediljka, and Matanović, Davorin. 2007. Wellbore instability: causes and consequences. *Rudarsko-geološko-naftni zbornik* **19** (1): 87-98.

- Patel, Dipal, Thakar, Vivek, Pandian, Sivakumar, Shah, Manan, and Sircar, Anirbid. 2019. A review on casing while drilling technology for oil and gas production with well control model and economical analysis. *Petroleum* **5** (1): 1-12.
- Patil, Prajakta, Muthusamy, Ramesh, and Pandya, Nisha. 2013. Novel controlled-release breakers for high-temperature fracturing. *Proc.*, North Africa Technical Conference and Exhibition.
- Paul, James M and Strom, Edwin T. 1987. Oil reservoir permeability control using polymeric gels. US Patent Application No. 737,617
- Pavković, Bojan, Bizjak, Renato, and Petrović, Bojan. 2016. Review of casing while drilling technology. *Podzemni radovi* (29): 11-32.
- Peter-Borie, Mariane, Loschetter, Annick, Merciu, IA, Kampfer, G, and Sigurdsson, O. 2018. Borehole damaging under thermo-mechanical loading in the RN-15/IDDP-2 deep well: towards validation of numerical modeling using logging images. *Geothermal Energy* **6** (1): 17.
- Plank, Johann P. 1992. Water-Based Muds Using Synthetic-Polymers Developed for High-Temperature Drilling. *Oil & Gas Journal* **90** (9): 40-45.
- Qiu, Liewei, Shen, Yiding, Wang, Tao, and Wang, Chen. 2018. Rheological and fracturing characteristics of a Novel sulfonated hydroxypropyl guar gum. *International journal of biological macromolecules* **117**: 974-982.
- Rabia, Hussain. 2002. *Well engineering & construction*: Entrac Consulting Limited London.
- Rafati, Roozbeh, Smith, Sean Robert, Sharifi Haddad, Amin, Novara, Rizky, and Hamidi, Hossein. 2018. Effect of nanoparticles on the modifications of drilling fluids properties: A review of recent advances. *Journal of Petroleum Science and Engineering* **161**: 61-76. <http://www.sciencedirect.com/science/article/pii/S092041051730949X>.
- Rahmanifard, H, Rasouli, AR, Mayahi, N, Amouri, AH, and Mafreshi, M. 2014. BEST PRACTICE IN MANAGING LOST CIRCULATION CHALLENGES DURING DRILLING AND CEMENTING OPERATIONS IN AZAR OIL FIELD. *Proc.*, Proceedings of the 2nd International Conference of Oil, Gas and Petrochemicals, Iran.
- Rajadurai, Hariharan and Gandhi, Usha Devi. 2020. A stacked ensemble learning model for intrusion detection in wireless network. *Neural Computing and Applications*: 1-9. <https://doi.org/10.1007/s00521-020-04986-5>

- Rana, Azeem, Saleh, Tawfik A., and Arfaj, Mohammad K. 2019. Improvement in Rheological Features, Fluid Loss and Swelling Inhibition of Water-Based Drilling Mud by Using Surfactant-Modified Graphene. Paper presented at the Abu Dhabi International Petroleum Exhibition & Conference, Abu Dhabi, UAE, 2019/11/11/. SPE. <https://doi.org/10.2118/197774-MS>.
- Reddy, B Raghava. 2014. Laboratory characterization of gel filter cake and development of nonoxidizing gel breakers for zirconium-crosslinked fracturing fluids. *SPE Journal* **19** (04): 662-673.
- Reddy, B. R., Eoff, Larry, Dalrymple, E. Dwyann, Black, Kathy, Brown, David, and Rietjens, Marcel. 2003. A Natural Polymer-Based Cross-Linker System for Conformance Gel Systems. *SPE-182266-PA* **8** (02): 99-106. <https://doi.org/10.2118/84937-PA>.
- Rehm, Bill, Haghshenas, Arash, Paknejad, Amir Saman, Al-Yami, Abdullah, and Hughes, Jim. 2013. *Underbalanced drilling: limits and extremes*: Elsevier.
- Remont, Larry J, Rehm, William A, McDonald, WJ, and Maurer, William C. 1976. Evaluation of commercially available geothermal drilling fluids, Maurer Engineering, Inc., Houston, TX (USA).
- Sabins, Fred L. 1990. Problems in cementing horizontal wells. *Journal of petroleum technology* **42** (04): 398-400.
- Saleh, Fatemeh K, Teodoriu, Catalin, Ezeakacha, Chinedum P, and Salehi, Saeed. 2020. Geothermal Drilling: A Review of Drilling Challenges with Mud Design and Lost Circulation Problem.
- Saleh, Tawfik A and Ibrahim, Mukaila A. 2019. Advances in functionalized Nanoparticles based drilling inhibitors for oil production. *Energy Reports* **5**: 1293-1304.
- Salehi, Saeed. 2012. Numerical simulations of fracture propagation and sealing: Implications for wellbore strengthening.
- Salehi, Saeed, Ghalambor, Ali, Saleh, Fatemeh K, Jabbari, Hadi, and Hussmann, Stefanie. 2015. Study of filtrate and mud cake characterization in HPHT: Implications for formation damage control. *Proc.*, SPE European Formation Damage Conference and Exhibition.
- Salehi, Saeed and Nygaard, Runar. 2011. Evaluation of New Drilling Approach for Widening Operational Window: Implications for Wellbore Strengthening. Paper presented at the SPE

- Production and Operations Symposium, Oklahoma City, Oklahoma, USA, 2011/1/1/. SPE. <https://doi.org/10.2118/140753-MS>.
- Salehi, Saeed and Nygaard, Runar. 2012a. Numerical Modeling of Induced Fracture Propagation: A Novel Approach for Lost Circulation Materials (LCM) Design in Borehole Strengthening Applications of Deep Offshore Drilling. Paper presented at the SPE Annual Technical Conference and Exhibition, San Antonio, Texas, USA, 2012/1/1/. SPE. <https://doi.org/10.2118/135155-MS>.
- Salehi, Saeed and Nygaard, Runar. 2012b. Numerical modeling of induced fracture propagation: a novel approach for lost circulation materials (LCM) design in borehole strengthening applications of deep offshore drilling. *Proc.*, SPE Annual Technical Conference and Exhibition.
- Salih, AH and Bilgesu, H. 2017. Investigation of rheological and filtration properties of water-based drilling fluids using various anionic nanoparticles. *Proc.*, SPE Western regional meeting.
- Sánchez, Francisco and Al-Harthy, Mansoor H. 2011. Risk analysis: Casing-while-Drilling (CwD) and modeling approach. *Journal of Petroleum Science and Engineering* **78** (1): 1-5.
- Sarwar, Muhammad Usman, Cawiezel, Kay E, and Nasr-El-Din, Hisham A. 2011. Gel degradation studies of oxidative and enzyme breakers to optimize breaker type and concentration for effective break profiles at low and medium temperature ranges. *Proc.*, SPE Hydraulic Fracturing Technology Conference.
- Seetharaman, Gomathi Rajalakshmi and Sangwai, Jitendra S. 2020. Effect of Nanoparticles on the Performance of Drilling Fluids. In *Nanotechnology for Energy and Environmental Engineering*, 279-297. Springer.
- Seybold, CA. 1994. Polyacrylamide review: Soil conditioning and environmental fate. *Communications in soil science and plant analysis* **25** (11-12): 2171-2185.
- Shaikh, Shifa MR, Nasser, Mustafa S, Magzoub, Musaab, Benamor, Abdelbaki, Hussein, Ibnelwaleed A, El-Naas, Muftah H, and Qiblawey, Hazim. 2018. Effect of electrolytes on electrokinetics and flocculation behavior of bentonite-polyacrylamide dispersions. *Applied Clay Science* **158**: 46-54.
- Shanker, Rishi, Ramakrishna, Cherla, and Seth, Prahlad K. 1990. Microbial degradation of acrylamide monomer. *Archives of Microbiology* **154** (2): 192-198.

- Sheng, James J. 2010. *Modern chemical enhanced oil recovery: theory and practice*: Gulf Professional Publishing.
- Shukor, MY, Gusmanizar, N, Azmi, NA, Hamid, M, Ramli, J, Shamaan, NA, and Syed, MA. 2009. Isolation and characterization of an acrylamide-degrading *Bacillus cereus*. *J Environ Biol* **30** (1): 57-64.
- Shupe, Russell D. 1981. Chemical Stability of Polyacrylamide Polymers. *SPE-9299-PA* **33** (08): 1513-1529. <https://doi.org/10.2118/9299-PA>.
- Song, Linjiang, Liang, Xiuqi, Yang, Suleixin, Wang, Ning, He, Tao, Wang, Yan, Zhang, Lan, Wu, Qinjie, and Gong, Changyang. 2018. Novel polyethyleneimine-R8-heparin nanogel for high-efficiency gene delivery in vitro and in vivo. *Drug Delivery* **25** (1): 122-131. <https://doi.org/10.1080/10717544.2017.1417512>.
- Steffe, James Freeman. 1996. *Rheological methods in food process engineering*: Freeman press.
- Stephansson, Ove, Hudson, John, and Jing, Lanru. 2004. *Coupled thermo-hydro-mechanical-chemical processes in Geo-Systems*: Elsevier.
- Stockmayer, Walter H. 1944. Theory of molecular size distribution and gel formation in branched polymers II. General cross linking. *The Journal of Chemical Physics* **12** (4): 125-131.
- Sun, Yixuan and Huang, Haiying. 2015. Effect of rheology on drilling mud loss in a natural fracture. *Proc.*, 49th US Rock Mechanics/Geomechanics Symposium.
- Swapnil DS, P, Ravindra Y, and L., Meenal. 2013. A Review on Polymers Used In Novel In situ Gel Formulation For Ocular Drug Delivery and Their Evaluation. *Journal of Biological and Scientific Opinion* **2** (1): 132-7.
- Sweatman, Ron, Wang, Hong, and Xenakis, Harry. 2004. Wellbore Stabilization Increases Fracture Gradients and Controls Losses/Flows During Drilling. *Proc.*, Abu Dhabi International Conference and Exhibition.
- Sydansk, Robert D. 1990. A Newly Developed Chromium(III) Gel Technology. *SPE-19308-PA* **5** (03): 346-352. <https://doi.org/10.2118/19308-PA>.
- Tangedahl, Michael J. 1996. Well Control: Issues of Under Balanced Drilling. Paper presented at the SPE Eastern Regional Meeting, Columbus. Ohio, 1996/1/1/. SPE. <https://doi.org/10.2118/37329-MS>.

- Tessarolli, Fernanda G. C., Souza, Sara T. S., Gomes, Ailton S., and Mansur, Claudia R. E. 2019. Gelation kinetics of hydrogels based on acrylamide–AMPS–NVP terpolymer, bentonite, and polyethylenimine for conformance control of oil reservoirs. *Gels* **5** (1): 7.
- Thaemlitz, CJ, Patel, AD, Coffin, George, and Conn, Lee. 1999. New environmentally safe high-temperature water-based drilling-fluid system. *SPE drilling & completion* **14** (03): 185-189.
- Thomas, Fabien, Masion, Armand, Bottero, Jean Yves, Rouiller, James, Genevrier, Francine, and Boudot, Denis. 1991. Aluminum (III) speciation with acetate and oxalate. A potentiometric and aluminum-27 NMR study. *Environmental science & technology* **25** (9): 1553-1559.
- Torlay, L, Perrone-Bertolotti, Marcela, Thomas, Elizabeth, and Baciú, Monica. 2017. Machine learning–XGBoost analysis of language networks to classify patients with epilepsy. *Brain informatics* **4** (3): 159-169.
- Trifunovski, Tony and Mostofi, Masood. 2020. Investigating the application of reactive polymers in fluid loss control. *Journal of Petroleum Exploration and Production Technology* **10** (3): 1137-1143.
- Uhl, Klaus, Bannerman, James K, Engelhardt, Friedrich J, and Patel, Arvind. 1984. *Water soluble copolymers containing vinyl imidazole as drilling fluid additives*, Google Patents (Reprint).
- Vasquez, Julio, Civan, Faruk, Shaw, Thomas M, Dalrymple, E Dwyann, Eoff, Larry, Reddy, BR, and Brown, David. 2003. Laboratory evaluation of high-temperature conformance polymer systems. *Proc.*, SPE production and operations symposium.
- Wang, Hong, Towler, Brian Francis, and Soliman, Mohamed Y. 2007. Fractured Wellbore Stress Analysis: Sealing Cracks to Strengthen a Wellbore. Paper presented at the SPE/IADC Drilling Conference, Amsterdam, The Netherlands, 2007/1/1/. SPE. <https://doi.org/10.2118/104947-MS>.
- Wang, Zhengzhou, Wu, Xiusheng, Gui, Zhou, Hu, Yuan, and Fan, Weicheng. 2005. Thermal and crystallization behavior of silane-crosslinked polypropylene. *Polymer international* **54** (2): 442-447.
- Wastu, ARR, Hamid, A, and Samsol, S. 2019. The effect of drilling mud on hole cleaning in oil and gas industry. *Proc.*, Journal of Physics: Conference Series2, 022054.
- Wenger, Lloyd M., Davis, Cara L., Evensen, Joseph M., Gormly, James R., and Mankiewicz, Paul J. 2004. Impact of modern deepwater drilling and testing fluids on geochemical

- evaluations. *Organic Geochemistry* **35** (11): 1527-1536.
<http://www.sciencedirect.com/science/article/pii/S0146638004001780>.
- Wenjun, Shan, Shixian, Tao, Fan, Fu, Weimin, Yue, and Zhitao, Zhao. 2014. Research on the Drilling Fluid Technology for High Temperature over 240oC. *Procedia Engineering* **73**: 218-229.
- Wojtanowicz, A. K. and Zhou, D. 2001. Shallow Casing Shoe Integrity Interpretation Technique. Paper presented at the SPE/IADC Drilling Conference, Amsterdam, Netherlands, 2001/1/1/. SPE. <https://doi.org/10.2118/67777-MS>.
- Wong, Syieluing, Tumari, Hasnaa H, Ngadi, Norzita, Mohamed, Nurul Balqis, Hassan, Onn, Mat, Ramli, and Amin, Nor Aishah Saidina. 2019. Adsorption of anionic dyes on spent tea leaves modified with polyethyleneimine (PEI-STL). *Journal of cleaner production* **206**: 394-406.
- Work, WJ, Horie, K, Hess, M, and Stepto, RFT. 2004. Definition of terms related to polymer blends, composites, and multiphase polymeric materials (IUPAC Recommendations 2004). *Pure and applied chemistry* **76** (11): 1985-2007.
- Zaba, Joseph and Lyons, Ph DPE. 1996. *Standard Handbook of Petroleum and Natural Gas Engineering: Volume 2*: Elsevier Science.
- Zamora, M., Broussard, P. N., and Stephens, M. P. 2000. The Top 10 Mud-Related Concerns in Deepwater Drilling Operations. Paper presented at the SPE International Petroleum Conference and Exhibition in Mexico, Villahermosa, Mexico, 2000/1/1/. SPE. <https://doi.org/10.2118/59019-MS>.
- Zhang, Xiaotian, Lin, Donghai, and Chen, Weixing. 2015. Nitrogen-doped porous carbon prepared from a liquid carbon precursor for CO 2 adsorption. *RSC Advances* **5** (56): 45136-45143.
- Zolfaghari, Reihaneh, Katbab, Ali A, Nabavizadeh, Javad, Tabasi, Ramin Yousefzadeh, and Nejad, Majid Hossein. 2006. Preparation and characterization of nanocomposite hydrogels based on polyacrylamide for enhanced oil recovery applications. *Journal of applied polymer science* **100** (3): 2096-2103

APPENDIX A: COST ANALYSIS FOR THE GELLING MUD, PILLS, AND COMMERCIALY AVAILABLE FORMULATIONS

A.1. Cost Analysis of Drilling Fluids

| Component | PAM/PEI-Based Mud | | Water-Based mud | |
|-------------------|-------------------|--------------|-----------------|--------------|
| | Amount, lb/bbl | Cost, \$ | Amount, lb/bbl | Cost, \$ |
| Caustic soda | 0.5 | 0.07 | 0.5 | 0.07 |
| Lignite | 0 | 0 | 4 | 1.28 |
| Bentonite | 3.5 | 0.49 | 20 | 2.8 |
| Mud deflocculant | 0 | 0 | 4 | 1.28 |
| Calcium Carbonate | 0 | 0 | 55 | 8.8 |
| PAM | 25.6 | 17.408 | 0 | 0 |
| PEI | 3.4 | 3.842 | 0 | 0 |
| Total | 1 bbl | 21.81 | 1 bbl | 14.23 |

A.2. Cost Analysis of PAM/PEI Pills

| Pill | Additive | Concentration, lb/bbl | Price per pound, \$ | Cost, \$ |
|-----------------------------|-----------------------|-----------------------|---------------------|-----------------|
| Pill-1 (PAM/PEI) | PAM | 27.10 | 0.68 | 18.43 |
| | PEI | 3.61 | 1.13 | 4.08 |
| | Amonium Chloride | 18.06 | 0.11 | 2.05 |
| | Total | 1 bbl | | 24.56 |
| Pill-2 PAM/Al/Ac | PAM | 28.57 | 0.68 | 19.43 |
| | Aluminium acetate | 11.43 | 0.39 | 4.41 |
| | Nano silica | 3.81 | 544.22 | 2073.20 |
| | Amonium Chloride | 19.05 | 0.11 | 2.16 |
| | Total | 1 bbl | | 2099.20 |
| Pill-3 (PAM/FS) | PAM | 27.04 | 0.68 | 18.39 |
| | Functionalized silica | 10.82 | 1206.35 | 13047.38 |
| | Nano silica | 3.61 | 544.22 | 1962.01 |
| | Amonium Chloride | 18.03 | 0.11 | 2.04 |
| | Total | 1 bbl | | 15029.82 |

A.3. Cost Analysis Commercially Available Pills

| Losses | Additive | Concentration, lb/bbl | Price per pound, \$ | Cost, \$ | |
|--|--|--------------------------|---------------------|--------------|--------------|
| Seepage losses < 40 bbl/hr pump 15-20 bbl | Bentonite | 25 | 0.14 | 3.5 | |
| | Calcium carbonate 50µm | 3 | 0.187 | 0.561 | |
| | Calcium carbonate 150µm | 3 | 0.217 | 0.651 | |
| | Calcium carbonate 600µm | 3 | 0.22 | 0.66 | |
| | Composite LCM | 3 | 0.7888 | 2.3664 | |
| | Fiber | 3 | 0.7504 | 2.2512 | |
| | Walnut shell | 3 | 0.1864 | 0.5592 | |
| | Total | | 1 bbl | | 10.55 |
| Losses between 40-150 bbl/hr pump 20-40 bbl | Bentonite | 25 | 0.14 | 3.5 | |
| | Calcium carbonate 50µm | 6 | 0.187 | 1.122 | |
| | Calcium carbonate 150µm | 6 | 0.217 | 1.302 | |
| | Calcium carbonate 600µm | 6 | 0.22 | 1.32 | |
| | Composite LCM | 12 | 0.7888 | 9.4656 | |
| | Total | | 1 bbl | | 16.71 |
| | Losses between 150-300 bbl/hr pump 20-40 bbl | Bentonite | 25 | 0.14 | 3.5 |
| Calcium carbonate 50µm | | 5 | 0.187 | 0.935 | |
| Calcium carbonate 150µm | | 5 | 0.217 | 1.085 | |
| Composite LCM | | 10 | 0.7888 | 7.888 | |
| Fiber | | 10 | 0.7504 | 7.504 | |
| Total | | | 1 bbl | | 20.91 |
| Losses >300 bbl/hr pump 20-40 bbl | Bentonite | 25 | 0.14 | 3.5 | |
| | Composite LCM | 30 | 0.7888 | 23.664 | |
| | Fiber | 15 | 0.7504 | 11.256 | |
| | Total | | 1 bbl | | 38.42 |
| Complete Loss pump 20-40 bbl | Bentonite | 25 | 0.14 | 3.5 | |
| | Fiber | 60 | 0.7504 | 45.024 | |
| Total | | 1 bbl | | 48.52 | |